DECOMPOSITION OF ORGANIC MATERIALS WITHIN BURIAL ENVIRONMENTS

Adam Phillip Pinder

PhD

University of York

Chemistry

September 2016

ABSTRACT

The funerary practices of many past cultures in Northwestern Europe involve the burial of the deceased in clothing and in wooden coffins. Although objects made from wood, textiles and leather that exhibit exceptional levels of preservation, or that hold great significance, are commonly analysed by a wide range of analytical techniques, fragments of degraded coffin wood and funerary clothing materials have not, to date, been chemically analysed. This material therefore represents a wealth of potential information that has yet to be investigated.

By identifying and examining the preservation state of wood, textiles and leather placed in archaeological human burials, this research sought to explore the information that could be gained from analysing these degraded materials, and to develop an understanding of the long term decomposition trajectories of different archaeological materials buried in a range of burial environments. This analysis was complemented with data obtained from relatively shorter term burial experiments, aimed at investigating the short term diagenetic processes.

A suite of appropriate analytical chemistry techniques were employed to assess the degradation that had occurred in wood, textiles and leather by comparison with undegraded modern analogues. Using this approach, it has been shown that by examining the component biopolymers, not only can their preservation state be assessed, but a greater depth of information regarding their provenance may be gained in comparison to traditional archaeological methods. The degradation modifications that have occurred within the burial environments were shown to be attributable to a range of fungal, microbial and chemical factors. The type and extent of the degradation allow conditions within the burial environments to be elucidated. These findings have potential implications for the understanding, interpretation and conservation of buried archaeological and forensic materials.

This study found that well drained, sandy soils and permanently waterlogged environments are most conducive to the preservation of wood, textile, and leather fragments, while other environments lead to advanced states of decomposition. The data also indicate that conditions needed for inhibition of microbial decay are not immediately present, the burial environment changing as a result of decompositional, geological or hydrological processes. Evidence of proximity to copper altering the decay of wood by white rot fungus was found. Finding that the colour of a woollen textile is due to degradation rather than intentional dyeing and the chemical identification of lignin in soil stains thought to be due to heavily decayed wood are important findings that could guide future interpretation of archaeology and prevent incorrect conclusions from being arrived at. The removal of conservation treatments from wood sampled from a Bronze Age logboat allows for the future analysis of artefacts conserved using similar techniques.

CONTENTS

LIST OF FIGURES

LIST OF TABLES

ACKNOWLEDGEMENTS

I would like to thank Brendnan (*sic*) Keely for the opportunity to conduct this research project and for his advice and guidance (not to mention him driving us to conferences and field work sites, like a boy racer, in a car held together with gaffer tape). The members of the BJK group, both past and present, provided an atmosphere of humour, humility and comradeship. Thanks go to Scott (for letting me tag EA samples on your runs, for providing me with free biscuits, for being a lovable buffoon and for that night we shared in a Plymouth hotel room), Cezary (for the pickles, cake and heated debates), Marina (for keeping me supplied with Greek coffee and for helping me to wind up Scott), Kim (for driving us to meetings, her outfits, and motherly talks), Chris (for being a fellow night owl who would keep me company in the lab at night and go halves on a takeaway pizza at 2am) and Neung (for sharing with me her native cuisine and the use of her fan heater on those cold nights in the office). A special mention must go to Matt Pickering, who taught me all of my lab and instrumentation skills, kept the lab running, read my work and was a constant source of calm and encouragement (as well as decorating my work areas with drawings, lending me his drill and always being there to enjoy 'pub' and random Simon Pegg quotes). Without Matt, you wouldn't be reading this.

Thanks must also go to the archaeologists and micromorphologists of the InterArChive project; Fabio, Sabina, Raimonda, Helen, Annika, Bone and Allen. Carol must get a special mention for her support and friendship (and for the mutual angry rants about our left wing politics and for all the gin).

The support, advice, encouragement and use of the lab facilities of Kirsty Penkman are greatly appreciated (as was the invitation to the Christmas gathering at her house and, more importantly, taking on 'My Kirsty' as a PhD student). I am also indebted to Kirsty for acting as my internal examiner, who together with Chris Vane of the British Geological Survey (who acted as my external examiner) gave me the most intense four hour grilling of my life. Thank you for your time, compliments, constructive criticism and feedback (and the much needed lunch break!).

The members of Kirsty Penkman's group, who I shared an office and lab with, were of great help and provided me with much support. Thank you Sheila (for keeping the lab running, being my office mother and for putting up with me stealing your label maker and labelling your personal possessions), Marc (for our mutual love of aquariums and letting me use your HPLC), Jo (for being an awesome housemate and letting me love/sniff your lovely cat) and John (for your sense of humour, our deep conversations and for inviting me to your amazing wedding in one of my favourite parts of the UK).

The use of instrumentation provided by Geoff Abbott (Py-GC-MS, University of Newcastle), Meg Stark (SEM, York) and Karl Heaton (GC-MS, York) is greatly appreciated. Thanks go to Sarah Bell, Nick Short and colleagues at Forestry Commission England who provided samples of modern wood, the farmers at the Great Yorkshire Show in 2014 who provided me with wool from their beautiful sheep and all of the archaeologists who gave us their time and allowed us to take samples of archaeological material.

I would also like to thank all of my friends who have put up with my moaning and short temper, provided moral support and welcome distractions and tried to make me feel 'normal'.

I am truly grateful to my family, especially my parents, for providing me with emotional and financial support, for always encouraging and believing in me and for fostering my obsession of asking "why?"

My beautiful furry son Darwin has been a constant source of joy, love and distraction that has helped me to carry on. Thank you for accompanying me on walks (although not when it's raining), for making sure my ears are always clean and for sharing my food, my bed, your toys and your doggy friends.

Most importantly, I would like to express my eternal gratitude to my partner Kirsty. Thank you so much for supporting me, picking me up off the floor, listening to my thoughts, proofreading my scrawlings, putting up with my moods and sleeping habits, for sharing your life with me and for being an amazing person. You made me carry on when I wanted to give up, you made me happy and you saved me. I love you babe.

This study was funded by the European Research Council (ERC) under the European Communities Seventh Framework Programme (FP7/2007-2013; ERC grant agreement no 230193) and by the Natural Environment Research Council (grant number NE/H025545/1).

In memoriam: Don Brothwell

Several days after this thesis was submitted for examination (my thesis mania had barely begun to subside) the archaeological science community lost one of its inspirational and pioneering founders. Don Brothwell had a long and distinguished career that spanned the globe and led the way in applying scientific techniques to archaeological questions. As well as being an academic paragon, Don was also a wonderful human being. From helping to understand the horrors that humans inflict on each other and bringing the transgressors to justice (Brothwell, 2016), to giving encouraging words and a hearty shoulder pat to a self-doubting young research student, Don was an amazingly good person.

I only knew Don Brothwell for a few short years, but in that time he shared with me his vast insight into the archaeological world and infected me with his enthusiasm, passion and curiosity. A chat with Don was always engaging and entertaining (and often light-hearted and witty). Don's stewardship of the InterArChive Project was imperative to its findings and impact. Don also opened his home to the project, letting the InterArChive team bury piglets in his back garden at Hovingham, waving burning newspaper like something out of The Wicker Man to ward off the flies whilst we excavated them (Figure 1) and providing us all with a banquet to honour their sacrifice in the name of science. Don was truly an inspirational human being who I am privileged to have worked with and to have known. I hope that I make a fraction of the contribution to our collective knowledge that Don has, and that I am as good a person.

Figure 1. Wicker Don. 'If I have seen further it is by standing on the shoulders of giants.'

DECLARATION

I hereby certify that the work presented in this thesis is original and my own, with the exception of the collaborative works outlined below and where otherwise acknowledged throughout the text. This work has not previously been submitted for the fulfilment of a research degree at this or any other university.

The following manuscripts arose as a result of the work carried out during this PhD project:

- **Pinder, A. P**., Panter, I., Abbott, G. D., & Keely, B. J. (2017) *Deterioration of the Hanson Logboat: chemical and imaging assessment with removal of polyethylene glycol conserving agents*. Manuscript submitted for publication.

- Burns, A., Pickering, M. D., Green, K. A., **Pinder, A. P**., Gestsdóttir, H., Usai, M. R., Brothwell, D. R., & Keely, B. J. (in press). Micromorphological and Chemical Investigation of late-Viking Age Grave Fills at Hofstaðir, Iceland. *Geoderma*.

- Lang, C., Hicks, S. A., **Pinder, A. P**., Usai, M. R., Wilson, C. A., Brothwell, D. R., & Keely. B. J. *Micromorphological and Chemical Investigations the of First World War mass graves at Fromelles, France*. Manuscript in preparation.

- Pickering, M. D., Hicks, S. A., Green, K. A. , **Pinder, A. P**., Keely, B. J. and Brothwell, D. R. *Organic chemical signatures related to interred human remains and mortuary practise in coffin burials dating from Medieval to the 19th century: factors controlling their preservation and distribution.* Manuscript in preparation.

- Pickering, M. D., Hicks, S. A., **Pinder, A. P**., Usai, M. R., Keely, B. J., & Brothwell, D. R. *Intra-site variation in the preservation of organic matter in archaeological grave soils linked to hydrology of the burial environment.* Manuscript in preparation.

'The Brothers Grimm. Lovely fellas.

They're on my darts team.

According to them, there's this

Emperor and he asks this shepherd's boy,

"How many seconds in eternity?".

And the shepherd's boy says,

"there's this mountain of pure diamond,

it takes an hour to climb it,

and an hour to go around it.

Every hundred years a little bird comes

and sharpens its beak on the diamond mountain.

And when the entire mountain is chiselled away,

the first second of eternity will have passed".

You might think that's a hell of a long time.

Personally, I think that's a hell of a bird.'

…

'And if they ask you who I am,

tell them, "I came the long way round".'

The Doctor

(Steven Moffat)

Enjoy my mound of diamond dust. I'm off to find another mountain.

CHAPTER 1

INTRODUCTION

1.1 Information contained within human burials

For human beings death is an unavoidable fact of life. Eloquently put by one of our greatest and most revered wordsmiths, “Well, we were born to die” (Shakespeare, 1599). Unsurprisingly, societies have developed practices for dealing with death: the remains of the deceased are variously treated according to legal requirements, spiritual and religious beliefs, to ease the grief of the family and to prevent odour and the spread of disease (de Goyet, 2004). The earliest undisputed evidence of intentional burial comes from the remains of early *Homo sapiens* in Skhul Cave, Israel, and is thought to have occurred around 100 thousand years ago (Lieberman, 1991). As our ancestors evolved, formed communities and began to hold shared beliefs, a range of burial practices developed. High status individuals in ancient Egyptian civilisations were mummified and placed within tombs, Viking age Norse leaders were burned in their ships, and Catholics (until relatively recently; Jupp, 1992) believed they had to be buried to ensure their resurrection (Taylor, 2000).

The predominance of the Christian faith in Europe during the last millennium ensured that the most common form of mortuary sequestration was burial (Latourette, 1978; Jupp, 1992). The excavation of archaeological burials has long been of interest as they can provide a wealth of information about both the individual and the wider community. This hidden archive can serve as a record of past cultures and civilisations, giving information on health and disease, culture, society and religious beliefs (Brothwell, 1958; Brothwell, 1981; Kelley and Angel, 1987; Huisman, 2009).

1.1.1 Skeletal remains

The most obvious and some of the most widely studied objects found during the excavation of archaeological burials are the osseous remains. Grave goods, such as coffins, clothing and personal effects, often degrade entirely, leaving the skeleton as the only surviving record (MacKinnon, 2007). Bone is a composite material, consisting of both organic and inorganic components, enabling it to survive in conditions where wholly organic or inorganic materials have completely decayed (Collins *et al.,* 2002).

The earliest analyses of bone recovered at archaeological sites focussed on observation and dimensional measurements of individual bones and skeletal features (Virchow, 1882; MacKinnon, 2007). The focus of the field was on information such as the size, gender and ethnicity of the individual (Jacobsen and Cullen, 1990). Little advance in the analysis of human remains was made until the 1980s, at which point their potential became fully realised (MacKinnon, 2007). Thus, more comprehensive examinations of individual bones and their features became widespread, enabling interpretations of premortem injuries, disease and cause of death (Brothwell, 1981).

The modern study of archaeological osseous remains is a diverse and active area of research involving both physical and chemical analysis (Brothwell, 1981). Isotope analysis is used to infer diet and geographical movements (Sealy *et al*., 1991) and radiocarbon dating is used to estimate the temporal range in which an individual died (Arneborg *et al*., 1999). Analysis of DNA recovered from bones has been used to suggest death due to disease (Abbott, 2001), determine the lineage (Hagelberg *et al*., 2015) and even the identity of a skeleton (a recent and high profile example being the identification of the remains of Richard III; King *et al*., 2014).

1.1.2 Grave goods

Early excavations of archaeological burials were often performed in the interests of financial gain, with burial goods fetching high prices from collectors of antiquities (MacKinnon, 2007). As the field of archaeology developed, the non osseous contents of inhumations began to be studied, in order to improve the understanding of social structures, beliefs, customs, movement and trade relating to the individual and their wider community (Pearson, 1999; Łucejko *et al.,* 2015; Pearce, 2016). The presence of a coffin, burial clothing and objects placed in the grave with the deceased can all be vastly significant (Kim and Singh, 2016) and are deserving of explicit consideration.

1.1.2.1 Coffin remains

The shape, methods and quality of construction, and adornments or fastenings of a coffin may give an indication as to the person's status (Bell, 1990). The religion of the deceased may also be inferred from the coffin, an example being the strict construction methods and lack of any metal parts on coffins used by followers of Judaism (Cutter, 1992). The type of wood used in the construction of coffins can also be indicative of past ecological conditions; the predominance of one type of wood being used for the construction of coffins in a cemetery can indicate a readily available source of that wood to a community (Cevasco and Moreno, 2015). An incongruous wood, on the other hand, can indicate a person of high status and provide evidence for trade links (El Hadidi, 2016).

For all but the most high profile or well preserved coffins, chemical analysis on coffin wood is rare (for example: Blanchette and Simpson, 1992; Blanchette, 1991; Crestini *et al*., 2009). However, the analysis of fragments of coffins wood recovered from archaeological burials has the potential to reveal information about the individual and their society, as well as the conditions and degradation processes that occurred within the burial environment.

1.1.2.2 Clothing remains

In addition to coffins, textiles and animal skins have also been found in human burials (Good, 2001). In many cases, however, the component polymers that make up these materials decay rapidly when buried, which results in them being uncommon in excavations from all but the most recent burials (Janaway, 2001). Examples that do survive can be extremely informative, a recent example being the analysis of the clothes and possessions of 'Ötzi the Iceman'. The naturally mummified and exceptionally preserved individual, discovered frozen in an Alpine glacier in Italy in 1991, was estimated to have lived around 3300 BC by ^{14}C dating (Bonani *et al*., 1994). O'Sullivan *et al*. (2016) analysed mitochondrial DNA from his clothing and hide arrow quiver, concluding that his coat was made from the hides of two goats and two sheep, his loincloth and leggings were goat hide, his shoelaces were cow leather, his hat was the fur of a brown bear and his arrow quiver came from a roe deer. These analyses provided evidence for the hunting and

domestication of these animals, while earlier analyses of the items provided insight into the tailoring techniques of the period (Dickson *et al.,* 2003).

1.1.3 The grave and burial soils

The earliest recordings of grave morphology were in the form of rough plans and sketches done to mark out the locations where finds were recovered; detailed and systematic recording of excavations of human burials did not become commonplace until the 1960s (MacKinnon, 2007). Modern archaeological excavation practice is far more methodical, with every aspect of the site recorded in detail. Accurate recording of grave dimensions using surveying techniques and precise location mapping using global positioning technology are commonplace, allowing greater detail of the site and individual burials to be elucidated (Grant *et al*., 2015; Fagan, 2016). Features such as the orientation of the burial often infer religious practices (Pearson, 1999; Mackinnon, 2007). Mass graves can be related to the location and outcome of historic battles, or the outbreak and mortality rate of communicable disease (Loe *et al*., 2014a; Frisk, 2015; Pearce, 2016).

The analysis of soil from archaeological contexts is a well established field, with soil micromorphology (Courty, 1992; Grave and Kealhofer, 1999) and inorganic elemental compositions (Parnell *et al*., 2002*;* Wilson *et al*., 2008) being routinely studied as part of many archaeological investigations. The analysis of the organic residues found in archaeological soils is also widely applied and has been used to detect sites of human habitation, infer land use and hint at historical agricultural processes (Bull *et al*., 1999; Evershed, 2008). By contrast, little work has been reported on the soils from archaeological human burials (Usai *et al.,* 2014). Notably, however, analyses of soils from modern graves (Forbes *et al*., 2003) and during forensic investigations (Bull *et al*., 1999) have shown the potential for biomarkers of cadaver degradation to be retained by the burial environment. This work on modern human burials led to the question: what chemical and micromorphological signatures remain in the burial matrices of archaeological graves?

1.2 The InterArChive project

A pilot study carried out by Tongue and Keely (2008) examined the potential for organic residues from decayed human remains to be retained in the soils of archaeological burials. Based on this work the project titled *"'Interred with their bones' – linking soil micromorphology and chemistry to unlock the hidden archive of archaeological human burials"*, or InterArChive for short, was funded by the European Research Council (European Community's Seventh Framework Programme (FP7/2007-2013) / ERC grant agreement no. 230193).

The InterArChive project aimed to investigate the information contained within the burial soils of graves, using a combination of analytical chemistry techniques (including carbon, nitrogen, hydrogen, sulphur, oxygen (CHNSO) and total organic carbon (TOC) elemental analysis and gas chromatography – mass spectrometry analysis of solvent extracts) and soil micromorphology carried out on thin sections of resin impregnated soil samples (Usai *et al.,* 2014).

A high intensity sampling strategy was developed to collect soil samples from 17 positions associated with each grave studied for chemical analysis, and four positions for micromorphological analysis, in order to maximise the information that could be obtained (Figure 2). Additional samples of any other soils perceived to be of potential value were also taken into account in the strategy.

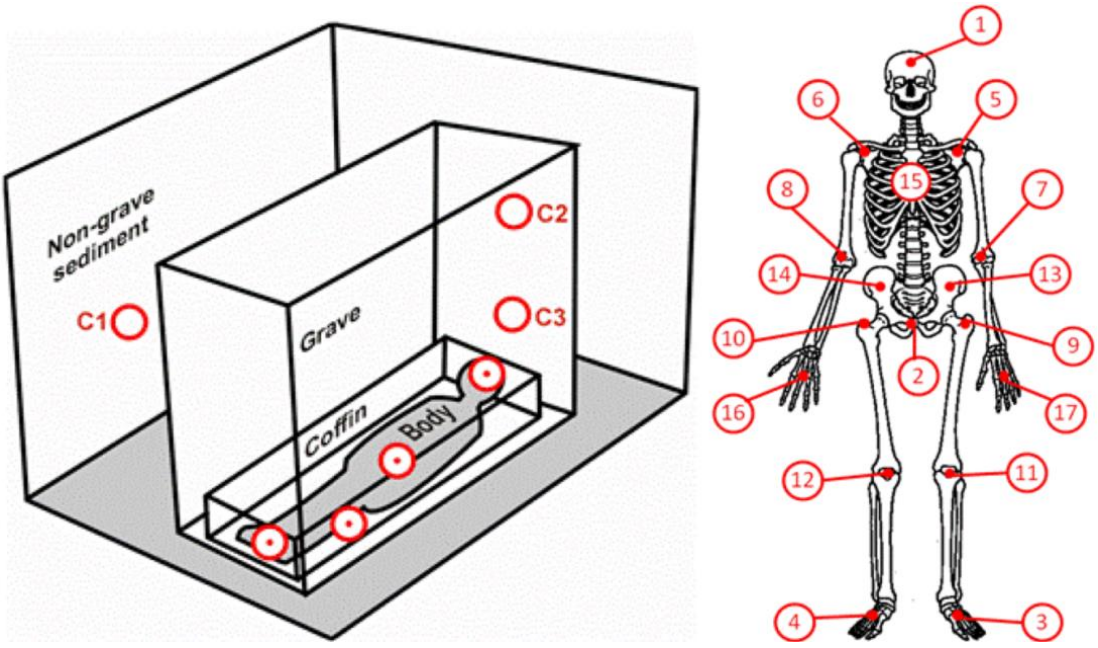

Figure 2. The sampling strategy for collection of soils from archaeological human burials. C1, C2 and C3 are soil control samples used to establish background chemistry and soil features. Circles with dots are soil samples taken for micromorphology analysis from the head, pelvis, hand and foot. The numbered circles are soil samples taken for chemical analysis. Image credit: Matt Pickering, University of York.

During the sampling of burial soils from sites across Northwestern Europe, fragments of surviving wood and clothing materials were also collected. The vast amounts of these wood (primarily from coffin remains) and clothing fragments presented a unique opportunity to compare preservation states and postulate the decomposition trajectories of grave goods from a range of different burial environments.

1.3 Archaeological wood

Since our primate ancestors first learned to use rudimentary implements, wood has played a crucial role in human history and development (Perlin, 2005). Heat, tools, shelter, weapons and transport aids have all been provided by the shed branches and fallen trunks of native trees. Wood is still intrinsic to modern day societies, prized for its strength, renewability and ease of processing. Many currently available building materials are stronger and more resistant to degradation, yet wood is still chosen over many materials due to its sustainability, aesthetics, and links to our past.

The oldest worked wooden object to be discovered is the Clacton Spear, found in Clacton-on-Sea in Essex, UK in 1911 and has been dated to 400,000 years ago (Allington-Jones, 2015). A set of hunting spears found in Schöningen, Germany, have survived for 300,000 years (Thieme, 1997; Barham, 2013) and the Shigir Idol found in Russia is the oldest wooden sculpture, the ^{14}C date indicating an age of 11,000 BP (Liesowska, 2015). Physical and chemical analysis of such materials can provide a wealth of information regarding the environment and the societies from which they originated.

1.3.1 The chemical composition of wood

1.3.1.1 Lignin

Lignin is a large, cross-linked phenylpropanoid biopolymer contained within the plant cell wall. It is one of the most abundant plant biopolymers – second only to cellulose – and is the largest biological source of aromatic hydrocarbons (Calvo-Flores and Dobado, 2010). The main lignin monomers are three phenylpropanoid alcohols (or monolignols): para-coumaryl alcohol (4-[(E)-3-hydroxyprop-1-enyl]phenol), coniferyl alcohol (4-(3-hydroxy-1-propenyl)-2-methoxyphenol) and sinapyl alcohol (4-(3-hydroxyprop-1-enyl)-2,6-dimethoxyphenol). The exact composition of lignin and ratio of the phenylpropanoid subunits in the structure is dependent on the type of tree. The lignin of 'softwood' gymnosperm trees comprises exclusively guaiacyl (2-methoxyphenol) subunits, whereas that of 'hardwood' angiosperm trees contains both guaiacyl and syringyl (2,6-dimethoxyphenol) subunits (Figure 3 and Figure 4; Obst, 1982; Boerjan *et al*., 2003).

Lignin is a highly complex and heterogeneous polymer that has thus far confounded definitive characterisation of its three dimensional structure, despite the application of a wide array of analytical techniques (Vanholme *et al*., 2010). Although it will differ slightly to the intact polymer (Alves, *et al*., 2006), the alkaline soluble lignin content of angiosperm wood has an approximate molecular formula of $C_{31}H_{34}O_{11}$ (King and Solomon, 1983).

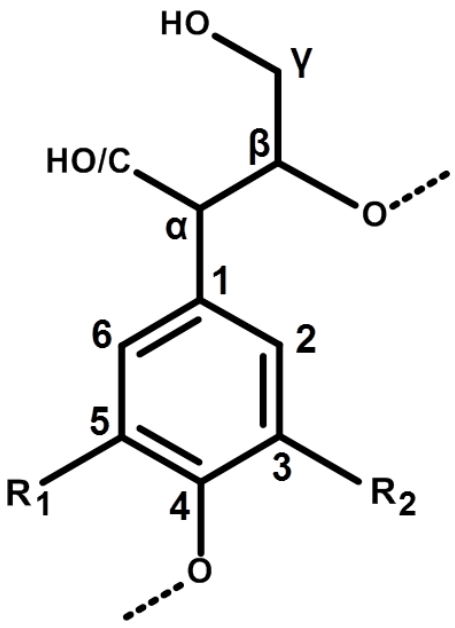

Figure 3. The structure of a typical lignin subunit, showing the numbering of the phenolic ring carbon atoms and the propenyl carbon chain. In guaiacyl lignin subunits, R_1 = H and R_2 = OMe; in syringyl lignin subunits both R_1 and R_2 = OMe.

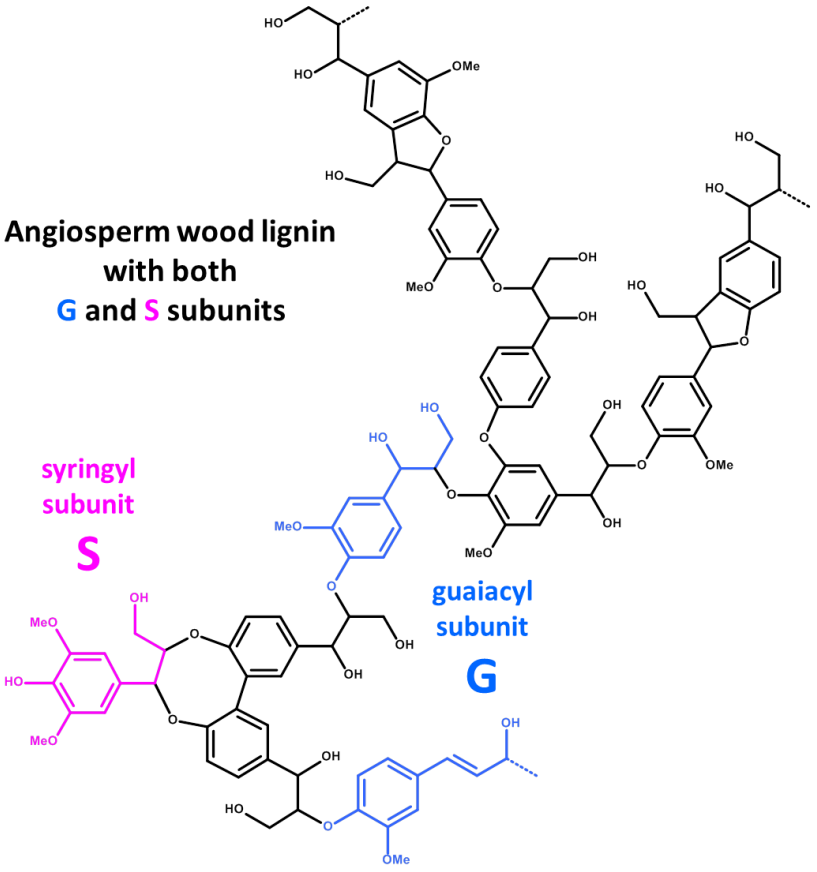

Figure 4. A structural representation of a typical fragment of a larger lignin polymer, showing the structure of guaiacyl (blue) and syringyl subunits (pink) and some common interunit linkages (Leonowicz et al.,1999).

1.3.1.2 Cellulose

The structure of cellulose, the dominant biopolymer of wood, comprises chains of D-glucose molecules linked by β(1-4) glycosidic bonds (Figure 5; Updegraff, 1969), the repeat unit having the formula $C_6H_{10}O_5$ (Payen, 1838). The sugar rings of cellulose all occupy the same orientation and the resulting polymer has a straight chain with no branching (Fengel and Wegener, 1984). The number of glucose molecules in each cellulose polymer in wood varies from 7000 to 10,000 (Goring and Timell, 1962).

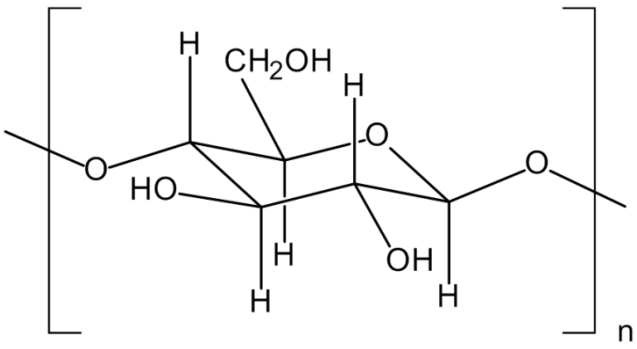

Figure 5. The structure of the repeat unit of cellulose.

1.3.1.3 Hemicellulose

Hemicellulose has shorter chain lengths and a more varied structure than cellulose, incorporating both five and six membered heteroatomic rings and containing many saccharide side chains (Bauer *et al*., 1973; Fengel and Wegener, 1984). As with lignin, hemicellulose biosynthesis exhibits a degree of phylogenic specificity. The hemicellulose of softwoods contains more mannose and galactose units, whereas that of hardwoods has a higher proportion of xylose and contains more acetyl functional groups (Fengel and Wegener, 1984; Hoch, 2007; Scheller and Ulvskov, 2010).

1.3.1.4 Variation in biopolymer composition

The proportions of the three biopolymers in any given sample of wood is dependent on the tree species, age, the location the sample is taken from within the tree, and the soil and environmental conditions in which the tree is rooted (Pandey and Pitman, 2003). The approximate compositional ranges of softwoods and hardwoods are shown in Table 1.

Table 1. Ranges of the relative amounts of cellulose, hemicellulose and lignin that have been observed in wood from softwood and hardwood trees (Fengel and Grosser, 1975).

Wood type	Cellulose content	Hemicellulose content	Lignin content
Softwood	40-60%	5-15%	25-40%
Hardwood	35-50%	20-35%	15-30%

1.3.2 The structure of wood

1.3.2.1 Macrostructure

A generalised cross section of a tree trunk is shown in Figure 6. The outer layers of the bark serve a similar purpose to that of skin in animals, offering protection to the tree from microbial attack and damage from external factors (Salisbury and Ross, 1992; Silvester, 2013). The inner layers of the bark and the underlying vascular cambium are responsible for the biosynthesis of new wood cells. Each growth season (typically the local spring and summer months) results in the addition of a new layer of growth to the wood beneath the bark, leading to the addition of another annual growth ring and an increased diameter of the tree trunk (Salisbury and Ross, 1992; Silvester, 2013).

Sapwood is tissue of the tree where the wood cells are still living and playing a biologically active role in the tree and is responsible for the transport and storage of water (Silvester, 2013). When a tree grows to dimensions that necessitate a greater degree of structural integrity and strength the sapwood nearest the centre of the tree undergoes conversion to heartwood (Silvester, 2013). Heartwood differs from sapwood in that it is stronger, no longer living and has a greatly reduced water content due to it not being used for water transport and storage (Silvester, 2013). Due to its superior strength and reduced propensity to shrink and warp when dried, heartwood is commonly favoured for use in woodworking and construction (Taylor *et al*., 2002).

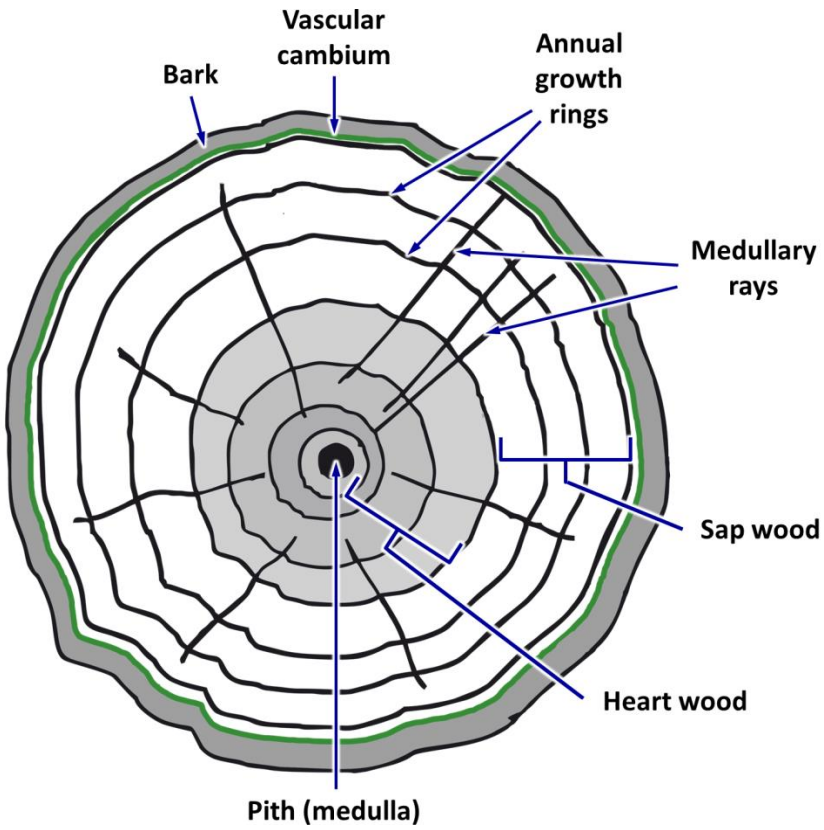

Figure 6. The structure of a tree trunk, showing the key tissues and features.

1.3.2.2 Microstructure

On the microscopic scale, the wood of gymnosperm trees is profoundly different to that of their broadleaved angiosperm cousins (Fengel and Wegener, 1984). Gymnosperm wood – commonly referred to as softwood – has a relatively simple structure composed chiefly of tracheid cells (Figure 7; Hoffmann and Jones, 1990). The tracheid cells produced during the earlier part of the annual growth season are typically larger in diameter and more thinly walled than those grown during the later growing months, these being smaller but have thicker walls (Fengel and Wegener, 1984). The different cells are termed earlywood and latewood, respectively. In many gymnosperm woods the early and latewoods occur in distinct bands (Fengel and Wegener, 1984; Blanchette, 2000).

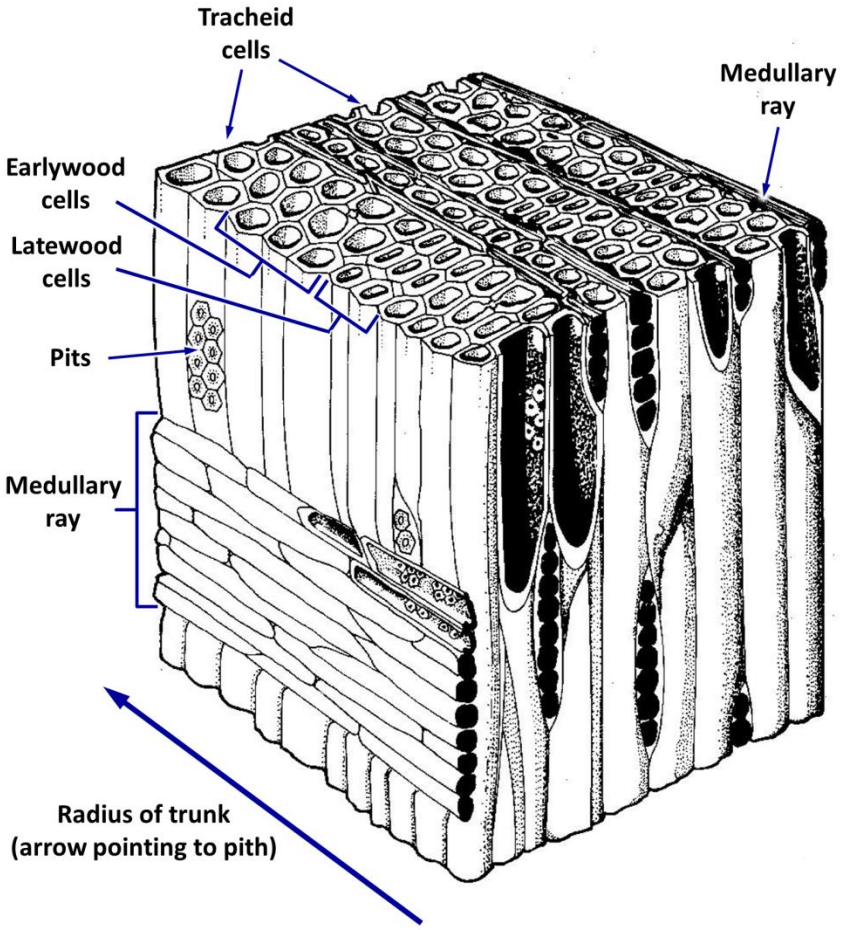

Figure 7. The microstructure of softwoods from gymnosperm trees. Adapted from Fengel and Wegener (1984).

In comparison to those found in gymnosperm trees, the tracheid cells of angiosperm woods (Figure 8) are smaller and have relatively thicker walls; the difference between early and latewood is also less distinguishable (Fengel and Wegener, 1984). Hardwoods contain many vessel elements that are not present in softwoods, which are responsible for the transport of water within the wood (Wilson, 1986). The vessels are typically several times larger than the tracheid cells and contain tyloses, which act as valves that can halt the transpiration stream during times of drought (Fengel and Wegener, 1984).

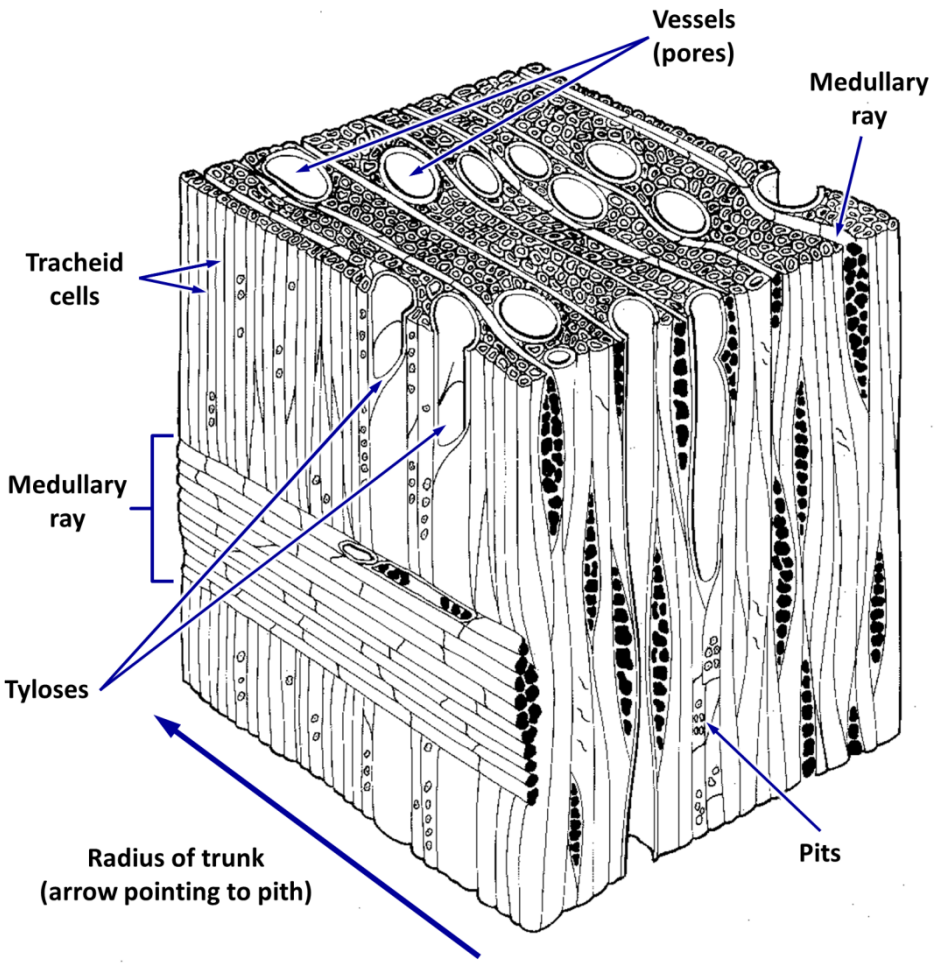

Figure 8. The microstructure of hardwoods, from angiosperm trees. Adapted from Fengel and Wegener (1984).

Although the size and density of tracheid cells of softwoods and hardwoods differ, the structure of the cells in both wood types is similar (Figure 9). Each cell is essentially a long tube made up of several layers: the primary cell wall layer; the secondary cell wall S1 layer; the secondary cell wall S2 layer; and the secondary cell wall S3 layer (Hoffmann and Jones, 1990). Some species of tree have an additional warty layer that sits atop the S3 layer, inside the lumen (Fengel and Wegener, 1984). Each cell wall layer consists of fibrils, made up of the three major component biopolymers of wood (lignin, cellulose and hemicellulose). All the fibrils in a particular cell wall layer have the same orientation and each cell wall layer has a different fibril orientation (Fengel and Wegener, 1984; Figure 9). Each cell is attached to the neighbouring cells by the middle lamella.

The different layers within each wood tracheid cell contain different proportions of biopolymer. The middle lamellae are almost entirely lignin, giving them a high degree of strength and acting as a structural scaffold which supports the embedded tracheids (Fengel and Grosser, 1975). The primary cell wall layer also has a high lignin content, but it is comparatively lower than that of the middle lamella. The proportion of lignin decreases and that of holocellulose increases in successive secondary cell wall layers, with the S3 layer being almost completely cellulose (Fengel and Grosser, 1975).

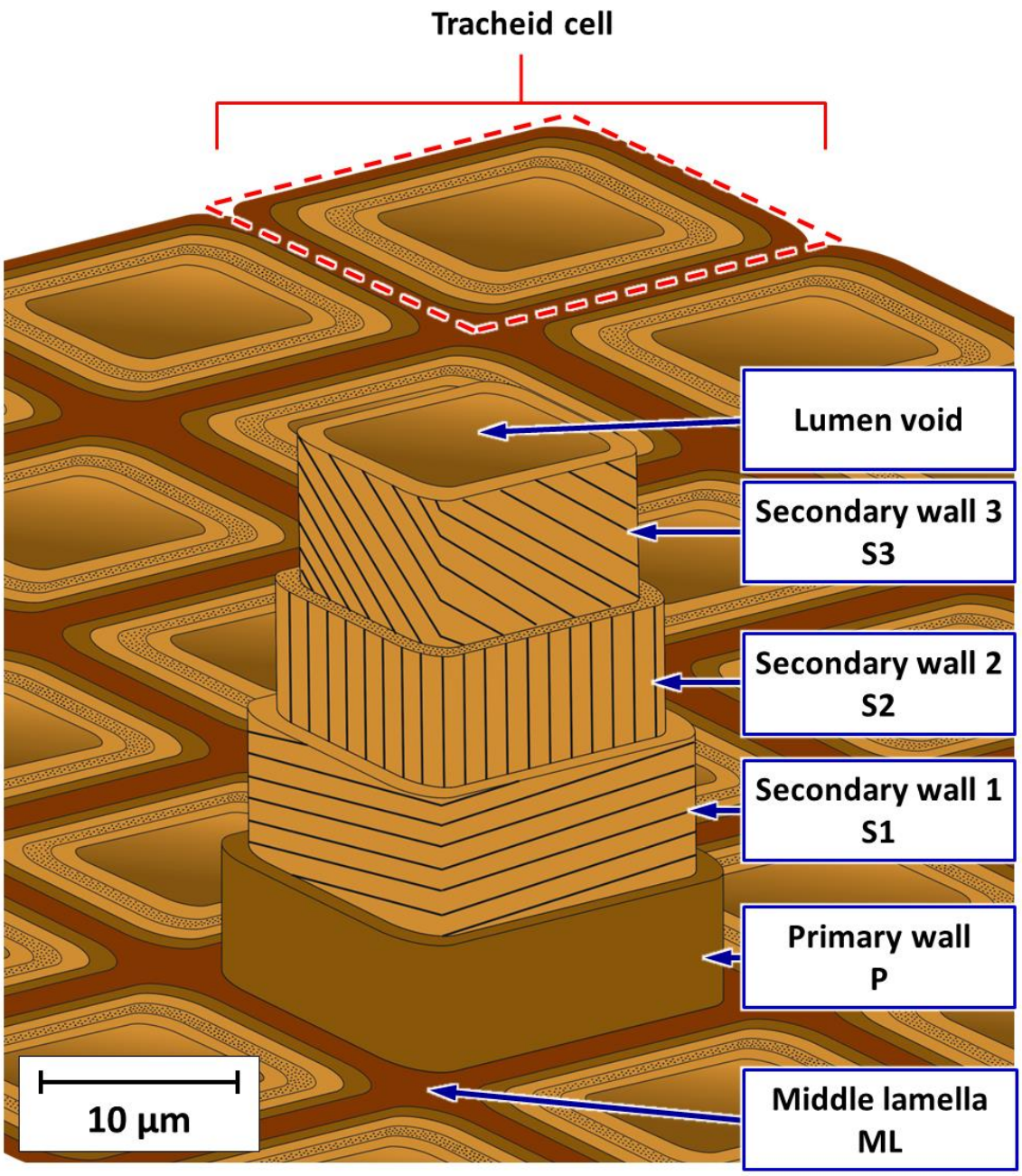

Figure 9. The generalised microstructure of wood tracheid cells, showing the composition and packing of individual cell wall layers (Fengel and Wegener, 1984; Eriksson et al., 1990).

1.3.3 Wood degradation

Although wooden objects that have survived for hundreds of thousands of years have been recovered during archaeological excavations (Thieme, 1997), the survival of wooden objects for such extended periods of time is atypical: when cut from the parent tree wood is readily degraded by fungi or bacteria. The cellulose and hemicellulose components of wood decay relatively quickly on the archaeological timescale due, in part, to the ability of microorganisms to metabolise these polysaccharides using a range of hydrolysing and oxidising enzymes (Blanchette *et al.,* 1990; Sánchez, 2009). Brown rot and soft rot fungi are the most commonly observed holocellulose fungal degraders in wood, and a wide range of bacteria are known to be capable of metabolising holocellulose (Blanchette, 2000; Martinez *et al*., 2005). Extremes of pH can also lead to the breakdown of holocellulose, although the damage caused by the chemistry of the burial environment is typically negligible compared with that attributable to microbes (Fengel & Wegener, 1984; Jones & Eaton, 2006).

Lignin, on the other hand, is far more recalcitrant, being found in prehistoric samples of wood (albeit in a modified form) where all of the carbohydrates have been degraded (Blanchette, 2000; Blanchette *et al*., 2013). The polysaccharide degrading activity of microbes that are not capable of metabolising lignin – including brown rot fungi, soft rot fungi and a range of bacteria – do however lead to modification of lignin (Blanchette, 2000; Martinez *et al*., 2005). These changes are typified by the demethylation and demethoxylation of the methoxy groups attached to guaiacyl and syringyl lignin phenols (Martinez *et al*., 2005).

There are two currently acknowledged classes of lignin degradation; those performed by bacteria, and those by fungi. Bacterial lignin degradation has only been successfully probed relatively recently. Although it is less well understood, it has been shown to be performed by a range of microorganisms; including *Streptomyces viridosporus* (Bugg *et al*., 2011a). It must be noted that the observed activity of bacterial lignin modifiers is far less than that of fungi, which are thought to be the most common degraders of lignin (Blanchette *et al*., 1990; Kim & Singh, 2000).

Fungal degradation has been studied very extensively and has been shown most commonly to be caused by white rot fungi (Schwarze *et al*., 2000). Two distinct types of white rot mediated wood degradation are known; simultaneous rot and selective delignification. Simultaneous rot sees the degradation of both lignin and holocellulose, destroying all cell wall components (Eriksson *et al*., 1990; Blanchette, 2000; Schwarze *et al*., 2000). Selective delignification attacks only the lignin rich middle lamellae and primary cell wall layers, leaving disconnected tubes of the remaining holocellulose rich secondary cell wall layers (Eriksson *et al*., 1990; Schwarze *et al*., 2000; Martinez *et al*., 2005).

The mechanisms of action of white rot lignolytic enzymes are well characterised (Bugg *et al*., 2011b; Martinez *et al*., 2005; Sánchez, 2009). The lignin is depolymerised by a range of enzymes having transition metal containing active sites, including lignin peroxidase (LiP), manganese peroxidase (MnP) and laccase. A comprehensive scheme for the biodegradation of lignin indicates that these enzymes lead to the cleavage of Cα-Cβ bonds of the three carbon side chains of lignin subunits (D, K and R in Figure 10) and result in the oxidation of the attached hydroxyl groups. The peroxidase enzymes are hydrogen peroxide dependant, and oxidize lignin via two consecutive one-electron oxidation steps, with the formation of an intermediate radical cation and subsequent bond cleavage or ring opening (Leonowicz *et al.,* 1999; Martinez *et al*., 2005). Laccase is an oxygenase (requiring oxygen as a co factor) that catalyses single electron oxidation.

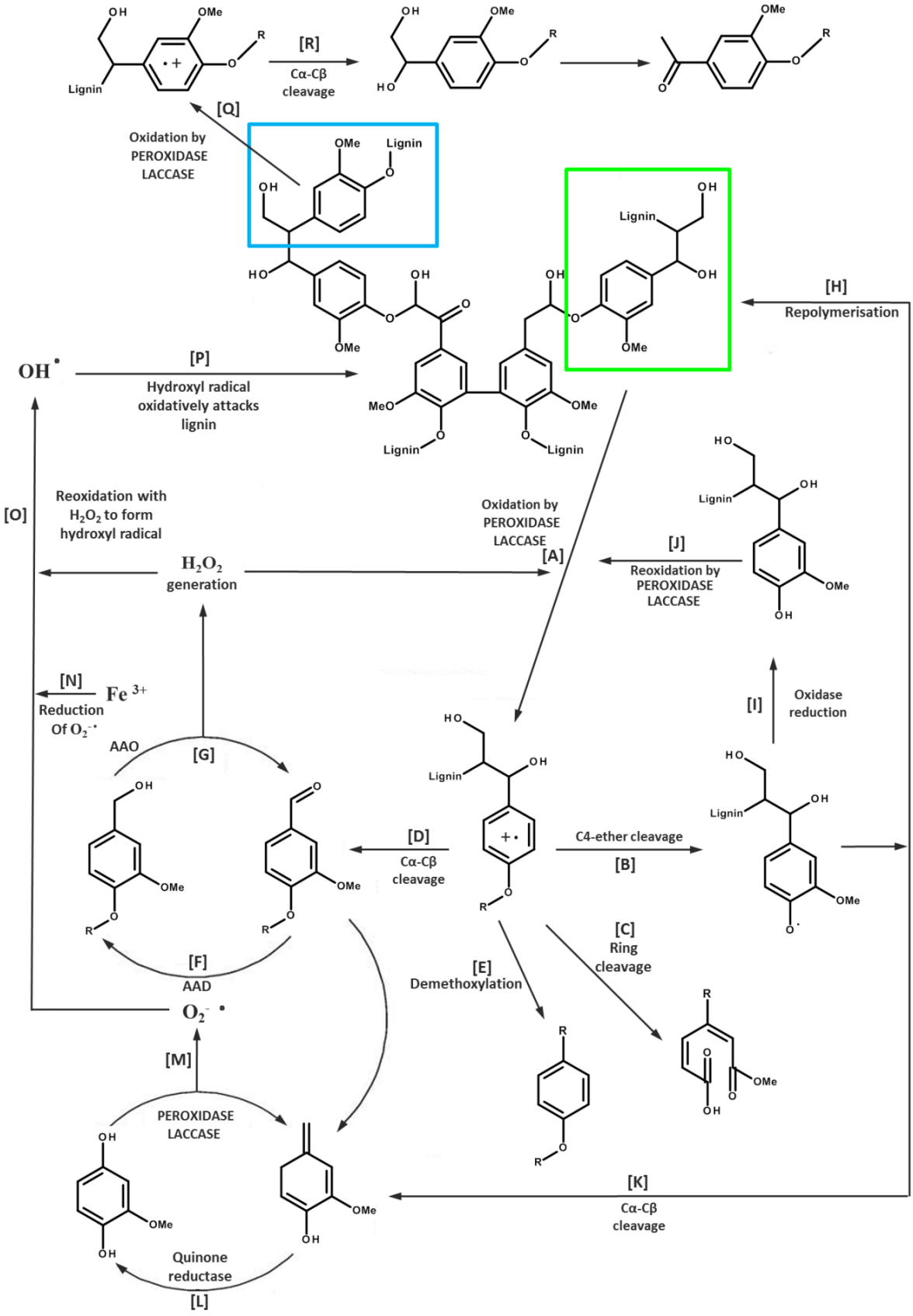

Figure 10. Scheme showing the enzymatic degradation of lignin. AAO = aryl-alcohol oxidase; AAD = aryl-alcohol dehydrogenases Adapted from Martinez et al., (2005) using Tien and Kirk (1984), Tien (1987) and Rencoret et al., (2010).

1.3.4 Wood preservation

The first evidence of a solution to the degradation of wood used in construction comes from the Egyptians over 4000 years ago, who coated wood with natural oils (Graham, 1973). Early Roman records document the use of cedar oil to prevent microbial or insect damage, and pitch to waterproof wooden boats and ships (Rackham, 1945). Until the beginning of the 20th century, wood preservatives were relatively expensive and reserved for more important construction projects (Graham, 1973; Schultz *et al*., 2007), with the coffins of even the Egyptian pharaohs being made from untreated wood (Weiss, 1916). Due to leaching or breakdown of the applied substances, rudimentary preservative treatments often required periodic reapplication to maintain their protective effects (Schultz *et al*., 2007). Thus, either with or without such treatment, for a wooden object to have survived in the burial environment for any considerable length of time the actions of degrading microorganisms must have been either slowed or arrested.

The endurance of the Schöningen spears and the Shigir Idol was due to their burial in waterlogged peat bogs, the environments being anoxic and limiting microbial degradation (Ajuong and Redington, 2004). The survival of wooden objects from burials depends on a narrow range of conditions. The majority of wood processing fungi require moist, oxic environments to metabolise and decay wood (Boer *et al*., 2005). Conditions in which the amounts of water or oxygen are insufficient may well lead to the survival of lignocellulosic materials. These conditions occur relatively rarely, and the survival of objects is dependent on the conditions remaining unchanged until discovery. A change in the burial environment may lead to the destruction of the object. Despite the dependence on static burial environmental conditions, some wooden objects do survive. A unique and fascinating example is the Bronze Age settlement at Must Farm in Cambridgeshire, where logboats and wooden houses and their contents have been preserved in the silt of a former river (Malim, *et al.,* 2015; www.mustfarm.com).

Although rare and often heavily degraded, coffin woods can be found when the remains of buried individuals are excavated (Henderson, 1987; Hunter *et al*., 1996). As the focus of the InterArChive Project was to examine the residues remaining in archaeological graves, fragments of coffin wood were the main source of archaeological wood samples analysed during this investigation.

1.3.5 Analysis of wood

1.3.5.1 Optical microscopy and SEM

The preservation state of wood can be assessed by means of microscopy, by examining the physical condition of the remaining cellular structure (Hoffmann and Jones, 1990; Blanchette, *et al*., 2013). Optical microscopy is of limited use, as the resolution limit of visible light and the need to produce and stain thin sections of fragile archaeological woods is difficult and time consuming (Schwarze, 2007). Scanning electron microscopy (SEM) provides nanometre resolution using incident and reflected photons, negating the need for the production of thin sections (Blanchette *et al*., 2004). The sample preparation and imaging is time consuming and expensive, but the amount of detail in insight provided far outweigh the investments.

Chemical analysis of wood can provide similar information to that of microscopy, as well as much more detailed information regarding the preservation state of the component biopolymers. Instrument based techniques such as elemental analysis (EA), Fourier transform infrared spectroscopy (FTIR), nuclear magnetic resonance (NMR) and pyrolysis – gas chromatography (Py-GC) as well as an array of wet chemical techniques can be used to make detailed studies of modifications to archaeological wood in comparison to modern, undegraded woods.

1.3.5.2 Wet chemical analysis

Given that the holocellulose and lignin components of wood are often degraded by different microorganisms and conditions (see Section 1.3.3), wet chemical techniques can be used to investigate the content of different cellulose fractions and lignin. Such methods are routinely used in the paper production industry, where a high cellulose content is often desired. Raw wood starting materials, as well as paper that is being recycled, are analysed to assess the cellulose and lignin contents, and hence their suitability for different paper applications (TAPPI standards). These methods have been adapted for use in the analysis of archaeological wood (Hoffman, 1981).

There are, however, considerable drawbacks with using these adapted methods in the analysis of archaeological wood. The methods have inherent inaccuracies, which can lead to inaccurate quantitation of the different components, illustrated by total compositions of the various components that are in excess of 100% being reported (Fengel and Wegener, 1984). When analysing precious archaeological objects, one of the key compromises is minimising destruction to the artefact while maximising the information gained from the investigation. Wet chemical techniques (such as lignin and cellulose extraction) often require large amounts of material for accurate and conclusive results, making them less applicable when smaller objects (such as fragments of coffin wood) need to be studied (Hoffman, 1981).

1.3.5.3 EA

Compared to other techniques, EA provides very basic information on the atomic composition of woods, losing much data on the higher order of composition. It is, however, useful to analyse woods that may contain materials other than the native lignocellulose. For example, the sulfur content of waterlogged archaeological woods is known to lead to problems with decay after excavation (Ghisalberti *et al.,* 2002; Sandström *et al*., 2005). Analysis of materials by EA to determine their carbon, hydrogen, nitrogen oxygen and sulfur contents is useful in cases where organic and inorganic contamination is expected.

1.3.5.4 FTIR

When used with an attenuated total reflectance attachment, FTIR is non destructive and can be used to analyse objects without the need to remove subsamples. The analysis of lignin:holocellulose is often performed using FTIR (Pandey, 1998; Pandey and Pitman, 2003; Gelbrich *et al*., 2008). The main drawback with FTIR is that molecules with small variations in structure can produce little difference in the wavenumber of resonant bonds, making it difficult to gain more detailed structural information. There is also a lack of quantitation of the observed bonds, meaning that the data is less informative than other techniques.

1.3.5.5 NMR

Solid state ^{13}C NMR analysis gives detailed information about both the two and three dimensional structure of the biopolymers of wood (Wilson *et al*., 1993; Almkvist, 2008). The loss or modification of polymer subunits or functional groups that result from the degradation of wood lead to differences in the peak intensities and chemical shift values in comparison with undegraded wood, thus allowing the degradational modifications to be investigated (Wilson *et al*., 1993). Solid state NMR has the potential to be a powerful tool in the analysis of wood, but technical, computational and financial limitations prevent the technique from being widely applied (Almkvist, 2008). The analysis must be performed using specialist solid state NMR instrumentation, which is expensive and not widely available to researchers studying archaeological wood. In addition, solid state NMR has lower resolution and broader linewidth than solution phase NMR, leading to the need for the data to be digitally reprocessed prior to analysis (Vogt, 2010). The variation contained within the polymers that constitute wood result in very complex spectra, which require significant computing power to process. In combination, these factors limit the application of solid state NMR analysis to archaeological wood, and mean that it is not often used (Hedges, 1990, Almkvist, 2008).

1.3.5.6 Analytical pyrolysis

Analytical pyrolysis techniques are widely used for the study of archaeological materials made from wood (Bonaduce *et al*., 2016). Studies of modern and of archaeological woods have illustrated the suitability of sequential thermal desorption, pyrolysis, and gas chromatography (TD/Py-GC) to the characterisation of the lignin component; examples include the ancient ships of Pisa San Rossore in Pisa, Italy and several Indian Ocean shipwrecks (Wilson *et al*., 1993; Colombini *et al*., 2003; Łucejko *et al*., 2009). Thermal desorption - using temperatures less than 300°C - removes any volatile and semi-volatile organic molecules from materials, including degraded polymer subunits that are loosely bound or no longer bonded to the remaining structure. This allows a clearer picture of the remaining polymer to be gained. The pyrolysis step involves heating material to temperatures typically in excess of 500°C, resulting in the breaking of bonds between monomeric units. The liberated species are subsequently separated by gas chromatography and detected by either mass spectrometry (MS) or a flame ionisation detector (FID). MS provides the mass and fragmentation pattern of the resolved species but, due to the differences in ionisability, the quantitation of each molecule is variable. FID, on the other hand, allows for better quantitation of each resolved compound but provides no definitive identification. Each peak must instead be identified by use of retention order and peak patterns in comparison with those of standards and data acquired using MS detection. Despite the complexity of the data analysis, Py-GC techniques have many advantages. Small samples of material are required (less than 1 mg), sample preparation is minimal (due to removal of non-polymeric materials by TD) and the resulting data is extremely informative as to the state of the polymers of the wood.

1.3.5.7 Techniques applied in this study to analyse wood

This investigation employed a combination of TD/Py-GC with FID and MS detection to assess the chemical state of the holocellulose and lignin of the buried archaeological woods, together with SEM to aid in the interpretation of results and to provide an assessment of the preservation state of the physical microstructure of the woods. EA was used to analyse materials from waterlogged environments to assess the sulfur content in order to ascertain if there had been any accumulation of sulfur from the burial environment.

1.4 Archaeological textiles and leathers

All extant animals have adapted to the climate in which they survive. The selection pressures of cold local climates have led to many different solutions to the problem of heat loss, whether it be fur, feather or fat. Humans are unique in their use of clothing to control the rate of heat loss from the body, a behaviour which has enabled *Homo sapiens* (and other extinct hominins) to spread to a vast range of environments.

The earliest evidence of hominins wearing clothing is the genetic divergence of clothing lice from head lice, which occurred between 83,000 and 170,000 years BP (Toups *et al*., 2011). The earliest forms of artificial insulation probably came in the form of the furs and hides obtained from prey animals (Gilligan, 2010). As the methods of fashioning these raw materials into more suitable clothing progressed, the use of plant material or animal connective tissues as cordage and rudimentary stitching developed (Barber, 1991). The skills needed to perform these tasks probably evolved into the origins of weaving fibres into textiles (Gilligan, 2010).

The oldest known textile materials are dyed flax fibres from Dzudzuana Cave, Georgia, which date from between 35,500 and 37,500 years BP (Kvavadze *et al*., 2009). Other examples of textile finds from prehistory are 8500 year old linen recovered from Namal Hemar, Israel (Schick, 1986), and 8000 year old textiles from Çatal Hüyük, Turkey (Burnham, 1965). The routine use of sheep wool came about after the domestication of goats and the subsequent selective breeding to produce modern sheep, with the use of wool in Europe emerging between 3650-3100 BC (Pipes *et al*., 2014).

1.4.1 Plant derived textiles

1.4.1.1 Structure and composition

Different structures and tissues from a range of plants can be used to create textiles. The most common plant textile in use in modern Europe is cotton (Smith and Cothren, 1999). Made from the seed pods of plants in the genus *Gossypium* (found in tropical and subtropical regions across the globe), cotton is almost entirely made of cellulose (95.5 – 99.9%), with very small quantities of lignin (0.3 – 0.5%) and hemicellulose (0.1 – 0.9%; de Morais Teixeira *et al*., 2010). The strong, yet fine, fibres of cotton enable it to be weaved into thin, comfortable materials.

Before the modern dominance of cotton, textiles produced from the bast fibres of plants including flax (*Linum usitatissimum*) and hemp (*Cannabis sativa*) were commonly used for clothing as well as other domestic and commercial applications (Mohanty *et al.,* 2005). Bast fibres (layer 5 in Figure 11) run the entire length of the stem and have a higher lignin content than cotton (≈ 2.2% for flax and 3.7 – 13.0% for hemp; Li *et al*., 2007), allowing them to impart structural strength to the stems of many plants. When harvested, the stems are beaten and the outer layers stripped away, allowing the bast fibres to be isolated. Bast fibres from flax are used to produce linen, a fabric which is still in use and was a major part of the economy on northern Europe before mass imports of cotton from Asia (Van der Wee and Aerts, 1978).

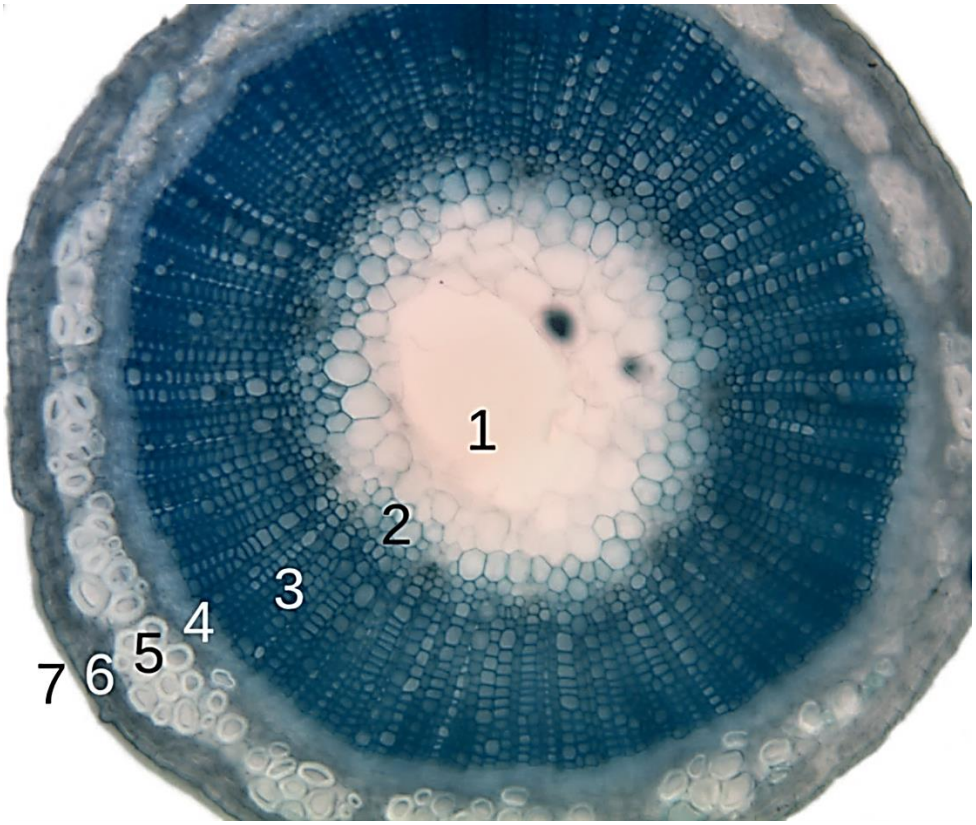

Figure 11. A light microscopy cross section of a flax stem, showing the interior structure. Image key: 1 = pith; 2 = protoxylem; 3 = xylem; 4 = phloem; 5 = bast fibres (sclerenchyma cells); 6 = cortex; 7 = epidermis. Image by McKenzie (2006) from the Wikimedia Commons.

1.4.2 Animal derived textiles and leathers

1.4.2.1 The structure and composition of wool

Textiles produced from the wool or hairs of animals are primarily made up of keratin proteins (Robbins, 2012). Proteins are long chains of amino acids linked by peptide bonds (Figure 12). There are 22 different amino acids that are incorporated into mammalian proteins, each having a different R group attached to the carbon adjacent to the nitrogen atom (Jakubke and Sewald, 2008; Popescu and Wortmann, 2010). The R groups of the different amino acids lead to different intermolecular interactions, which then dictate the three dimensional folding and shape of the protein. Slight variations in the amino acid sequence of a protein can lead to vast differences in shape and geometry. The amino acids incorporated into proteins by biological systems are exclusively L-stereoisomers (Michal and Schomburg, 1999).

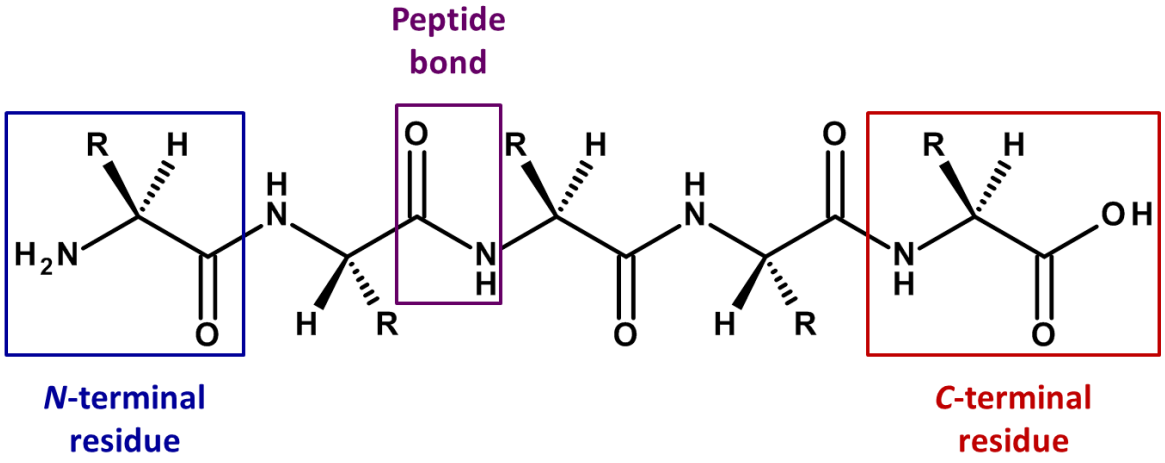

Figure 12. The basic structure of a peptide, showing a chain of five amino acids. The R groups are the location of amino acid side chains, of which there are 22 different variants in biological systems.

The structure of wool fibres is shown in Figure 13. The proteins of the cuticular layers have hydrophobic surface residues and a waxy coating which give wool and hair a water repellent quality and also enhances their resistance to microbial attack. The cells of the cortex are surrounded by the cell membrane complex which binds the cells together. Each cortical cell is made up of many macrofibrils, which in turn are composed of microfibrils. The microfibrils are bundles of protein chains that have a helical conformation (Robbins, 2012).

Wool is very similar to hair, likely having evolved from the fur of the mouflon forbearers (*Ovis orientalis orientalis*) of modern sheep during selective breeding and domestication (Hiendleder *et al*., 2002). The hair from mammals other than sheep (including humans) has very similar fibre morphology, physical properties and chemical composition to wool, with some variation in the fibre diameter and component proteins (Menkart *et al*., 1966; Hearle, 2000; Adelson *et al*., 2004).

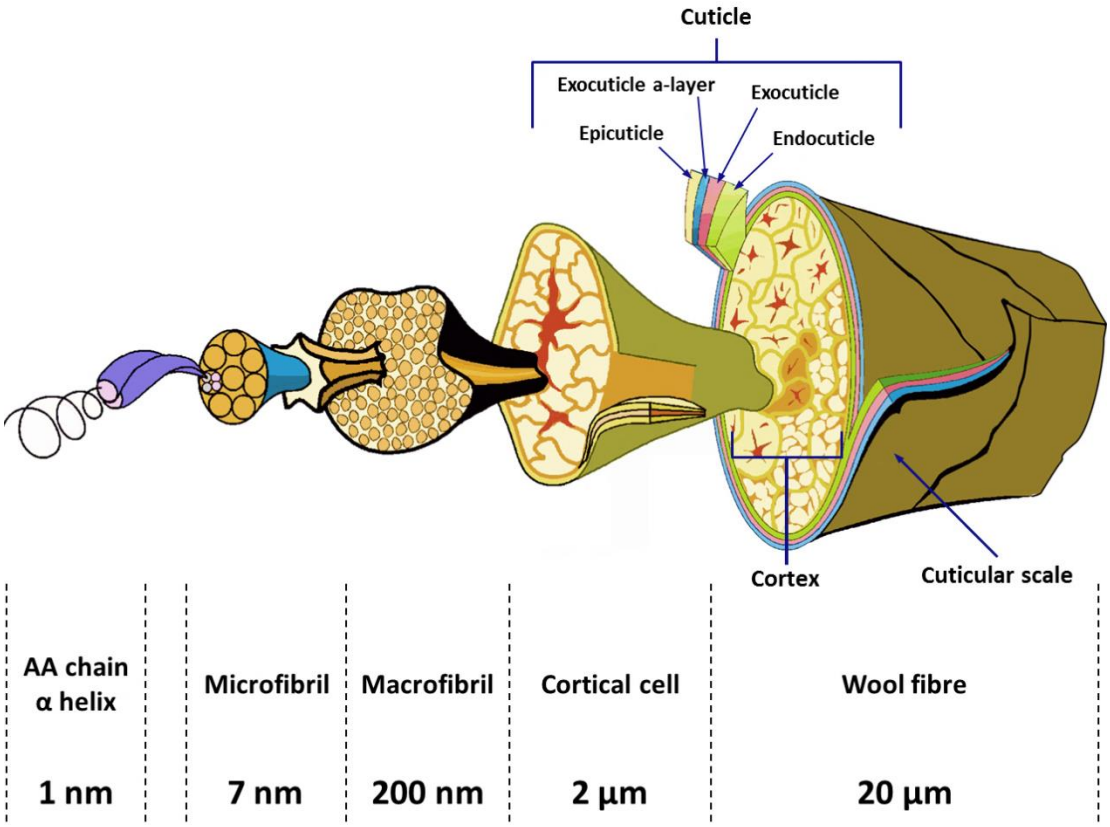

Figure 13. The structure and composition of wool fibres. Modified from Textile and Fibre Technology, CSIRO.

When sheared from the host animal, wool is typically washed and mechanically agitated to remove dirt (Australian Wool Exchange, 2010). The overlapping cuticular scales of wool act like barbs, each fibre having much more friction when rubbed in the direction of the root than towards the tip of the shaft (Gupta, 2008). This enables wool fibres to be spun into yarn of a range of thicknesses, which can then be woven or knitted to form textiles.

Felt is also produced from wool. Unlike spun woollen textiles, the raw wool is processed directly into sheets of material. As with wool spinning, felting relies on the friction of overlapping cuticles. The felting process involves the mechanical and chemical 'roughing' of the cuticular scales of wool fibres in order to create microscopic barbs that hold the material together (Schroeder *et al.,* 2004).

1.4.2.2 The structure and composition of leathers

Leather is a material that is manufactured from the skins of animals, typically ruminants such as cattle and sheep, but can also be made from the skins of fish and other animals (Bienkiewicz, 1983). The skin is a complex organ made up of many layers. For the purposes of the analysis of leather, a simplified cross section can be seen in Figure 14. The majority of skin is collagen, a protein in which three peptide chains interact by hydrogen bonding to form a triple helix (Rich and Crick, 1961). Bundles of triple helices stack to form a collagen fibril, which in turn forms layers of collagen fibres (Figure 14). Leather is produced from layers split from the dermis which have been processed to prevent the degradation of the native collagen (Haines, 2006).

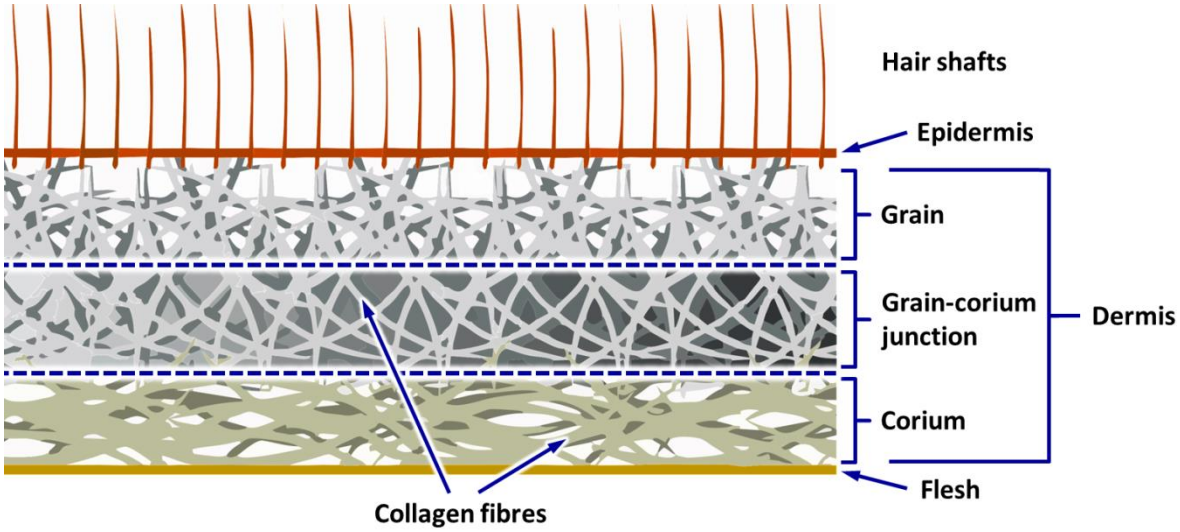

Figure 14. The composition of mammalian skin, showing the layers of collagen fibres that exist between the hair and the underlying flesh (Haines, 2006).

Once the hide is removed from the animal it must be treated to prevent putrefaction. Liming involves soaking the skins in high pH solutions of calcium hydroxide and sodium sulfide, which degrades glycosaminoglycans, triglyceride fats and hair keratins (Covington, 1997). This leads to more supple leather and causes the collagen fibres to swell, allowing subsequent treatments to penetrate into the skin. The pH is reduced before treatment with proteolytic enzymes to degrade non collagenous proteins (such as globulins and elastin) which further softens the skin, a process carried out historically by the application of dog faeces (Covington, 1997).

Once the skins have been pretreated the process of tanning begins. Until the discovery of chromium tanning processes in 1858, all leather was tanned by the application of plant extracts (Sreeram and Ramasami, 2003). These 'vegetable tanning' methods employ polyphenols that were typically extracted from the bark of trees (Covington and Covington, 2009). These polyphenols attach to the peptides of the collagen via hydrogen bonding and electrostatic interactions, which protect the protein from microbial attack (Covington, 1997). The tanned leather can then be split to give different exterior textures. Finishes such as dyes, polishes, waxes and oils are then applied depending on the intended purpose of the material.

1.4.3 Degradation of textiles and leathers

The recovery of textiles and tanned skins from all but the most recent archaeological burials is rare. Both animal and plant derived materials are readily degraded by microfauna and unfavourable soil chemistry (Janaway, 2001). Biota present in burial environments secrete enzymes that cleave the peptide and disulfide linkages of proteinaceous materials. Bacterial and fungal cellulases readily degrade the cellulose of plant based materials by converting it into glucose (Schlegel, 1986). Any material that does remain does so due to a very specific range of conditions existing within the particular burial environment (Janaway, 1983). The conditions most noted for producing such preservation are typically extremes of moisture levels and temperature, which limit the growth of microorganisms (Janaway, 1983).

Strongly acidic or basic conditions lead to the chemical hydrolysis of protein based clothing materials. Extremely high or low pH hydrolyses peptide bonds and some amino functional groups, and disrupts the disulfide bridges of cysteine that are integral to the structure of wool (Janaway, 2001). Proteins are also susceptible to degradation in weak alkaline conditions (Cook, 1988). Mildly alkaline pH can lead to deprotonation, disrupting the ion-ion interactions and hydrogen bonds which define the three dimensional structures of the proteins. By contrast, proteinaceous materials are resistant to acid induced degradation when the pH is above 2, leading to their preservation in acidic soils (Sibley and Jakes, 1984; Janaway, 2001). Conversely, plant derived materials made of primarily cellulose will rapidly degrade in acidic environments, due to the susceptibility of the β-1,4 glycosidic bonds to acid hydrolysis (Cardamone *et al*., 1991). Plant textiles with lower cellulose contents and higher amounts of incorporated hemicellulose and lignin are marginally more resistant to acidic conditions, with a proportional increase in lability in alkaline conditions (Cook, 1988; Janaway, 2001). The preservation of cellulosic materials is therefore more favoured in alkaline environments. Lower temperatures slow the chemical modification of all materials (Janaway, 2001).

1.4.4 Analysis of textiles and leathers

Methods of analysis differ depending on whether the material is derived from plant or animal tissues. In cases where the provenance of the material is not known, optical light microscopy and elemental analysis may be of use in differentiating between lignocellulose and protein based matter.

1.4.4.1 EA

EA is a relatively cheap bulk analytical technique that is widely available, making it an appropriate method for screening archaeological samples. Minimal sample preparation, automated running of large batches of samples and the ease of data analysis make the technique quick, easy and reliable. In all but the most heavily degraded materials there is sufficient difference in the elemental composition of plant and animal derived materials to differentiate between those composed of protein and those of lignocellulose composition. Based on the indications from the EA data, further analyses using more informative, polymer specific techniques can then be carried out.

1.4.4.2 Py-GC

Py-GC is widely regarded as one of the most suitable techniques for analysing plant polymers (Crighton, 1977; Hardin and Wang, 1989; Zhu *et al.*, 2004; Sobeih *et al.,* 2008). Unlike animal derived materials such as wools and skins – which are composed predominantly of proteins – plant based textiles are made up of a range of different polymers, with lignin and polysaccharides in the form of celluloses being the dominant species. These biopolymers are readily amenable to analysis by Py-GC.

Detection of resolved species resulting from the pyrolysis of a material by MS is expensive, both in terms of the substantial initial cost of the instrumentation and in the costs of consumables and maintenance. Py-GC with more affordable means of detection (such as a flame ionisation detector (FID), nitrogen-phosphorus detector (NPD) or an electron capture detector (ECD)) make the technique more appealing and accessible. Without the benefit of compound identification by MS, Py-GC must rely on the use of standards to indicate the retention times and elution order of the chromatographed pyrolysis products. Comparison of the peak patterns (or 'fingerprint') with published Py-GC-MS data can also aid assignment (Sobeih *et al.,* 2008).

The Py-GC facilities at the University of York do not currently include MS detection capability; FID is used to detect but not directly identify the species resolved by GC. Py-GC-MS facilities at Newcastle University's School of Civil Engineering and Geosciences were used to analyse selected samples of plant based materials. To aid in the interpretation of data produced using FID, the same method and a similar GC column were employed in both facilities.

1.4.4.3 RP-HPLC

Many proteomic methods are available to study the component proteins of materials such as wool and leather. These generally involve enzymatic digestion of wool proteins to smaller peptide fragments, followed by analysis by mass spectrometric techniques (Solazzo *et al*., 2014). The peptide sequences are elucidated from their mass spectral fragmentation patterns, focusing on ions relating to losses of individual amino acids (Brandt *et al*., 2014). Such techniques require specialist and expensive equipment as well as complex data analysis.

RP-HPLC analysis of the constituent amino acids can offer a cheaper and faster method of identifying changes to the compositions of certain proteins and to establishing degradation pathways (Marte, 2003; Demarchi *et al*., 2011).

Amino acid analysis techniques are much more accessible to the archaeological community than other methods of analysis. Peptide analysis may be more informative but it is more costly to run, both in terms of the high cost of the equipment and in the consumables used per sample analysed. Peptide analysis is more challenging than amino acid analysis and takes a substantial amount of time in terms of sample preparation and data analysis. The ability to analyse a greater number of samples from a wider range of burial environments may allow more relevant and accurate conclusions to be drawn about the decompositions of organic clothing materials in archaeological burial environments.

Amino acid composition data can be useful to determine the identity of unknown, amorphous materials that have no discernible weave or fibre structure (Tridico, 2009). This must, however, take account of alterations to the composition of materials by biologically mediated decay, as microorganisms can preferentially degrade certain tissues and substructures (Wilson *et al.*, 2007a, Wilson *et al.,* 2010). Hence, it is also important to gain an understanding of the degradation pathways and how they may affect the analysis. The modification or loss of the proteins that are attacked is detectable by a change in the amino acid composition of the remaining material.

Peptides and proteins are cleaved during both biological and chemical deterioration of proteinaceous material. Cleavage of the polypeptide chain produces a greater number of terminal residues, most of which are vulnerable to racemisation (Bada, 1985a). With the exception of Asp and Ser, which have been shown to racemise in chain (Stephenson and Clarke, 1989; Demarchi *et* al, 2013), the racemisation of L form amino acids to a racemic mixture of D and L occurs predominantly in amino acids bound at the N-terminal position or free amino acids (Mitterer *et al.,* 1984). Thus, increases in the D/L ratio of the amino acids that are not capable of in chain racemisation indicates that there has been some degree of cleavage of the component proteins. An increase in the D/L ratio with no observed change in the amino acid composition would

indicate a chemically induced decay of material, involving processes such as oxidation or hydrolysis.

The total amino acid content per unit of mass of a protein based material decreases as it is degraded (von Holstein *et al.*, 2014). Materials from the burial environment replace the lost structure or become incorporated into the voids created. This adds mass, leading to a measurable decrease in the amino acid content per unit of mass analysed. Samples that display a low total amino acid content are therefore likely to have undergone degradative processes.

1.4.4.4 SEM

SEM is an imaging technique that exploits the wavelength of electrons being orders of magnitude shorter than those of visible light photons. This generates an image resolution which enables structures to be viewed that are too small to been seen by optical microscopy (Rudenberg and Rudenberg, 2010). SEM studies of a range of archaeological textiles and animal hide materials are widely reported in the literature (Janaway, 1983; Wortmann and Arns, 1986; Bergfjord and Holst, 2010). Such analysis can provide information of the type of fibre used, manufacturing methods and the preservation state.

1.4.4.5 Techniques applied in this study to analyse textiles and leathers

The main focus of the textile analysis was to investigate the chemical modifications that occur to polymeric organic materials in archaeological burials. To achieve this, a combination of elemental analysis and analytical pyrolysis were applied to differentiate between materials made from animal and plant derived tissues. Materials that were identified as being of animal origins were analysed by RP-HPLC to examine the amino acid compositions. Materials that were indicated to be made from plant matter were analysed by Py-GC-FID and Py-GC-MS.

The ‘real world’, visible changes to these materials reflect the cumulative effects of chemical modifications. The interpretation of the chemical data can be further evaluated by looking for the cumulative effects on structures visible at the micrometre and nanometre scale. SEM is the best and most widely available technique to achieve this. Although the time and monetary expense per sample are high, it was hoped that the refinement offered to the interpretation of the data from chemical analytical techniques would justify the cost and that the published results will aid in the analysis of materials by others who may lack access to SEM.

1.5 Aims and objectives

The overall aim of this project was to analyse the preservation state of the biopolymers of artefacts recovered from archaeological burials; objects which represent an underexploited repository of information. Attempting to understand how wood, textiles and leather have degraded in the ground may provide information on the conditions within the burial, complementing the data provided from the chemical and micromorphological analyses performed on the grave soils and giving insights into previous soil biota and the past conditions within the burial environment. Understanding how objects have been degraded during their interment is also an important factor in understanding any changes in the archaeological data (such as tool marks, the provenance of any textiles, and the species of wood used). This additional information may be critical in ensuring that archaeological evidence is appropriately interpreted.

A better understanding of the decay of wood, textiles and leather also has the potential to aid in forensic cases, complementing information gained from the examination of the human remains. An additional benefit of better understanding the degradation processes that organic polymeric artefacts have undergone prior to excavation, is that the state of preservation of remains is often crucial for the conservation of these objects. This is particularly imperative for wood, where the application of appropriate treatments and preservatives depend on an accurate preservation assessment, enabling the better survival of these precious objects (Unger *et al.*, 2001).

In order to achieve this aim, the key objectives of this project were:

- to analyse fragments of wood (Chapter 5), textiles and leather (Chapter 6) recovered from archaeological burials using appropriate analytical chemistry and imaging techniques;
- to identify and examine the preservation state of organic materials placed in archaeological burials with human remains (Chapters 5 and 6);
- to develop an understanding of the long term decomposition trajectories of different archaeological materials buried in a limited range of burial environments, and to compare this to data obtained from relatively shorter term burial experiments (Chapter 4);
- to examine the potential information available from the chemical analysis of organic materials from archaeological inhumations and to assess its significance (Chapters 5 and 6).

CHAPTER 2

EXPERIMENTAL

2.1 General laboratory procedures

2.1.1 Reagents

Unless stated otherwise, solvents used for analytical work were HPLC or AR grade (VWR International). HPLC grade water was deionised and filtered using a Millipore water purifier fitted with a 0.2 µm filter. Carrier gas used for all gas chromatography work was analytical grade (BOC Gases). Unless stated otherwise, reagents were supplied by Sigma Aldrich or Fisher Scientific.

2.1.2 Glassware and tool cleaning

All laboratory glassware and tools used to handle samples were extensively cleaned to remove any potential contaminants, using methods developed by Green (2013). Equipment was soaked for 24 hours in an aqueous solution of DECON 90 (1%, Decon Laboratories Ltd). The cleaning solution was removed by rinsing, in sequence, with copious amounts of tap water, deionised water and laboratory grade acetone followed by drying in air for approximately 2 hours. Dried glassware and tools were baked in a Pyro-Clean oven at 450°C for 6 hours (Barnstead/ Thermolyne Pyro-Clean).

2.2 Sample collection and preparation

2.2.1 Sample collection

Sampling of archaeological graves was carried out according to the protocol of the InterArChive project. Briefly, where possible, three control samples were collected to assess: the background organic matter content of non-grave fill soil (C1 in Figure 15a) and the soil from within the grave fill above the remains (C2 and C3 in Figure 15a). Soil samples were collected from as many of the 17 standard points around the skeletal remains (Figure 15b) as possible. The vertical relationship of samples to the skeletal remains at each sampling point was designated as: x (above), y (adjacent) or z (below). Additional samples (designated with the prefix A) of any notable materials found within the grave fill were collected including, but not limited to, coffin wood, coffin fixtures and decoration, textiles and hair. Samples of stained areas within the grave fill were also sampled.

All samples were lifted using trowels and placed directly into aluminium foil that had been cleaned by baking in a Pyro-Clean oven (Barnstead/Thermolyne Pyro-Clean) at 450°C for 6 hours. The foil was sealed by wrapping, and placed into geological sampling bags (Whirl-Pak, Nasco). Packaged samples were kept cool in the field using domestic cool boxes, before being frozen at -20°C at the earliest available opportunity.

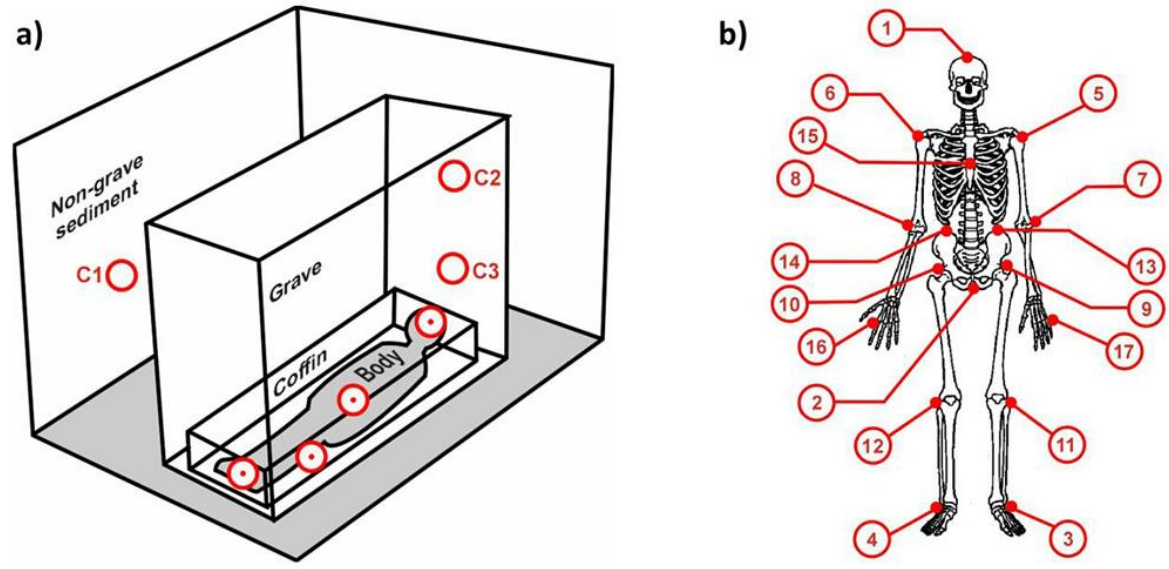

Figure 15. Soil sampling positions in relation to the skeletal remains. a) C1 is a site control taken away from the grave fill, C2 and C3 are control samples taken from the grave fill above the level of the remains; b) locations of the 17 standard soil sampling positions for organic residue analysis. Image courtesy of Matt Pickering.

2.2.2 Sample preparation

2.2.2.1 Subsampling

Frozen samples were allowed to thaw at room temperature. Once thawed, small subsamples were removed using cleaned tweezers and blades. The subsamples were frozen at -20°C until required.

2.2.2.2 Wood subsample processing

Subsamples of wood were dried and ground using a method modified from those published by van Bergen *et al*. (2000) and Vane *et al*. (2000). Frozen subsamples of wood were freeze dried in a low pressure environment of approximately 1 hPa for 2 hours using a Thermo Heto PowerDry PL3000. Dried samples were ground to a fine powder with an agate pestle and mortar before storage at -20°C in sealed glass vials (cleaned as described in Section 1.2).

2.2.2.3 Textiles and leather subsample processing

Samples of suspected textiles and animal hide were cleaned using a protocol modified from that published by Hedges *et al*. (2005). Samples were placed in pre-cleaned 7 ml glass vials and sonicated (using a Decon F5100b sonic water bath) for 30 minutes in 1:2 DCM:methanol. After 30 minutes, the solvent was poured off, replaced with 2:1 DCM:methanol and sonicated for a further 30 minutes. Each step was repeated twice. Finally, samples were sonicated in HPLC water (× 3), before being freeze dried and stored at -20°C.

2.2.2.4 Accelerated solvent extraction

Dried samples were weighed into stainless steel cells (5 ml internal volume), which had been previously cleaned by sonication of component parts in acetone followed by blank extraction (using the following method). The cells were loaded on to the sample cell carousel of a Dionex/Thermo Scientific ASE 350 accelerated solvent extractor system and the system programmed to fill the cells to 50% volume with HPLC purity grade solvent before heating the cells to 100°C for 5 minutes. A nitrogen purge (1 minute) was used. The solvent from the heated cells was transferred by an automated needle arm into pre-cleaned 90 ml ASE vials. The extraction process was carried out three times on each individual cell using 9:1 (v/v) dichloromethane/methanol. The extracted samples were allowed to dry in air before analysis. The solvated residues were taken to dryness using a rotary vacuum concentrator (Christ RVC; 25°C; 1500 rpm; 40 minutes) before being transferred to pre-weighed glass vials (cleaned as described in Section 1.2) using DCM (3 x 0.5 ml). Extracts were dried, weighed and stored at -20°C.

2.3 Elemental analysis

Elemental analysis was performed using a Flash 2000 (CHNS/O) elemental analyser (Thermo Fisher Scientific) equipped with an MAS 200 autosampler unit, using a method developed by M. Pickering (unpublished data). A sequence of standards was run with each set of samples to check and calibrate the instrument. The standards included a bypass (an aliquot of standard to check the instrument functions), a blank (an empty, folded capsule), calibration standards (two compounds to check detector responses and the accuracy of peak integration) and a drift check standard (run after the final analytical sample in the sequence). A typical elemental analysis sequence, including standards, is outlined in Table 2.

All standards and samples were weighed accurately using a 6 figure microbalance (Mettler Toledo XS3DU). The weighing utensils were cleaned between samples using DCM and lint free tissue (Kimtech Scientific). Samples were weighed into tin or silver soil capsules (depending on the type of analysis). The capsules were folded, using tweezers, and loaded into the autosampler.

Table 2. A typical sample sequence used for elemental analysis.

Sequence no.	Sample type	Composition	Notes	Approx. mass (mg)
1	Bypass	Sulfanilamide	Instrument check	2-3
2	Blank	Empty capsule	-	-
3	Standard	Sulfanilamide	Calibrant	2-3
4	Standard	Sulfanilamide	Calibrant	2-3
5	Check standard	Methionine	Calibrant accuracy	2-3
6 to *n*	Samples for analysis	Unknown	Material for analysis	0.5-20
n + 1	Drift check standard	Methionine	Calibration of drift	2-3

2.3.1 Carbon, hydrogen, nitrogen and sulfur (CHNS) analysis

Standards and samples were weighed into tin foil capsules, sealed and loaded into the autosampler. Samples were analysed as described in Section 3.

2.3.2 Total organic carbon (TOC) analysis

Standards and samples were weighed into silver foil capsules and placed in a heating block. Aqueous HCl (18.5% w/v, 2 drops) was added to each capsule to remove inorganic carbon. Samples were heated to 80°C for 6 minutes to complete the reaction and remove excess HCl.

Once cooled, the capsules were folded and loaded into the autosampler for analysis (following the procedure outlined in Section 3).

2.3.3 Oxygen analysis

Standards and samples were weighed into silver foil capsules, sealed and loaded into the autosampler. The samples were analysed as described in Section 3.

2.4 Pyrolysis – gas chromatography

2.4.1 Sequential thermal desorption/pyrolysis gas chromatography – flame ionization detection

TD/Py-GC-FID was utilised to screen all archaeological samples in order to indicate the nature of the organic material and preservation state. Further sample analyses were performed based upon the results of the TD/Py-GC-FID analysis. The following methods were adapted from those reported by Buckley *et al*. (1999), van Bergen *et al*. (2000) and Arias *et al*. (2006).

Quartz boats for analysis of samples were cleaned by heating in the pyrolyser to 1000°C for 15 s. Samples of organic materials (c. 0.5-2 mg) or soil (10-20 mg) were weighed into the pre-cleaned quartz boat and analysed using a CDS Pyroprobe 5150 coupled to a Thermo Scientific Trace GC Ultra gas chromatograph. The TD/Py-GC method was adapted from that of Buckley *et al,* (1999). Samples were subjected to thermal desorption at 290°C for 15 s then analysed by pyrolysis at 610°C for 15 s in a flow of 9 ml/minute analytical grade helium. The valve oven, transfer line and GC inlet were held at 310°C. Separation of the species liberated was achieved using a fused silica capillary column (DB-5, 60 m x 0.32 mm i.d., 0.25 mm film thickness) with the oven temperature programmed as follows: 50°C (5 minutes) to 320°C (20 minutes) at a rate of 4°C/minute. The column carrier gas used was helium at a flow rate of 2 ml/minute. Species were detected using a flame ionisation detector and assigned by comparison of retention times and peak patterns with commercially available compounds known to be produced by lignin pyrolysis (Sigma Aldrich), subsequently collected Py-GC/MS data (see Chapter 2.4.3 and Chapter 3.1.4) and published data (Ralph and Hatfield, 1991; van Bergen *et al*., 2000; del Rio *et al*., 2002; Vane *et al*., 2003; Arias *et al*., 2006).

2.4.2 Pyrolysis – gas chromatography – flame ionization detection

No thermal desorption was carried out prior to the pyrolysis. The pyrolysis temperature applied was dependant of the type of material being analysed (Table 2). All other Py-GC conditions and peak assignment methods were the same as those used for TD/Py-GC (outlined Section 4.1).

Table 3. Pyrolysis temperatures for the various materials analysed.

Material type	Pyrolysis temperature (°C)
Wood	610
Plant-based textiles	750
Soil	Dependent on the material contained within the soil matrix

2.4.3 Pyrolysis – gas chromatography – mass spectrometry

Samples of organic materials (c. 0.5-2 mg) or soil (10-20 mg) were weighed into quartz tubes and plugged with defatted glass wool. The sample tubes were placed into the filament of a CDS Pyroprobe 1000, which was inserted into a CDS1500 valved interface, connected to a Hewlett-Packard 6890 gas chromatograph. Samples were subjected to pyrolysis at 610°C for 15 s in a flow of 9 ml/minute analytical grade helium. The valved interface and GC inlet were held at 310°C. Separation of the species liberated was achieved using a fused silica capillary column (HP-5, 60 m x 0.25 mm i.d., 0.25 mm film thickness), with the oven temperature programmed as follows: 50°C (5 minutes) to 320°C (20 minutes) at a rate of 4°C/minute. The column carrier gas used was helium at a flow rate of 1 ml/minute. Species were detected using a Hewlett-Packard 5973 mass selective detector with the following set values: electron voltage 70 eV, filament current 220 µA, source temperature 230°C, quadrupole temperature 150°C, multiplier voltage 2200 V and interface temperature 320°C. The acquisition was controlled by a HP kayak xa Chemstation computer in full scan mode (50-650 amu). Total ion chromatogram (TIC) data were assigned by comparison of mass spectra with the NIST 08 database and the online NIST Mass Spectrometry Data Center Reference Database (NIST WebBook; National Institute of Standards and Technology, USA), and by comparison of retention times and peak patterns with published data (Ralph and Hatfield, 1991; van Bergen *et al*., 2000; Vane *et al*., 2003; Arias *et al*., 2006).

2.5 Amino acid analysis

2.5.1 Sample preparation

Cleaned samples were accurately weighed into pre-cleaned 2 ml vials, and 7 M HCl (200 µl per mg of sample) was added. Sample vials were purged with nitrogen, sealed with Teflon lined lids and incubated at 110°C for 18 hours to hydrolyse the peptide bonds between the constituent amino acids. The caps were re-tightened after the vials had been in the oven for 10 minutes. After the hydrolysis time had elapsed, the samples were removed from the oven dried using a rotary vacuum concentrator (Christ RVC; 25°C; 1500 rpm). Dried, hydrolysed samples were stored at -20°C.

For analysis by reversed phase HPLC, samples were solvated in rehydration buffer (200 µl per 1 mg of pre-hydrolysis sample mass) and diluted 1 in 20 with the same buffer. The rehydration buffer contained 0.01 M HCL, 1.5 mM sodium azide and 0.01 mM L-homoarginine (used as an internal standard) in HPLC water.

2.5.2 Reversed phase high performance liquid chromatography

The amino acid compositions of the hydrolysed samples were analysed by revered phase HPLC, using a modification of the method of Penkman *et al*. (2008) for unbleached samples. An Agilent 1100 series HPLC fitted with a degasser, quaternary pump, autosampler unit, temperature controlled column compartment and a fluorescence detector was used. The fluorescence detector utilised a xenon-arc flash lamp at 55 Hz, with a 280 nm cut off, 230 nm excitation wavelength and a 445 nm emission wavelength.

Samples were derivatised online by drawing 1.1 µl of derivatising agent (260 mM N-iso-L-butyryl L-cysteine, 170 mM o-phthaldialdehyde in 1 M potassium borate buffer, pH adjusted to 10.4 (±0.01) using potassium hydroxide), 2 µl of sample and a further 1.1 µl of derivatising agent into the sample injection loop, and mixing 13 times using needle aspiration. Separation was achieved using a HyperSil BDS C18 column (250 mm x 3 mm i.d., 5 µm particle size, 120 Å pore size) held isothermally at 25°C. A ternary solvent gradient was used, consisting of sodium acetate buffer (23 mM sodium acetate trihydrate, 1.5 mM sodium azide, 1.3 µM EDTA, adjusted to pH 6.00 ±0.01 with acetic acid and sodium hydroxide), methanol, and acetonitrile (see Table 4). Fluorescence data was collected for the first 95 minutes, with the remaining 20 minutes being used to equilibrate the column for the subsequent run. Blanks and standards were analysed periodically throughout the analyses.

Table 4. The tertiary solvent gradient of sodium acetate buffer, methanol and acetonitrile used in the elution of derivatised amino acids.

Run time (minutes)	Flow rate (ml/minute)	% A (sodium acetate buffer)	% B (methanol)	% C (acetonitrile)
0	0.56	95.0	5.0	0.0
31	0.56	76.6	23.0	0.4
95	0.60	46.2	48.8	5.0
95.9	0.60	0	95.0	5.0
99	0.60	0	95.0	5.0
100	0.60	95.0	5.0	0.0
115	0.56	95.0	5.0	0.0

Asparagine and glutamine undergo deamidation during the hydrolysis procedure, forming aspartic acid and glutamic acid respectively. Asparagine and aspartic acid are reported collectively as Asx, glutamine and glutamic acid are reported as Glx. The amino acids detected and their three letter abbreviation codes are shown are shown (in order of elution) in Table 5.

Table 5. The amino acids detected using the RP-HPLC method and their abbreviation codes. The amino acid retention time increases down the table, with the first eluting at the top and last eluting at the bottom.

Amino acid	Amino acid abbreviation
L-asparagine and L-aspartic acid	L Asx
D-asparagine and D-aspartic acid	D Asx
L-glutamine and L-glutamic acid	L Glx
D-glutamine and D-glutamic acid	D Glx
L-serine	L Ser
D-serine	D Ser
L-threonine	L Thr
Glycine	Gly
L-arginine	L Arg
D-arginine	D Arg
L-alanine	L Ala
L-homoarginine	L hArg
D-alanine	D Ala
L-tyrosine	L Tyr
L-valine	L Val
L-methionine	L Met
D-methionine	D Met
D-valine	D Val
L-phenylalanine	L Phe
L-isoleucine	L Ile
D-phenylalanine	D Phe
L-leucine	L Leu
D-alloisoleucine	D Alle
D-leucine	D Leu

2.6 Scanning electron microscopy

Subsamples for SEM were cleaned by washing with three portions of deionised water in 7 ml glass vials. Samples were immersed in water, agitated by gentle shaking to remove surface debris and the water was decanted. This procedure was repeated two more times with fresh portions of deionised water. Textile samples were placed in watch glasses, covered with loose fitting lids and allowed to air dry for 24 hours at room temperature and pressure. Wood samples were prepared using a general method under the supervision of M. Stark (personal communication, September 2015). Samples were immersed in a fixative solution of 4% paraformaldehyde and 2.5% glutaraldehyde in 100 mM phosphate buffer at pH 7 for 3 hours, after which the liquid was decanted and replaced with fresh 100 mM phosphate buffer and left to stand for 30 minutes. The buffer was decanted and replaced a total of two times. The samples were dehydrated using solutions of increasing concentration of acetone: 25%, 50%, 70%, 90% and 100% (v/v in deionised water). Thus, samples were covered in each acetone solution for and left for 15 minutes. The acetone solution was decanted and the next, more concentrated, acetone solution was added. The final 100% acetone soak was repeated a total of 3 times. The dehydrated samples were dried using an E3000 carbon dioxide critical point dryer (Quorum Technologies). The acetone immersed samples were held at 10°C under 8 MPa of CO_2 for 1 hour. The samples were then heated to 32°C before the CO_2 was vented.

Dried samples were cut with razor blades and mounted to aluminium stubs using epoxy resin. Surface imaging samples were mounted horizontally and adhered directly to the stub. Cross sectional samples were stuck to the vertical face of copper tape that was bent at a 90 degree angle into an L shape, the bottom of the tape was attached to the stub. Samples were earthed using Acheson Silver DAG glue (Agar Scientific). A 7 nm layer of gold/palladium was applied to the mounted samples using a Quorum SC7640 sputter coater (Quorum Technologies). Images were obtained under vacuum using a JSM-6490LV scanning electron microscope (JEOL Incorporated).

CHAPTER 3

METHOD DEVELOPMENT

3.1 Pyrolysis – gas chromatography

3.1.1 Selection of pyrolysis temperatures for the analysis of wood and plant based textiles

Pyrolysis temperatures of 450°C to 800°C are widely reported in the analysis of woods (Shedrinsky *et al*., 1989; Alves *et al*., 2006; Łucejko *et al*., 2009). Temperatures below 500°C have been reported to give poor yields of guaiacyl type subunits, which would lead to an overestimation the abundance of syringyl subunits (Shedrinsky *et al*., 1989). Temperatures above 750°C give the best yields of cellulose whereas temperatures in excess of 800°C result in excessive fragmentation of the lignin subunits, reducing their diagnostic value and limiting the information available (Shedrinsky *et al*., 1989). A balance between maximising pyrolytic yields of holocellulose and lignin whilst minimising further thermal degradation of compounds was therefore sought.

Analyses of buried, degraded and archaeological lignocellulose materials using temperatures of 610°C were reported to give representative yields of all wood biopolymers whilst limiting the thermal breakdown on the released subunits (Saiz-Jimenez *et al*., 1987; van Bergen *et al*., 2000; del Rio *et al*., 2001). As a result, analytical pyrolysis of woods in this study was performed at 610°C.

The predominance of cellulose in textiles made from plant fibres requires a higher pyrolysis temperature than wood to provide an accurate assessment of the cellulose content. The pyrolysis of these materials is commonly carried out at 750°C (Hardin, 1996; Morrison and Archibald, 1998; Wampler, 2006). A pyrolysis temperature of 750°C was used for the analysis of all plant derived textiles.

3.1.2 Removal of non-polymeric components from wood prior to Py-GC analysis

The non polymeric, extractable compounds commonly found in fresh woods include lipids (fats, fatty acids and alcohols, waxes), terpenoids, flavonoids as well as the phenolic precursors of lignin polymers (Fiebach and Grimm, 2000). These non-polymeric compounds account for approximately 1% of the mass of fresh wood (Todaro *et al*., 2013; Kebbi-Benkeder *et al*., 2015). The porous nature of wood makes it highly like that a significant amount of non-polymeric residues from the burial environment will have been incorporated into archaeological wood samples collected during the InterArChive project. The polymer breakdown and subsequent thermal transformations that occur during analytical pyrolysis lead to highly complex pyrograms with large numbers of peaks (Moldoveanu, 1998; Wampler, 2006). The presence of non-polymeric components further convolute the data, with the possibility of coelution of peaks that are key to the analysis of preservation state of the wood polymers. To avoid such issues, non-polymeric components are removed from samples prior to analysis (Wampler, 2006).

Thermal desorption (TD) is used to liberate volatile or loosely bound compounds, allowing for their analysis by gas chromatography. In the analysis of wood samples, TD can be used to remove volatile, non-polymeric compounds from the material prior to analysis of the structural polymers by pyrolysis (Pe´rez-Coello *et al*., 1997). Removal of the volatile compounds is necessary as they can compromise data analysis due to coelution and increased complexity in the pyrograms. This is of particular concern in the archaeological materials where a wide range of unknown compounds may have been transferred into the wood from the burial environment.

A substantial proportion of the wood fragments recovered as part of the InterArChive project's sampling were very small (less than one gram). Testing with solvent extraction techniques demonstrated that such small samples often yielded insufficient material for analysis by analytical pyrolysis. The suitability of sequential thermal desorption – pyrolysis – gas chromatography (TD/Py-GC) techniques in the analysis of milligram scale archaeological lignocellulose samples using TD at 290°C has been demonstrated in previous studies (Wilson *et al*., 1993; Buckley *et al*., 1999; Colombini *et al*., 2003; Łucejko *et al*., 2009; see Chapter 1.3.5.6). Compared with other methods (such as solvent extraction) TD is rapid (taking 15 to 30 seconds) and requires no additional sample pretreatments that are costly in terms of time and consumables. Temperatures greater than 350°C are typically avoided to prevent pyrolytic degradation of the sample; temperatures below this will desorb any volatiles or loosely bound residues – such as degraded polymer fragments which would erroneously contribute to quantitation of the remaining intact polymer – that are not fully incorporated into the polymer. (Saiz-Jimenez, 1994; Hays *et al*., 2003; Yokoi *et al*., 2003; High, 2014). As a result of this, it was decided that all archaeological wood

samples would need to be pre-treated by thermal desorption to remove the extractable components.

One of the approaches employed in the InterArChive project involved the analysis of organic residues contained within burial soils. This is achieved by accelerated solvent extraction, followed by derivatisation and analysis of the extracts by GC-MS (Pickering *et al*., unpublished). In certain cases, the non-polymeric components of the woods needed to be analysed by other InterArChive project team members to identify compounds that may have leached into the coffin woods from the burial matrices. In addition to the analysis of the archaeological materials, the InterArChive project conducted a series of burial experiments that used piglets as human proxies. The majority of these burials featured a wooden box, which enclosed the piglet and replicated the conditions experienced in coffined human burials. The analysis of the wood from these coffins was one of the objectives of this thesis (see Chapter 4). Concomitant with these analyses, other members of the InterArChive team analysed the solvent extractable components of the materials sampled from the experimental burials, among which was the wood from the coffins. The removal of modern wood treatments and adhesives from the experimental piglet burial coffins was also of concern, as was the removal of conservation treatments applied to wood samples from the Hanson Logboat (see Chapter 5.8). These requirements meant that solvent extraction by ASE had to be carried out on the piglet coffins and wood from the Hanson Logboat.

Given that the archaeological woods had to be cleaned using TD and the piglet coffins had to be solvent extracted with ASE, the question was posed: will treating some woods with TD and others with ASE lead to sufficient differences in the analytical pyrolysis data to prevent comparison of the two datasets? As a result of this, the analytical pyrolysis data following pre-treatment with TD and ASE was evaluated.

Samples of modern pine and modern oak were pyrolysed after pre-treatment with TD and ASE, according to the procedures outline in Chapter 2.4. Pyrograms and lignin subunit compositional data for the analyses of modern pine are shown in Figure 16 and Figure 17 respectively. The data for modern oak are not shown but display similar trends to those observed in the modern pine.

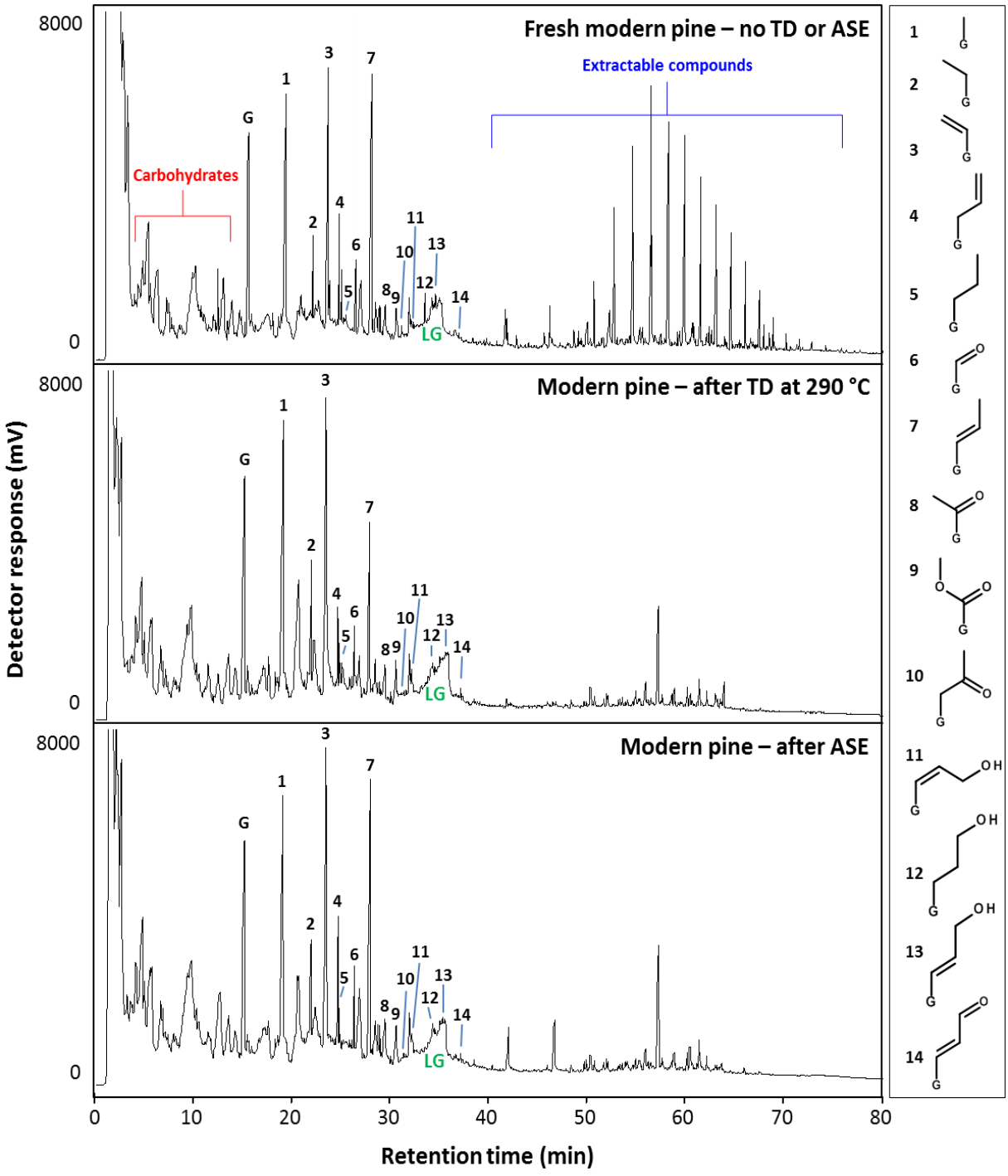

Figure 16. Partial Py-GC-FID pyrograms of modern pine, showing the differences with no sample pre-treatment, pre-treatment with TD at 290°C and pre-treatment with ASE. LG = levoglucosan, a pyrolysis product of cellulose.

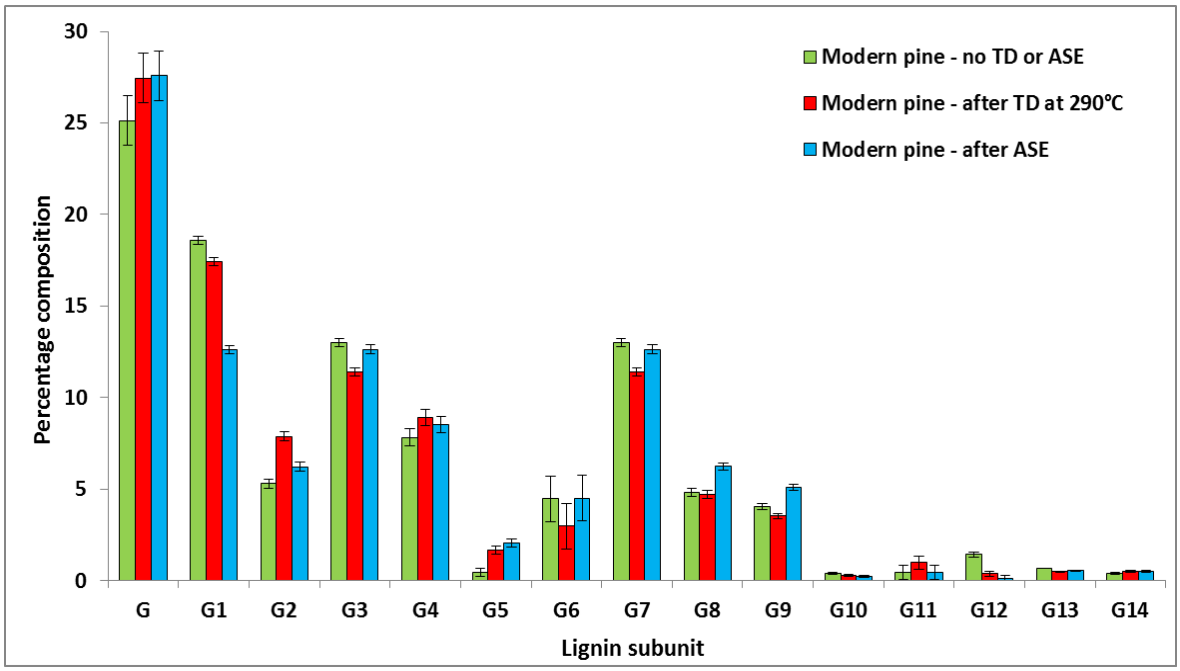

Figure 17. Lignin subunit percentage compositions for modern pine pyrolysed after no pre-treatment, after TD at 290°C and after ASE. The values were calculated from the pyrograms shown in Figure 16, by normalising the peak areas of individual lignin subunits to the sum of the peak areas for all G lignin derived peaks. Error bars represent +/- 1 standard deviation from n=2 replicate analyses.

Both TD and ASE remove the majority of the non-polymeric compounds from the modern pine, with ASE removing slightly fewer extractable compounds than TD. The pyrograms obtained following TD at 290°C and ASE show differences in the relative amounts of some of the lignin peaks compared with the material analysed without pre-treatment. For modern pine that had been subjected to thermal desorption, the relative abundances of peaks corresponding to guaiacyl compounds 1 (4-methylguaiacol), 4 (4-vinylguaiacol), 7 (4-propenylguaiacol) and 12 (guaiacylpropanol) are statistically lower than in the pyrogram of pine that had not been thermally desorbed (Student's t tests; all p values <0.05). ASE extraction of the modern pine also reduced the relative amounts of 1 (4-methylguaiacol) and 12 (guaiacylpropanol) that were recovered. Although low temperature pyrolysis of lignocellulose materials has been reported to occur at temperatures as low as 350°C (Arias *et al*., 2006), the lower yields of 1 (4-methylguaiacol) and 12 (guaiacylpropanol) after ASE extraction suggests that these components are lignin precursors, not structural polymers. Thus they are not incorporated into the polymer and are removed by both solvent extraction and TD at 290°C. The lower abundances of 4 (4-vinylguaiacol) and 7 (4-propenylguaiacol) on the pyrogram following TD are likely due to the losses of non-structural lignin residues that are loosely bound to the lignin polymer being removed by the TD and not the ASE (Arias *et al*., 2006). The increases of the abundances of some guaiacyl compounds in the ASE and TD treated woods are likely due to the large decreases in G1 altering the overall percentage compositions of other compounds.

The use of TD at 290°C and ASE to remove volatile compounds prior to pyrolysis seems to have little detrimental effect on the structural wood polymers. Some differences are apparent in the

compositions of the lignin pyrolysis products when the two methods of pre-treatment are employed, although the differences are small in comparison to the values of the relative abundances. As a result of these analyses it was decided that using ASE to remove residues from the wood of the piglet coffins and TD in the archaeological materials may have some impact on the comparison between the two data sets; although the differences are small, comparisons using multivariate statistical methods should be interpreted with caution.

3.1.3 Analysis of pyrolysis – gas chromatography data

Since the advent of FID in the 1950s it has become the most widely used detection method for compounds resolved by GC (Crockford *et al*., 2006). FID is cheap by comparison with other detection methods and offers an excellent lower limit of detection, good reproducibility and detects all organic compounds in a predictable manner (Pacchiarotta *et al*., 2010). The universal detection of organic molecules makes FID an excellent technique for quantitative analysis of complex mixtures. The primary limitation of FID is that it offers no structural information on the analytes, with peak identification relying on the comparison of retention times and peak profiles with those of standards and published data (Harris, 1999).

MS detection allows for the identification of analytes based on their masses and the masses of fragment ions as a result of ionisation (Higson, 2004). Hence, MS detection is invaluable in determination of the molecular structures of unknown components (Higson, 2004). The benefits of compound identification are offset by the lower limit of detection, lower reproducibility and differences in ionisation efficiency (Pacchiarotta *et al*., 2010). Resolved compounds that are not readily ionised are detected in lower abundance or not detected at all, leading to inaccurate quantitation. MS detectors are also expensive, with basic mass selective detector (MSD) units typically costing more than the accompanying GC.

The primary Py-GC system used during this project was fitted with an FID. To aid with the identification of the peaks in the FID generated pyrograms, a sample of wood from each archaeological site, as well as a series of modern gymnosperm and angiosperm woods were analysed by Py-GC-MS using the same instrument settings and column type (Figure 18a). The individual peaks of the Py-GC-MS total ion chromatograms (TICs) were identified by comparison with data from the NIST 08 mass spectral library (NIST, 2008) and the online NIST Mass Spectrometry Data Center Reference Database (NIST WebBook). Selected mass spectra of peaks from the TIC of modern oak are shown in Figure 19.

Each day that Py-GC-FID data was acquired, 5 µl of a solution of hexane containing phenol (P), guaiacol (G), 4-methylguaiacol (G1), 4-ethylguaiacol (G2), 4-vinylguaiacol (G3), syringol (S), *cis*-4-propenylguaiacol (G6), 4-methylsyringol (S1) and *trans*-4-propenylguaiacol (G7) was pyrolysed. All of these compounds are known to be produced by the pyrolysis of lignin (Vane *et al*., 2003). This standard mixture (Figure 18b) allowed for the retention times of seven lignin peaks to be accurately identified. The remaining peaks in the FID pyrograms were identified by comparison of the retention times and peak order with those in the MS data.

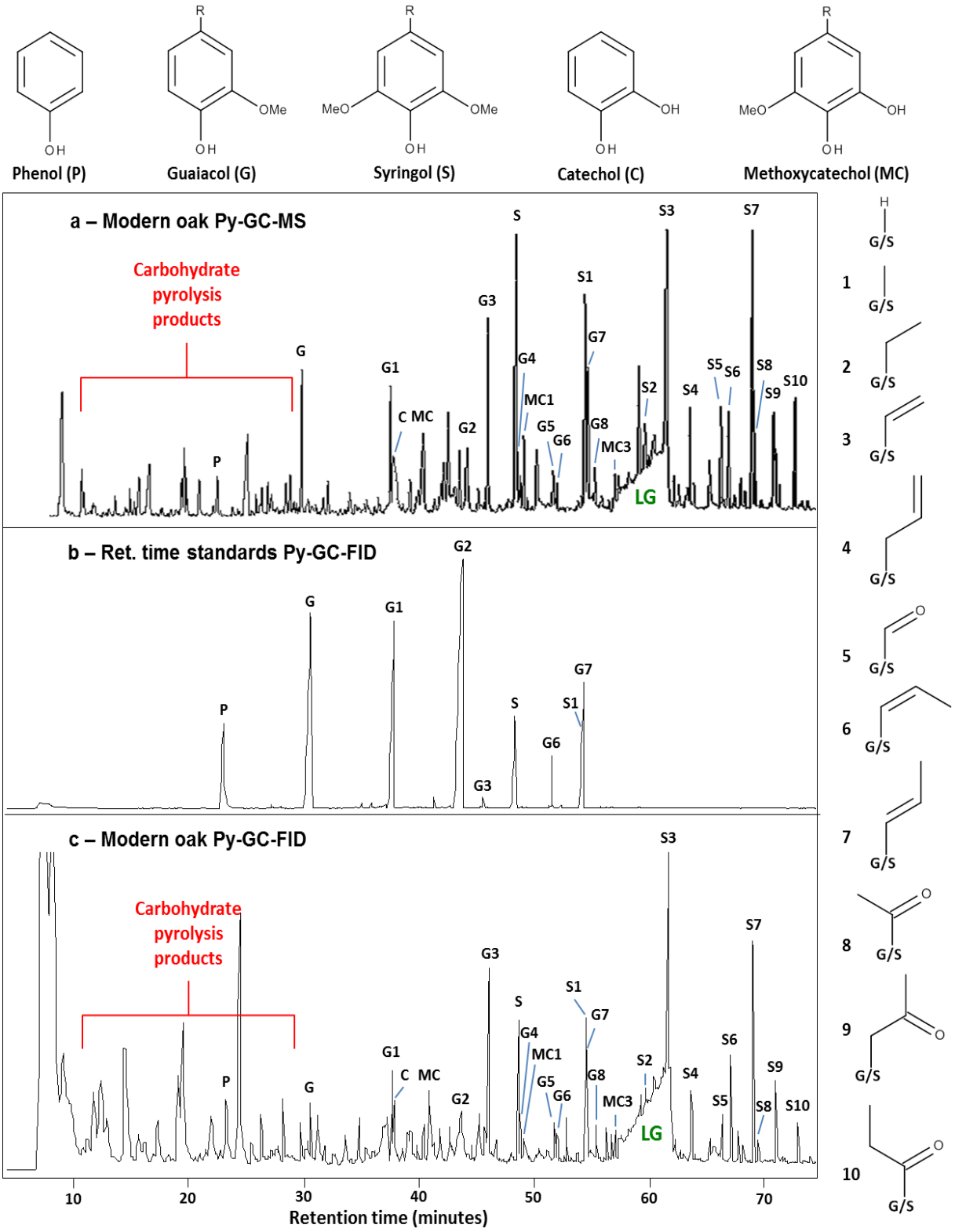

Figure 18. Partial pyrograms of a – modern oak acquired using Py-GC-MS, b – the pyrolysis standard mixture acquired using Py-GC-FID and c – modern oak acquired using Py-GC-FID.

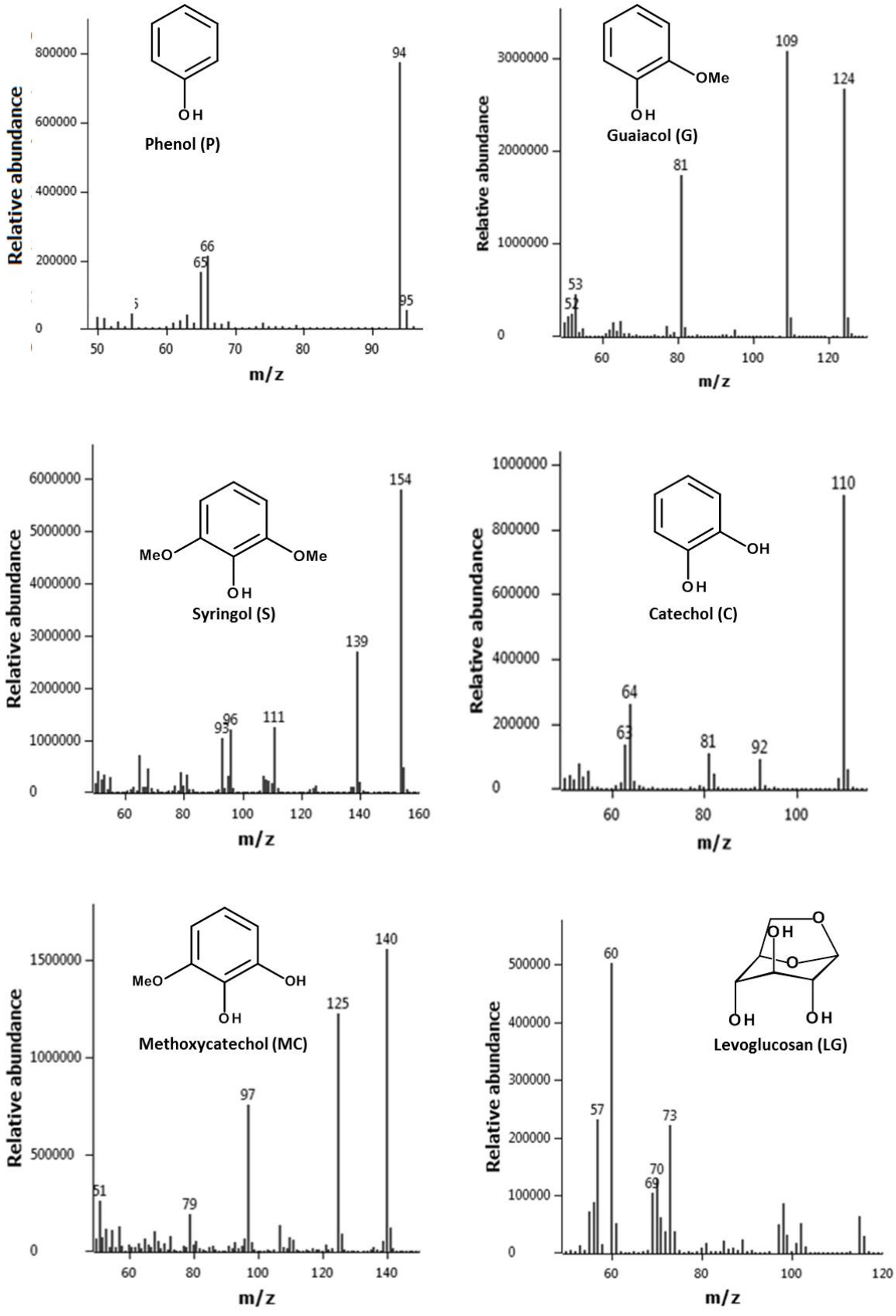

Figure 19. Selected mass spectra from the total ion chromatogram of pyrolysed modern oak.

3.1.4 Modern analogues for archaeological woods

The identification of woods is typically performed by preparation of thin sections and examining the microfeatures using transmission light microscopy. There is often difficulty in determining the exact species, genus and even family of tree a wood has come from using microscopic techniques, as cellular structure varies in response to a range of environmental stresses (Blanchette *et al*., 1994; Yeh *et al*., 2006; Foston *et al*., 2011; Cartwright, 2015). Processes that affect wood in archaeological burial environments include shrinkage, swelling and collapse of the cellular structure due to decay or compression, further complicating the identification of wood (Florian, 1990; Schoch, 2011). As a result of this, the identifications provided by such analyses can be unreliable. Preparation of the samples is also very difficult, especially for archaeological woods which are often heavily degraded and too fragile to produce the thin sections required (Cartwright, 2015; Braovac *et al*., 2016).

Small variations in S:G ratios have been found between different *Eucalyptus globulus* trees and in wood taken from different sites within the same tree. Such differences are, however, very limited compared with the changes in S:G ratios that occur during wood decay (Rodrigues *et al*., 1999; van Bergen *et al*., 2000). The differences in the relative abundances of long chain, short chain, carbonyl, demethylated and demethoxylated subunits in lignin between wood from trees of the same genus (gymnosperm or angiosperm) is very small compared to the changes that are the result of degradation within burial environments (Braovac *et al*., 2016). The lack of chemical variation is most likely due to the different species of tree of the same genus having evolved from a common ancestor, resulting in them possessing very similar lignin biosynthetic pathways (Higuchi, 1990; Bojeran *et al*., 2003).

Braovac *et al*. (2016) found that comparison of pyrolysis data from unidentified archaeological woods with a range of modern angiosperm woods provided a sufficient level of certainty to draw conclusions regarding the degradation of the wood. The analysis of lignin derived pyrolysis products, individually or as groups, indicated that the variations caused by degradation far outweighed species variation.

The chemical variation within the holocellulose content of woods is, like that of lignin, very limited. There is, however, clear variation in the holocellulose to lignin ratio (H:L; Fengel and Wegener, 1983; Braovac *et al*., 2016). The percentage composition of lignin and holocellulose in woods has been shown to vary between trees of the same type grown in different locations (Campbell *et al*., 2007). Variation in the biopolymer percentages also exists across the diameter of a tree trunk: in the heartwood and sapwood, in normal, tension and compression wood and at different heights within the same tree (Yeh *et al*., 2006; Campbell *et al*., 2007; Foston *et al*., 2011). These variations in composition indicate that care must be taken when comparing the

holocellulose and lignin contents of wood. As a result of this, only qualitative assessment of the holocellulose fraction in the archaeological wood samples was carried out, with comment only being made when the peaks in the carbohydrate region (due to cellulose and hemicellulose) and the levoglucosan peak (from cellulose) were significantly different in intensity to those in the modern comparator of the same genus.

To summarise, modern angiosperm or gymnosperm wood of any species will provide a sufficient comparison for archaeological wood of the same type. The chemical lignin variation between species is negligible compared with the changes brought about by degradation processes, allowing semiquantitative analysis to be carried out. The variation in cellulose and hemicellulose contents of woods are such that only large changes in the relative compositions of holocellulose and lignin should be interpreted as being due to degradation processes. As a result of this, only large differences between the holocellulose contents of archaeological woods and their the modern analogues were interpreted as being due to decay.

3.1.5 Definition of error in TD/Py-GC analysis of archaeological woods

The small size of the wood fragments recovered from the majority of archaeological burials, combined with limitations of time and resources meant that replicate analyses were not possible for the majority of archaeological wood samples analysed by Py-GC. Replicate analyses of each sample of archaeological material would be the best method of investigation, as it would have enabled an understanding of the accuracy of the data collected from each sample and for more robust statistical comparisons to be employed. Lack of repeat analyses mean that no exact confidence interval can be defined for the analysis of each sample and no exact error limits can be calculated. To mitigate against this, samples of modern and archaeological gymnosperm wood (Figure 20), as well as modern and archaeological angiosperm wood (Figure 21) were subjected to repeat analysis by TD/Py-GC-FID (using the methods outline in Chapter 2.4.1), in order to examine the potential variation and to establish a set of standard errors that could be applied to the data from other samples of archaeological wood for which replicate analyses were not possible.

The standard deviations for respective subunit composition means are similar in the modern and archaeological material for both gymnosperm and angiosperm woods. This suggests that the variation in TD/Py-GC analyses of the other archaeological woods (Chapter 5) may also be similar. Clear differences are apparent between the compositions of the modern and archaeological materials for both wood types, all the differences being statistically significant to a confidence level of at least 95% (Student's t tests; all p values <0.05). The +/- 1 standard deviation error bars are very small by comparison with the differences seen between both modern and the archaeological woods. Although the error bars applied based on these repeat analyses will likely not reflect the exact error that would have been observed if repeat analyses were performed for each individual archaeological wood sample, the large difference between modern and archaeological materials likely mean that errors calculated for these materials will be sufficient to characterise the within-sample variation for the majority of archaeological woods where such large differences are apparent. This approach is far from ideal. It will, however, account for any variation that occurs due to systematic errors inherent to the instrumentation and methods used. Results will therefore be interpreted with caution, especially in cases where there is little difference between the archaeological material and the modern comparator. Any hypotheses made based on the analytical pyrolysis data will also be tested using SEM.

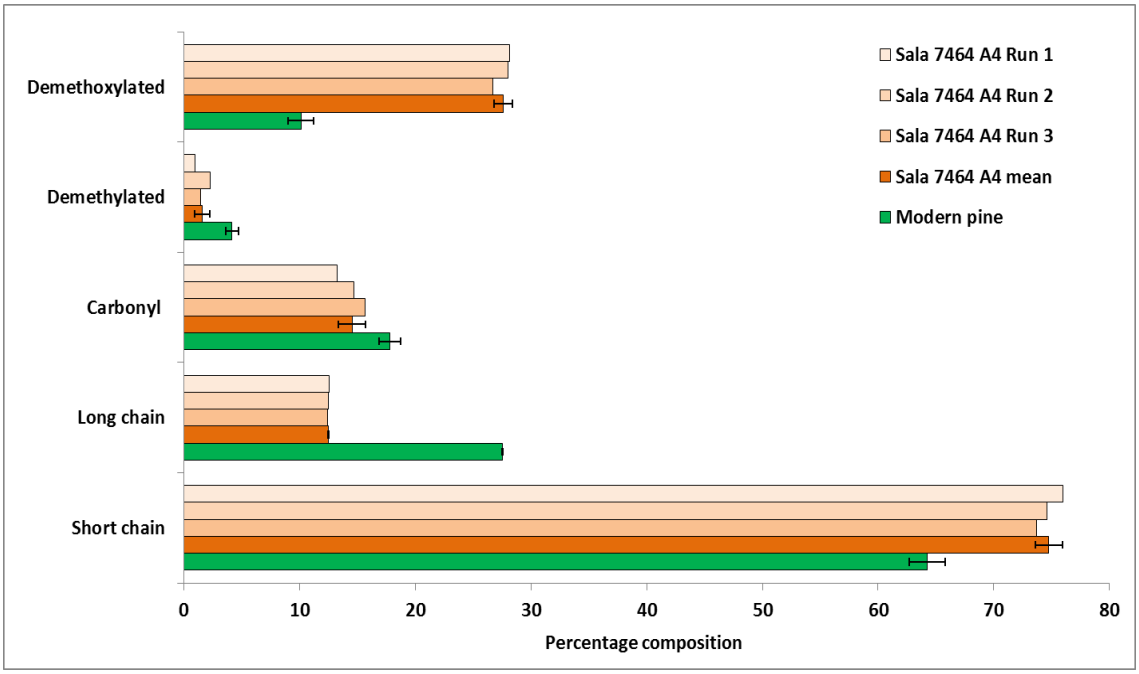

Figure 20. Percentage compositions of demethoxylated, demethylated, carbonyl, long chain and short chain compounds detected in three replicate Py-GC-FID analyses of an archaeological gymnosperm wood from grave 7464 in Sala, Sweden (see chapter 5.6) and modern pine. Lignin pyrolysate compound classifications are given in Table 6. Values are calculated as a percentage of the total area of lignin derived peaks in the pyrograms. Error bars represent +/- standard deviation.

Table 6. Classifications of the detected compounds resulting from the pyrolysis of gymnosperm woods.

Compound	**Classification**
Toluene (T)	Demethoxylated/short
Phenol (P)	Demethoxylated/short
2-Methylphenol	Demethoxylated/short
3-Methylphenol	Demethoxylated/short
Guaiacol (G)	Short
4-Methylguaiacol (G1)	Short
Catechol (C)	Demethylated/short
4-Ethylguaiacol (G2)	Short
4-Vinylguaiacol (G3)	Short
4-Allylguaiacol (G4)	Long
4-Propylguaiacol (G5)	Long
4-Formylguaiacol (G6)	Carbonyl
trans-Isoeugenol (G7)	Long
4-Acetylguaiacol (G8)	Carbonyl
Vanillic acid-methyl ester (G9)	Ester/long
Guaiacylacetone (G10)	Carbonyl/long
cis-Coniferyl alcohol (G11)	Long
Guaiacylpropanol (G12)	Long
trans-Coniferyl alcohol (G13)	Long
Coniferyl aldehyde (G14)	Carbonyl/long

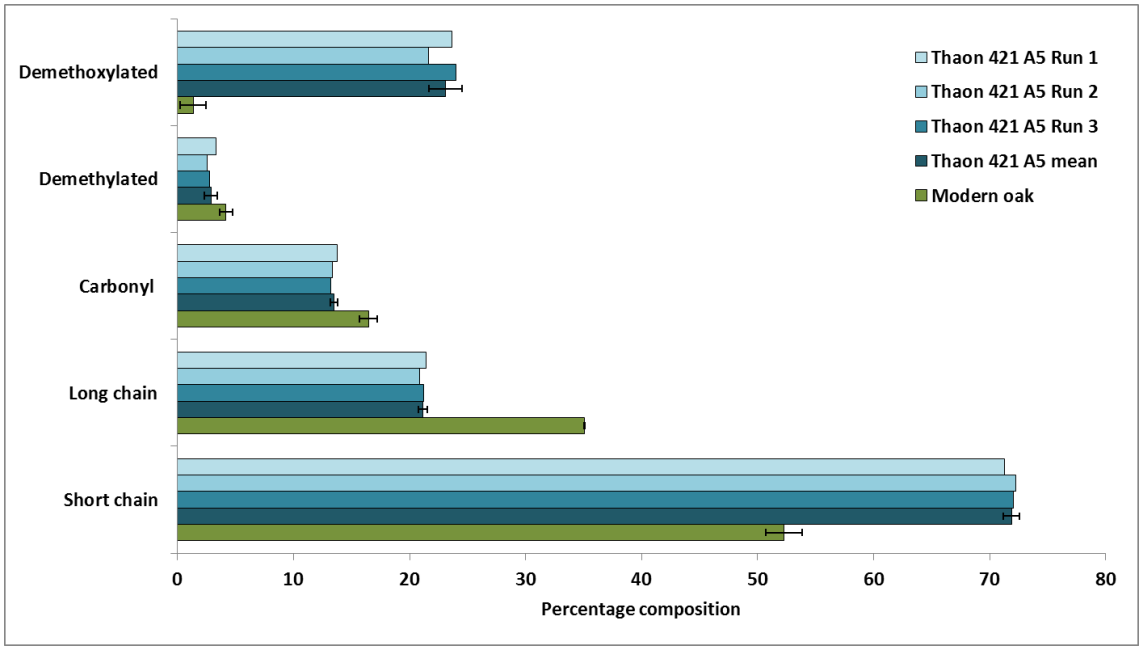

Figure 21. Percentage compositions of demethoxylated, demethylated, carbonyl, long chain and short chain compounds detected in three replicate Py-GC-FID analyses of an archaeological angiosperm wood from grave 421 in Thaon, France (see chapter 5.7) and modern oak. Lignin pyrolysate compound classifications are given in Table 7. Values are calculated as a percentage of the total area of lignin derived peaks in the pyrograms. Error bars represent +/- standard deviation.

Table 7. Classifications of the detected compounds resulting from the pyrolysis of angiosperm woods.

Compound	**Classification**
Toluene (T)	Short/Demethoxylated
Phenol (P)	Short/Demethoxylated
2-Methylphenol	Short/Demethoxylated
3-Methylphenol	Short/Demethoxylated
Guaiacol (G)	Short
(G1) 4-Methylguaiacol	Short
(MC) Methoxycatechol	Demethylated
(G2) 4-Ethylguaiacol	Short
(G3) 4-Vinylguaiacol	Short
(S) Syringol	Short
(G4) 4-Allylguaiacol	Long
(MC1) 4-Methylmethoxycatechol	Demethylated
(G5) 4-Formylguaiacol	Carbonyl
(G6) *cis*-Isoeugenol	Long
(S1) 4-Methylsyringol	Short
(G7) *trans*-Isoeugenol	Long
(G8) Acetoguaiacone	Carbonyl
(MC3) 4-Vinylmethoxycatechol	Demethylated
(S2) 4-Ethylsyringol	Short
(S3) 4-Vinylsyringol	Short
(S4) 4-Allylsyringol	Long
(S5) Syringaldehyde	Carbonyl
(S6) *cis*-4-Propenylsyringol	Long
(S7) *trans*-4-Propenylsyringol	Long
(S8) Acetosyringone	Carbonyl
(S9) Syringylacetone	Long/carbonyl
(S10) Propiosyringone	Long/carbonyl

3.2 Amino acid analysis

3.2.1 Wool protein hydrolysis: evaluation of the time required

Whilst Py-GC and EA can give indications as to whether an unidentified material is of plant or animal origin, as well as limited data on degradation relative to modern materials, a method to accurately quantify the amino acid content of proteinaceous materials was required. The North East Amino Acid Racemisation Laboratory (NEaar) based in York has developed a method to analyse the amino acid content of hydrolysed protein samples (Penkman *et al.,* 2008). The method allows both the amino acid composition and the relative ratios of the D and L forms of most of the amino acids to be determined. Racemisation of the biological configuration (L form) amino acids to produce a racemic mixture of D and L amino acids occurs naturally over time. For the majority of the constituent amino acids in proteins, racemisation can only occur when the residue is in the C or N terminal position, with N- terminal residues racemising faster than their C-terminal counterparts (Bada, 1985b). The racemisation half lives of many amino acids are too long to be of use for samples from the most recent archaeological time periods. For example, the racemisation of Ile in bone collagen is approximately 100 ka at 20°C (Bada *et al*., 1973). Asp, Asn and Ser have been shown to undergo in-chain racemisation (Demarchi *et al*., 2013) at rates that would be appropriate for dating archaeological materials. Comparison of the D/L values of amino acids liberated by hydrolysis of modern materials with those obtained from analogous archaeological materials allows the extent of peptide bond hydrolysis to be assessed. Degradation by hydrolysis of peptide bonds would lead to a greater number of N-terminal residues being generated, increasing the number of amino acids able to undergo racemisation and generating higher D/L ratios than those of modern standards.

The method outlined by Penkman *et al.* (2008), involving hydrolysis for 24 hours at 110°C in 7M HCl, was established for materials with significantly lower protein contents than textiles, hair and hide products. In theory, longer hydrolysis times break more peptide bonds, releasing more of the amino acids that comprise the material (Fountoulakis and Lahm, 1998). In particular, peptide linkages between the hydrophobic residue Val and Ile are difficult to cleave, giving only 50 – 70% recovery when a 24 hour hydrolysis at 110°C is employed (Hirs *et al*., 1954). Amino acids racemise rapidly during hydrolysis at 110°C (Kaiser and Benner, 2005) and acid labile amino acids such as Ser, Thr and Tyr are partially destroyed, incurring increasing losses as the hydrolysis time is extended (Hunt, 1985; Fountoulakis and Lahm, 1998; Darragh and Moughan, 2005). The ideal hydrolysis time for the archaeological materials examined in this study would maximise amino acid yield whilst minimising racemisation and destruction of amino acids.

An investigation into a suitable hydrolysis time (T_H) for protein based materials was carried out using modern sheep wool from a single breed (Herdwick Tops) and a sample of archaeological wool that had been buried for approximately one hundred years in a First World War mass grave at Fromelles, Northern France (Chapter 6.2). Samples were incubated in an oven maintained at 110°C for 6, 18, 24 and 48 hours. The percentage compositions of the amino acids liberated during the hydrolysis treatments of modern wool and the archaeological material are broadly similar, though some small differences in the relative abundances of particular amino acids are apparent and the error bars are greater for the archaeological material (Figure 22 and Figure 23).

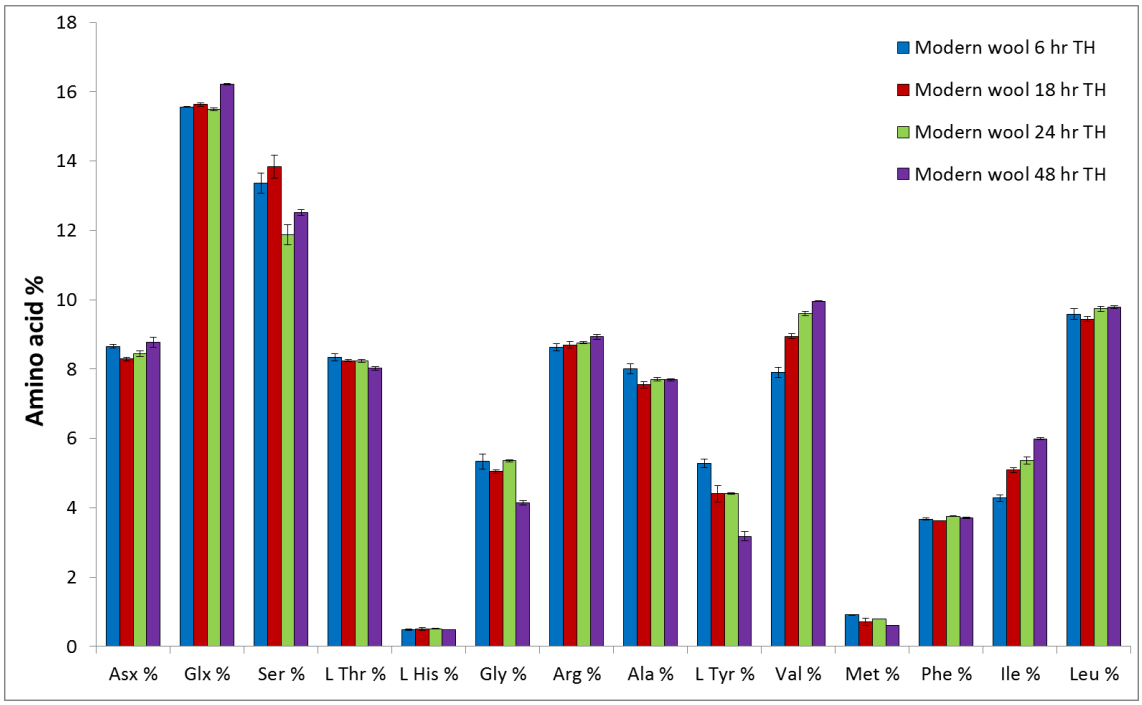

Figure 22. Percentage amino acid compositions of modern Herdwick Tops sheep's wool hydrolysed at 6, 18, 24 and 48 hours. The data are expressed as percentages of the sum of all amino acid peak areas. Error bars represent +/- 1 standard deviation; n=3.

Prolonging the hydrolysis time from 6 to 48 hours gives increasing yields of Val and Ile and progressively lower amounts of Ser, Gly and Tyr. The error in the Ser measurement from both modern and archaeological wools is higher than for the other amino acids, though a general decrease is evident. The increase in hydrolysis time from 6 to 18 hours causes the greatest proportional increases in Val and Ile in both modern and archaeological wool samples. This indicates that an 18 hour hydrolysis time leads to a more complete hydrolysis of keratin and that a 6 hour hydrolysis would be insufficient for obtaining an accurate assessment of the archaeological materials. The losses of the acid labile species (Ser and L Thr) are minimal for 18 hours hydrolysis, with the exception of Tyr which shows a much larger decrease between 6 and 18 hours than for 18 to 24 hours. Hydrolysis for 48 hours leads to the greatest losses of all acid labile amino acids and the largest recovery of the aliphatic amino acids (Val and Ile). The resultant skewing of the composition indicates 48 hour hydrolysis to be unsuitable for the analysis of archaeological samples.

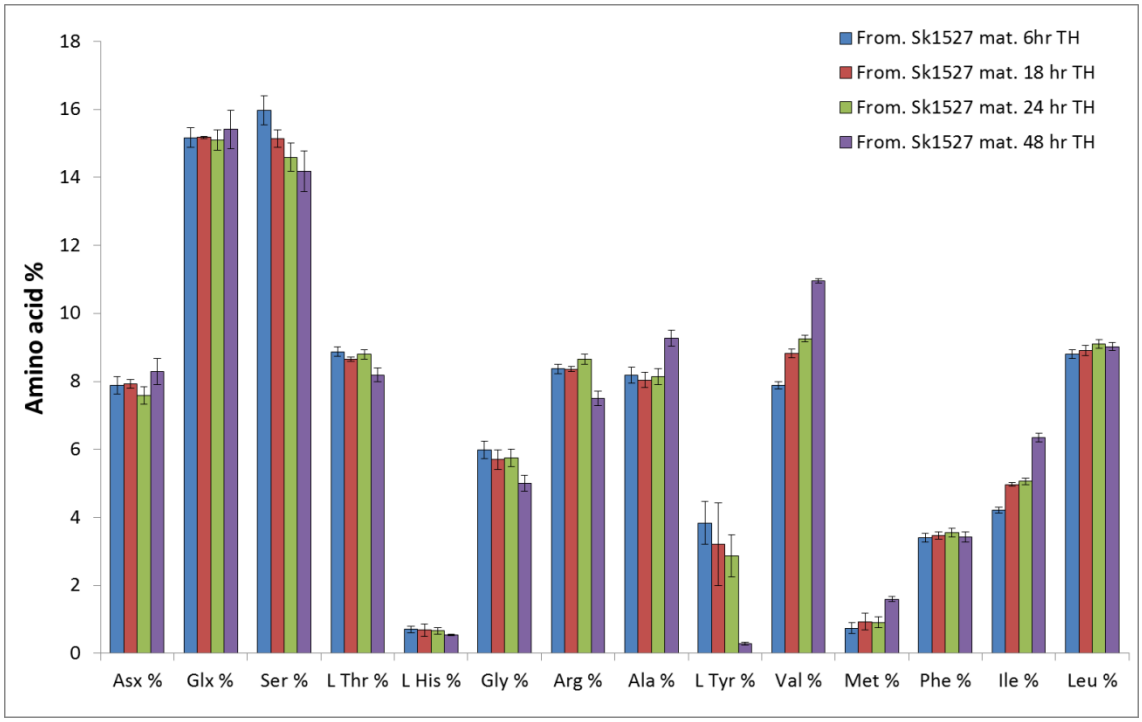

Figure 23. Percentage amino acid compositions of archaeological wool (Fromelles SK 1527 pelvis material) hydrolysed at 6, 18, 24 and 48 hours. The data are expressed as percentages of the sum of all amino acid peak areas. Error bars represent +/- 1 standard deviation; n=3.

The increase in time that the wool is subjected to hydrolysis also increases the extent of racemisation of the amino acids that are liberated, as has been observed with other proteins (Kaiser and Benner, 2005). Thus, the D/L ratios of the amino acids recovered from wool keratin show increasing, though different, values with increasing T_H (Figure 24 and Figure 25).

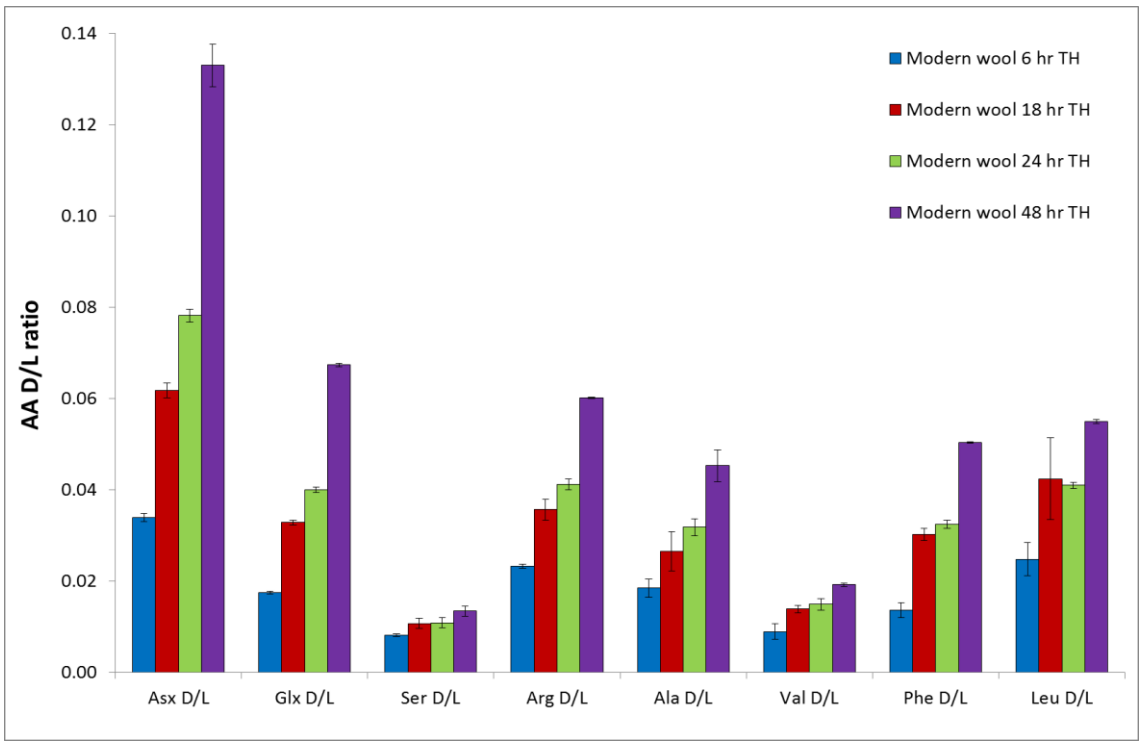

Figure 24. Amino acid D/L peak area ratios of Herdwick Tops wool hydrolysed at 6, 18, 24 and 48 hours. Error bars represent +/- 1 standard deviation; n=3.

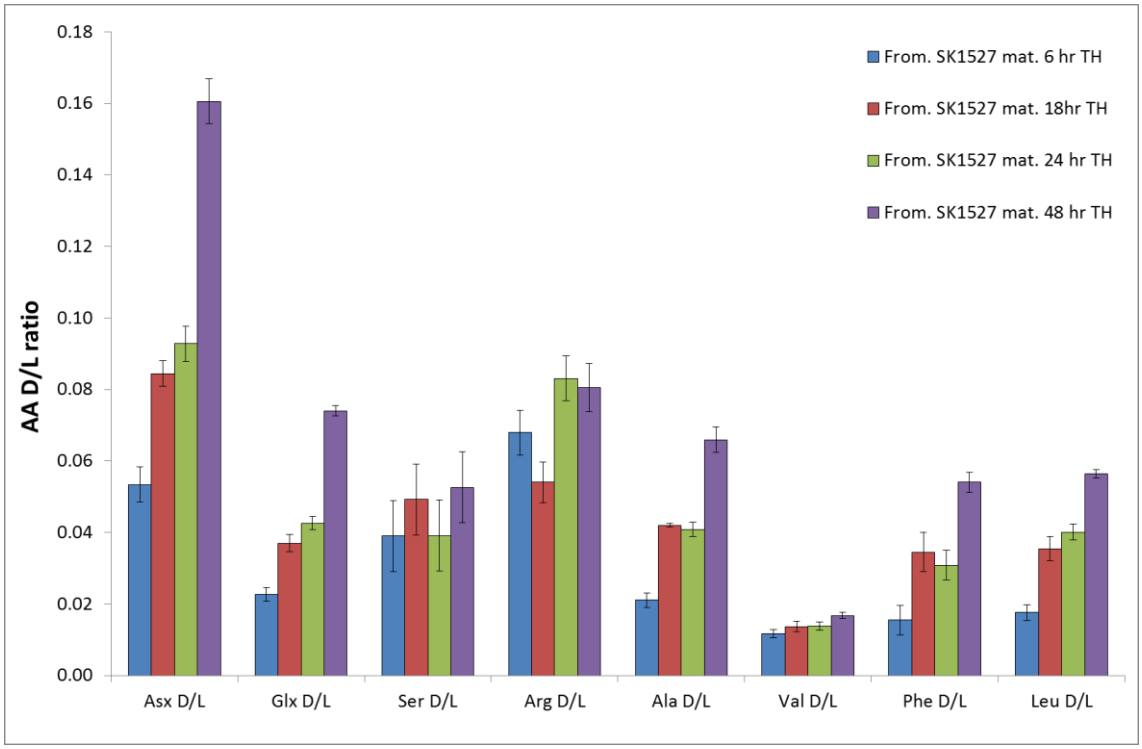

Figure 25. Amino acid D/L peak area ratios of archaeological wool (Fromelles SK 1527 pelvis material) hydrolysed at 6, 18, 24 and 48 hours. Error bars represent +/- 1 standard deviation; n=3.

In an effort to maximise keratin hydrolysis while minimising amino acid degradation and racemisation, a hydrolysis time of 18 hours was selected for use in the analyses of protein based materials recovered from archaeological burial environments.

3.2.2 Modern analogues for archaeological wool, hair and leather

Many different methods are used to study amino acid compositions of proteinaceous materials commonly recovered from archaeological burials (Robbins, 2012). The range of sample preparation, hydrolysis and chromatographic techniques employed is much more diverse than those used in the analysis of woods, resulting in a wider variation in the amino acid compositions reported in the literature (Block, 1939; Bowes and Kenten, 1948; Corfield and Robson, 1955; Eastoe, 1955; Ward *et al*., 1955; Felix *et al*., 1963; Chapman and Bradbury, 1968; Robbins, 2012). Consequently, it was deemed necessary to assess the variability in amino acid compositions of typical archaeological materials likely to be recovered from burial environments, using the hydrolysis and analytical methods to be employed in the study. Samples of modern human hair, leather, suede, silk and sheep wool (Table 8) were cleaned, hydrolysed and analysed using the methods outlined in Chapter 2.5.

Table 8. Protein based modern materials analysed to establish the extent of variability in amino acid composition using the hydrolysis and analysis methods employed in the study.

Material type	Source	No. of repeat analyses
Human hair	British male, age 23, light brown hair	2
	Greek female, age 24, black hair	2
	British male, age 25, blonde hair	2
	British male, age 32, black hair	2
	British male, age 83, white hair	2
Leather	Tanned South American cow hide	3
	Tanned British cow hide	3
Suede	Lamb hide, unknown provenance	3
Silk	Cultivated *Bombyx mori* moth cocoons	3
Wool	Herdwick Tops, sheep, female	2
	Jacob, sheep, female	2
	Lincoln Longwool, sheep, female	2
	Shetland, sheep, female	2
	Whitefaced Woodland, sheep, female	2

The total amino acid contents of all of the modern materials (Figure 26) show large variations, suggesting that this parameter may be of limited use in the analysis of archaeological materials. Given the ranges indicated by the standard deviations, only very large differences in the values in the archaeological materials would be statistically significant.

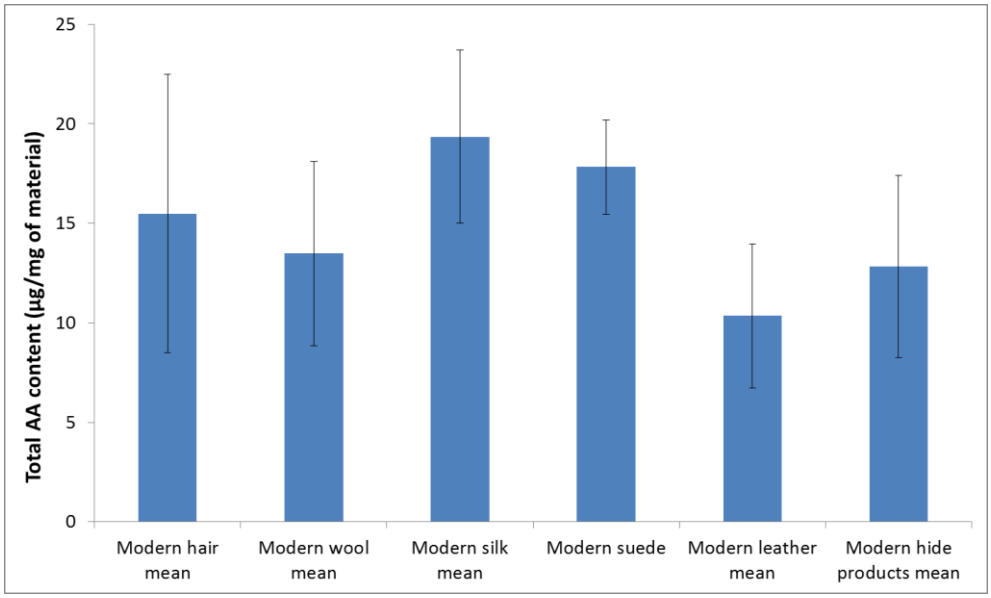

Figure 26. Mean total amino acid concentrations of modern hair and clothing materials. Error bars represent +/- 1 standard deviation; n=10 for modern hair and wool, n=3 for modern silk and suede, n=6 for modern leather and n=9 for modern hide products.

The standard deviations for the individual amino acids of all of the modern materials are low, the greatest values being for Gly in the two leathers, indicating that the biosynthetic pathways in different organisms of the same species are very similar (Figure 27). Microbially mediated enzymatic digestion of protein based materials often leads to a change in amino acid composition (Wilson *et al*. 2007a, Wilson *et al*. 2010). Thus, the limited variation in the compositions of the modern materials may allow detection of changes in the archaeological materials.

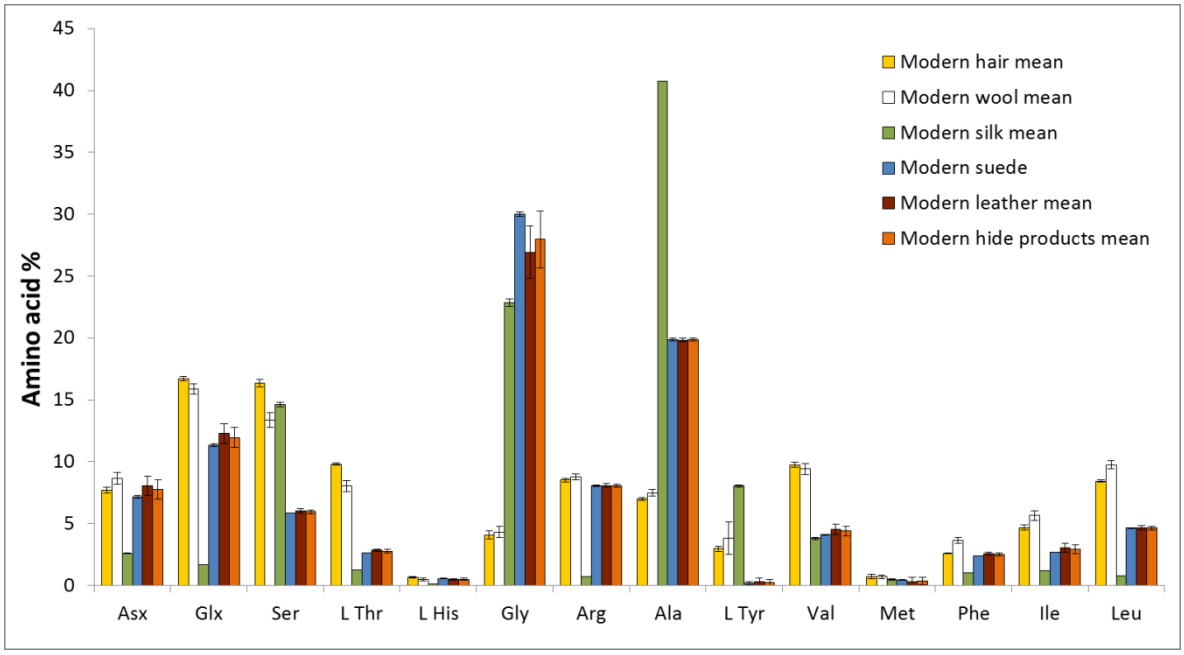

Figure 27. Mean amino acid compositions of the modern materials analysed. The data are expressed as percentages of the sum of all amino acid peak areas. Error bars represent +/- 1 standard deviation; n=10 for modern hair and wool, n=3 for modern silk and suede, n=6 for modern leather and n=9 for modern hide products.

The amino acid D/L ratios exhibit larger error bars than the amino acid composition data, indicating a greater degree of variability between samples of the same material (Figure 10). The extent of racemisation that can occur in degraded protein based materials is typically greater than that determined for the modern materials (von Holstein *et al*., 2014). Thus, the control materials and methods of analysis were deemed suitable for assessing the racemisation of the amino acids in archaeological materials.

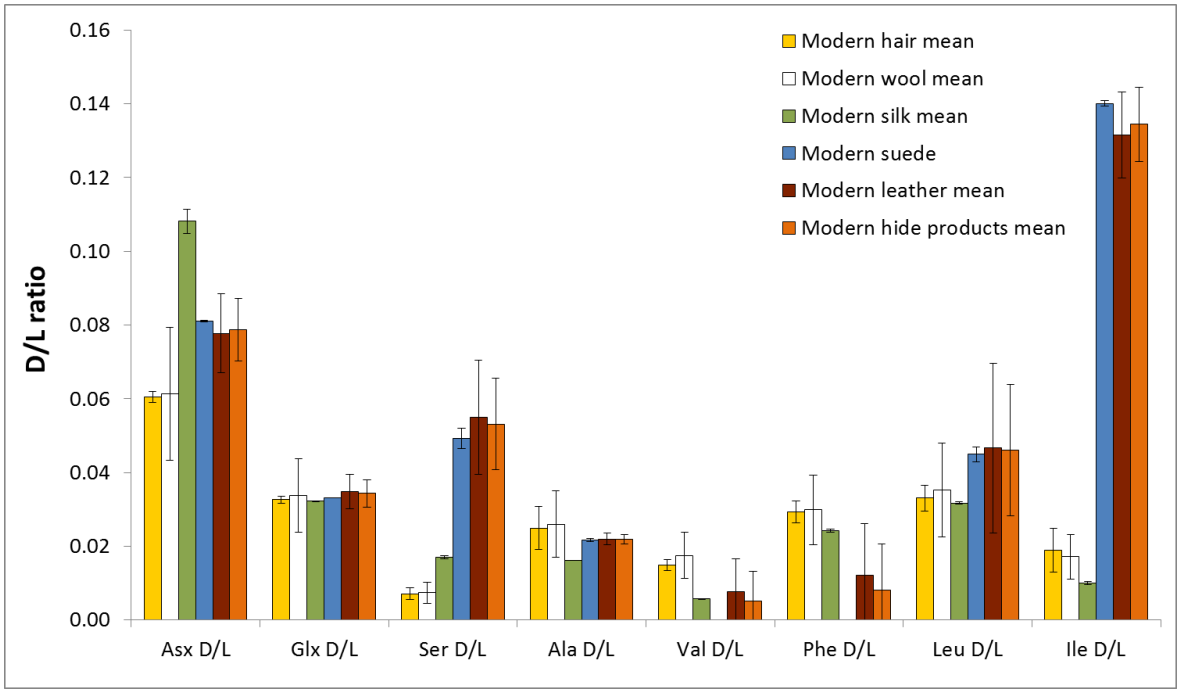

Figure 28. Selected mean amino acid D/L values of the modern materials analysed. Error bars represent +/- 1 standard deviation; n=10 for modern hair and wool, n=3 for modern silk and suede, n=6 for modern leather and n=9 for modern hide products.

CHAPTER 4

BURIAL EXPERIMENTS

4.1 Introduction

In order to complement the archaeological data and to look at short term diagenetic processes that occur within burials, *in situ* experiments were conducted to replicate the burial environments and materials commonly found in archaeological graves. Using a range of different burial environments and by analysing known buried materials alongside unburied controls as a means to assess any short term alterations, this chapter aims to further advance the overall goals of the InterArChive project: to study the information contained within the soils of archaeological inhumations. The InterArChive project had a total research timescale of five years and the experimental burials were started early in the investigation to allow time for the excavations, sample analysis and data interpretation. The experiments were therefore planned and executed before the commencement of this PhD project.

Due to the legal restrictions surrounding the disposal of human remains and the control of disease, cadavers cannot currently be used for decomposition studies in the UK (Public Health Act, 1984; Peachey, 2015). Pigs have a similar skin structure, hair coverage and fat content to that of humans and are commonly used as substitutes for human cadavers in experimental burials (Turner and Wiltshire, 1999; Wilson *et al*., 2007b; Janaway *et al*., 2009). Ten piglets were sourced from a pig farm in North Yorkshire; the majority of the animals were stillborn, whilst some died not long after birth from natural causes. The piglets were buried at five locations in the North Yorkshire area (Figure 29) which represent a range of different soil types (Table 9).

Figure 29. A map showing the locations of sites where experimental piglet burials were carried out.

Each piglet was buried with a range of grave goods. As the majority of the piglets had never suckled and had empty digestive tracts, a fibre bag containing foodstuffs was sewn into the abdominal cavity to simulate the gut contents. A second bag containing simulated burial offerings (such as tobacco, cloves and beeswax) was deposited by the snout of each animal, to investigate if the signatures relating to these materials could be detected in the burial soils. Some piglets wore leather shoes and all had human hair scattered on their heads, to simulate the scalp hair of humans. Five piglets were buried in wooden boxes to simulate coffins. In the majority of archaeological coffined burials, the action of water or structural collapse allows sediment to accumulate in the base of the coffin (Pokines and Baker, 2013). As the burials were only planned to be for a period of three years (insufficient time to allow such an accumulation to occur) the base of each coffin was therefore filled with sediment matching that of the burial environment. Images of typical piglet burials are shown in Figure 30 and the inventory and burial soil type of each piglet grave is shown in Table 9.

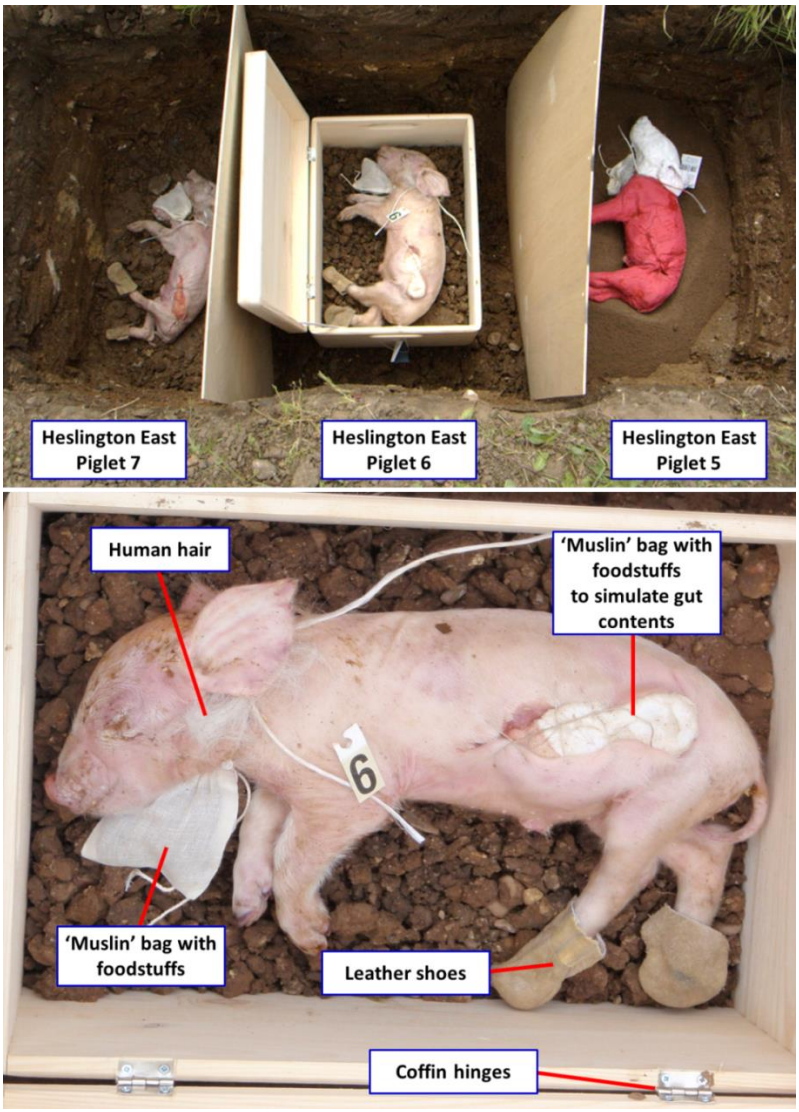

Figure 30. Images of the experimental piglet burials at West Heslerton. The top image shows the three piglets, one of which was in a coffin. The bottom image shows piglet 6 before burial. The positions of both 'muslin' bags and the leather shoes were similar in all other burials.

Table 9. Details of the location, burial soil type, coffin fill (where relevant) and grave goods of each of the ten experimentally buried piglets. Soil information provided by Carol Lang.

Location (including latitude and longitude)	**Soil type**	**Piglet**	**Coffin**	**Coffin fill**	**Leather shoes**	**Human hair**
Hovingham	Sandy/loam	1	Yes	Sand	N	Y
(54.170043, -0.980173)		2	Yes	Limestone chips	N	Y
Folkton	Peat bog	3	Yes	Burial soil	N	Y
(54.20797, -0.38202)		4	No	-	N	Y
Heslington East	Extremely aggregated clay	5	No	-	N	Y
(53.95232, -1.0213)		6	Yes	Burial soil	Y	Y
		7	No	-	Y	Y
West Heslerton	Sandy	8	No	-	N	Y
(54.171765, -0.60794)		9	Yes	Burial soil	Y	Y
Kings Manor	Urban soil (technosol)	10	No	-	Y	Y
(53.96251, -1.08727)						

Samples of all materials were retained to act as unburied controls. Once buried in their respective locations, the piglets were left for a period of approximately three years, after which they were excavated. Samples of the burial soil were taken following the sampling strategy for human burials that is outlined in Chapter 2.2.1. Any remaining textiles, leather, hair and the coffins were taken in their entirety. Soil micromorphology and soil extractable organic matter were studied by other members of the InterArChive team (Hicks, 2017). This thesis focused on the analysis of the materials buried alongside the piglet, specifically the coffin wood, human hair, textiles and leather.

4.2 Analysis of buried coffin woods

4.2.1 Sampling information

Two samples were collected from the same positions from each of the five experimentally buried coffins and from an unburied control coffin; a 10 cm by 6 cm section from the centre of the front panel, and the wood directly underneath the right hinge were cut out using a band saw (shown by the blue areas in Figure 31). The wood from the front panels was chosen as representative of the overall condition of the wood at all five of the sites, and to allow for comparisons to be made between the different burial environments. The brass from which the hinges were made contains copper, which is known to have antimicrobial properties (Ramsay *et al*., 1999; Levin *et al.,* 2002). Organic materials that have survived due to their association with metal are often recovered from archaeological burials (Beukens *et al*., 1992; Chen *et al.,* 1998; Janaway, 2001). With the exception of the coffin recovered from Folkton (which was not fitted with hinges) the wood in proximity to the hinges was therefore sampled to examine any differences in preservation state compared to the wood from the front panels.

Several of the coffins exhibited areas where the wood was of a different texture and visibly more degraded than the rest. Others had fungal growth on specific parts of the wood. These areas are shown in Figure 31 and detailed in Table 10. Samples of the degraded wood and of the wood beneath the fungal growths were taken for analysis and comparison with the wood that was not in proximity to these features.

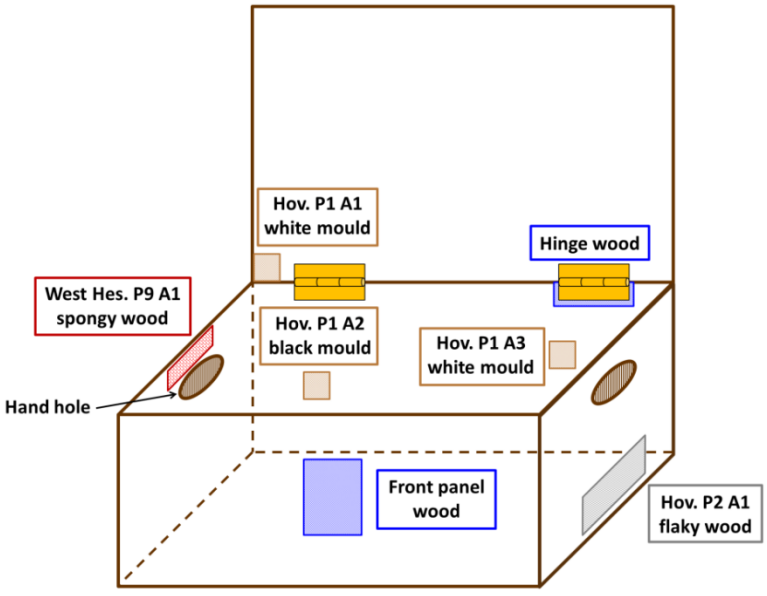

Figure 31. Diagram showing the wood sampling strategy of the excavated piglet burial coffins. The blue areas represent samples that were taken from all coffins (wood from the front panel and from the right hinge). Other colours show samples taken from individual coffins in areas where the wood looked to be more degraded or was beneath fungal growth. Light brown = Hovingham piglet 1, grey = Hovingham piglet 2 and red = West Heslerton. See Table 10 for sample descriptions. No obvious areas of degradation were noted for the coffins from Folkton and Heslington East.

Table 10. Descriptions of the samples taken from areas of the piglet coffins that exhibited degradation or were in proximity to fungal growth.

Piglet coffin	Sample/feature location	Description
Hovingham piglet 1	A1: back/bottom left corner of coffin lid	Spongy and compressible wood beneath an area of white fungus
	A2: back panel, down from left hinge	Wood beneath black 'fuzzy' mould
	A3: back panel, down from right hinge	Wood beneath white fungus
Hovingham piglet 2	A1: bottom of right side panel	The entire lower third of the coffin was flaky and very soft, this sample was from the most degraded area
West Heslerton piglet 9	A1: above left handle hole	Spongy and compressible wood

All samples of piglet coffin wood were solvent extracted using the methods outlined in Chapter 2.2.2.4. The solvent extracts were retained for GC-MS analysis by other members of the InterArChive team. Samples were then analysed using Py-GC-FID and the results discussed in Chapter 4.2.2.

4.2.2 Analysis by Py-GC

4.2.2.1 Issues discovered following Py-GC analysis

The presence of syringyl lignin compounds in the majority of the Py-GC data obtained from the piglet coffins shows that they are constructed of wood from both gymnosperm and angiosperm trees; examples of pyrograms from both gymnosperm and angiosperm wood samples are shown in Figure 32 and Figure 33 respectively. This is contrary to what was believed at the time of burial, as the coffins were purchased on the understanding that they were all made from wood from pine trees, which are gymnosperms. Of the 16 wood samples from the piglet coffins that were analysed, four are from gymnosperm trees, including that from the unburied control coffin. The different panels of the coffins being constructed with different types of wood with no discernible pattern indicates that they were made from offcuts of wood, likely from large scale manufacturing of larger wooden products.

Comparison of the coffin wood pyrograms and the lignin subunit data with those of freshly cut modern pine and oak reveals differences in the lignin content. Both the gymnosperm woods (Figure 34) and the angiosperm woods (Figure 35) that were buried with the piglets have more demethoxylated and short chain lignin components, and fewer long chain and carbonyl lignin components than the fresh modern gymnosperm and angiosperm comparisons. However, these differences are also apparent in the control sample, implying that the burial of these woods was not the cause of the lignin modifications. The modern wood industry employs a range of techniques to modify the physical and chemical properties of the raw materials. Some aim to increase the lifetime of the wood by limiting microbial attack, others impart fire retardant properties while some modify softer woods for use in applications which the native wood would not be suitable (Tjeerdsma *et al*., 1998; Weiland and Guyonnet, 2003; Tame *et al*., 2007). The most common methods of treating fresh wood for commercial applications are impregnation with metal-containing inorganic compounds and thermal modification by heat treating. Both of these processes could account for the differences between the lignin of the piglet coffins and the untreated modern woods.

Ions of the metals K, Cu, Fe, Mn and Co are commonly used in wood preservatives and have been shown to have catalytic effects during the pyrolysis of woods, altering the pyrolysis products (DiCosimo and Szabo, 1988; Wu *et al*., 1994; Richards and Zheng, 1991; Fu *et al*., 2008). The presence of such compounds could therefore explain the differences in the lignin of the piglet coffin woods (including the unburied controls) compared to fresh woods.

Thermal modification typically involves the exposure of woods to temperatures ranging from 150 to 200°C, first in an atmosphere of steam followed by heating under gaseous nitrogen, for durations of up to ten hours (Yildiz *et al*., 2006). These treatments improve the dimension stability

and durability of the wood whilst making the wood less hydroscopic, reducing the water content and thus the habitability toward potential microbial degraders (Tjeerdsma *et al*., 1998; Tjeerdsma and Militz, 2005). These changes are a result of modification of the component biopolymers. The cellulose and hemicellulose are degraded to liberate volatile compounds, and the lignin structure is modified by cleavage of β-O-4 linkages, oxidation of Cγ and autocondensation at Cα, which forms linkages with surrounding lignin subunits (Tjeerdsma *et al*., 1998; Tjeerdsma and Militz, 2005; Brosse *et al*., 2010). Such modifications could also be an explanation for the observed differences in the piglet coffin control and the untreated modern woods.

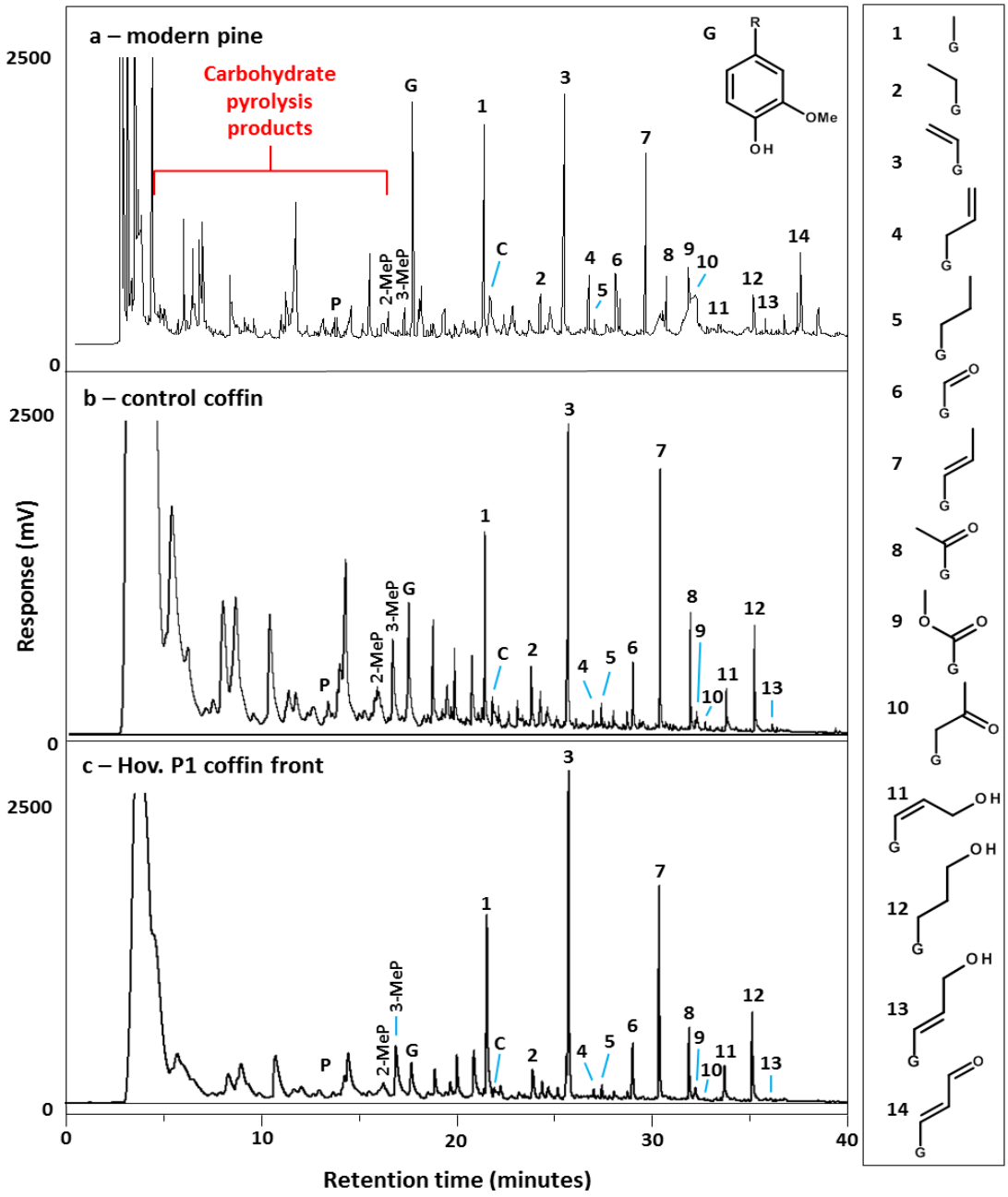

Figure 32. Assigned partial Py-GC-FID pyrograms of a – untreated modern pine wood, b – wood from the front panel of an unburied control coffin, c – wood from the front panel of the coffin buried with piglet 1 at Hovingham. P = phenol, MeP = methoxyphenol, G = guaiacol and C = catechol. The identities of the numbered peaks are shown in the key to the right of the pyrograms.

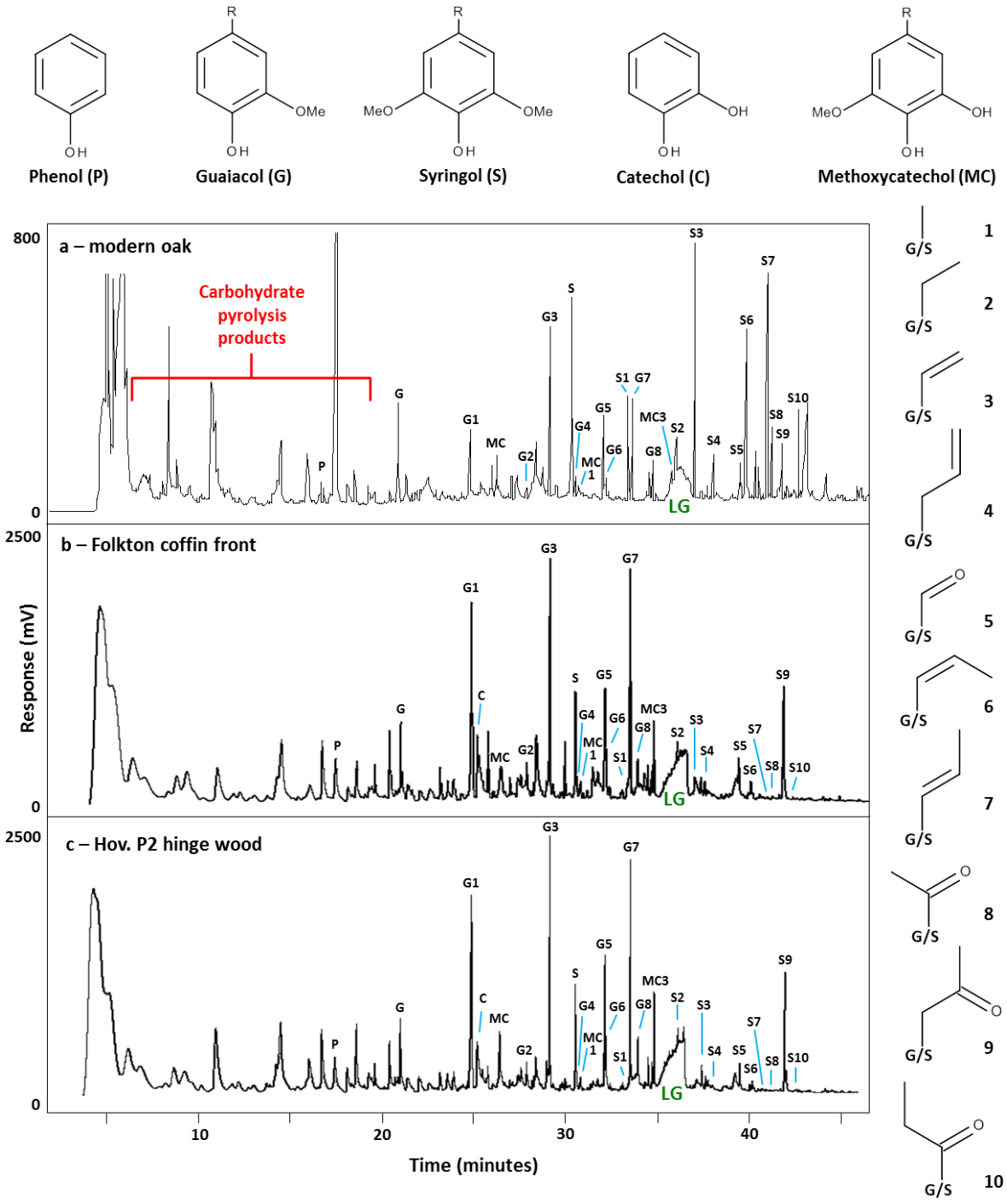

Figure 33. Assigned partial Py-GC-FID pyrograms of a – untreated modern oak wood, b – wood from the front panel of the coffin buried with piglet 3 at Folkton and c – wood from the hinge of the coffin buried with piglet 2 at Hovingham. P = phenol, MeP = methoxyphenol, G = guaiacol, C = catechol and LG = levoglucosan (a cellulose pyrolysis product). The identities of the numbered peaks are shown in the key to the right of the pyrograms.

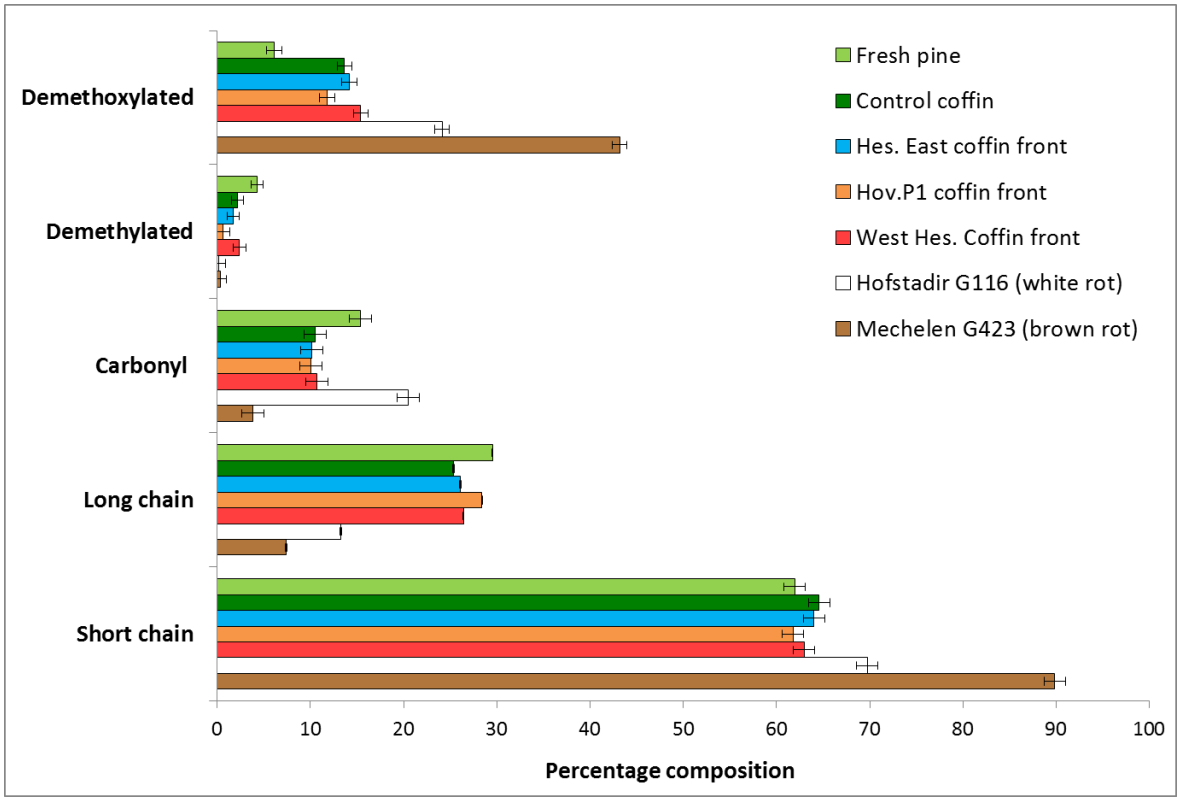

Figure 34. Percentage compositions of demethoxylated, demethylated, carbonyl, long chain and short chain compounds in untreated modern pine, the unburied control coffin, coffins buried containing piglets 1, 6 and 9 and archaeological woods degraded by white rot and brown rot fungi (see chapter 5). Values are calculated as a percentage of the total area of lignin derived peaks in Py-GC-FID pyrograms. Error bars represent +/- standard deviation and are the standard analytical error calculated in Chapter 3, based on n=3 replicates of an archaeological gymnosperm wood.

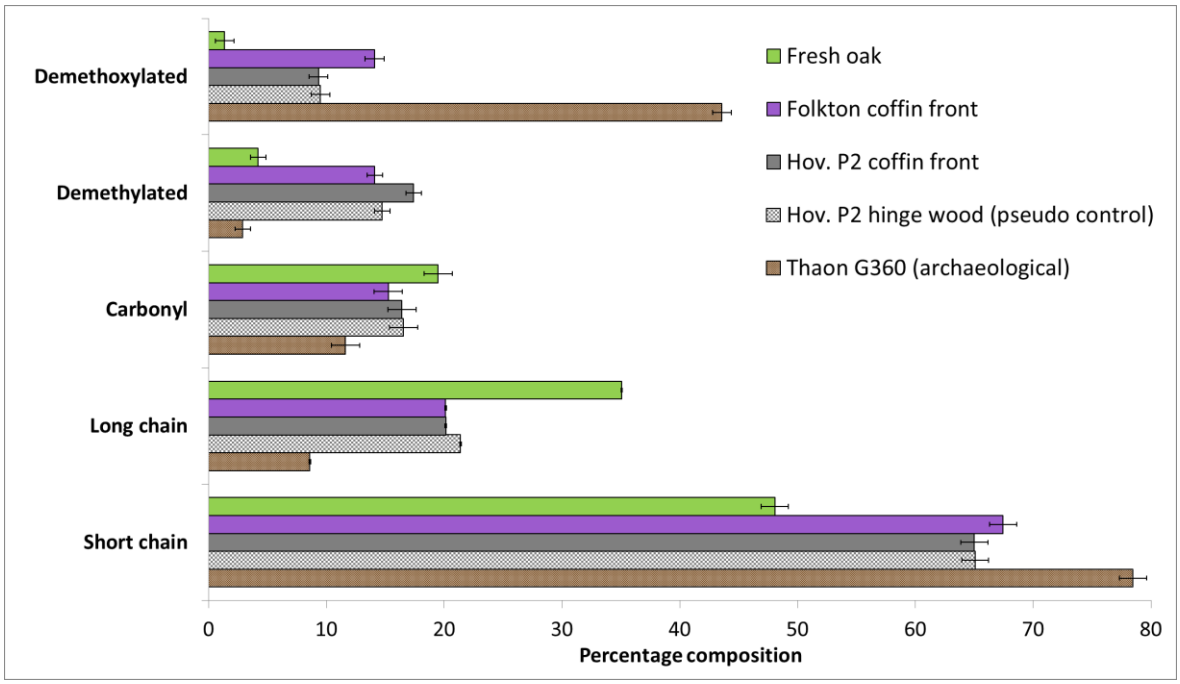

Figure 35 . Percentage compositions of demethoxylated, demethylated, carbonyl, long chain and short chain compounds in untreated modern oak, wood from the front panels of the coffins buried containing piglets 2 and 3, wood from the right hinge of the piglet 2 coffin (used as a pseudo control) and a degraded archaeological wood (see chapter 5). Values are calculated as a percentage of the total area of lignin derived peaks in Py-GC-FID pyrograms. Error bars represent +/- standard deviation and are the standard analytical error calculated in Chapter 3, based on n=3 replicates of an archaeological angiosperm wood.

Due to a lack of -20 °C storage space, only the coffin subsamples detailed in Section 2.1 were retained, meaning that further subsamples could not be taken. The only sample of the unburied control coffin being gymnosperm greatly complicates the analyses of the 12 experimentally buried angiosperm samples, as there is no unburied control that has been treated using the same preservative techniques. The differences in the lignin subunit data of the fresh modern wood that has not been treated and the buried woods show that the fresh woods are unsuitable for use as undegraded comparators.

Comparison of all the pyrolysis data from the angiosperm piglet coffins shows that the wood from the hinge of the Hovingham piglet 2 coffin is the least chemically different from untreated modern oak, which suggests that this material has been least affected by degradation within the burial environment. This wood showed no physical or mechanical signs of decay during the subsampling. Using this wood as a pseudo control, by setting it as a baseline from which to assess the degradation of all other buried samples allows for a better assessment of preservation state than the use of fresh modern oak.

All of the hinge wood samples are from angiosperm trees and (with the exception of the coffin front from Hovingham piglet 2) the coffin fronts are from gymnosperm trees. The result of this is that the planned comparison between the two, to investigate metal fittings retarding decay, is not possible.

4.2.2.2 Overall preservation state of the piglet coffins

The proportions of different categories of lignin pyrolysis products from the gymnosperm coffin fronts were compared with archaeological gymnosperm woods from Mechelen and Hofstadir that have been interpreted to be degraded by brown rot and white rot fungi (Figure 34; Chapter 5) None of the buried coffin woods show higher abundance of short chain lignin pyrolysis products than the unburied control, suggesting that the three carbon lignin side chains have not been shortened as occurs during depolymerisation of wood through the actions of fungi . Similarly, no demethylation or demethoxylation is apparent, and there is no difference in the proportion of lignin subunits with carbonyl groups, changes that are seen in the archaeological wood that has been attacked by biological degraders. Curiously, increases in the abundances of the long chain lignin subunits are apparent in the buried woods. This could be due to these treated woods having greater variation in the lignin composition or less reproducible pyrolysis products in comparison to native, untreated woods.

The only gymnosperm coffin front to show any alteration of the holocellulose component is that from Hovingham piglet 1. Figure 32c shows peaks in the carbohydrate region with significantly lower abundances than those in the unburied control, pointing to degradation of the holocellulose fraction of the wood. The peaks that correspond to 2-methylphenol, 3-methylphenol and guaiacol also show lower relative abundances than those of the control. None of the other gymnosperm pyrograms exhibited the same features, implying a cause of degradation that was unique to the Hovingham burial, possibly as a consequence of the nature of the burial matrix or the burial environment.

The lignin pyrolysis product compositions of the two angiosperm coffin fronts reveal observable signatures of decay when the hinge wood from the coffin of Hovingham piglet 2 is used as a pseudo control (Figure 35). The material from the front of the Hovingham piglet 2 coffin shows lower amounts of long chain lignin compounds, and an increase in demethylated units (Figure 35). The decrease of long chain lignin phenols would be expected to be accompanied by an increase in those with short chains, as the three carbon chains are broken down to form shorter chain derivatives. The disparity between the short and long chain components could either reflect a larger error in the measurement of the former or, perhaps more likely, that the longer chain compounds were broken down and lost to the burial environment rather than being converted to short chain components retained within the remaining polymer.

The wood buried at Folkton produced higher proportions of short chain and demethoxylated lignin products and lower proportions of long chain lignin products than the pseudo control. These differences are also seen in degraded archaeological materials (Figure 35). The differences in the proportions of the short and long chain lignin products are typically much larger in archaeological wood than those observed for the material from Folkton, suggesting that the

Folkton material represents an early stage of decay. The differences in the lignin structure compositions of the Folkton and Hovingham piglet 2 coffins suggest that the two have been modified by different decay agents within the burial environments. Similar consideration suggests that the wood from Folkton is more degraded than that from the Hovingham piglet 2 burial.

The Folkton burials took place in boggy, waterlogged soil. On excavation in late June of 2013, the water level was found to be above that of the burials. The decision was made to rebury the piglets and return at the end of the summer. This was done to allow for pumping equipment to be sourced and in the hope that the hot, dry months to follow would reduce the water level below that of the burials. On re-excavation in early October of the same year, the water level had indeed dropped below the level of the burials. Combined with the deterioration seen in the Folkton coffin, it is unlikely that the burials were waterlogged for the duration of the three year burial period. Permanent waterlogging would have generated anoxic conditions, which are known to limit microbial growth, leading to better preservation of wood (Rowell and Barbour, 1990; Björdal *et al*., 1999).

The lignin of the angiosperm coffin fronts is more degraded than that of the gymnosperm counterparts. Syringyl methoxy groups have been shown to be preferentially demethylated over those of guaiacyl subunits, possibly due to the lower degree of condensation found in guaiacyl lignin (van Bergen *et al*., 2000). The lack of a methoxy group at C6 of guaiacyl aromatic ring allows for the formation of cross links at this position (del Rio *et al.,* 2002; Vane *et al*., 2003). Another theorised reason for the increased resistance of guaiacyl subunits is that many microbes preferentially attack the secondary cell wall layers which are richer in syringyl lignin, leaving the middle lamella (which is richer in guaiacyl lignin) intact (Backa *et al*., 2001). It has also been suggested that syringyl lignin moieties can be demethylated in the early stages of wood diagenesis (van Bergen *et al*., 2000). The higher abundance of demethylated lignin phenols in the Hovingham piglet 2 coffin wood combined with the relative brevity of these burials suggests this may indeed be the case.

4.2.2.3 Areas of the coffins exhibiting signs of degradation

Several areas of the buried piglet coffins exhibited clear signs of degradation (Table 10 and Figure 31). Of all the piglet coffins that were excavated, that buried with Hovingham piglet 1 had the greatest number of areas where decay was apparent. Three distinct areas were colonised by fungi and the structural integrity the wood was affected. The proportions of different categories of lignin pyrolysis products calculated from the Py-GC-FID data show distinct differences between modern oak and the Hovingham coffin wood samples (Figure 36).

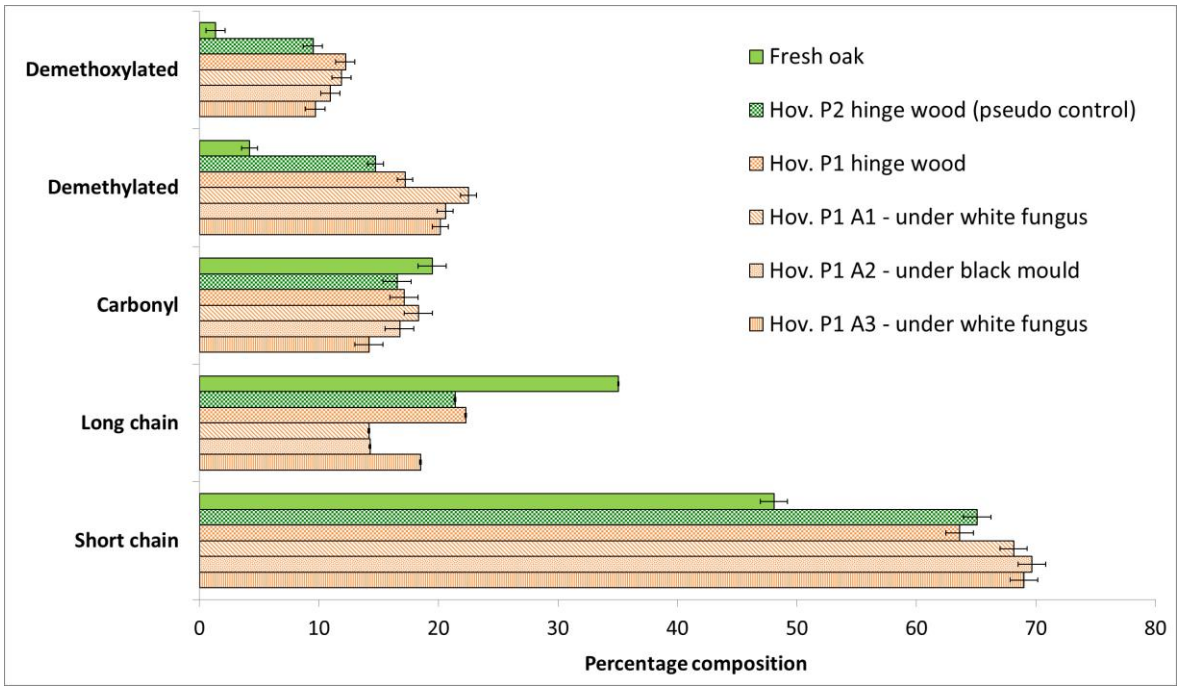

Figure 36. Percentage compositions of demethoxylated, demethylated, carbonyl, long chain and short chain compounds in untreated modern oak, wood from the right hinge of the piglet 2 coffin (used as a pseudo control), wood from the front panel of the coffin buried containing piglet 1 and three additional wood samples from the coffin of piglet 1 which showed visible signs of degradation. Values are calculated as a percentage of the total area of lignin derived peaks in Py-GC-FID pyrograms. Error bars represent +/- standard deviation and are the standard analytical error calculated in Chapter 3, based on n=3 replicates of an archaeological angiosperm wood.

The samples A1 and A3 were both collected from areas affected by a white fungus. Both woods have higher relative abundances of demethylated and short chain lignin phenols and lower relative abundances of long chain phenols than the hinge wood from the same coffin and from the pseudo control wood. Carbohydrate components and levoglucosan were less abundant in the material from A3 than in the pseudo control wood, suggesting that the hemicellulose and cellulose of this part of the coffin had been degraded. By contrast, the holocellulose fraction of A1 appeared unaffected, being very similar to the pseudo control. The larger extent of damage to the lignin in sample A1 and lack of evidence for alteration of the carbohydrate suggest that the wood from this area of the coffin was degraded by a fungus capable of selective degradation of lignin. The only fungi known to degrade wood in this way are preferential lignin degrading white rot fungi, making them the most likely candidates for the degradation of the wood of sample A1

(Blanchette, 1991; Blanchette, 2000). The lesser modification of the lignin in sample A3 combined with the observed holocellulose degradation suggests that the modification to the lignin may have occurred indirectly, as a result of the fungus directly attacking the carbohydrate component. Brown and soft rot fungi both lead to limited lignin modification and a loss of a large proportion of the carbohydrate component of wood. Based on these decay signatures being identified from the pyrolysis data, brown and soft rot fungi are more likely candidates for the decay than white rots (Blanchette, 1991; Blanchette, 2000; Blanchette *et al.,* 2004).

The black fungus that had colonised the wood represented by sample A2 has produced similar modifications the carbohydrate and levoglucosan peaks as that seen in sample A3, but, the changes to the lignin profile seen in Figure 36 are similar to that of sample A1. This suggests that both the holocellulose and the lignin may have undergone direct microbial attack, a feature commonly seen in white rot fungi that do not preferentially attack lignin (Blanchette, 1991; Blanchette, 2000).

The entire lower third of the coffin buried with Hovingham piglet 2 was heavily degraded, the wood having little structural integrity and bundles of tracheid cells easily flaked away. The decayed material was much lighter in colour than the unaffected wood. The pyrogram (not shown) exhibits a significant attrition of peaks that correspond to cellulose and hemicellulose. The lignin subunit compositions are shown in Figure 37. The degraded wood contains larger amounts of short chain and demethoxylated lignin phenols and fewer long chain and carbonyl containing lignin phenols than the pseudo control wood.

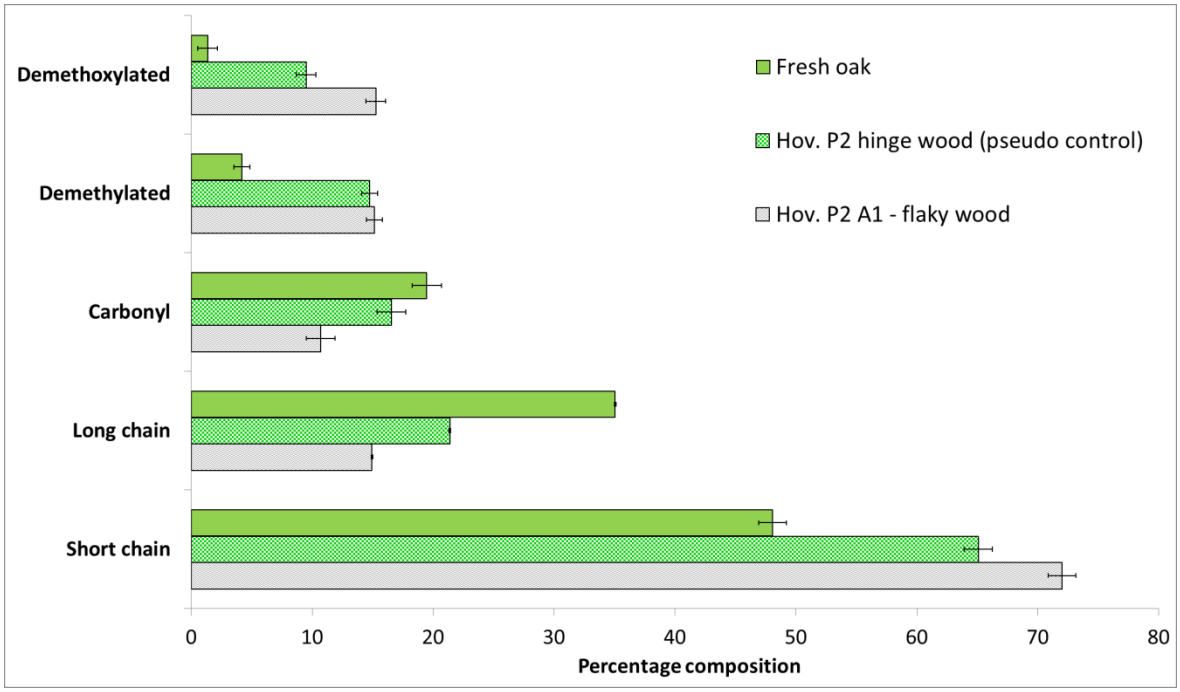

Figure 37. Percentage compositions of demethoxylated, demethylated, carbonyl, long chain and short chain compounds in untreated modern oak, wood from the right hinge of the piglet 2 coffin (used as a pseudo control) and the degraded, flaky wood that made up the entire lower third of the piglet 2 coffin. Values are calculated as a percentage of the total area of lignin derived peaks in Py-GC-FID pyrograms. Error bars

represent +/- standard deviation and are the standard analytical error calculated in Chapter 3, based on n=3 replicates of an archaeological angiosperm wood.

Prior to burial, the bottom of the coffin was layered with limestone chips, the piglet placed on top and the remaining space filled with the limestone. Limestone, primarily $CaCO_3$, is known to impart high alkalinity to soils (Obreza *et al*., 1993). Alkali treatment of wood removes hemicellulose and lignin and modifies the crystalline cellulose (Jackson, 1977; Borysiak and Doczekalska, 2005). These effects are exploited in wood pulping, which uses strong alkaline solutions to break down wood and solubilise the modified lignin, cellulose and hemicellulose (Patt *et al*., 2002). Blanchette (1991) reported the analysis of wood from a reagent shelf in the historic Thomas Edison Research Laboratory, Fort Myers, Florida. The wood was found to have been degraded by "… a spill of a concentrated caustic material such as potassium hydroxide" (p8). The description of the physical condition of the wood is essentially identical to that of the lower part of the Hovingham piglet 2 coffin. Blanchette's analysis of the shelf wood shows a depletion of lignin and hemicellulose. Given the limestone burial matrix and the similarity in degradation to that reported in the literature, it is likely that the coffin from Hovingham piglet 2 was affected mainly by chemical rather than microbial degradation.

The wood above the left hand hole of the West Heslerton coffin (West Hes. A1) was very soft and easily compressed, indicating deterioration of the wood biopolymers. Analysis by Py-GC-FID shows that the holocellulose of the wood is no different from that of the pseudo control or wood from the hinge of the coffin. There are, however, differences in the lignin content of the wood above the hand hole (Figure 38). With the exception of a higher short to long chain lignin phenol ratio, the wood from the hinge has a very similar lignin composition to that of the pseudo control. The handle wood, on the other hand, contains higher proportions of demethylated, demethoxylated and short chain lignin subunits, and lower proportions of long chain and carbonyl subunits. The degradation of the lignin without alteration to the holocellulose component reflects a selective process. Fungal colonisation was not observed on either the surface or cut sections of the wood. Fungi grow from spores which attach to a surface and grow by the spreading of hyphae. Hence, the absence of fungal bodies suggests that the degradation was mediated by bacteria. Although the understanding of bacterial degradation of lignin is far less well developed than that of fungi, it has been shown that soil bacteria, including *Amycolatopsis sp. 75iv2*, digest lignin by secreting heme peroxidases (Brown *et al*., 2011; Brown and Chang, 2014). Therefore, it is likely that the degradation of the A1 wood sample was caused by bacteria.

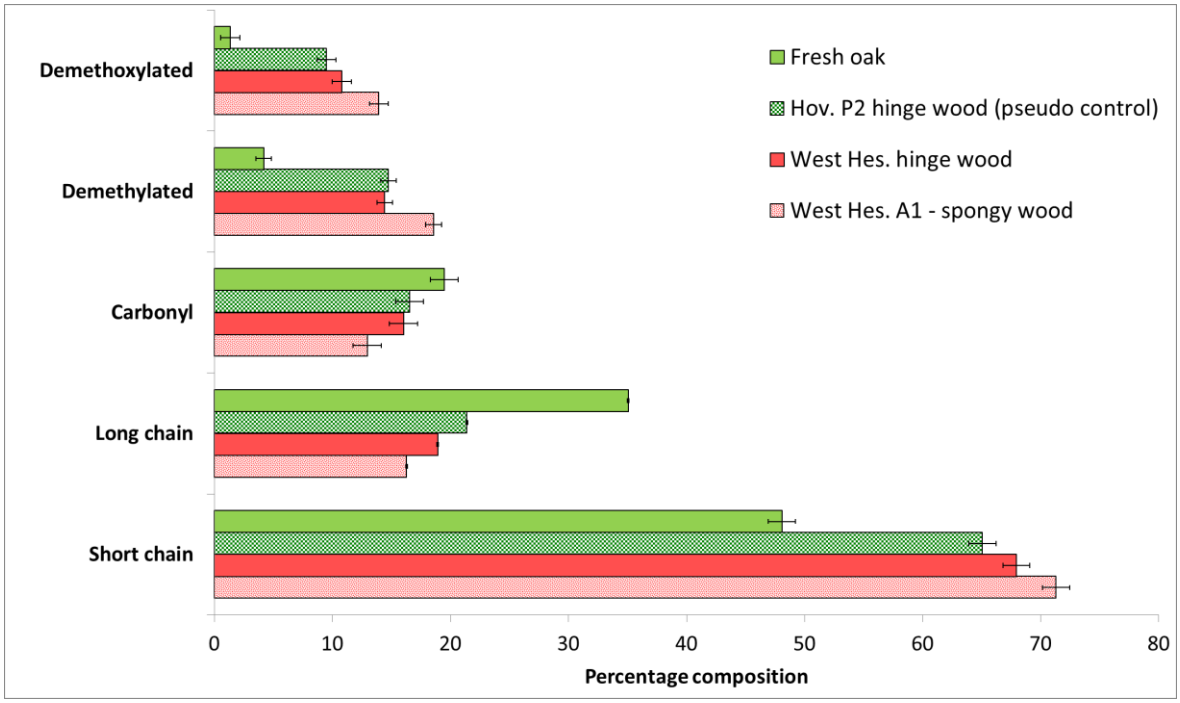

Figure 38. Percentage compositions of demethoxylated, demethylated, carbonyl, long chain and short chain compounds in untreated modern oak, wood from the right hinge of the piglet 2 coffin (used as a pseudo control) and the degraded, wood from the hinge of the coffin buried with piglet 9 at West Heslerton and the spongy wood from the piglet 9 coffin. Values are calculated as a percentage of the total area of lignin derived peaks in Py-GC-FID pyrograms. Error bars represent +/- standard deviation and are the standard analytical error calculated in Chapter 3, based on n=3 replicates of an archaeological angiosperm wood.

4.2.3 Summary and conclusions

The analysis of the buried piglet coffins was complicated and limited by the wood being from a range of gymnosperm and angiosperm trees and not exclusively the pine that was intended. The apparent use of preservative treatments on the wood also caused issues with the analysis of the coffins, preventing the use of modern, untreated woods as undegraded comparators. Such treatments can be expected to have altered the degradation of the coffins owing to the wood being more resistant to attack from the majority of microbial wood degraders. Hence, the experimental results may differ to those from archaeological coffins.

Despite the limitations, degradation of the buried woods can be observed. Information about the individual burial conditions, the observed physical characteristics and the modification of the lignin and holocellulose biopolymers revealed by Py-GC enable likely causal agents to be identified. The observation of chemically induced decay and biologically mediated decomposition due to a range of different burial fauna show that the degradation of the wood in the burial environments studied is diverse and variable.

Overall, the coffins buried with the piglets have undergone relatively little degradation, with the majority of the wood being little different from that of the controls. This is likely due to the short timescale of the burial experiment. The most severely degraded was that which enclosed piglet 2 at Hovingham, where corrosion by the alkaline limestone burial matrix is the likely cause of the observed damage. The coffin of piglet 1 at Hovingham featured the most areas of biologically induced decay. The fact that the damage was caused by at least three different microorganisms illustrates the diverse microbial populations that can exist within burial soils. The burial soil at Hovingham was a sandy loam, which likely allowed the burial to remain oxic. The grave was at the bottom of a hill, which would have allowed water to run off the slope and keep the burial soil moist but not waterlogged. The localised nature of the degradation for all of the coffins suggests that the activity of wood degrading microorganisms is a relatively slow process and that the complete mineralisation of a buried coffin would need far longer than the three years for which these burial experiments were conducted. Nevertheless, clear evidence for degradation has been revealed and the results show that the Py-GC enables condition assessment of the wood polymers and provides evidence of different degradation mechanisms.

4.3 Analysis of buried hair samples

4.3.1 Sampling information

Each of the piglets were buried with human hair scattered about the head, as an analogue for the scalp hair of humans. During the excavation of the piglet remains, hair was only recovered from piglets 8 and 9 at West Heslerton. The hair buried with the other piglets had either completely degraded in the burial environment, leaving no detectable remnants, or the consistency of these soils made the hair very difficult to find, resulting in the hair being missed during the excavations. Given the extreme care and precision with which the piglets were excavated, the latter is far less likely than the former. Samples of the hair were cleaned, subjected to hydrolysis and derivatisation and the amino acid content analysed by RP-HPLC, following the procedures described in Chapter 2.5.

4.3.2 Analysis by RP-HPLC

4.3.2.1 Amino acid composition

The amino acid compositions of the buried hair samples from the piglets at West Heslerton (piglets 8 and 9) are very similar to that of the unburied control (Figure 39), demonstrating that the samples were not contaminated by amino acid or non-keratin protein

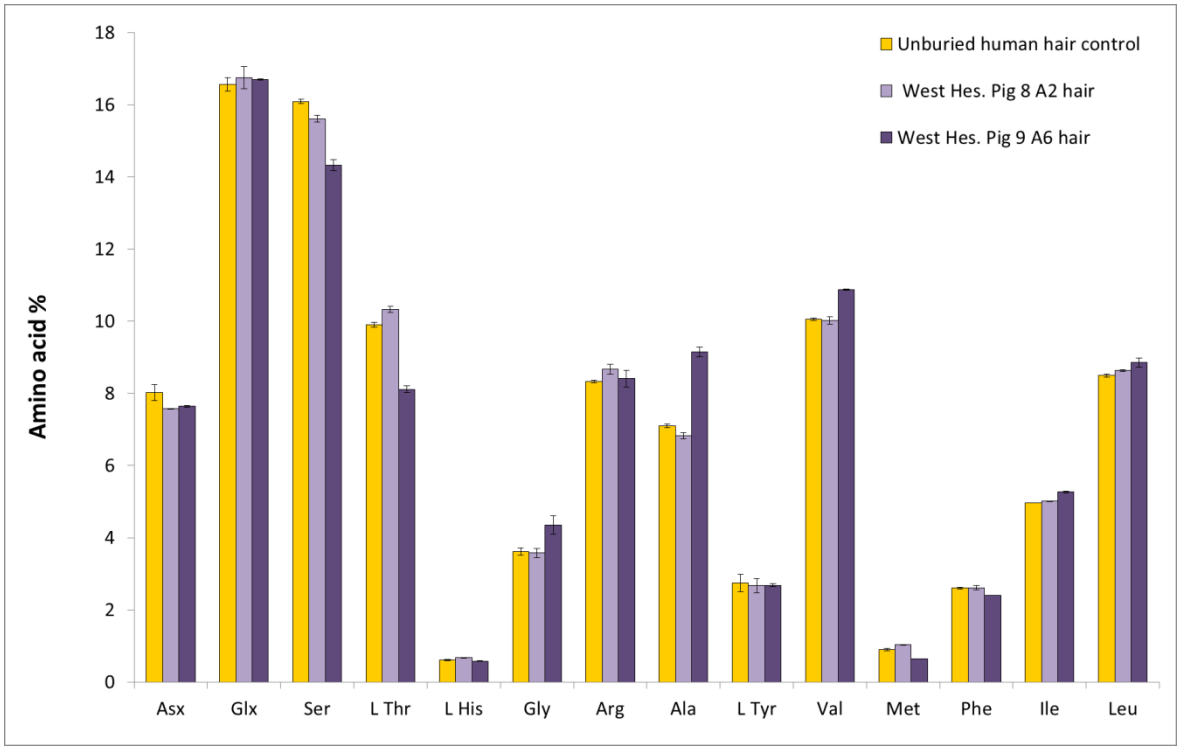

Figure 39. Amino acid compositions for the human hair recovered from the piglet burial experiments compared with an unburied sample of the same hair. Error bars represent +/- 1 standard deviation; n=3 for the control hair and n=2 for the experimental samples.

Both buried hair samples exhibit small but statistically significant amino acid compositional differences with respect to the unburied control (Student's t tests; all *p* values = <0.014), suggesting that they have both undergone degradative processes. Although a sample size of two is the smallest possible on which a t test can be performed, the low *p* value obtained likely indicates that the result is statistically significant. Ideally, a sample size of at least four would have been used, but the amount of material available for analysis in the majority of cases precluded this. Increases in the L Thr and Met content of the hair buried with piglet 8 are opposed to the decreases seen for the same amino acids in the material from piglet 9, suggesting they have likely been decayed in different ways.

In addition to the increases in the L Thr and Met content, the lower amounts of Asx, Ser and Ala seen in the hair from piglet 8 are small but statistically significant differences (Student's t tests; all *p* values = <0.022). The individual structures within hairs have slightly different amino acid sequences (Robbins, 2012). A large change in amino acid composition would suggest that certain tissues within the hair have been degraded more than others. As this is not the case it either

indicates very limited degradation by attack of a single hair substructure or it means that the hair has been decayed uniformly, with all hair tissues being damaged.

In contrast with the small changes in the hair from piglet 8, that from piglet 9 shows larger statistically significant changes in the amino acid composition; increases in Gly, Ala, Val, Ile and Leu, and decreases in Ser, L Thr and Met (Student's t tests; all *p* values = <0.018). Such changes are likely due to the attack of one or more specific hair substructures by bacteria of fungi, leading to a large change in the overall amino acid composition of the remaining material (Wilson *et al*. 2007a, Wilson *et al*. 2010). The proteins of the hair cuticle have a larger proportion of Ser than other hair tissues (Wolfram and Lindemann, 1971; Swift and Bews, 1976). The large decrease in Ser seen here likely reflects damage to the cuticle layers. The intercellular δ-layer is the cuticle component that has least resistance to microbial attack; the loss of this material leads to delamination and flaking of the cuticular scales (Wilson *et al*., 2007a). This hypothesis could be investigated using SEM, which was unfortunately not possible during the analysis of this material.

4.3.2.2 Amino acid D/L values

The hair buried with both West Heslerton piglets shows increased racemisation of selected amino acids (Figure 40). The hair from Piglet 8 shows repeatable increases in the D/L values of Ser, Val, Phe and Leu (Student's t tests; all *p* values = <0.049). The reproducibility of these changes in both hair samples that were analysed (indicated by the error bars) implies that there has been uniform degradation throughout the hair, giving rise to new terminal residues in all hair tissues, which were able to racemise. Microbial decay is the major route of decomposition for buried hair, especially when buried with decomposing animal remains (Wilson *et al*., 2007a). A range of fungi are known to degraded hair by 'tunnelling' across hair shafts, creating uniform voids by degrading all tissues in the path of the hyphae by keratinase enzyme secretion (DeGaetano *et al*., 1992; Wilson *et al*., 2007a). The observed increase in racemisation of the amino acids from the piglet 8 hair could be indicative of keratinase enzymes cleaving at predictable amino acid sequences in all proteins, supporting the postulated fungal tunnelling activity. The fact that the increase in racemisation is small could either reflect that there has been a small amount of damage, or that the rates of racemisation were slow enough to prevent much conversion between the two chiral amino acid forms.

The hair recovered from piglet 9 has large variations in the recorded Ser and Ala D/L values. Analysis of the two individual samples used to produce the mean and standard deviations revealed that one hair sample has Ala and Ser D/L values similar to that of the modern material and the other sample has large increases in the racemisation of these amino acids (data not shown). Ser and Ala are two of the most abundant amino acids in the cuticle proteins of hair, implying that attack was focussed on the outer layers of the hair that has increased racemisation of these amino acids (Wolfram and Lindemann, 1971). The large deviation in the measurements of the D/L values could be due to one hair strand being decayed well in advance of the other, the earlier degraded hair having more time for the newly generated terminal residues to racemise. The standard deviations for the Ala and Ser values in the compositional data for this material (Figure 39) do not show the large deviations seen in the D/L data, being similar to those for the other amino acids and for the other materials. This fits with the hypothesis of both hairs being degraded but one being more racemised than the other.

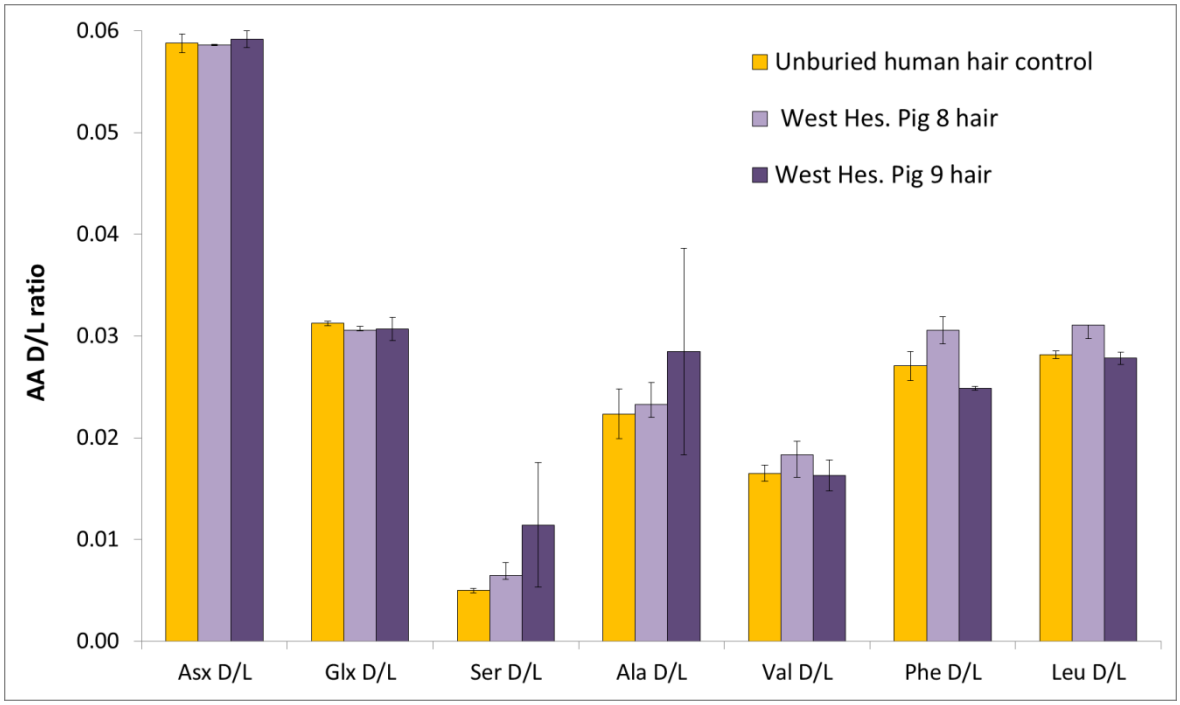

Figure 40. Selected amino acid D/L values for the human hair recovered from the piglet burial experiments compared with an unburied sample of the same hair. Error bars represent +/- 1 standard deviation; n=3 for the control hair and n=2 for the experimental samples.

4.3.3 Summary and conclusions

Of the human hair buried with each of the 10 piglets, excavation only recovered this material from two of the burials: piglets 8 and 9, both buried at West Heslerton. Either the hair completely degraded in all of the other burials or was missed during the excavations. The soil at the West Heslerton site was extremely sandy and likely offered excellent drainage. Low moisture levels are conditions that are known to preserve protein based textile materials (Janaway, 2001). Sandy soils often have a low pH and acidic conditions are known to retard the growth of a range of soil biota (Day and Ludeke, 1993; Rousk *et al*., 2010). As a result of this, archaeological protein based materials commonly survive when buried in acidic soils (Sibley and Jakes, 1984; Janaway, 2001). A combination of the low water content and low pH of the West Heslerton burial matrix was therefore probably responsible for the survival of hair.

Despite the hair still being physically present at the West Heslerton burials, both materials exhibited changes in their amino acid compositions and D/L values that indicate degradation may have occurred, likely by microbial attack. The piglet 8 hair shows evidence of attack by tunnelling fungi while that buried with piglet 9 shows erosion of the cuticle, likely by attack on the intercellular δ-layer. SEM imaging of these materials was not performed during this study but could be used to further test these conclusions. Degradation experiments in which samples of hair are exposed to microorganisms known to cause degradation similar to those hypothesised in this section could be useful in determining the underlying causes of any change in the amino acid compositions or racemisation values.

4.4 Analysis of buried leather samples

4.4.1 Sampling information

Piglets 6 and 7 at Heslington East, piglet 9 at West Heslerton and piglet 10 at Kings Manor were buried with a leather shoe placed on each hind leg (Figure 30). All eight of the shoes were recovered on excavation. A shoe from each of the West Heslerton and Kings Manor piglets was taken for analysis by the micromorphology team. The remaining shoes were cleaned, subsamples of the material were hydrolysed and the amino acid content analysed by RP-HPLC, following the procedures described in Chapter 2.5.

4.4.2 Analysis by RP-HPLC

4.4.2.1 Amino acid composition

The amino acid compositions of six leather shoes recovered from the piglet burials are shown in Figure 41. The vast majority of the buried leathers do not have amino acid compositions that are statistically different from those of the unburied control (Student's t tests; all *p* values = >0.05). However, there are statistically significant differences in the Gly content of the leathers buried with piglets 9 and 10, which are considerably lower in comparison with the unburied control (Student's t tests; all *p* values = <0.047). The piglet 9 leather also shows a significantly decreased Ala content, whereas the piglet 10 leather shows an increase in Ala (Student's t tests; all *p* values = <0.05). The degree of change in composition of these materials suggests they are more degraded than the other buried leathers, with the chemical or biological degraders specifically acting upon different tissues or proteins to different extents. The fact that the changes in amino acid composition are different suggests that the degradation in each had a different causal agent.

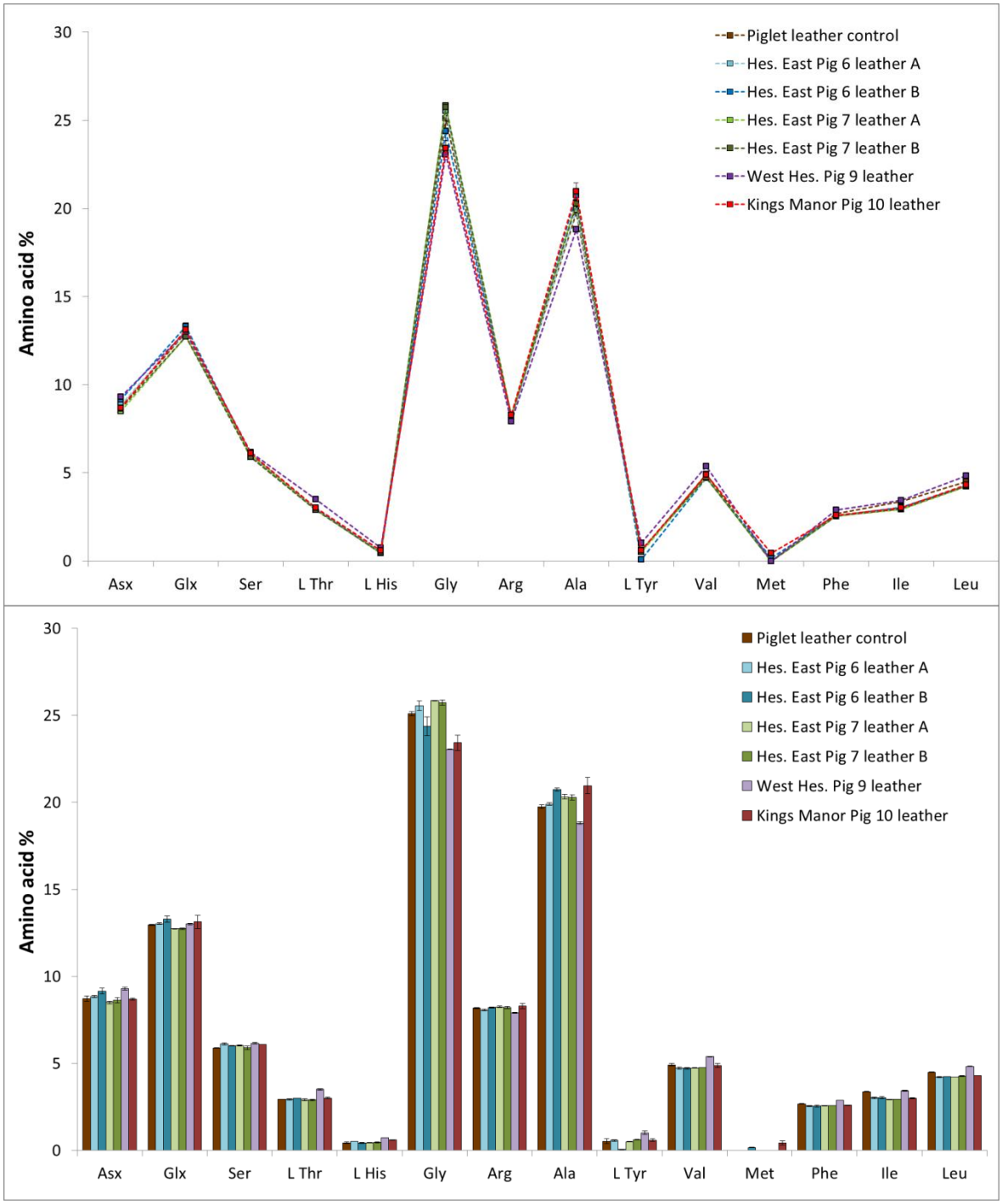

Figure 41. Amino acid compositions for the leather shoes recovered from the piglet burial experiments compared with an unburied sample of the same leather. Error bars represent +/- 1 standard deviation; n=3 for theunburied control leather and n=2 for the experimental samples.

4.4.2.2 Amino acid D/L values

The D/L values for the buried leather samples are shown in Figure 42. With the exception of Val, Heslington East Piglet 6 leather A shows consistent increases in D/L values that are greater than all of the other buried leathers. This suggests that this burial environment may have led to faster rates of racemisation or that many more terminal amino acids were generated, leading to more sites at which the amino acids can racemise. Chemical hydrolysis could have resulted in the scission of the amino acid chains of the constituent proteins and is a reported pathway for the decomposition of archaeological leathers (Larsen, 2008). There is little difference in the amino acid compositions of this material and that of the unburied leather. If biologically mediated degradation is the cause it must have degraded all tissues and proteins uniformly and in a similar fashion to the fungal tunnelling mentioned in the analysis of the buried hair (Section 3). The fact that the D/L values are increased for one of the leather samples from piglet 6 and not the other is an interesting observation. It implies either that an isolated microbial colony lived in the area of shoe A and did not spread to shoe B, or that there were minor fluctuations in the chemistry or hydrology of the burial, allowing one shoe to be chemically degraded and not the other.

Whereas differences in the amino acid compositions of the leather buried with piglets 9 and 10 from that of the control were observed (Section 4.2.1) the D/L values only differ for the piglet 9 material. The similarity of the extent of racemisation in piglet 10 leather to the material from the other burials suggests that either the burial environment limited racemisation of newly generated terminal residues or that degradation occurred shortly prior to the material being excavated; the -20°C storage temperature would have effectively arrested any further conversion of L form amino acids to D form.

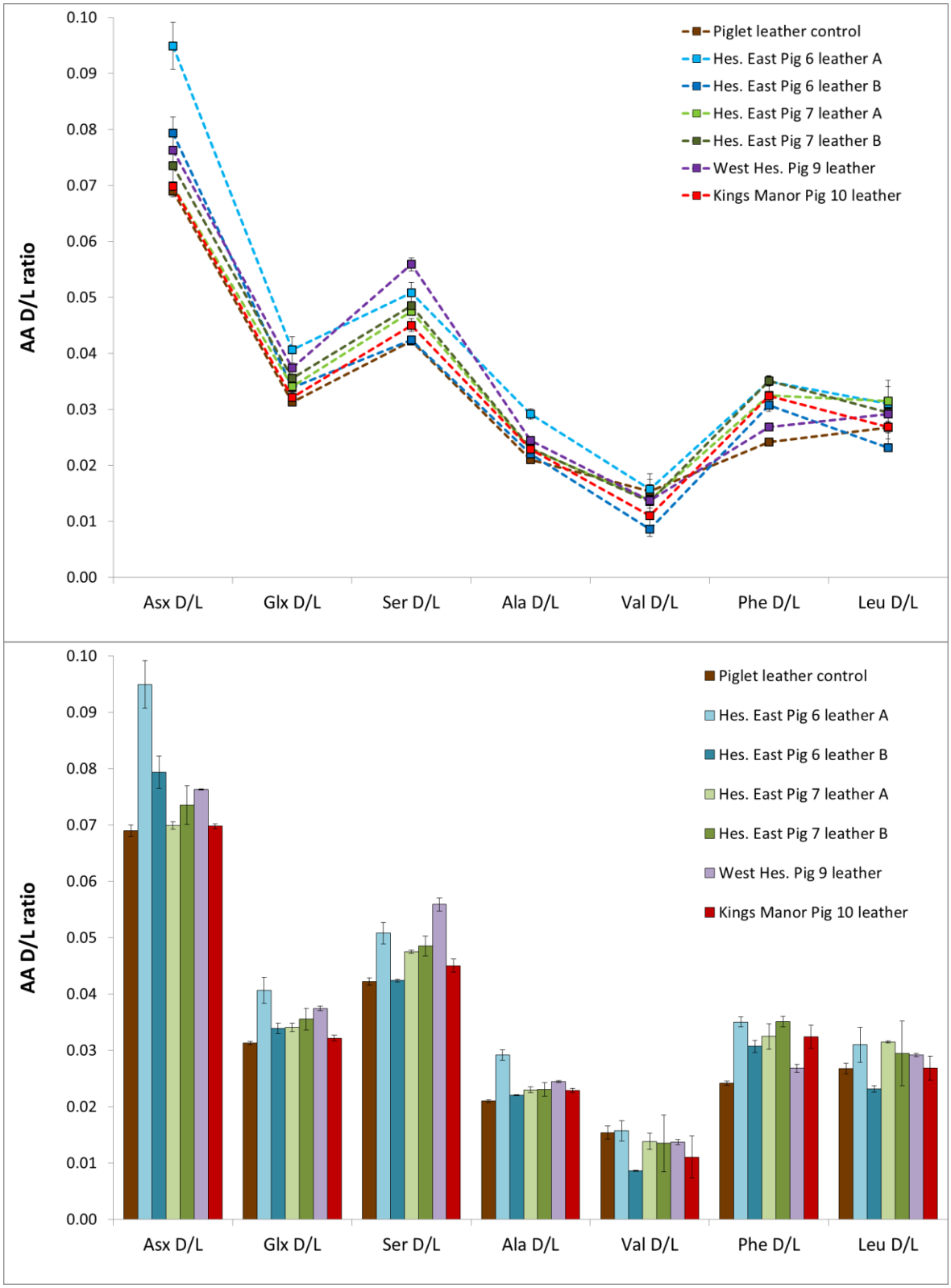

Figure 42. Selected amino acid D/L values for the leather shoes recovered from the piglet burial experiments compared with an unburied sample of the same leather. Error bars represent +/- 1 standard deviation; n=3 for the unburied control leather and n=2 for the experimental samples.

4.4.3 Summary and conclusions

From a chemistry perspective, the degradation of leather is far less well understood than that of wood and hair, hence the interpretation of the RP-HPLC data is limited. The data do, however, suggest that the leathers recovered from piglets 6, 9 and 10 have undergone limited extents of decay. The substantial increases in the D/L values of only one of the Heslington East piglet 6 shoes suggests that acute differences existed in the burial matrix that allowed one leather item to be preferentially degraded.

It is well documented that modern leather items buried in forensic contexts undergo very little degradation; the chromium tanning methods impart an increased resistance to decay compared with tanning with plant extracts as was common of antiquity (Strzelczyk *et al.*, 1987; Janaway, 2001). The results from the leather buried with the piglets substantiates the reported findings as the three year burial period resulted in little decomposition of these materials.

4.5 Limitations of the burial experiments

Woollen textiles were the most abundant form of textile found by the InterArChive team during the collection of archaeological samples. The piglet burials were conducted prior to the sampling of archaeological grave soils and, as a result of this, no woollen materials were buried with the piglets. The lack of any buried wool highlights the need for extensive literature research when planning experimental burials, as their lengthy duration often precludes further or repeat burials based on the results of post excavation analyses.

Bags in which foodstuffs and grave goods were buried were believed to be made from muslin (D. Brothwell, personal communication, 2014). When analysed by Py-GC-MS following their excavation, none of the pyrograms were found to contain any compounds produced by cellulose, the dominant biopolymer found in cotton from which muslin is made (Riello and Parthasarathi, 2011). Instead, a range of synthetic compounds were present, the most intense signatures were from benzoic acid, vinyl benzoate, biphenyl and ethylene glycol dibenzoate. These pyrolysis products are characteristic of polyethylene terephthalate (PET), a man made polymer which is commonly referred to as polyester when used in textile applications (Rosato *et al*., 2004; Tsuge *et al.*, 2011). Given the fact that no unburied control 'muslin' was retained, it cannot be ascertained as to whether the buried material was wholly man made or a blend of cotton and synthetic fibres, the former having degraded during the period of burial. As a result of this, conclusions cannot be drawn on the degradation of this material in the burial experiments, and the analysis of this material was discontinued. This issue draws attention to the vital need for certainty of the identity of the materials buried. Ideally, any buried materials should be analysed prior to burial to confirm their composition in order to prevent such problems arising. At the time that the burial experiments were set up however, the analytical instrumentation required for any preburial analysis of the textile was not in place.

4.6 Conclusions

Although the piglet burial experiments have provided insights into the early stages of degradation of wood, hair and leather in different burial environments, the usefulness of this data has been limited by several factors. These include: different wood types being used for the construction of the piglet coffins, which resulted in not having an unburied control for the majority of the buried wood samples; no wool being included in the burial inventories; and a synthetic material being buried in place of cotton, or 'muslin'. The extractable residues remaining in the soils from the degradation of the piglets, however, did give useful insights into the degradation of mammalian tissue and the resultant chemical signatures imparted on the burial matrix (Hicks, 2017).

A major lesson learned from the analysis of the materials buried with the piglets is, therefore, the need for careful research and planning prior to conducting experimental burials. The inclusion of woollen textiles in the piglet burials would have complemented the analyses of textiles recovered from the archaeological inhumations. Whilst the human hair served as a useful proxy to wool, the subtle differences in the chemical and physical composition makes detecting any minute changes over the relatively short burial period difficult, and means that the observed changes may not be transferable to the archaeological textiles analysed in the later chapters of this thesis.

The issues of the 'muslin' being polyester, and the wood being a mix of varieties and being modified by modern treatment methods could be avoided in future burial experiments by analysing the materials using the analytical techniques intended for the post excavation analysis of the objects. Future burial experiments must have a much clearer understanding of the materials being buried to maximise the information that will be gained from such a large investment of time and resources.

Modifying these burial experiments to make them more relevant to the archaeological materials would involve burying materials that have been processed using methods similar to those employed in antiquity. Leather tanned with a range of plant derived tanning agents (such as vegetable and oak bark extracts) would be better than those used in the burial experiments, which were treated with chromium compounds. Wooden coffins for future burials should be made using historically accurate building techniques and incorporate both angiosperm and gymnosperm woods of known species, with the identity of each wood face known and unburied controls kept in suitable conditions for each wood. This will enable the decay of both angiosperm and gymnosperm woods in all of the planned burial environments to be studied, with comparisons made between the two types. The woods should be treated in a similar manner to those found in the burial record and not using modern methods, which will undoubtedly lead to different degradation trajectories to the coffin woods excavated from archaeological burials. A range of different burial times would also be prudent, with the longest period of interment being

more than the three years of the study discussed in this chapter. All of these issues highlight the difficulty of conducting burial experiments on a research-project timescale. Lab-based degradation experiments may have, in hindsight, been more appropriate. Previous studies have employed microcosm burial experiments conducted in the laboratory to regulate and monitor variables including soil type, mineral and oxygen content, temperature, hydrology and pH within the burial environment (Lillie and Smith, 2007; Gelbrich *et al*., 2012; High *et al*., 2016).

The recovery of human hair from only the West Heslerton site could suggest that of the burial environments studied, dry, sandy soils hold the most potential for preserving keratin based materials. It could also be interpreted to indicate that recovery of such fine materials from archaeological burials is unlikely in soils that are not sandy, with more loam or clay rich soils adhering to the material and preventing it from being detected during excavation. If either of these theories are correct, finding traces of human hair (and possibly woollen textiles) from archaeological sites with soils that are highly aggregated may be less likely than in looser soils.

The pyrolysis analysis of the piglet coffins revealed that limited but observable degradation occurred within the three year burial period. The chemically induced degradation of the piglet 2 coffin demonstrates that burial environments with extremely high pH can lead to rapid and severe damage to buried wood. Overall, the limited biological degradation indicates that the complete mineralisation of a buried coffin takes far longer than three years; this is unsurprising given that coffins are often found during the excavation of recent archaeological burials (see Chapter 1.1.2.1 and Chapter 5). The observation of multiple organisms decaying the Hovingham piglet 1 coffin highlights the diversity of soil biota. Through its pH, oxygen levels, mineral concentrations and water content, the chemistry of the burial environment can prevent, facilitate or directly cause the decay of buried woods.

CHAPTER 5

ANALYSIS OF ARCHAEOLOGICAL WOOD

5.1 Introduction

The focus of this chapter is the analysis of wood fragments recovered from archaeological burials, obtained from seven sites across Northwestern Europe (see map in Figure 43), with burial matrices ranging from predominantly well drained sand to completely waterlogged environments. One aim of analysing these materials was to identify the woods, with the hopes of providing information that would aid in the interpretation of the archaeological sites. The chemical and physical preservation states were also investigated, the aim being to examine what information regarding degradation modifications, degradation agents and the conditions within the burial environments could be deduced.

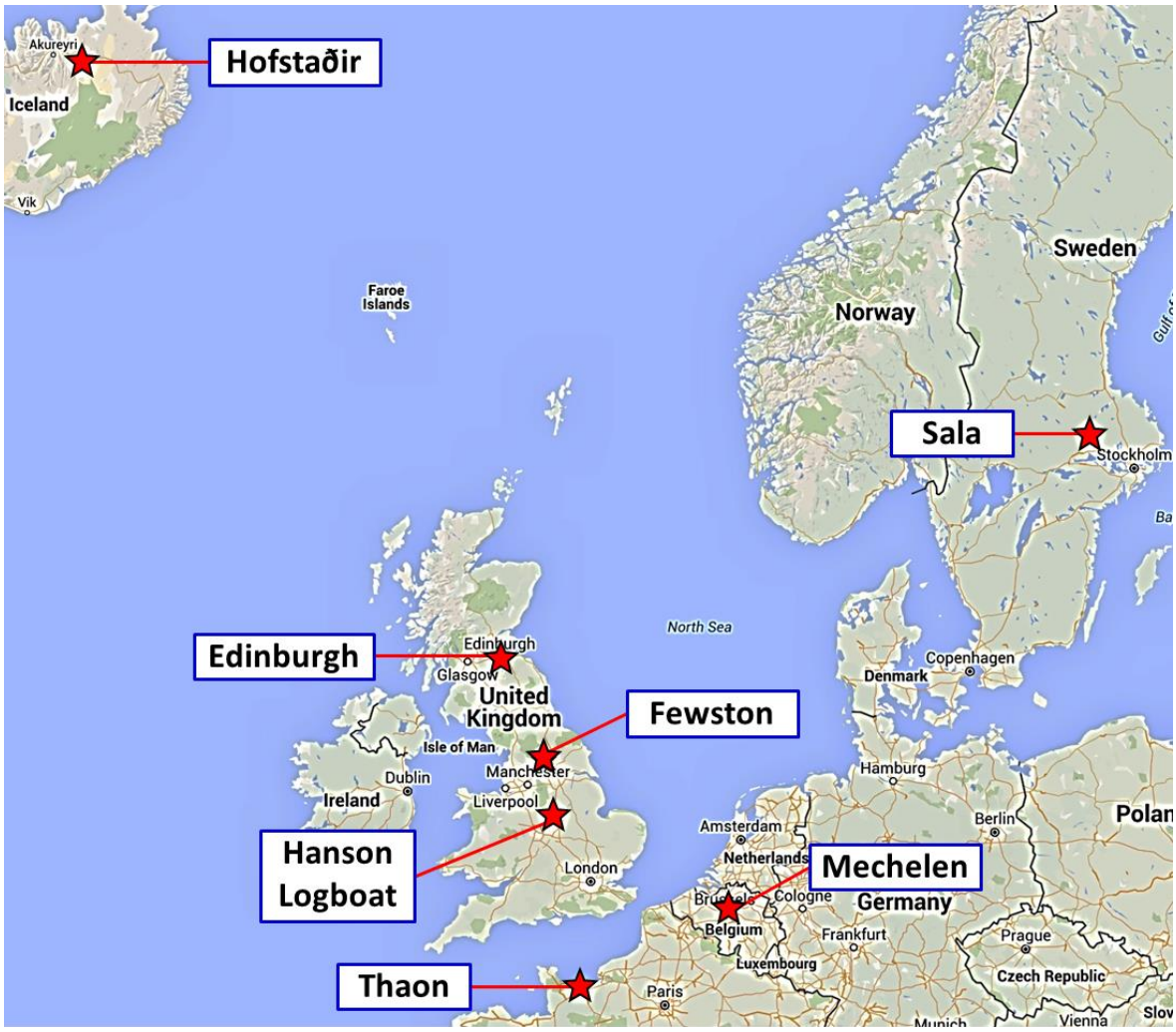

Figure 43. A map of Northwest Europe showing the sites from which archaeological woods were sampled as part of the InterArChive project.

The wood samples were prepared and analysed using a range of appropriate techniques (detailed in Chapter 3), including: analytical pyrolysis (Py-GC with FID and MS detection) to examine the cellulose, hemicellulose and lignin components of the wood; SEM to study the microstructure of the wood; and EA in a limited number of cases where it was though that this technique would

complement the data already obtained using pyrolysis, or where it was reasoned that materials other than holocellulose and lignin were present.

Several ‘coffin stains’, soil that is commonly believed by archaeologists to be the site of degraded wooden coffins, were also analysed. Postholes are a similar cut feature, often interpreted as sites where wooden posts were buried to support a larger aboveground structure (Drewett, 2011). Oonk *et al*. (2009) provide the only report of any previous analyses being performed on soil stains thought to be derived from the decomposition of wooden objects. Their investigation (focussed on inorganic analyses) found no lignocellulose components. The aim of analysing these soil stains was to examine the widely held belief that such soil features are caused by the remains of decayed wood. The presence of chemical signatures that are definitively relatable to wood would provide the first chemical evidence to contribute toward the understanding of the provenance of ‘coffin stains’.

5.2 Edinburgh

5.2.1 Site and sampling information

In the summer of 2009, during the construction of a new tram system in Edinburgh, groundworks in Constitution Street, Leith (latitude: 55.971814, longitude: -3.169501) uncovered human remains that lay within the original boundary of the graveyard of South Leith Parish Church. The graveyard dates back to the first half of the 15th century. Constitution Street was built in 1790 to give improved access to Leith harbour. The building of the road led to the contraction of the graveyard boundary to that seen in Figure 44 and the remains outside the new footprint were built over. The area is built on an ancient dune system, the burial matrix at the site being free draining sand (Spanou, 2012).

The InterArChive team collected samples from the remains of three coffined burials at the Leith excavation. SK434 lay supine in area 6 (Figure 44) with the head facing north east. The skull, cervical vertebrae and part of left shoulder were exposed; the rest of skeleton was beyond the limit of excavation to the south east and was left buried (Spanou, 2012). The remains of the sides and the lid of the coffin were present but very fragile and only traces of the coffin base had survived. The wood was notably thin, suggesting a low status or low cost burial. SK749 was a supine inhumation in area 8 with the skull facing south. Much of the coffin was present although in places only stained soil remained. The age of the individual was determined to be 'adult' but no definite sexing was possible. SK758 was a supine burial also in area 8. The skull and right arm were missing and only the left humerus was present. The bone was in an advanced state of decay and was very fragile. Osteological analysis indicates that the remains are of a juvenile, the estimated age being 2 years. Very little of the coffin remained; the few fragments that were found were extremely fragile. Samples of the remaining coffin wood were taken from each of the three burials. SK749 also presented several areas of stained soil, the locations of which suggested them to be the remains of a coffin that had mostly decayed during the period of burial. A sample of this material was also taken for analysis.

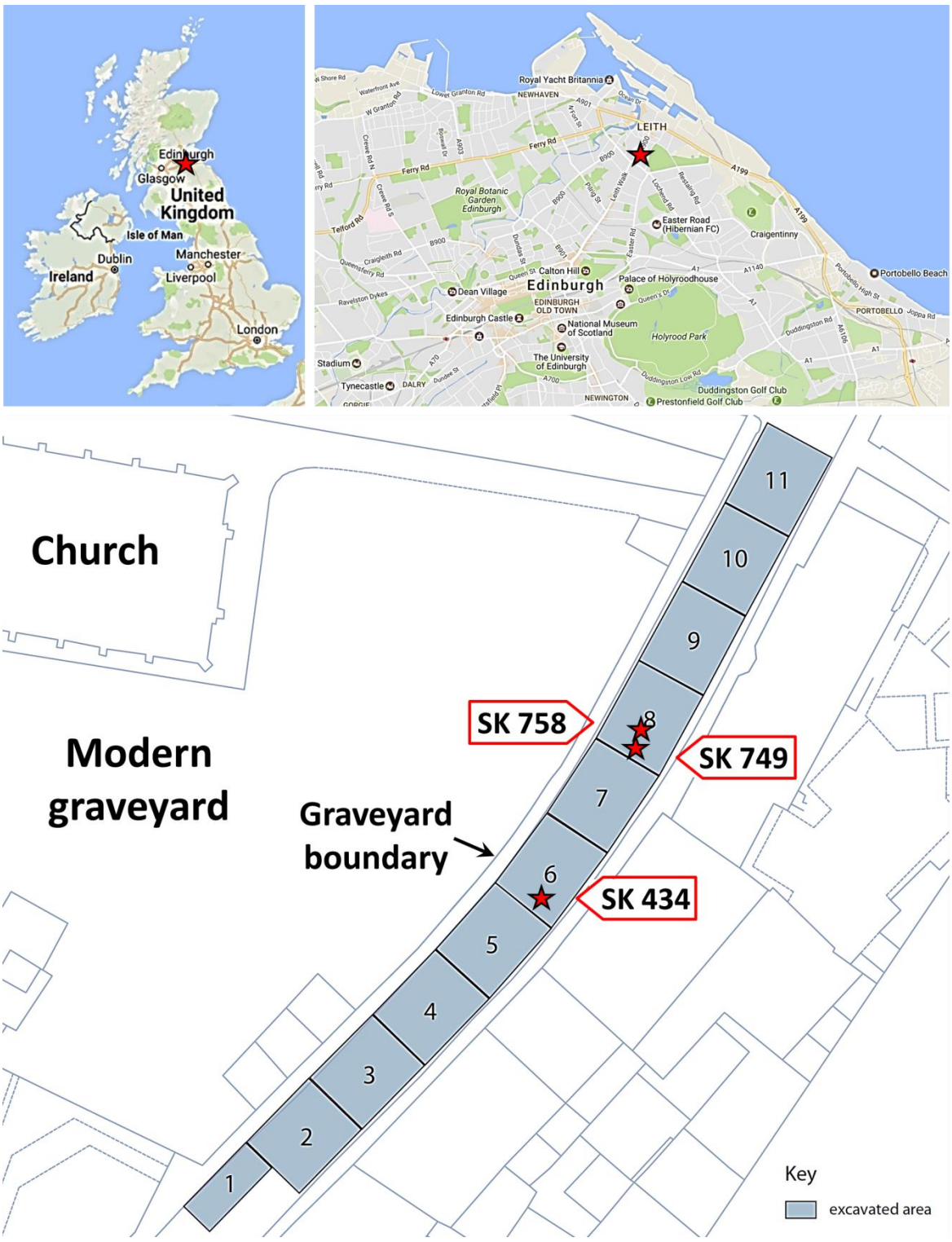

Figure 44. A map showing the area surrounding the excavation site in Edinburgh (top) and a plan of the excavation on Constitution Street in Leith, showing the location of graves 434, 749 and 758 (bottom; adapted from Spanou, 2012).

5.2.2 Analysis of archaeological material

5.2.2.1 Py-GC

The thin wood sampled from grave 434 produced a pyrogram with no syringyl subunits, indicating that it is softwood, from a gymnosperm tree. The profile showed a complete absence of components resulting from the pyrolysis of holocellulose, suggesting its complete decay. The guaiacyl lignin sub units were significantly defunctionalised with a higher proportion of demethoxylated lignin subunits and a larger predominance of short compared with long chain subunits than in the modern pine analogue (Figure 45). White rot fungi as well as several strains of bacteria native to soil environments are known to degrade both lignin and holocellulose in woods by demethoxylation and hydrolysis, respectively (Blanchette, 1991; Blanchette, 2000; Martínez *et al*, 2005).

The pyrograms of the fragile and scattered remnants of coffin wood from grave 758 contained few peaks that were identifiable as being from wood polymers. Only phenol, 2-methoxyphenol, 3-methoxyphenol and toluene were detected, albeit in very small amounts. Given the lack of any other lignin derived peaks no quantitation was performed of these data sets, and no taxonomic assignment can be made.

In previously reported cases sandy soils have resulted in the excellent preservation of buried organic materials, possibly due to the acidic conditions and the free drainage offered by the matrix that allows the exfiltration of water and inhibits microbial growth (Day and Ludeke, 1993; Rousk *et al.,* 2010). The fact that the burials at Constitution Street had been built over may have compacted the grave soils, altering the hydrodynamics of the sediments and resulting in an increased propensity for degradation of organic materials. Human input to the soils is also a factor that must be considered. The presence of water containing increased amounts of nitrogen containing inorganic compounds has been shown previously to increase the rate of degradation of lignocellulosic materials buried in soils (Scott *et al.*, 1996).

Both the coffin wood and the stained soil from grave 749 display pyrogram peak profiles consistent with that of degraded gymnosperm wood (Figure 46). The coffin wood shows no peaks which indicate that any of the holocellulose remains. The soil stain pyrogram, on the other hand, does contain peaks in the carbohydrate region that match the retention times of those corresponding to furan containing molecules in modern pine, which are characteristic of the thermal degradation products of hemicellulose (Vane *et al*., 2003). Both the carbohydrate and lignin pyrolysis peaks are not present in the soil control pyrogram (Figure 46d), which proves that the signatures of wood observed in the pyrogram of the soil stain are not due to background components that are common throughout the grave soil. With no previous finding of wood

biopolymers in a suspected wood soil stain in the literature, this represents the first reported case.

The compositional differences between the soil stain and the remaining coffin wood suggests the operation of more than one degradation mechanism. The extent of lignin degradation and the survival of some carbohydrate in the coffin stain may be indicative of attack by of non-lignin preferring white rot fungi (Blanchette, 1991; Blanchette, 2000).

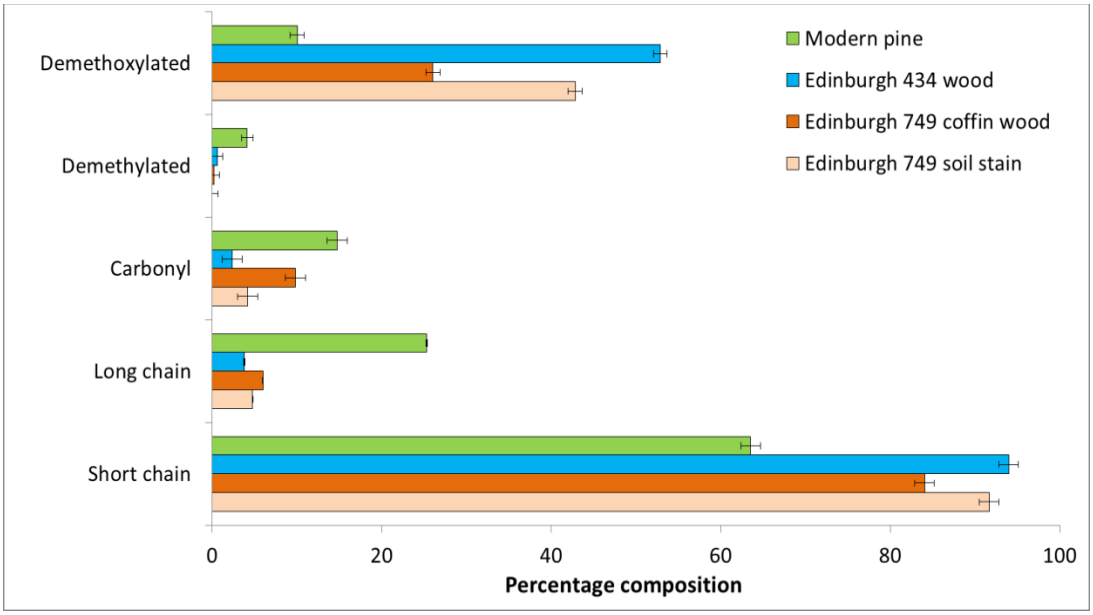

Figure 45. Percentage compositions of demethoxylated, demethylated, carbonyl, long chain and short chain compounds in modern pine, the coffin woods from graves 434 and 749, and the soil stain in grave 749 at Edinburgh (see Table 11 for compound classifications). Values are calculated as a percentage of the total area of lignin derived peaks in Py-GC-FID pyrograms. Error bars represent +/- standard deviation and are the standard error calculated in Chapter 3, based on n=3 replicates of an archaeological gymnosperm wood.

Table 11. Classifications of the detected compounds resulting from the pyrolysis of gymnosperm woods.

Compound	**Classification**
Toluene (T)	Demethoxylated/short
Phenol (P)	Demethoxylated/short
2-Methylphenol	Demethoxylated/short
3-Methylphenol	Demethoxylated/short
Guaiacol (G)	Short
4-Methylguaiacol (G1)	Short
Catechol (C)	Demethylated/short
4-Ethylguaiacol (G2)	Short
4-Vinylguaiacol (G3)	Short
4-Allylguaiacol (G4)	Long
4-Propylguaiacol (G5)	Long
4-Formylguaiacol (G6)	Carbonyl
trans-Isoeugenol (G7)	Long
4-Acetylguaiacol (G8)	Carbonyl
Vanillic acid-methyl ester (G9)	Ester/long
Guaiacylacetone (G10)	Carbonyl/long
cis-Coniferyl alcohol (G11)	Long
Guaiacylpropanol (G12)	Long
trans-Coniferyl alcohol (G13)	Long
Coniferyl aldehyde (G14)	Carbonyl/long

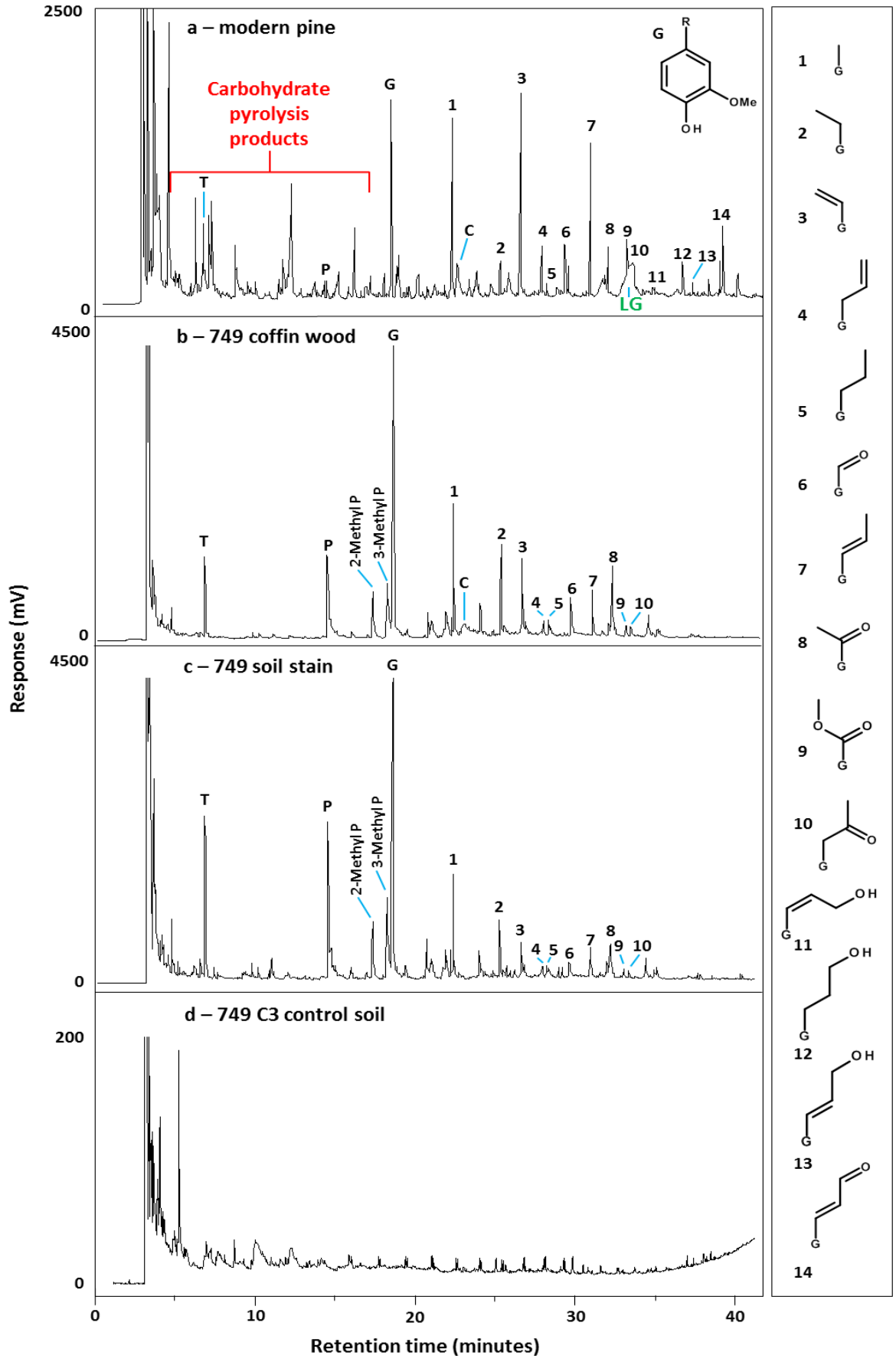

Figure 46. Assigned partial Py-GC-FID pyrograms of the coffin wood and soil stain from grave 749 at the Edinburgh excavations. a – modern pine wood, b – a representative sample of coffin wood, c – an example of the soil stains analysed that were thought to be due to degraded coffin wood, d – C3 control soil from the

grave. T = toluene, P = phenol, G = guaiacol, C = catechol and LG = levoglucosan (a cellulose pyrolysis product). The identities of the numbered peaks are shown in the key to the right of the pyrograms.

5.2.2.2 SEM

Analysis by scanning electron microscopy (Figure 47) shows the coffin wood from grave 749 to be in an advanced state of decay. A large proportion of the material displays no structural resemblance to that of wood. Some of the cell structure is still distinguishable in the cross sectional cuts, but the tracheid cells that remain have undergone intensive compression into dense wafers of the remaining cell wall material. This may be due to compaction of the burial matrix by the building work of the above street.

The secondary cell wall layers are no longer present (Rowell and Barbour, 1990), which fits with there being no detectable holocellulose in the analytical pyrolysis. What remains is a lignin rich skeleton of middle lamellae and primary cell wall layers. The lignin rich middle lamella observed under SEM appear relatively intact, despite the lignin component differing chemically from that of modern pine. This suggests that the decay agent was primarily able to degrade the holocellulose and the modification of the lignin component is a secondary effect. Many microorganisms (such as soft rots, brown rots and a wide range of bacteria) are able to degrade the cellulose component of wood but are not capable of producing lignolytic enzymes; their attack of the carbohydrate results in modification but not complete decomposition of the lignin (Blanchette et al., 1991; Blanchette, 2000; Martinez et al., 2005; Sánchez, 2009).

The coffin wood and the soil stain from grave 749 both have different degrees of lignin modification and the stain still contains residual hemicellulose. It was reasoned on the basis of the Py-GC data (in Section 2.2.1) that the two materials were degraded by different types of grave microfauna. If this is indeed the case then – based on the SEM evidence – lignin degrading microorganisms were far less prevalent in the wood, the carbohydrate degrading microfauna being much more active and mediating the complete attrition of the holocellulose to leave a lignin rich skeleton (Blanchette, 1991; Blanchette, 2000).

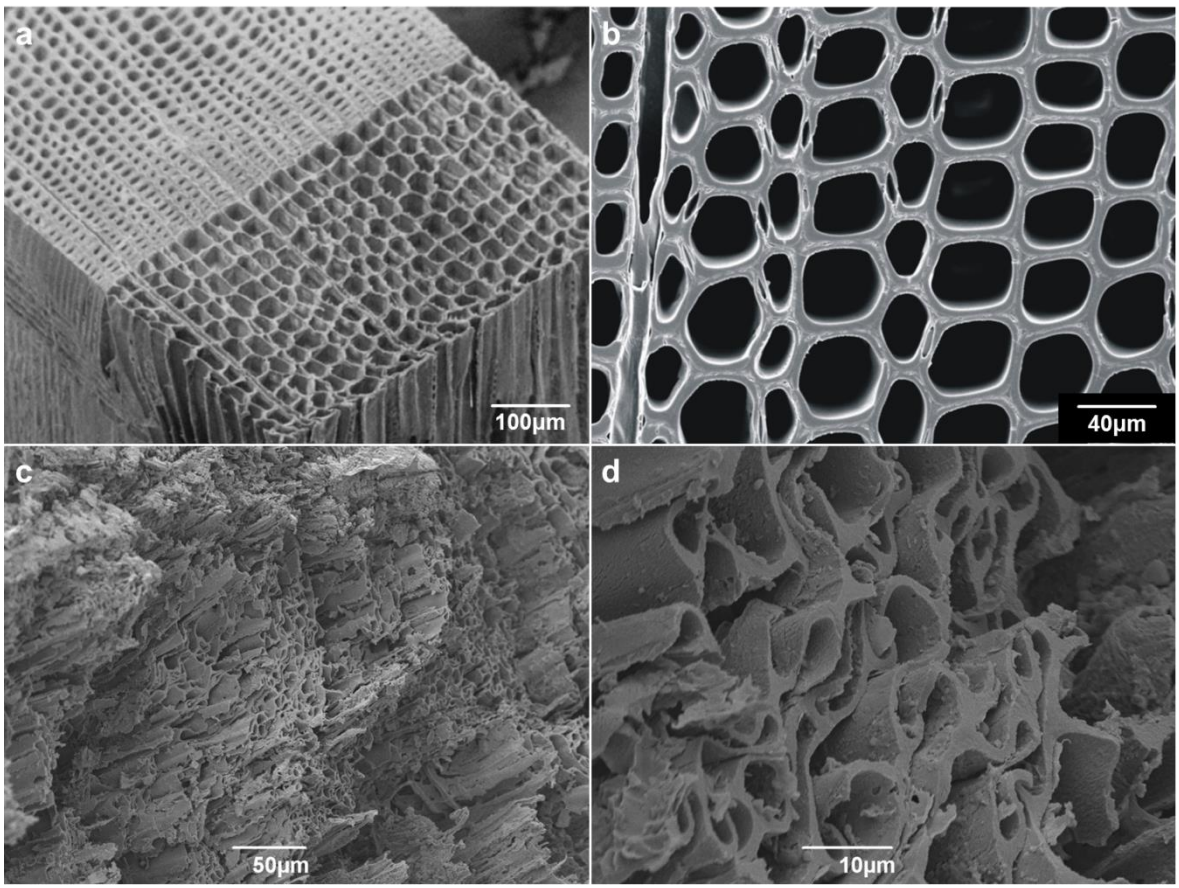

Figure 47. SEM images of modern pine wood (a – image from Radboud University, Dept. of Biology online reference collection; b – image from Hori et al., 2014) and coffin wood from grave 749 at the Constitution Street excavation in Edinburgh (c and d). The left image (a) shows a cross sectional slice of the wood. The right image (b) is a closer view of the cross section, showing attrition of secondary cell wall components and subsequent structural collapse.

5.2.3 Summary and conclusions

The wood from grave 434 is softwood, showing no presence of syringyl lignin subunits. The holocellulose polymers are completely decayed and the lignin is heavily modified by demethoxylation and depolymerisation. This damage to both the holocellulose and the lignin is likely the result of the action of white rot fungi or a range of soil bacteria (Blanchette, 1991; Blanchette, 2000; Martínez *et al*, 2005).

The fragments of wood from grave 758 produced only peaks characteristic of phenol, methylated phenols and toluene on pyrolysis, most likely to be the result of extreme modification and depolymerisation of the original lignin. As a result, no taxonomic assignment could be made. Congruent with the physical condition, the wood is chemically very degraded.

The coffin wood from grave 749 has a lignin profile consistent with that of degraded gymnosperm derived wood and has no remnant holocellulose. SEM reveals advanced physical decay; the majority of the tracheids being crushed and wafer like. The secondary cell wall layers are completely decayed, concordant with the lack of cellulose and hemicellulose derived peaks observed during pyrolytic analysis. The intact middle lamellae suggest that the holocellulose digestion was accompanied by limited modification of the lignin, suggesting the microorganisms responsible were not capable of direct lignin metabolism.

The soil stain from grave 749 has a detectable lignin content that is similar to that of the coffin wood, indicating that a gymnosperm wood once occupied the space now filled by the stained earth. The wood and the stain have different degrees of lignin modification and – unlike the coffin wood – the stain still contains residual hemicellulose. The differences in chemical and physical preservation state between the two materials suggest that the decay was mediated by two different types of microbes. The preferential lignin degradation with limited holocellulose degradation seen in the stain is characteristic of some white rot fungi (Blanchette, 2000).

With no previous reports in the literature, the finding of wood biopolymers in a soil stain is the first reported case. This demonstrates that Py-GC can be used to aid with the interpretation of soil colouration when the cause of staining is suspected to be the degradation of wooden objects.

The advanced decay of the wood is unusual, given that sandy soils typically aid in the preservation of organic materials (Day and Ludeke, 1993; Rousk *et al.,* 2010). Given the compression of the decayed wood tracheids seen in the SEM of wood from grave 749, compaction of the burial matrix is likely to have contributed, altering the hydrodynamics of the matrix and producing conditions that better support microbial growth. The decomposing human remains combined with the human activity in the street above may have increased the inorganic nitrogen content of the soil, conditions which enhance decay of buried lignocellulosic materials (Scott *et al.*, 1996).

5.3 Fewston

5.3.1 Site and sampling information

During March and April of 2010 an excavation was carried out to recover buried remains from graves in the construction footprint of a new Heritage Centre attached to the church of St Michael and St Lawrence at Fewston, North Yorkshire (latitude: 53.982745, longitude: -1.704312; Figure 48). A total of 163 sets of human remains were found and removed from graves in the churchyard (Buglass, 2010). The temporal range of the burials was from the church's founding in the 14th century through to the last recorded burial in 1921. The burial soils are well drained coarse loamy soils that lie atop Namurian millstone grit of the Upper Carboniferous period (Buglass, 2010).

The InterArChive team collected wood samples from the remains of two coffined burials. Wood was collected from the grave of SK271, heavily degraded skeletal remains on the western boarder of the cemetery excavation. Neither the age nor the sex of the individual were able to be determined. The burial was relatively shallow at 172.84 cm in depth. Very little remained of the coffin; only very fragile wood remnants persisted and were collected for analysis by TD/Py-GC.

SK310 was the remains of an elderly female, identified by parish records as Mary Dickinson who died on the 6th March 1886, aged 66 years. The skeleton was very well preserved and in the remains of a wooden coffin. The depth of the burial was not recorded. Several copper alloy nails that formed part of the coffin fixtures were still embedded in large fragments of wood. A section of wood with one of the copper pins still embedded was taken for analysis. The wood surrounding the coffin nail was soft and spongey at the top of the nail and firm at the bottom of the nail. Subsamples of material from both the top and bottom were taken for analysis by TD/Py-GC and SEM. A small sample of the coffin wood not in proximity to the nail was also analysed by TD/Py-GC.

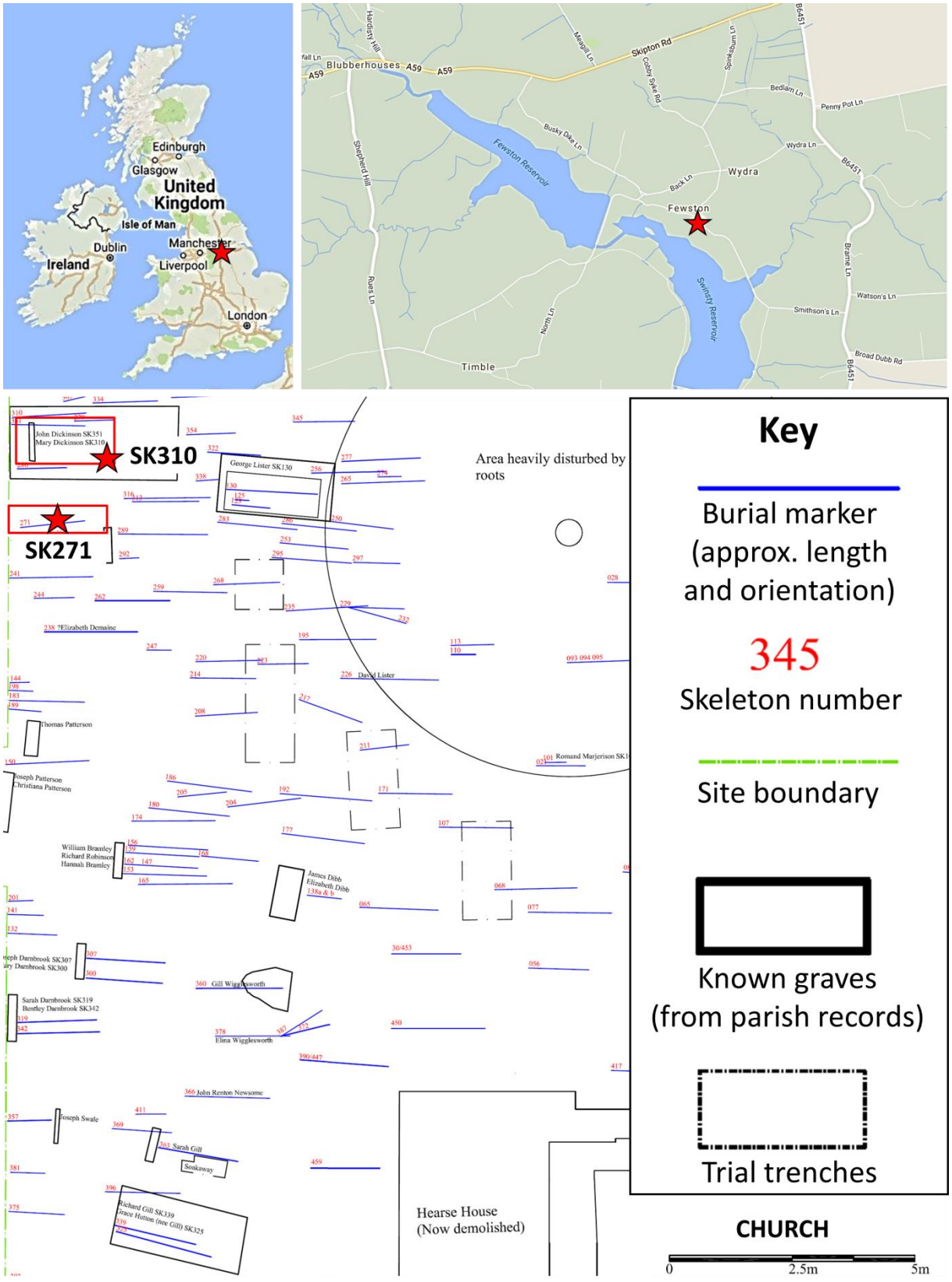

Figure 48. A map showing the area surrounding Fewston (top) and a plan of the excavation at showing the location of graves 271 and 310 (bottom; adapted from Buglass, 2010).

5.3.2 Analysis of archaeological material

5.3.2.1 Py-GC

Despite the materials from grave 271 having the physical appearance of wood none of the samples contain any peaks that could be assigned to compounds resulting from the pyrolysis of holocellulose or lignin biopolymers. The wood has completely degraded, leaving behind a mineralised pseudostructure. Interestingly, the osseous remains were also very heavily decayed (Caffel and Holst, 2010), which indicates that conditions within the burial environment were conducive to the extensive decay of organic materials. The conditions that led to the damage of the skeletal components could have also induced extensive degradation in the wood of the coffin.

The pyrogram of the wood from the base of the coffin in grave 310 (Figure 50b) shows only peaks corresponding to guaiacyl lignin, indicating that the wood used in the construction of the coffin is of wood from a gymnosperm tree. The presence of a levoglucosan peak and peaks with similar retention times to those found in the carbohydrate region of the modern pine indicate that there is significant cellulose and hemicellulose still present in the wood. The lignin of the wood is chemically different from that of the modern pine comparator, evidenced by the predominance of short chain lignin compounds over those with long chains, a lower abundance of carbonyl functionalities and an increase in the amount of demethoxylated lignin phenols (Figure 49). The preferential degradation of lignin, leaving some residual holocellulose, suggests that the wood has been metabolised by a white rot fungus (Blanchette, 1991; Blanchette, 2000).

The two samples from the wood surrounding the copper coffin nail are in very different states of preservation. When compared to the Py-GC data of modern pine (Figure 50a) the spongey wood taken from the top of the nail has fewer carbohydrate peaks, no levoglucosan peak and a very different lignin profile (Figure 50c). No carbonyl and catechol containing compounds were present and very few long chain lignin guaiacols remain: 97.1% short chain to 2.9% long chain, compared with 63.5% to 25.3% found in modern pine. The analysis shows the wood to be in a much more advanced state of decay than the wood from the base of the coffin.

In contrast, the wood from the around the bottom of the nail is in a better state of preservation than both the wood from the top of the nail and from the base of the coffin. Considerable amounts of cellulose and hemicellulose remain (evidenced by the carbohydrate and levoglucosan peaks in Figure 50d) and the sub unit type profile is the most similar to that of the modern pine standard (Figure 49).

The differences in preservation state of the three samples may relate to their relative proximities to the copper nail. The growth and activity of white rot fungi have been demonstrated to be dependent on copper concentration (Levin *et al.*, 2002). Concentrations of up to 1 mM copper

increase the rates of biosynthesis and secretion of key lignolytic enzymes in the white rot species *Trametes trogii*, including manganese peroxidase (MnP), laccase, and glyoxal oxidase (which produces hydrogen peroxide necessary for the function of lignin peroxidase (LiP)). Copper has also been demonstrated to have a strong effect on laccase induction in species including *Phanerochaete chrysosporium* (Dittmer *et al.*, 1997) and *Pleurotus eryngii* (Palmieri *et al*, 2000). Copper concentrations exceeding 1 mM inhibit fungal growth and drastically reduce the production of manganese peroxidase, as well as inhibiting enzymes crucial to many metabolic pathways (Ramsay *et al.*, 1999). The wood from the bottom of the nail, which is least degraded, may have been in close enough proximity to the nail to provide sufficient copper concentrations to retard fungal growth and lignolytic enzyme production and activity. The preservation of perishable organic materials in archaeological burials due to their proximity to copper objects is well documented (Beukens *et al*., 1992; Chen, 1998; Janaway, 2001). The more heavily degraded wood from the top of the nail may have been in an environment with copper concentrations that were not toxic to the fungus, but were sufficient to enhance the growth and lignin metabolism above that of the fungus which degraded the wood from the base, which was not close enough to the nail to experience a higher level of copper ions.

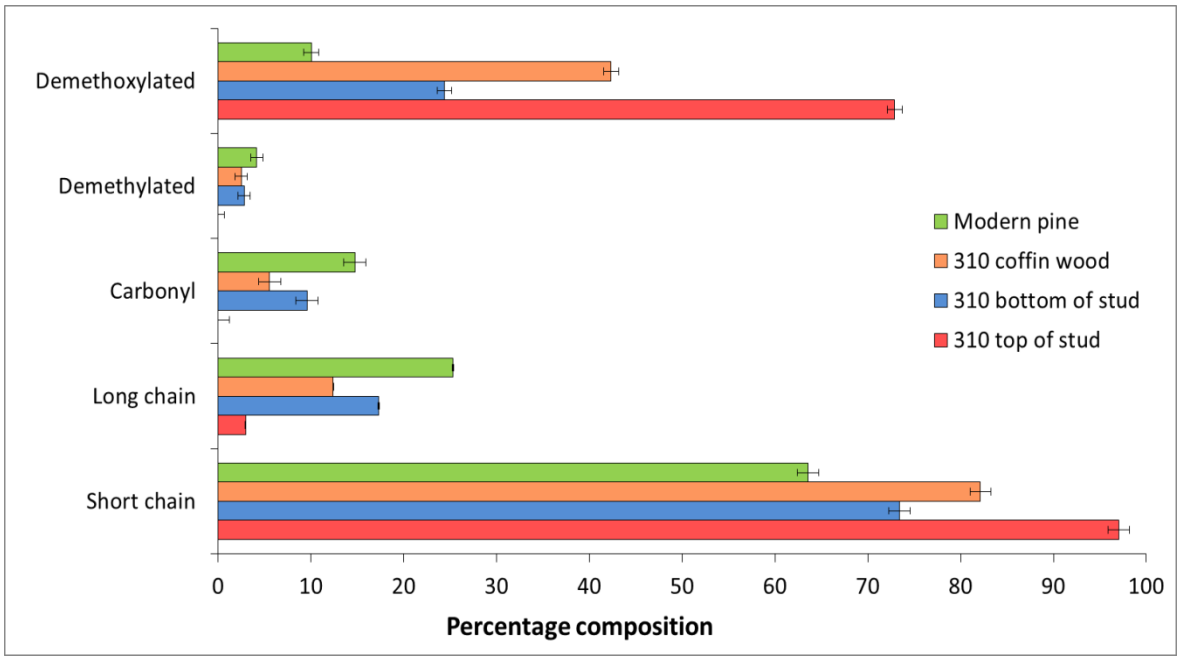

Figure 49. Percentage compositions of demethoxylated, demethylated, carbonyl, long chain and short chain compounds in modern pine, and the coffin woods from grave 310 at Fewston (see Table 11 for compound classifications). Values are calculated as a percentage of the total area of lignin derived peaks in Py-GC-FID pyrograms. Error bars represent +/- standard deviation and are the standard error calculated in Chapter 3, based on n=3 replicates of an archaeological gymnosperm wood.

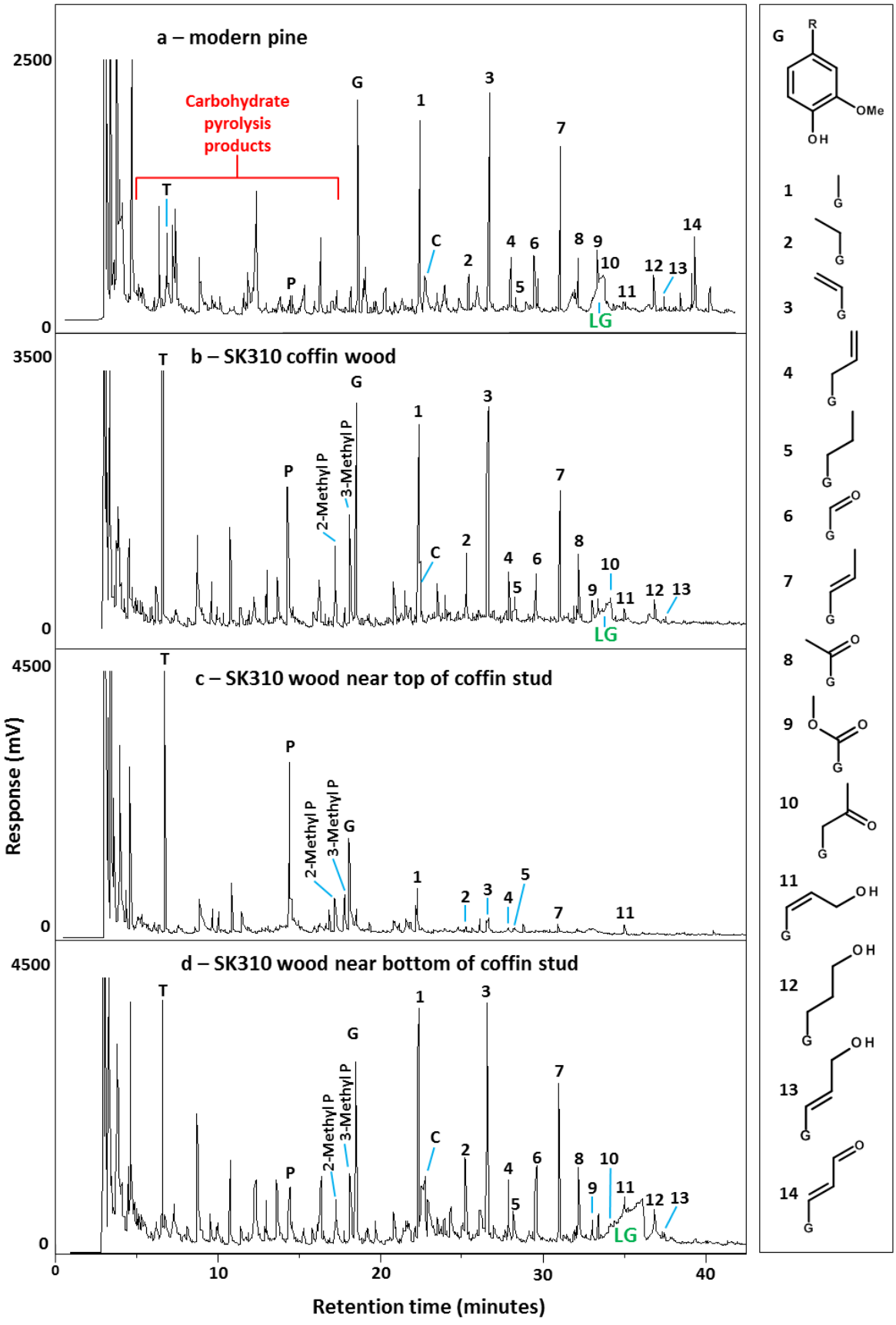

Figure 50 Assigned partial Py-GC-FID pyrograms of the coffin woods from grave 310 at the Fewston excavations. a - modern pine wood, b – wood from the coffin base, c – wood from the top of the coffin nail and d - wood from the bottom of the coffin nail. T = toluene, P = phenol, G = guaiacol, C = catechol and LG = levoglucosan (a cellulose pyrolysis product). The identities of the numbered peaks are shown in the key to the right of the pyrograms.

5.3.2.2 SEM

The wood from the top of the coffin nail in grave 310 appears heavily degraded under SEM (

Figure 51a and b). All cell wall layers are damaged, resulting in the separation of individual tracheid cells following the destruction of the lignin rich middle lamellae. There are many fungal bodies within the wood structure (labelled as F), indicating that the damage to the wood is due to a fungal microorganism. Coupled with the loss of both holocellulose and lignin revealed in the pyrolysis analysis, it is likely that the observed fungal features are the remnants of a white rot fungus that simultaneously degraded all components of the wood.

The wood from the bottom of the coffin nail is in much better condition than that analysed from the top of the coffin nail. The majority of the wood cells appear as those of modern, undegraded pine. Some distortion of the cell shape in the earlywood cells is evident (top right of

Figure 51c) and some swelling of the latewood cells with visible degradation to some of the S_3 cell wall layers. Such features have previously been attributed to attrition of hemicellulose (Hoffman and Jones, 1990).

The variation in preservation state and the prevalence of fungal features between the two wood samples that were only 15 cm from each other indicates that there was a factor involved in the protection of one and not the other. As mentioned in Section 3.2.2 the most likely candidate is the proximity to the copper coffin nail, copper concentration having been shown to enhance or retard the growth and activity of white rot fungi (Levin *et al.*, 2002). The large population of fungal bodies in the wood from the top of the coffin nail indicates that fungal growth was highly favoured in this location, with low enough copper concentrations to support or even enhance fungal activity, whereas the wood at the bottom of the nail was not supportive to the growth of microorganisms, likely due to toxic levels of copper.

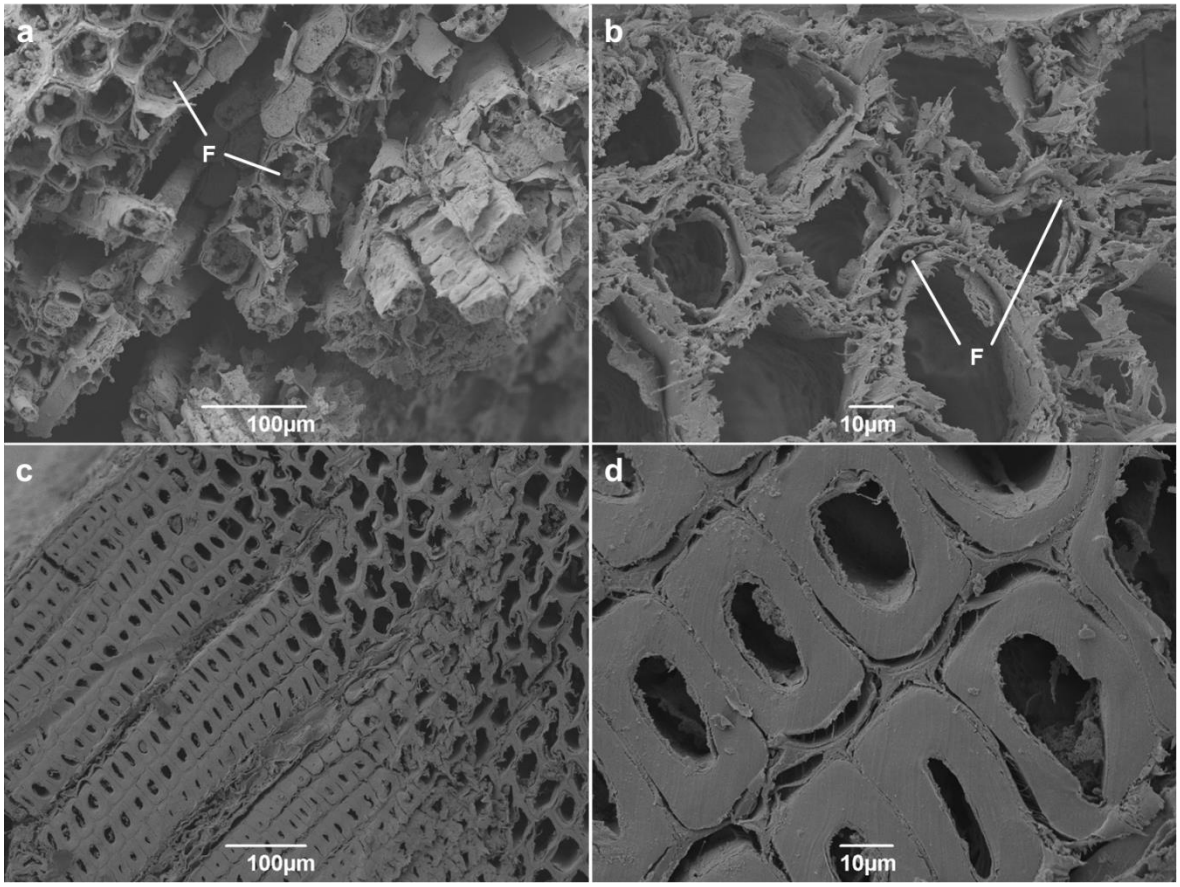

Figure 51. SEM images of coffin wood surrounding the top (a and b) and the bottom (c and d) of the copper coffin nail from grave 310 at the Fewston cemetery excavation. The top images (a and b) show heavily degraded tracheid cells with damage to all cell wall layers and the presence of fungal bodies (F). The bottom images (c and d) show that the wood is in a better state of preservation, with some swelling and damage to the cellulose rich secondary cell wall layers.

5.3.3 Summary and conclusions

Despite its appearance, the material from grave 271 does not contain any of the biopolymers (modified or otherwise) typically found in wood; the wood has completely decayed, leaving behind a mineralised pseudostructure made up of unknown inorganic components. The accumulation of the minerals is likely due to the hydrology of the grave, which has led to mineral rich water flow through and depositing inorganic salts within the burial matrix. The skeleton was also heavily degraded, suggesting that whatever conditions were present in the burial environments were able to facilitate the degradation of a range of materials.

The coffin wood from grave 310 provides strong evidence that proximity to a copper alloy alters the decomposition rates of lignin and cellulose by retarding or accelerating the growth and activity of white rot fungi. Wood from the base of the coffin (not in proximity to the copper nail) shows significant degradation of lignin but still retains the majority of the cellulose and hemicellulose components, preferential lignin degradation being characteristic of certain white rot fungi. Wood near the top of a copper coffin nail has undergone more extensive fungally mediated degradation of both lignin and cellulose, whereas wood from the bottom of the nail is in better condition than that from the coffin base. Copper concentrations up to 1 mM are known to increase the rates of biosynthesis and secretion of key lignolytic enzymes in white rots (Levin *et al.,* 2002), whereas concentrations exceeding 1 mM are mycotoxic, inhibiting metabolic pathways, fungal growth and lignolytic enzyme production and activity (Ramsay *et al.,* 1999). The wood from the top of the nail is likely to have been exposed to sufficient copper concentrations to enhance the degradation by white rot, the material at the bottom of the nail receiving much higher concentrations that severely restricted the activity of the fungus that thrived several centimetres away.

5.4 Hofstaðir

5.4.1 Site and sampling information

The remains of a church and the associated human burials at a site in Hofstaðir, Iceland have been under excavation by a volunteer led project during consecutive summer periods since 1999. The site lies on the banks of the River Laxá at latitude: 65.608613, longitude: -17.162163, 5 km west of Lake Mývatn and 80 km north east of Akureyri, the second largest city in Iceland. The earliest recorded activity at the site is in the late 9th century (Sayle *et al*, 2016). All of the burials are sealed by a tephra layer deposited by the eruption of Mount Hekla around 1300 BC, indicating that the site had become disused before that date. The soil at the site was a histic andosol, rich in basaltic glass from volcanic ash (Sigfusson *et al*., 2008). These soils are acidic, with pH values ranging from 4 to 6, have a fine grain size and are easily compacted, leading to a propensity for water retention and poor drainage (Arnalds, 2004).

The InterArChive team collected samples from several burials during the 2011 summer excavations. Alongside the remains of an adult female, grave 116 contained the remains of several fragments of wood believed to be from the remains of a coffin. Three samples of this wood as well as stained soil believed to be the decayed remains of coffin wood were taken and subjected to TD before analysis by Py-GC. A sample of the wood was also analysed by SEM.

Figure 52. A map showing the area surrounding the excavation site in Hofstaðir (top), a plan of the excavation showing the location of grave 116 (middle left; adapted from Gestsdóttir, unpublished), a photograph of the 2011 excavation showing grave 116 (bottom left) and a photograph of the excavated grave 116, showing the skeletal remains and the locations from which samples were taken (bottom right).

5.4.2 Analysis of archaeological material

5.4.2.1 Py-GC

All of the coffin woods were identified as being from gymnosperm trees; the pyrolysis peaks matching those of modern pine (see Figure 55). This is consistent with the finding of pimaric acid and abietic acid degradation products (dehydroabietic acid and didehydroabietic acid) in the soils of burial 116 (Green, 2013). These compounds are characteristic of resins found in woods of the *Pinaceae* family (Robinson *et al.,* 1987; Colombini *et al.*, 2003). The absence of aromatised terpenoids such as retene is evidence that the compounds were not derived from pine pitch produced by heating and are indeed from pine wood (Serpico and White, 2000; Colombini *et al.*, 2003). This corroborates the findings from the TD/Py-GC analyses that the wood is pine and was not treated with pitch as a preservative.

According to historical records and archaeological evidence the only tree species native to Iceland at the time of Norse settlement in 874 AD were downy birch (*Betula pubescens*), rowan (*Sorbus aucuparia*), and aspen (*Populus tremula*), all of which are angiosperms (Eysteinsson, 2004). Therefore, the wood used in the burial of this individual was either from an isolated or undocumented pine forest, was from driftwood, or was imported. These potential sources of the wood suggest that the individual was of high enough status to warrant a burial in a type of wood that would have been a scarce commodity.

The absence of any peaks that correspond to cellulose or hemicellulose pyrolysates indicates that the holocellulose fraction of the wood has been completely degraded within the burial matrix. Clear differences between the lignin component and that of modern pine wood are also apparent. Guaiacol (G), 4-formylguaiacol (G6) and 4-acetylguaiacol (G8) were all produced in greater relative abundance during the pyrolysis of the archaeological woods (shown in Table 12); all other guaiacyl subunits showed a lower relative abundance.

Table 12. Percentage compositions of guaiacol (G), 4-formylguaiacol (G6) and 4-acetylguaiacol (G8) in modern pine and Hofstaðir grave 116 coffin wood sample A3 (base of coffin between the femurs). Values are calculated as a percentage of the total area of lignin derived peaks in Py-GC-FID pyrograms.

Pyrolysis product	% abundance in modern pine	% abundance in 116 coffin wood
Guaiacol (G)	15.6	24.1
4-Formylguaiacol (G6)	4.3	8.6
4-Acetylguaiacol (G8)	3.9	8.1

The metabolism of lignin sub units by Cα-Cβ cleavage of the propyl side chain is widely reported in the literature as a feature of lignin peroxidase metabolism, a lignolytic enzyme found exclusively in white rot fungi such as *Phanerochaete chrysposporium* (Umezawa *et al.*, 1982; Tien and Kirk, 1984; Tien, 1987; Geib *et al.*, 2008; Bugg *et al.*, 2011a). These reactions (illustrated in Figure 53) lead to the depolymerisation and subsequent oxidation of lignin sub unit side chains, resulting in the production of guaiacol, 4-formylguaiacol and 4-acetyl guaiacol residues bound to the remaining structure (Tien and Kirk, 1984; Tien, 1987; Rencoret *et al.,* 2010). The high contents of short chain and carbonyl containing guaiacyl moieties in the archaeological woods, demonstrated in Figure 54, suggest that such degradation reactions have taken place. Micromorphological analysis of soils from grave 116 also found evidence for fungal activity that was identified to be a white rot fungus (Burns, 2015).

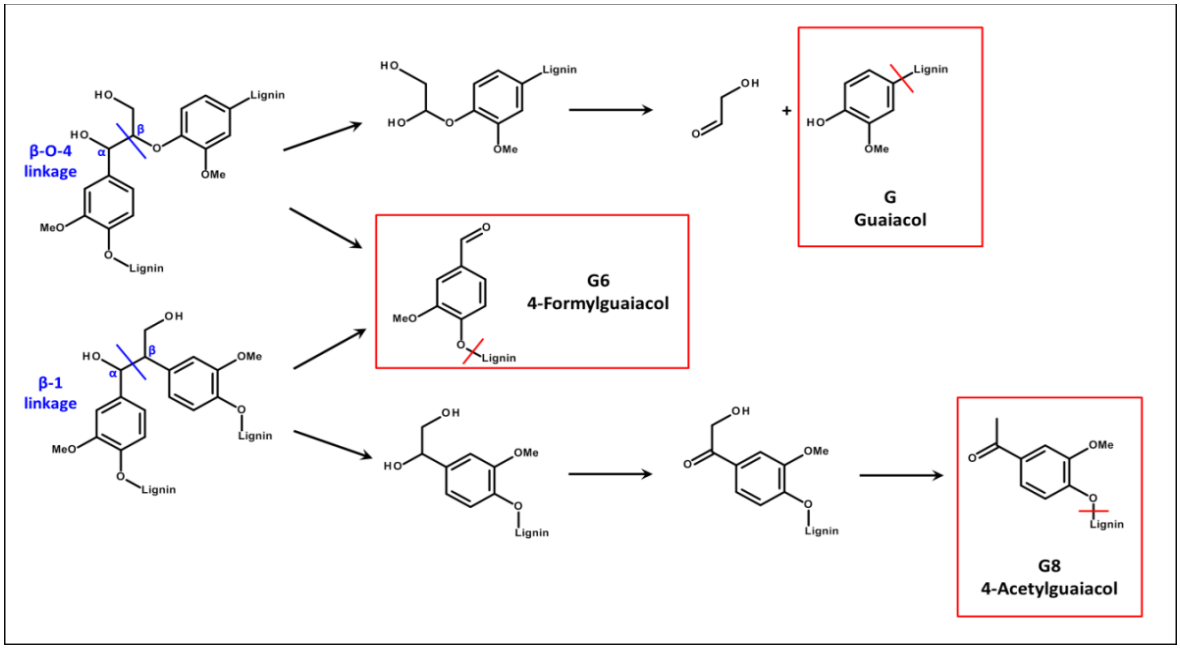

Figure 53. Lignin degradation reactions that proceed by C_{α}-C_{β} cleavage (blue lines) of β-O-4 ether (top) and β-1 (bottom) sub unit linkages with simultaneous hydroxylation of C_{β} followed by oxidation. The red lines represent bonds broken during pyrolysis (Tien and Kirk, 1984; Tien, 1987; Rencoret et al,, 2010).

The coffin woods from Hofstaðir also have a higher relative abundance of demethoxylated guaiacyl sub units than the modern pine standard (Figure 54). These phenols have been shown to be produced as a result of microbially mediated enzyme catalysed demethoxylation of guaiacyl subunits (Martínez *et al,*, 2005), another marker of lignin degradation.

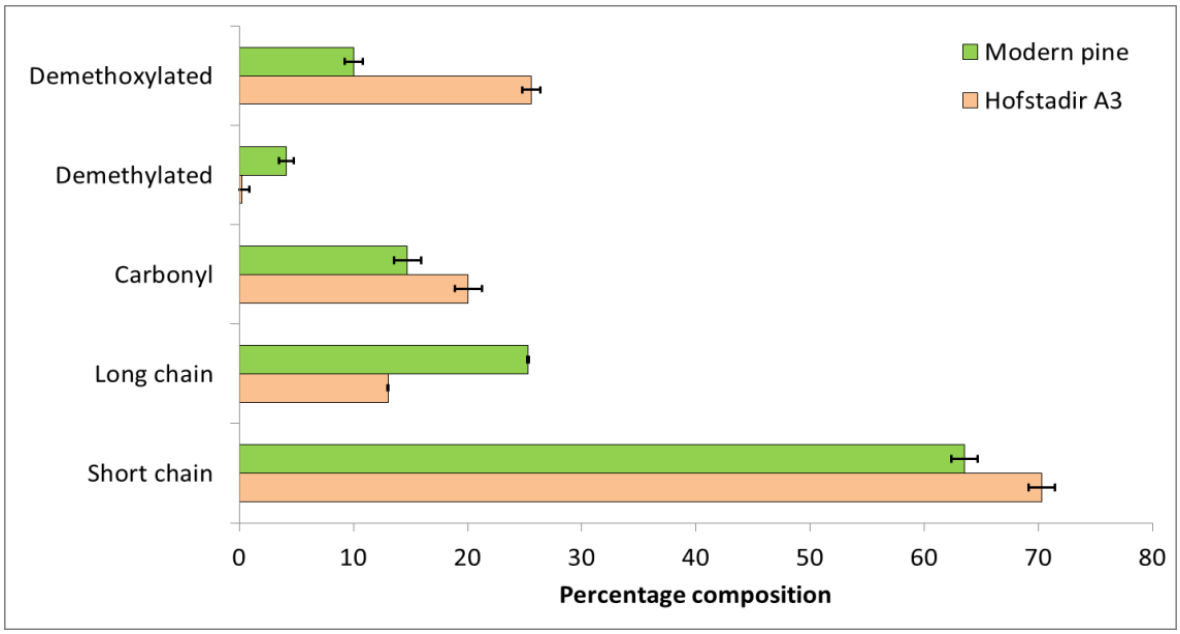

Figure 54. Percentage compositions of demethoxylated, demethylated, carbonyl, long chain and short chain compounds in modern pine and coffin wood sample A3 from grave 116 at the Hofstaðir excavations (see Table 11 for compound classifications). Values are calculated as a percentage of the total area of lignin derived peaks in Py-GC-FID pyrograms. Error bars represent +/- standard deviation and are the standard error calculated in Chapter 3, based on n=3 replicates of an archaeological gymnosperm wood.

The pyrograms of the soil stains from grave 116 display higher proportions of phenol than the C2 soil control (Figure 55 c and d). The elevated phenol content is indicative of the presence of a polymeric material that is not present in the soil control. As has been seen in the coffin wood, phenolic lignin derived compounds are produced by the defunctionalisation of guaiacyl lignins. The fact that the phenol liberated from the soil control is less than that from the soil stain may indicate the presence of heavily decayed wood in the latter. Analysis of the soil stain by Py-GC without TD and by Py-GC after solvent extraction with 9:1 DCM:methanol (see Chapter 2.2.2.4) showed no change in the pyrogram, indicating that depolymerised lignin metabolites were not present. Given the lack of peaks directly attributable to wood polymers, the source of the phenol cannot be identified definitively as a wood degradation product.

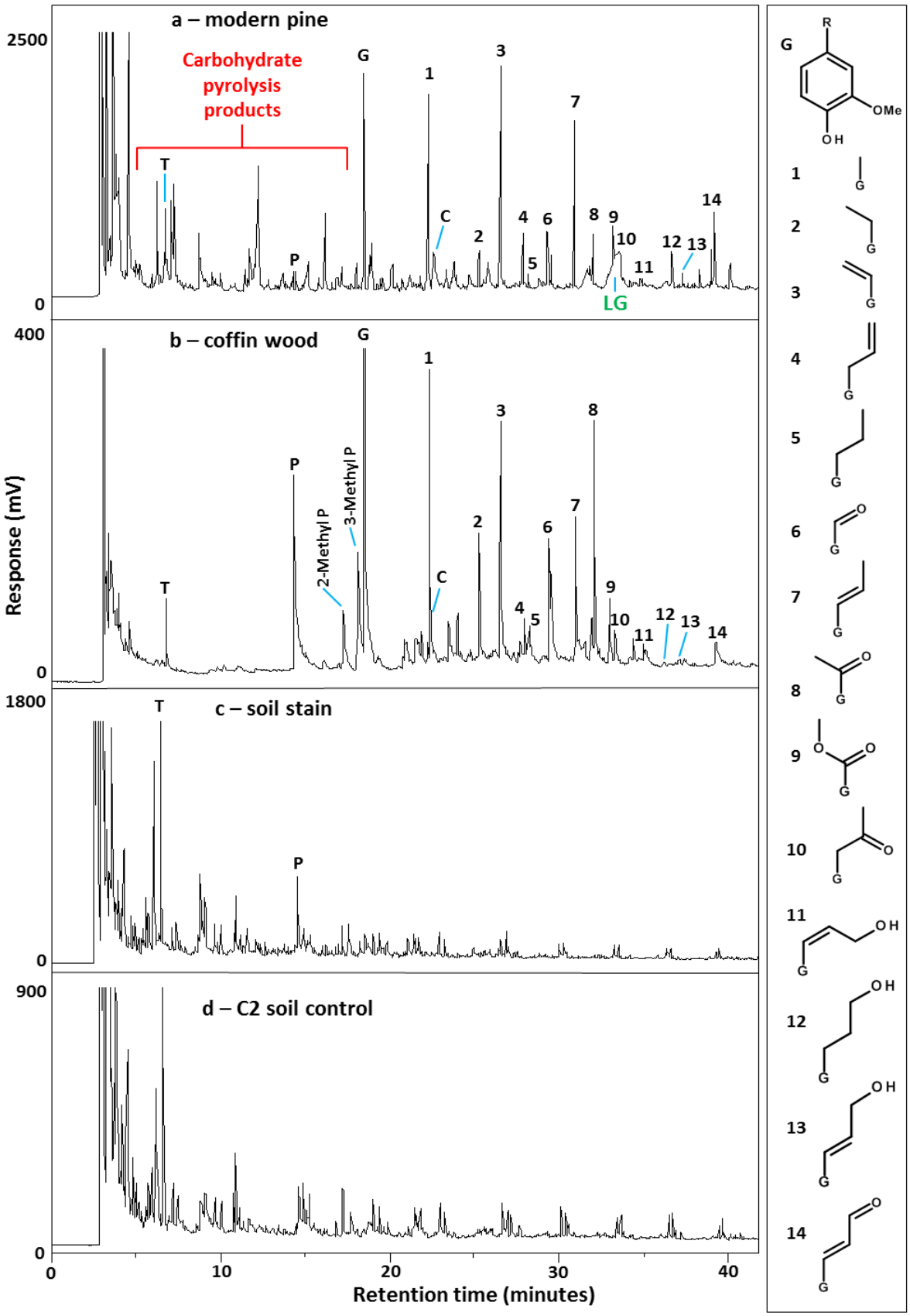

Figure 55. Assigned partial Py-GC-FID pyrograms of the coffin wood and soil stain compared with the C2 soil control from grave 116 at the Hofstaðir excavations. a – modern pine wood, b – a representative sample of coffin wood, c – an example of the soil stains analysed that were thought to be due to degraded coffin wood, and d – the C2 soil control for grave 116 that serves as a background measurement of any polymeric compounds present within the grave fill. T = toluene, P = phenol, G = guaiacol, C = catechol and LG = levoglucosan (a cellulose pyrolysis product). The identities of the numbered peaks are shown in the key to the right of the pyrograms.

5.4.2.2 SEM

Examination of the wood under SEM in cross section (Figure 56a) reveals that it is simple in structure, lacks vessels and show clear bands of earlywood and latewood, characteristics attributed to coniferous woods. Thinning of the inner layers of tracheids and localised areas where the cells have completely split open are evident. The cells of the wood are damaged in many areas, with degradation apparent in all cell wall layers. The cellulose rich secondary cell wall layers show signs of flaking and degradation, while the middle lamellae also exhibit symptoms of decay. The damage to both holocellulose and lignin rich layers of the wood structure bears a strong resemblance to that caused by white rot (Blanchette *et al.,* 1990). Fungal spores that appear similar to those produced by the white rot *Phanerochaete chrysosporium* (Rice *et al*., 2006) are also present.

Surface analysis by SEM (Figure 56b) reveals the presence of a fungal body embedded in the subsample, similar to those reported by Blanchette (2000). The fungal feature is approximately 100 µm in diameter, penetrates the wood at both ends and has produced numerous fungal hyphae that are adhering to the wood. In the immediate vicinity of the fungal hyphae the wood cells are heavily damaged and have separated into individual tracheids or bundles of tracheids.

The presence of fungus and spores which appear similar to those of a white rot fungus, combined with degradation of both lignin and cellulose suggests that the wood has been degraded by a non-lignin preferential white rot fungus (Blanchette, 2000).

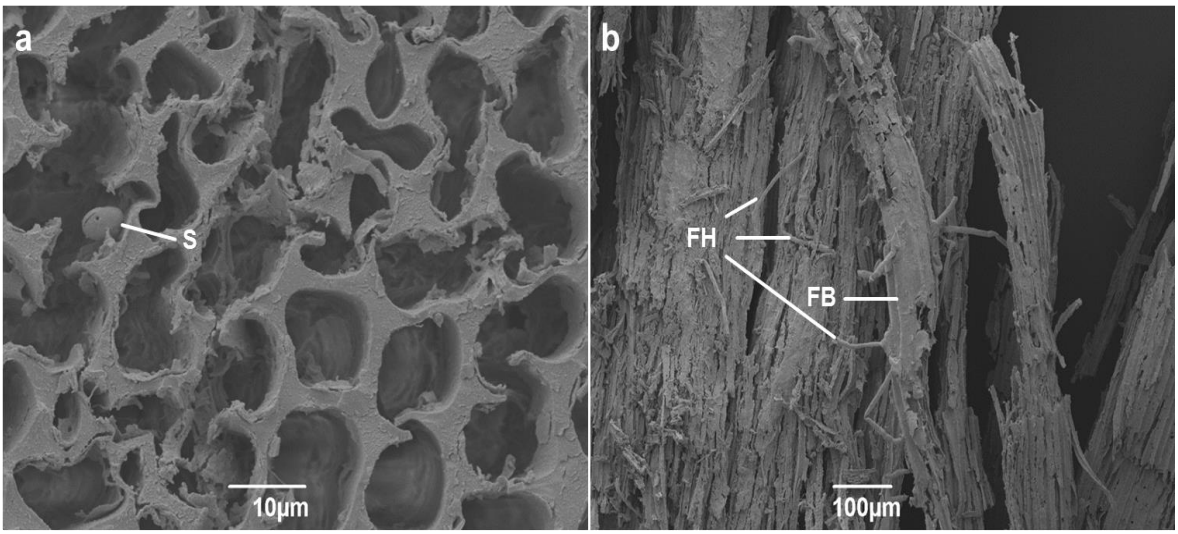

Figure 56. SEM images of coffin wood sample A3 from grave 116 at the Hofstaðir cemetery excavation. The left image (a) shows a cross sectional cut of degraded tracheid cells with damage to all cell wall layers and the presence of fungal spores (S). The right image (b) shows a fungal body (FB) approximately 100 µm in diameter adhered to the surface of the wood by fungal hyphae (FH) which have penetrated in to the wood.

5.4.3 Summary and conclusions

Pyrolysis data reveal that the coffin woods from grave 116 are from gymnosperm trees and have undergone decay of both lignin and holocellulose. This is confirmed by the damage revealed by SEM imaging. The presence of fungal bodies in the wood tissue allow for the identification of the degrading microorganism as a type of non-lignin preferential white rot. The lignin has underdone C_{α}-C_{β} cleavage of both β-O-4 ether and β-1 lignin sub unit linkages and oxidation of the resultant hydroxylated products.

The soil stains, thought to be due the presence of heavily decayed wood, show higher phenol content than the soil control, though no other compounds attributable to lignin were observed. As a result of this, the stain cannot be attributed definitively as resulting from degradation of wood.

5.5 Mechelen

5.5.1 Site and sampling information

Samples of coffin wood were collected from graves 26 and 423 during the excavations at St Rumbold's cathedral, Mechelen, latitude: 51.028858, longitude: 4.479221. (See Chapter 6.4.1 for a description of the Mechelen excavations, including soil analyses and historical information.)

Both materials were fragile and easily fragmented when handled. The wood from grave 26 was noticeably lighter in colour than that from grave 423. All materials were subjected to TD before analysis by Py-GC. The coffin wood from grave 423 was also analysed by SEM.

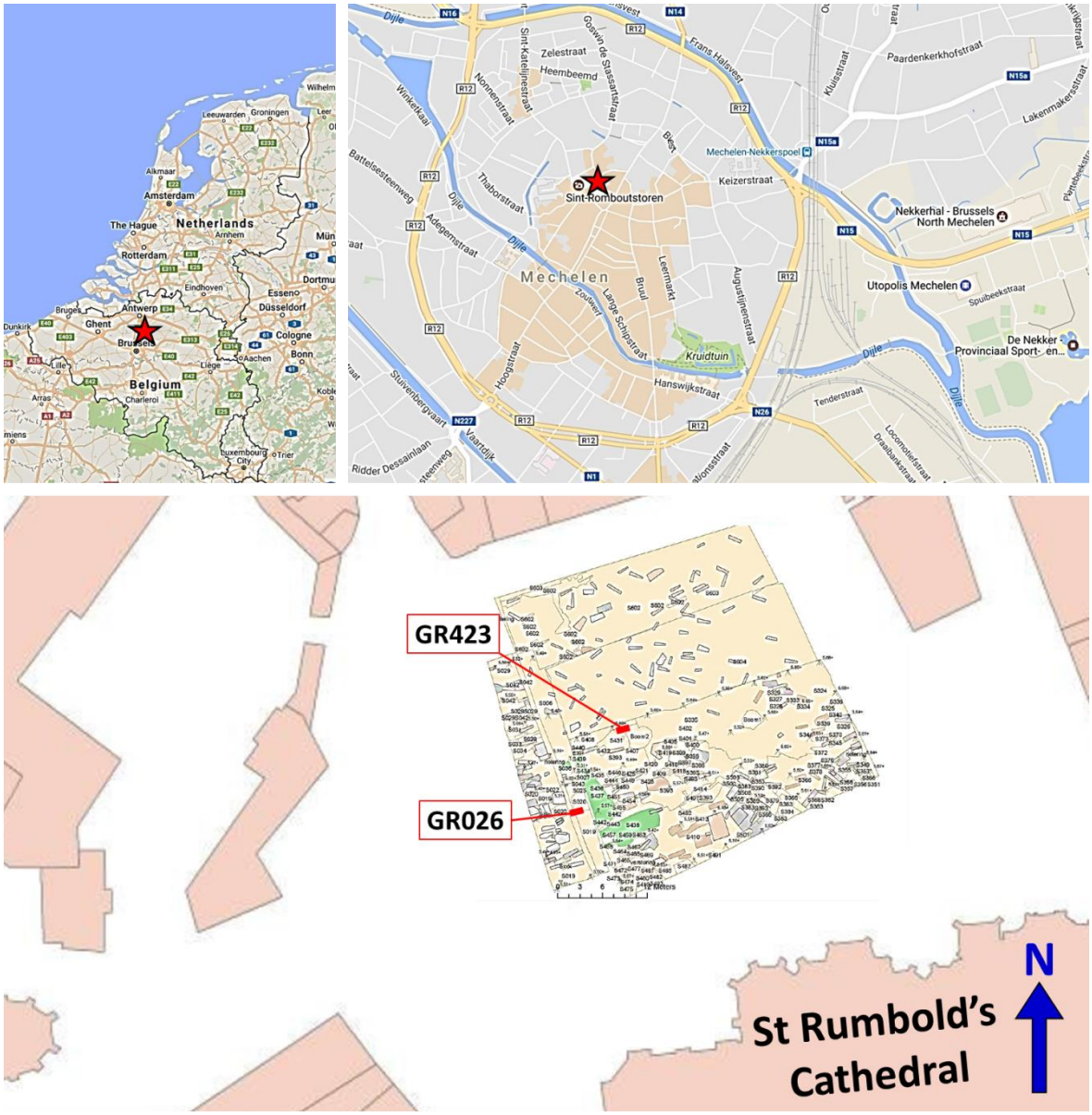

Figure 57. A map showing the area surrounding Mechelen (top) and a plan of the excavation at the cathedral in Mechelen, showing the location of graves 26 and 423 (bottom; image adapted from Depuydt et al., 2013).

5.5.2 Analysis of archaeological material

5.5.2.1 Py-GC

The coffin wood from grave 26 shows intensive modification and almost complete degradation of the lignin component of the wood by comparison with modern pine. The key characteristics are: a dominance of shorter chain lignin pyrolysis products over those with long chains, a lack of guaiacyl compounds with carbonyl functionalities, and an increased proportion of demethoxylated lignin phenols (Figure 58). The absence of compounds derived from syringyl lignin in the pyrogram suggests that the wood is from a gymnosperm tree, though due to the severe degradation of the lignin this conclusion is only tentative.

The pyrogram displays intense peaks in the region where carbohydrate pyrolysis products typically elute (5-25 min) that match the peak pattern of carbohydrate derived compounds in the modern pine (Figure 59). Levoglucosan, a characteristic of indicator of cellulose in pyrograms of wood (Mohan *et al.,* 2006), is absent. This suggests that the peaks in the carbohydrate region are due to the presence of only hemicellulose and not cellulose remaining in the coffin wood. Selective delignification is a phenomenon that has been previously been attributed to certain strains of white rot fungus (Blanchette, 1991; Blanchette, 2000), but selective microbial degradation of cellulose over hemicellulose is not reported to occur by any known microorganism. Although Iiyama *et al.* (1988) reported finding cellulose to be more heavily attrited than hemicellulose in heavily degraded buried woods, the degradation of hemicelluloses is typically more pronounced than that of cellulose in buried archaeological woods (Kim and Singh, 2000). Therefore, either an as yet unknown microorganism could be responsible for the degradation of the cellulose (and possibly the lignin), or the degradation is due to chemical factors within the burial environment.

The coffin wood from grave 423 contains only gymnosperm lignin derived compounds and no compounds from any carbohydrates (Figure 59). Figure 58 shows intensive demethoxylation of the guaiacyl subunits. While there is a larger ratio of short chain to long chain lignin sub units when compared to modern pine, there is no increase in the content of oxidised, carbonyl containing compounds. This would suggest that the lignin has been modified by demethoxylation but not broken down to any great extent. Combined with the holocellulose loss, these degradation signatures are consistent with a range of wood decaying microorganisms including brown rot and soft rot fungi, and wood decay bacteria including erosion, tunnelling and cavitation bacteria (Blanchette, 2000).

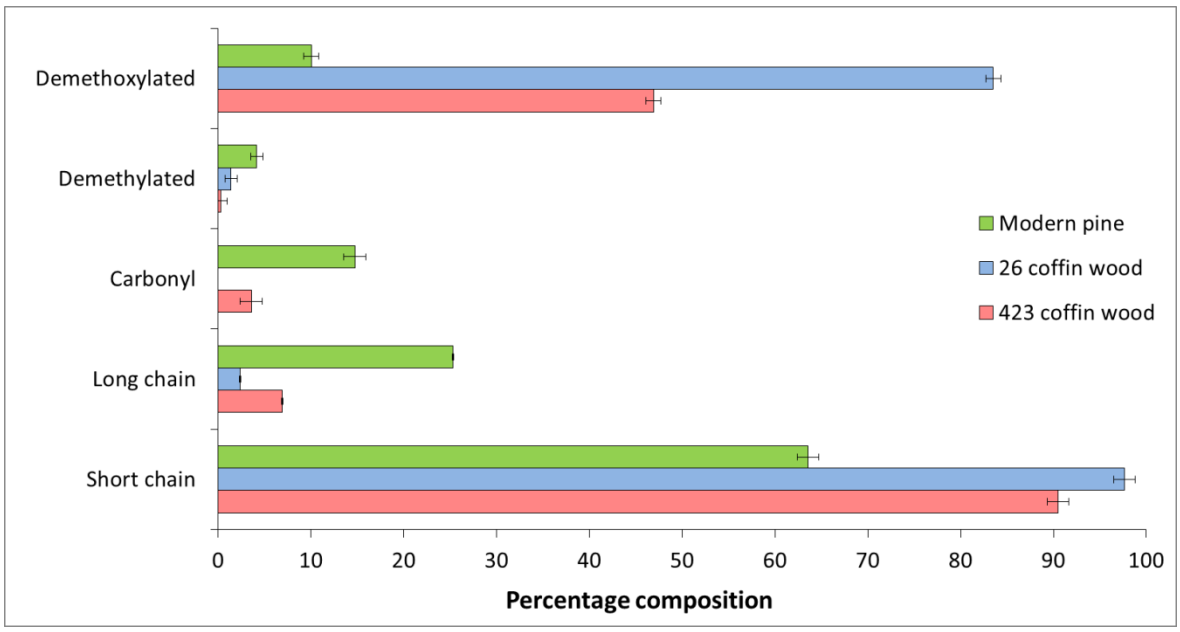

Figure 58. Percentage compositions of demethoxylated, demethylated, carbonyl, long chain and short chain compounds in modern pine and the coffin woods from graves 26 and 423 at Mechelen (see Table 11 for compound classifications). Values are calculated as a percentage of the total area of lignin derived peaks in Py-GC-FID pyrograms. Error bars represent +/- standard deviation and are the standard error calculated in Chapter 3, based on n=3 replicates of an archaeological gymnosperm wood.

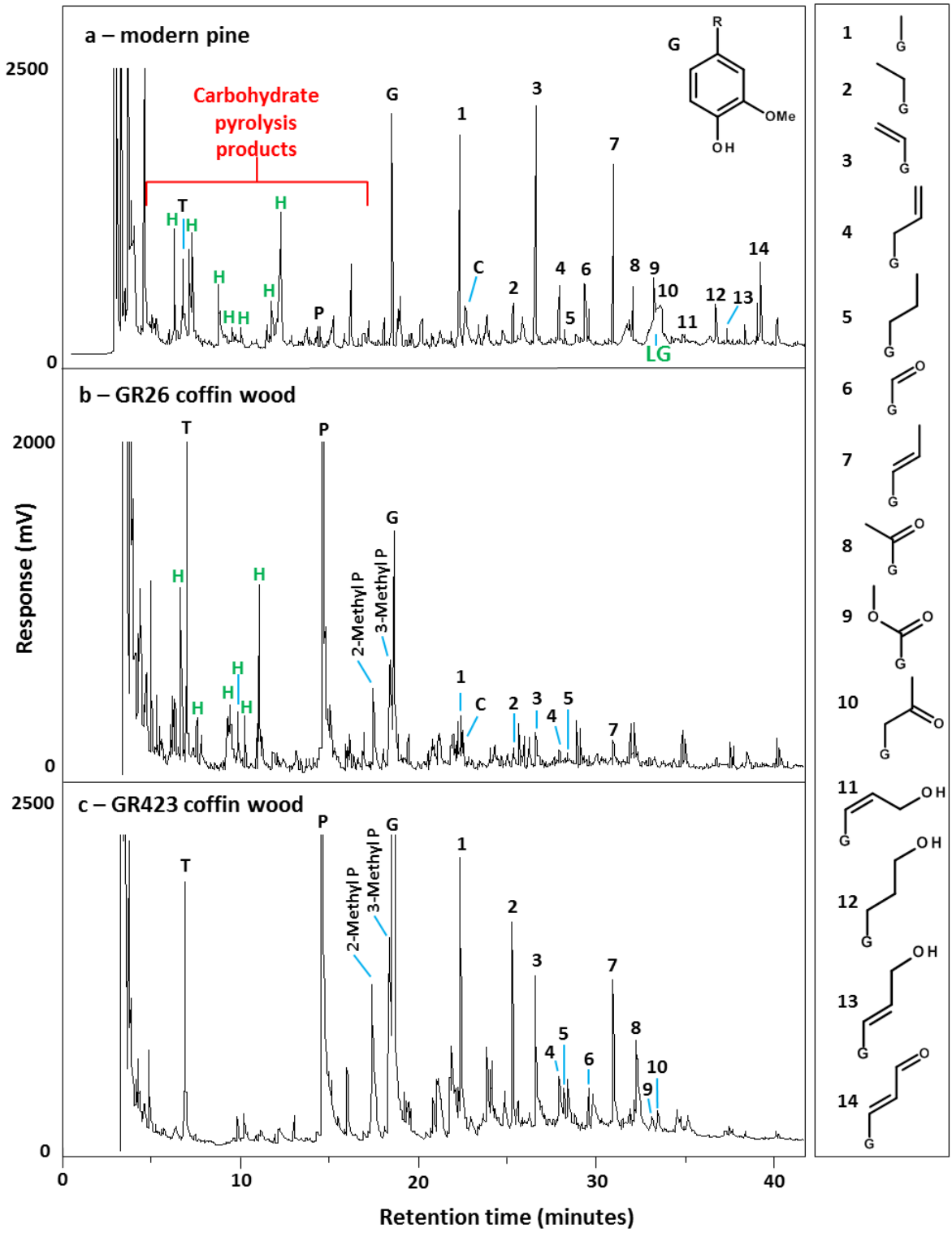

Figure 59. Assigned partial Py-GC-FID pyrograms of modern pine (a) and coffin wood from graves 26 (b) and 423 (c) at the Mechelen excavations. H = holocellulose pyrolysis products, T = toluene, P = phenol, G = guaiacol, C = catechol and LG = levoglucosan (a cellulose pyrolysis product). The identities of the numbered peaks are shown in the key to the right of the pyrograms.

5.5.2.2 SEM

The tracheid shape, absence of vessels, and the presence of resin ducts evident in the SEM images of wood from grave 423 indicate that the material is softwood (Figure 60). There are two distinct regions of the wood that show differing levels of degradation. One region shows less advanced deterioration of the cell walls, with evidence of flaking and attrition of the cellulose rich secondary cell wall components (Figure 60a and b). In this case, the overall shape of the cells is relatively undistorted and the structure of the wood is similar to that of undegraded softwood. The other region shows more complete destruction of the secondary cell wall material with significant thinning of the tracheid walls, leaving only a skeleton of the middle lamellae and primary cell wall layers (which are rich in lignin; Fengel and Grosser, 1975) that is warped and more heavily damaged (Figure 60c and d). Given that little holocellulose was observed in the pyrolysis data of this sample, it is likely that that there are very few areas where the tracheids are well preserved, those with heavily decayed secondary cell walls being the major component.

The two regions of differing preservation state both contain tube-like features that are approximately 2 µm in diameter within the lumen space of many of the cells. The tracheids in areas with more cellulose material remaining have features on the inner surfaces that appear to be very fine fungal hyphae. The pyrolysis data shows complete loss of holocellulose and modification of lignin by demethoxylation, but limited lignin depolymerisation. This kind of damage is known to be the result of brown rot and soft rot fungi (Blanchette, 2000). The SEM images do not show the cavities in the secondary cell wall layers that are typical of soft rot attack (Filley *et al.*, 2001; Blanchette *et al*., 2004), the degradation instead appearing similar to that carried out by brown rot fungus reported by Bouslimi *et al*. (2014).

There are several possible explanations as to why there are two regions with different levels of degradation. Proximity to metal objects may have limited the growth or metabolic activity of the fungus, impeding its ability to degrade the holocellulose in the more preserved areas. The depletion of oxygen within the burial environment is also a likely candidate for the arrest of the fungal decay. A change in the conditions from oxic to anoxic would have halted the metabolism of holocellulose, as brown rot fungi are not capable of degrading celluloses in anoxic environments (Boer *et al*., 2005).

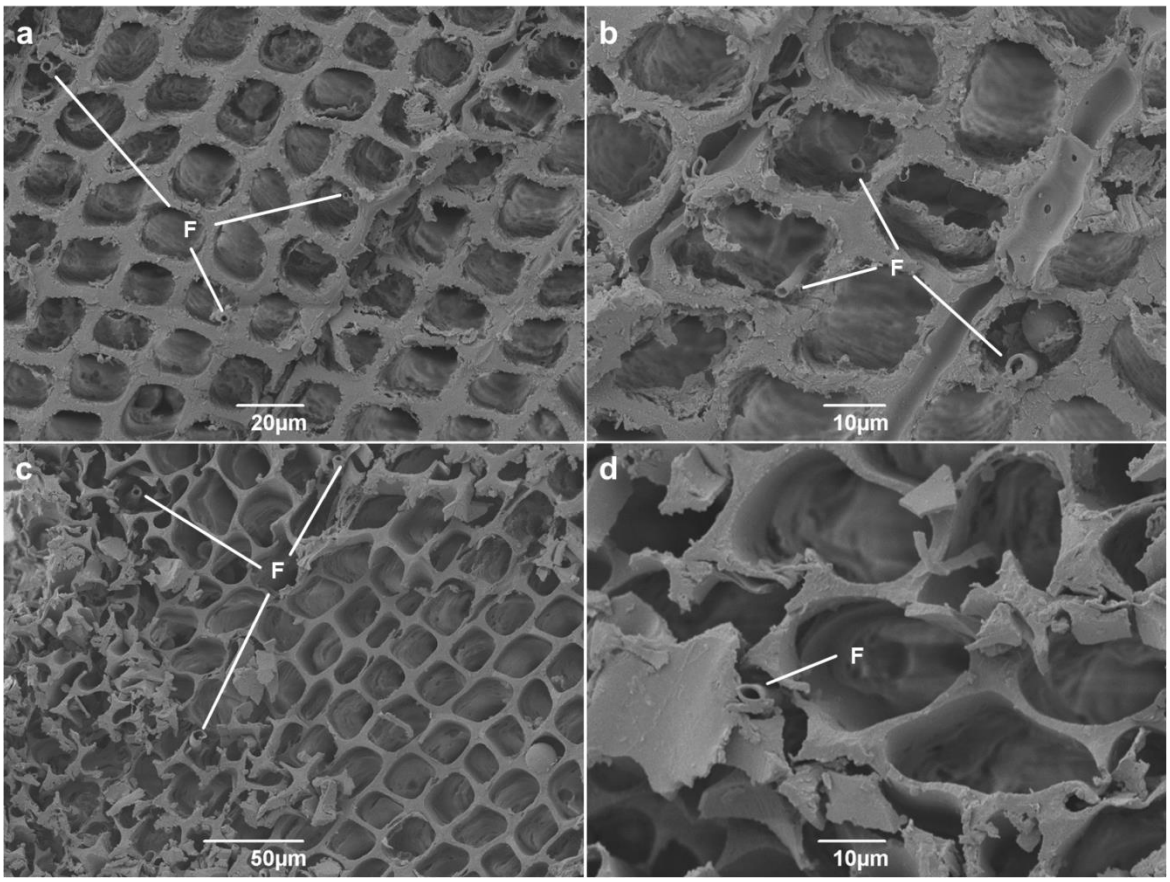

Figure 60. SEM images of coffin wood from grave 423 at the Mechelen cemetery excavation. The top images (a and b) show flaking and attrition of the cellulose rich secondary cell wall components and the presence of fungal bodies (F). The bottom images (c and d) show that the wood is more heavily degraded, with complete losses of all holocellulose components, structural collapse and apparent fungal bodies (F).

5.5.3 Summary and conclusions

Pyrolysis data of wood from grave 26 shows that the lignin component of the wood is heavily degraded but there is a large amount of hemicellulose still present. This is consistent with wood being selectively delignified, which is mediated by white rot fungus. All wood analysed was in this condition, suggesting similar conditions existed within all parts of the burial environment.

No cellulose or hemicellulose components are present in the pyrogram of the wood from grave 423. Some modification of the lignin is apparent (in the form of demethoxylation) but there was not a large amount of depolymerisation, suggesting that the wood was not attacked by microorganisms capable of metabolising lignin. The SEM shows two distinct areas of different preservation state, with one presenting more advanced decay of the cellulose rich secondary cell wall layers. Both areas have fungal bodies present in the cell lumen. The damage is consistent with that carried out by brown rot fungus, an interpretation that also fits with the damage to the biopolymers observed in the Py-GC analysis.

The presence of fungus in both woods and the differing levels of degradation indicates that the fungus was prevented from attacking the wood in one microenvironment more than the other, possible due to a change in the oxygen levels within the burial environment or the presence of a mycotoxin in one wood fragment and not the other.

5.6 Sala

5.6.1 Site and sampling information

Sala is a town in the Västmanland county of Sweden, approximately 60 km west of Uppsala. The town in best known for its silver mine that dates back to medieval times and closed in 1908. Periodic excavations at the town's cemetery have been ongoing since 2004 (latitude: 59.906881, longitude: 16.574256; Bäckström & Sundström, 2014). ^{14}C dating of bones together with coin finds suggest the cemetery was in use from the early 1400s to the late 1500s (Bäckström & Sundström, 2014). The burial matrix consisted of podzol, a soil typically found around coniferous forests. Podzols are most often sandy, well drained and have a low pH (Chesworth, 2008).

The InterArChive team collected samples of grave soil and wood during the third and final series of excavations at the Sala mining cemetery in August 2011. Grave 7464 was a supine burial that was at a depth of 0.17 m. It contained the remains of an older individual, at least 50 years of age, of an undetermined sex (Bäckström & Sundström, 2014). Parts of the coffin were still present and samples of the wood were taken for analysis.

A large sample of wood from the side of the coffin was trisected, to give three slices of wood that 1) had been exposed directly to the grave fill; 2) exposed to the interior of the coffin; 3) in between the two. Each was then processed as described in Chapter 2.2.2.2 before analysis by TD/Py-GC. A sample of the wood was also analysed by SEM.

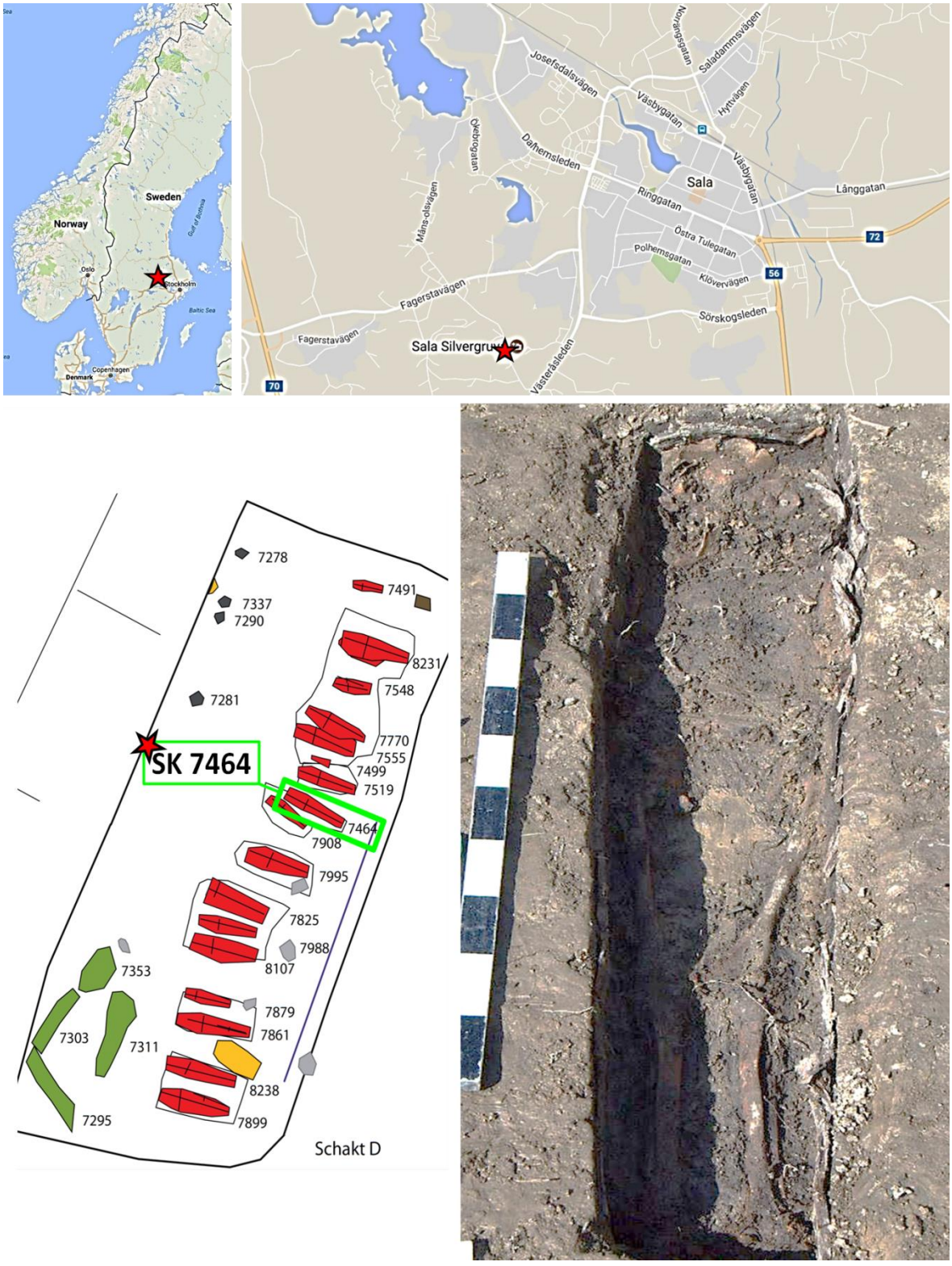

Figure 61. A map of the area surrounding the archaeological excavation at Sala silver mine (top) a photograph of grave 7464 (bottom left) and a plan of the 2009 excavation showing the position of grave 7464 (bottom right; image adapted from Bäckström & Sundström, 2014).

5.6.2 Analysis of archaeological material

5.6.2.1 Py-GC

The pyrograms of the coffin wood are similar to those of modern pine (Figure 62), and exhibit peaks attributed to guaiacyl units only, lacking any syringyl peaks. This is strongly indicative of the wood being gymnosperm in origin (Lewis and Yamamoto, 1990). Compared to the fresh pine, the coffin woods display several key differences. The most noticeable difference is in the region where carbohydrate pyrolysis products elute; the peaks in the archaeological wood being much smaller or absent compared those of modern pine. The levoglucosan peak present in the modern pine pyrogram is absent in those of the archaeological woods. The lack of any substantial peaks that are due to the pyrolysis of carbohydrates indicates that the holocellulose component (cellulose and hemicellulose) of the coffin woods is heavily degraded.

Figure 62 and Figure 63 show a high relative abundance of phenol, 2-methylphenol and 3-methylphenol which are likely the result of demethoxylated lignin compounds in the archaeological woods. These phenols have been shown to be produced as a result of microbially mediated enzyme catalysed demethoxylation of guaiacyl subunits, which leads to them being liberated as phenol on pyrolysis (Figure 68; Martínez *et al.*, 2005).

Unlike the wood analysed from other sites, the proportions of long and short chain lignin products are only slightly different than in modern pine, and the relative amounts of carbonyl containing lignin products are very similar to the modern wood (Figure 63). Combined with the evident removal of all the holocellulose, the damage is typical of that caused by fungi and bacteria that are not capable of extensively degrading lignin.

The preservation state of the wood is uniform in all of the samples from all parts of the coffin. Outer, centre and inner subsamples all show the same absence of holocellulose pyrolysis products and the same products attributed to transformation of lignin.

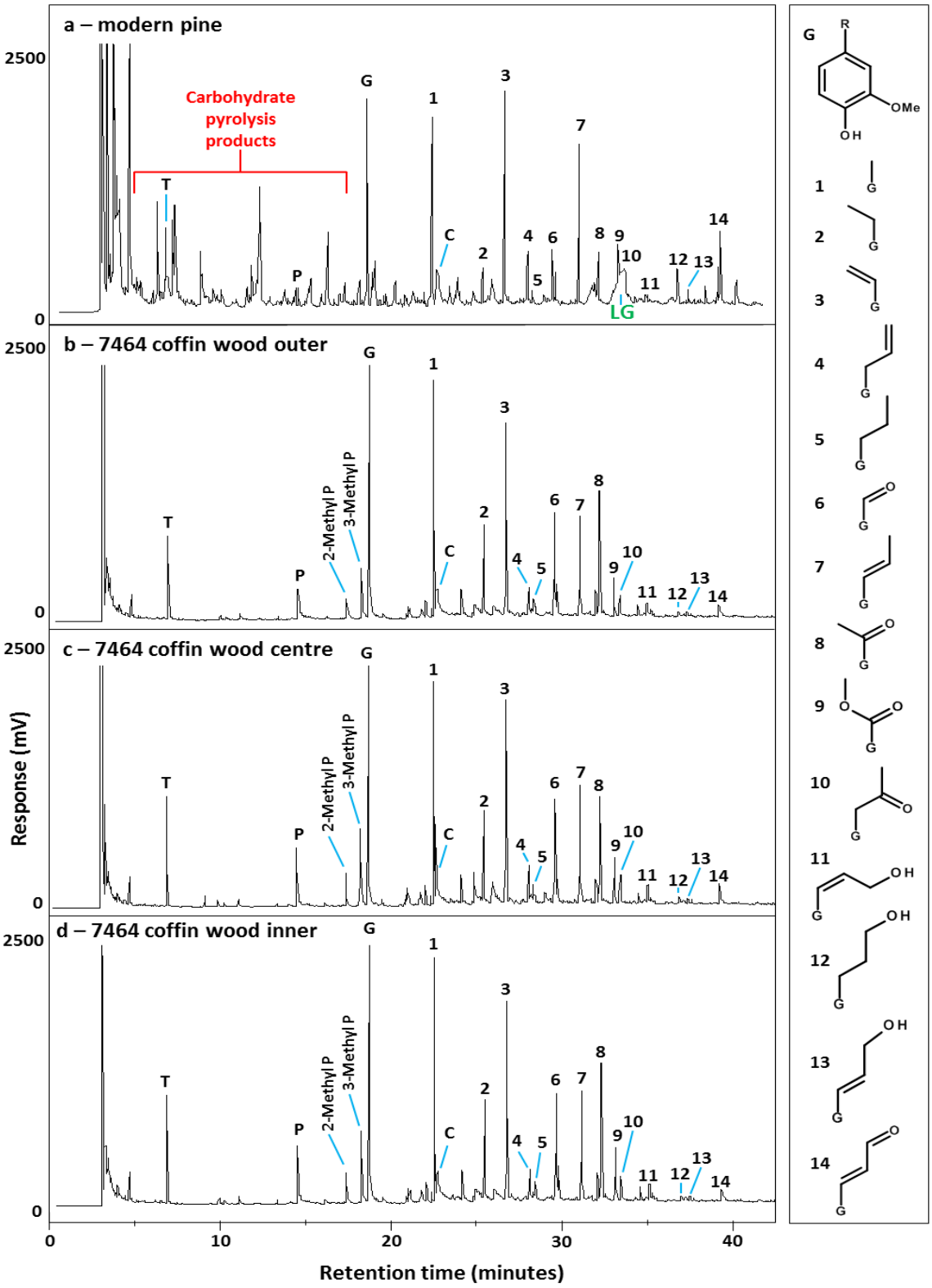

Figure 62. Assigned partial Py-GC-FID pyrograms of the trisected coffin wood from grave 7646 at the Sala silver mine excavations. a - modern pine wood, b - the outer layer of coffin wood (exposed to the grave fill), c - the inner 'sandwiched' layer of coffin wood and d - the inner layer of coffin wood (exposed to the inside of the coffin). T = toluene, P = phenol, G = guaiacol, C = catechol and LG = levoglucosan (a cellulose pyrolysis product). The identities of the numbered peaks are shown in the key to the right of the pyrograms.

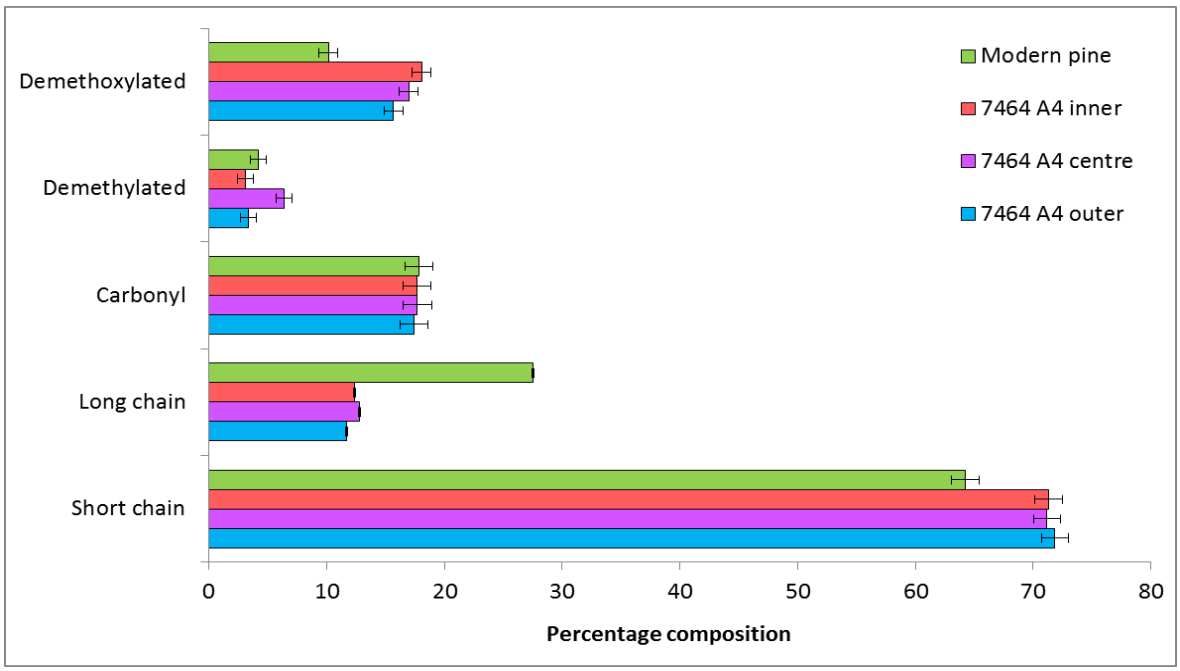

Figure 63. Percentage compositions of demethoxylated, demethylated, carbonyl, long chain and short chain compounds in modern pine and the trisected coffin wood sample A4 from grave 7646 at the Sala silver mine excavations (see Table 11 for compound classifications). Values are calculated as a percentage of the total area of lignin derived peaks in Py-GC-FID pyrograms. Error bars represent +/- standard deviation and are the standard error calculated in Chapter 3, based on n=3 replicates of an archaeological gymnosperm wood.

5.6.2.2 SEM

On first inspection of the SEM images (Figure 64), the wood appears to have vessels (labelled V), features that are not found in gymnosperm wood tissue (Salisbury and Ross, 1992). The pyrolysis data indicate that the material is from a gymnosperm tree, as does the simple structure apparent in the SEM images and the clear transition from earlywood cell to latewoods cells, which is less evident in angiosperms. Closer analysis however, shows the holes have poorly defined edges, with no structural linings typical of vessels. The edges of the voids appear to be made up of crushed and heavily degraded cells, which would be consistent with objects pushing though the wood, degrading the surrounding cells as they progressed, leading to compression and collapse of the cells. Several of the holes are over 1 mm in diameter, and have led to the splitting of the wood into distinct sections.

Several of the tunnels contain round, tubular features (labelled F) that have the same appearance as fungal bodies reported in SEM of wood reported by Blanchette *et al.* (1994) and Schwarze (2000). The fungus has penetrated the wood, leading to the observed damage. Whilst gymnosperm woods do not contain vessels, they do incorporate resin ducts. The resin ducts are normally much smaller than the features seen in the electron micrographs; the action of fungi, however, may have widened the resin ducts whilst using them to infiltrate the wood in its quest for nutrients. Bouslimi *et al*. (2014) degraded gymnosperm wood from white cedar (*Thuja occidentalis*) using brown rot fungus, producing similar damage to that observed in the SEM of the coffin wood.

The earlywood tracheid cells are distorted and less thick that those observed in undegraded gymnosperms (Meylan and Butterfield, 1972). This is likely to be due to the attrition of the holocellulose rich S1, S2 and S3 secondary cell wall components (Asunmaa and Lange, 1953; 1954). Cellulose and hemicellulose are of greater abundance in earlywood cells, leading to them being preferentially degraded and the decay being more likely to lead to structural collapse than the more intact latewood cells (Schwarze, 2007). The loss of the cellulose compromises the structural integrity and strength of the tracheids, leading to distortion of the cells. The distortion is much more apparent in the earlywood cells, whose wider lumen and thinner walls make them more susceptible to structural collapse when individual cell wall layers are degraded. Many of the earlywood tracheids contain thin fungal strands that have been observed previously in the decay processes of archaeological woods (Blanchette *et al.*, 1994; Schwarze, 2007). Fungal appendages of brown rot fungi are known to attack the holocellulose rich secondary cell wall layers, leaving behind a weakened skeleton of lignin in the middle lamella (ML), primary cell walls (P) and, occasionally, intact or partially degraded S1 material. The lower proportion of holocellulose in the ML, P and S1 cell wall layers makes them more resistant to fungal degradation (Schwarze, 2007).

The action of brown rot fungi would explain the observed thinning of the cell walls and structural deformation.

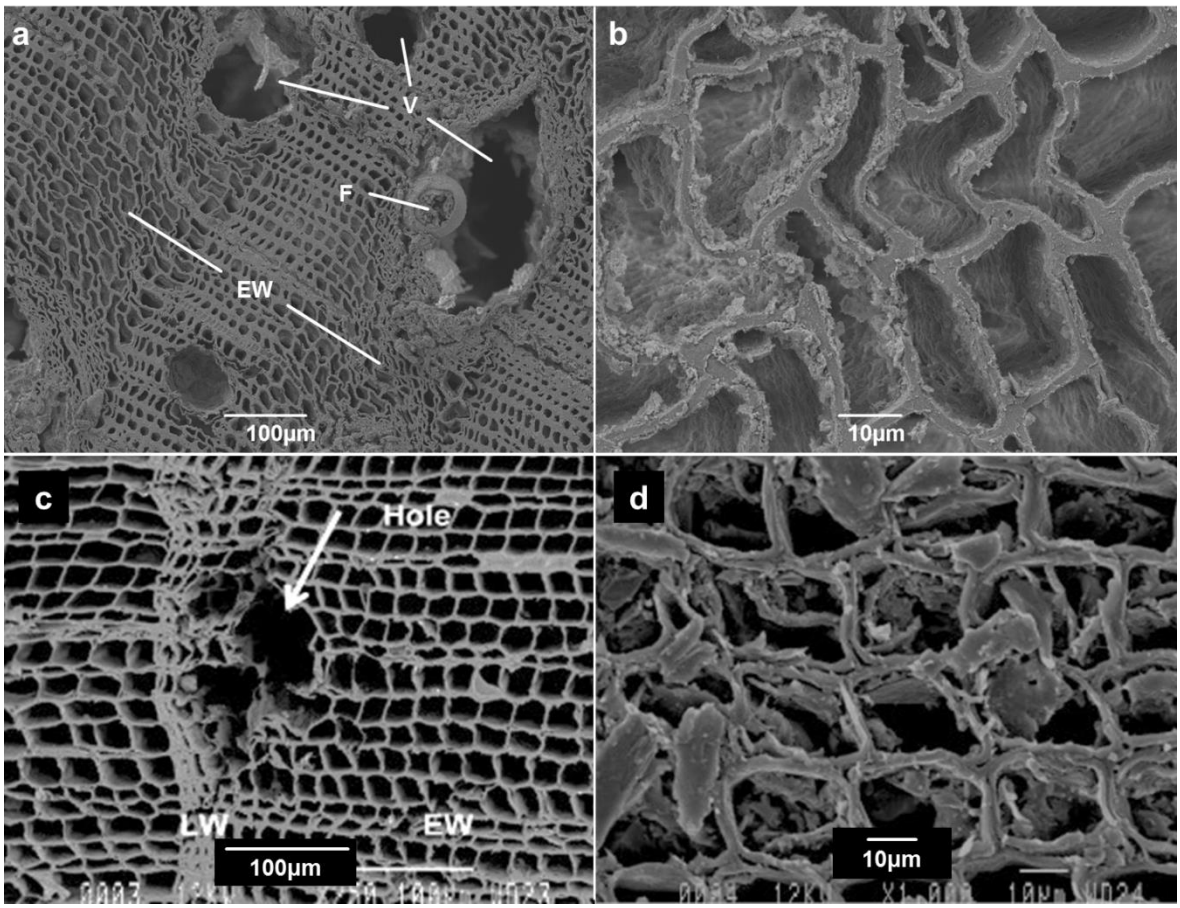

Figure 64. SEM images of coffin wood from grave 7467 at the Sala silver mine excavation (a and b), and SEM of white cedar that has been degraded by treatment with brown rot fungus, taken from Bouslimi et al (2014; c and d). The top left image (a) shows large voids (V) that are not consistent with the morphology of undegraded gymnosperm woods, fungal bodies filling one of the voids (F) and thinned, distorted tracheid cells of the earlywood layers (EW). The top right image (b) is a closer view of the decayed earlywood cells, showing significant losses to the secondary cell wall layers. The damage seen in the coffin wood from Sala grave 7464 is similar to that seen in c and d, suggesting that the damage to the archaeological material may be due to a brown rot fungus.

5.6.3 Summary and conclusions

Py-GC and SEM analysis both indicate that the coffin in grave 7464 is made from softwood. All cellulose and hemicellulose has been degraded, with some modification of the lignin by demethoxylation and limited depolymerisation. Fungal bodies are present within large voids that are atypical of undegraded gymnosperm wood and likely caused by the fungus (Salisbury and Ross, 1992; Schwarze, 2007). The secondary cell wall layers have been stripped away, accounting for the loss of holocellulose seen in the pyrolysis data. The middle lamellae remain, indicating that the lignin was modified as a result of the removal of the carbohydrates and not due to directed attack on the lignin. The degradation apparent in the chemical and morphological data suggests that the culprit is highly likely to be a brown rot fungus.

The preservation state was the same throughout the thickness of the side of the coffin wood and in all parts of the coffin, demonstrating the ability of brown rot fungi to permeate and proliferate within the burial environment.

5.7 Thaon

5.7.1 Site and sampling information

L'église Saint-Pierre de Thaon is a disused church in the Calvados region of Northern France, approximately 13 km from Caen and 20 km from Bayeux, latitude: 49.265572, longitude: -0.450441. The Romanesque tower of the church dates back to the 11th century, the remainder of the 11th century construction was demolished and the current nave and chancel added in the late 12th century. The church was finally closed in 1840. A ten year archaeological study of the church led by the University of Caen involved extensive excavations inside the church. Several hundred burials were uncovered below the floor of the church. The InterArChive team sampled coffin wood from the remains of two individuals (SEP 360 and SEP421) in the lowest levels of the burials within the nave of the church in the tenth and final season of excavation in 2009. The depth of the burials below the level of the original floor was in excess of one metre, below the water table of the site. Consequently, the burials were waterlogged at the time of excavation. The variability of the water level over time is not known, hence the duration of the waterlogging at the time of excavation was not determined.

Material from SEP360 and SEP421 was analysed by both TD/Py-GC-FID and TD/Py-GC-MS (to aid with peak assignment and data analysis). A sample of the material from SEP 360 also was analysed by SEM.

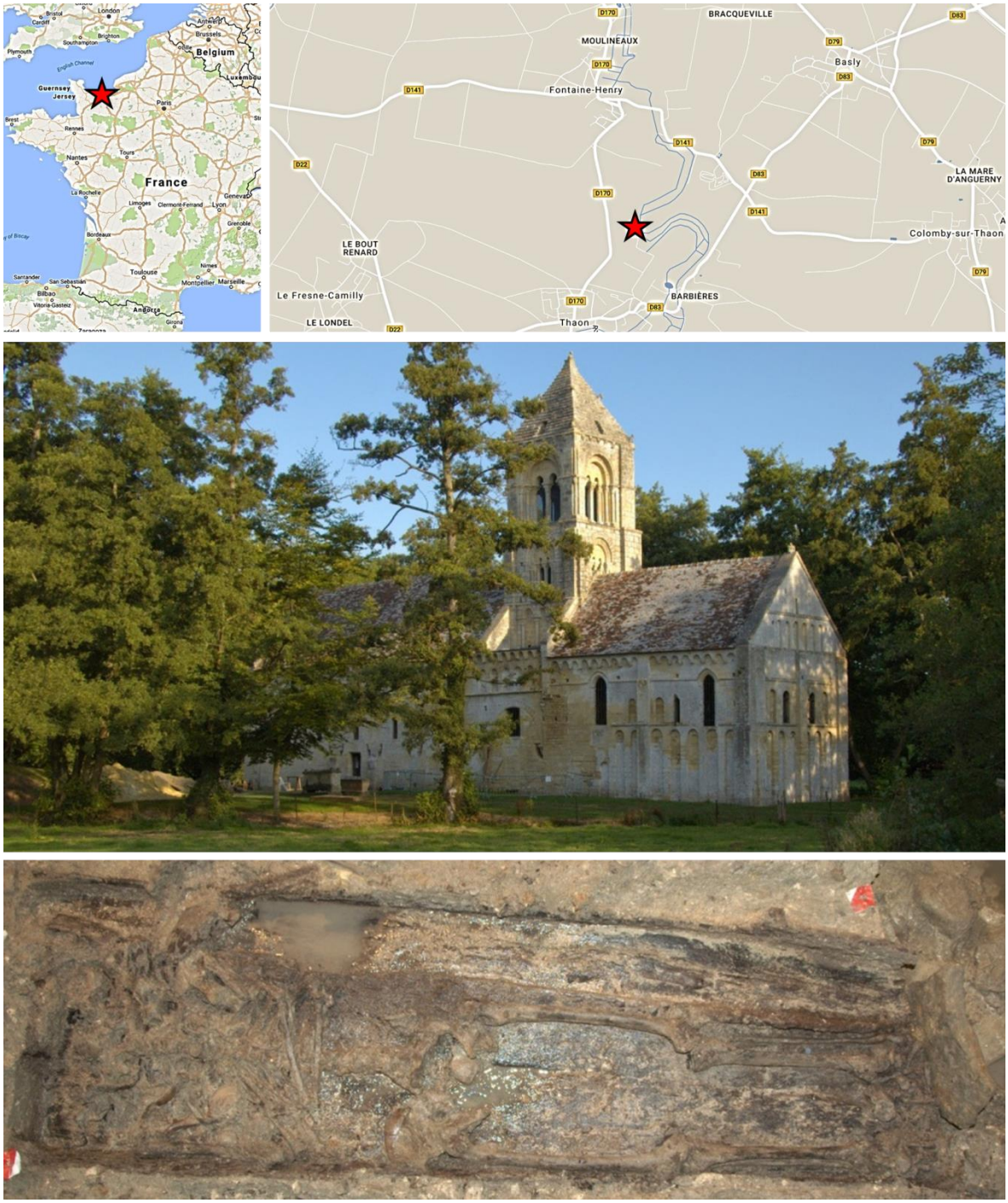

Figure 65. A map of the area surrounding the archaeological excavation at Thaon (top) a photograph of L'église Saint-Pierre de Thaon (middle) and a photograph of grave 420.

5.7.2 Analysis of archaeological material

5.7.2.1 Py-GC

Neither of the coffin wood samples from SEP360 and SEP421 yielded holocellulose derived compounds on pyrolysis, indicating that the carbohydrate components have completely degraded within the burial environment. Both materials produced pyrolysis products that correspond to guaiacyl and syringyl lignin sub units, indicating that the coffins were made with wood from angiosperm trees. The burials being under the floor of the church suggests that the individuals were of high status within the community; the coffins being made of expensive hardwoods indicates that they were of substantial wealth.

When analysed alongside modern oak the lignin of both archaeological woods have compositional differences (Figure 66). Larger ratios of short chain to long chain subunits and a higher predominance of demethoxylated subunits were detected, both parameters differing more in the wood from SEP360 than in that from SEP421. The wood from SEP360 also shows a measurably lower abundance of lignin components with oxidised side chains with respect to the amounts found in the modern oak. The greater difference in lignin composition in SEP360 samples suggest that this wood is more heavily degraded than that recovered from SEP421.

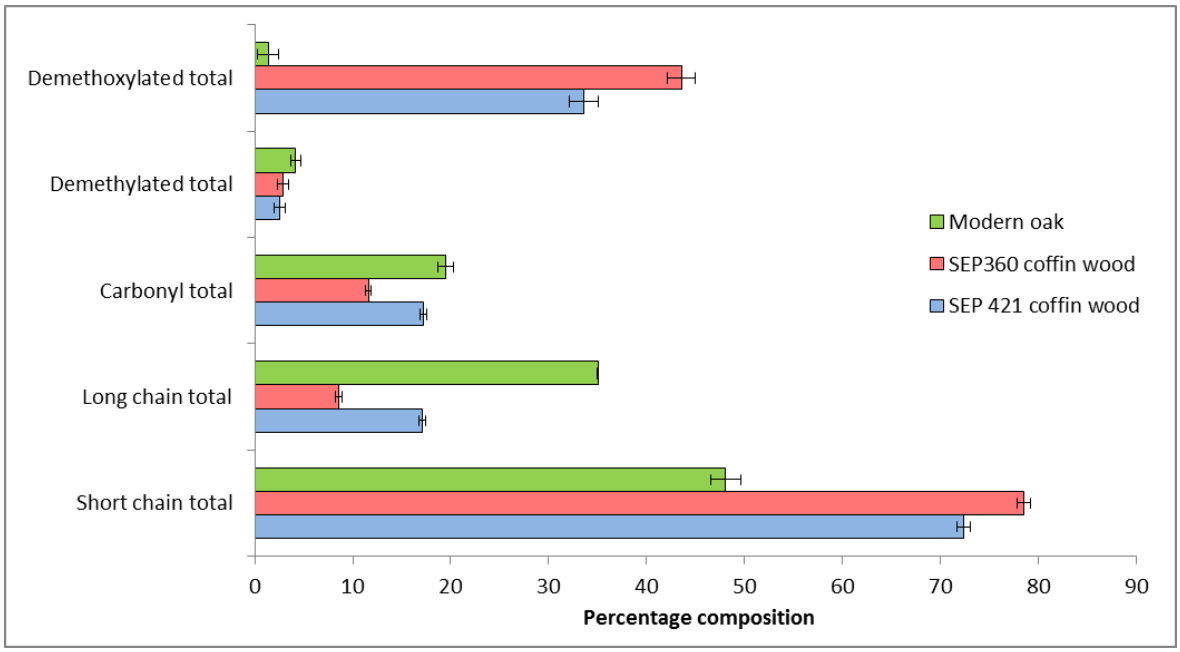

Figure 66. Percentage compositions of demethoxylated, demethylated, carbonyl, long chain and short chain compounds in modern oak and the coffin woods from graves 360 and 421 at Thaon (see Table 11 for compound classifications). Values are calculated as a percentage of the total area of lignin derived peaks in Py-GC-FID pyrograms. Error bars represent +/- standard deviation and are the standard error calculated in Chapter 3, based on n=3 replicates of an archaeological angiosperm wood.

Table 13. Ratios for corresponding syringyl, guaiacyl, phenol and methoxycatechol subunits from modern oak, SEP360 and SEP421 2003 coffin woods. ^ denotes an increase in the S:G ratio compared to modern oak.

Ratio	Modern oak	Thaon SEP360	Thaon SEP421
SH:GH	1.70	0.18	0.94
S1:G1	0.98	0.25	0.77
S2:G2	3.88	0.30	0.31
S3:G3	1.76	0.20	0.33
S4:G4	2.17	0.02	1.34
S5:G5	0.29	-	0.58
S6:G6	11.89	-	37.89^
S7:G7	2.57	0.26	0.98
S8:G8	1.22	0.05	0.10
Σ S:G	2.00	0.20	0.98
Σ S:MC	15.03	3.14	12.41
Σ G:P	23.26	1.16	1.15

A key parameter often used in assessing degradation of the lignin in hardwoods is the ratio of syringyl to guaiacyl lignin subunits (Faix *et al*., 1991; del Rio *et* al., 2001; Martínez *et al*., 2001; Łucejko *et al*., 2009). It is commonly observed that syringyl units are selectively degraded, either by being chemically modified in chain or by their complete removal from the lignin polymer, leading to a lower S:G ratio than in undegraded angiosperm wood. Side chain specific and total (Σ) S:G ratios for modern oak and the archaeological materials are shown in Table 13. With the exception of side chain 6 in SEP421 wood, all of the side chain specific and total S:G ratios for the archaeological woods are lower than the corresponding values from modern oak. This suggests that the degradation of the lignin was more focused on the syringyl subunits. The greater degree of variation observed among the SEP360 S:G ratios indicates that the attrition of syringyl moieties was more aggressive than for the wood from SEP421.

Several theories currently stand as to why the syringyl moieties of angiosperm lignin are more readily degraded than their guaiacyl counterparts. One possible reason is the fact that guaiacyl units can cross link by both β–O4 aryl ether linkages and by carbon–carbon bonds at the C6 position of the aromatic ring, whereas syringyl units have an extra methoxy group at C6 and therefore cannot form intermonomer carbon–carbon bonds. This leads to an increased degree of polymerisation of guaiacyl units, potentially making them more resistant to enzymatic attack (del Rio *et al.,* 2002; Vane *et al*., 2003). Another plausible explanation is that the mode of attack of many lignolytic microbes may be to preferentially attack the secondary cell wall layers that are richer in S lignin, leaving the G lignin rich inner lamella intact, leading to greater overall modification of syringyl units when compared to guaiacyl units (Backa *et al*., 2001).

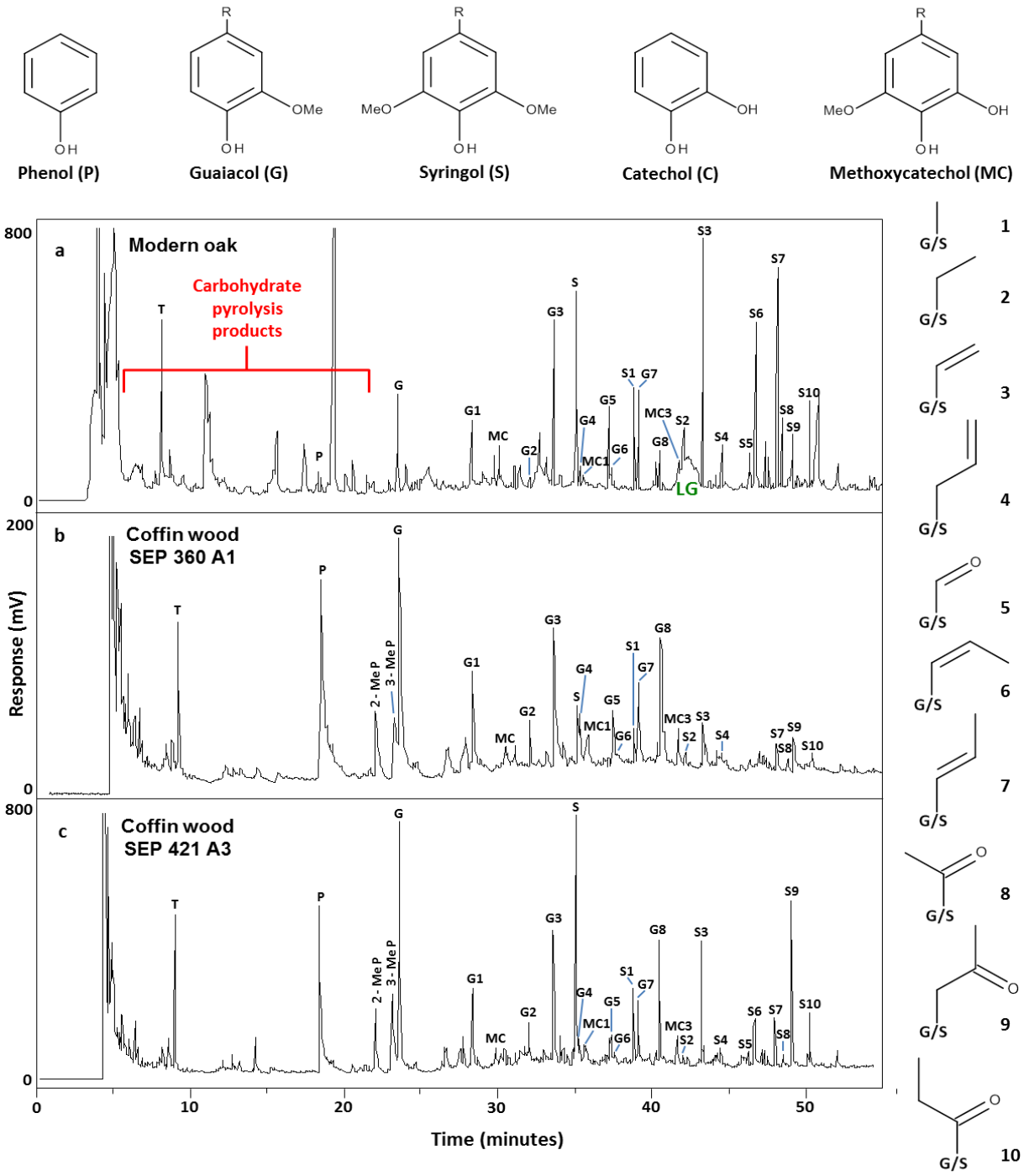

Figure 67. Assigned partial Py-GC-FID pyrograms of modern oak (a) and coffin wood from SEP360 (b) and SEP421 (c) at the Thaon church excavations. T = toluene, P = phenol, G = guaiacol, MC = methoxycatechol, S = syringol and LG = levoglucosan (a cellulose pyrolysis product). The identities of the numbered peaks are shown in the key to the right of the pyrograms.

Several mechanisms associated with the attrition of syringyl moieties have been proposed; two that are most often postulated being demethoxylation and demethylation. Demethoxylation (Figure 68) would result in an increase in mono-methoxylated guaiacyl units, contributing to an observed decrease in the S:G ratio (Saiz-Jiminez *et al*., 1987). One of the most characteristic pyrolysis signatures of heavily degraded lignin in archaeological wood is the increase in *para*-hydroxyphenyl with respect to guaiacyl and syringyl subunits. The increase is typically a result of

the complete demethoxylation of guaiacyl and syringyl subunits, leading to the liberation of large amounts of phenol on pyrolysis (Figure 68; Saiz-Jiminez *et al*., 1987; Martínez *et al*., 2001). The reaction scheme for the increase in phenol detected by Py-GC is shown in Figure 68. Larger amounts of phenol and smaller G:P ratios are evident in both coffins from Thaon, suggesting that demethoxylation of guaiacyl subunits or di-demethoxylation of syringyl subunits has occurred.

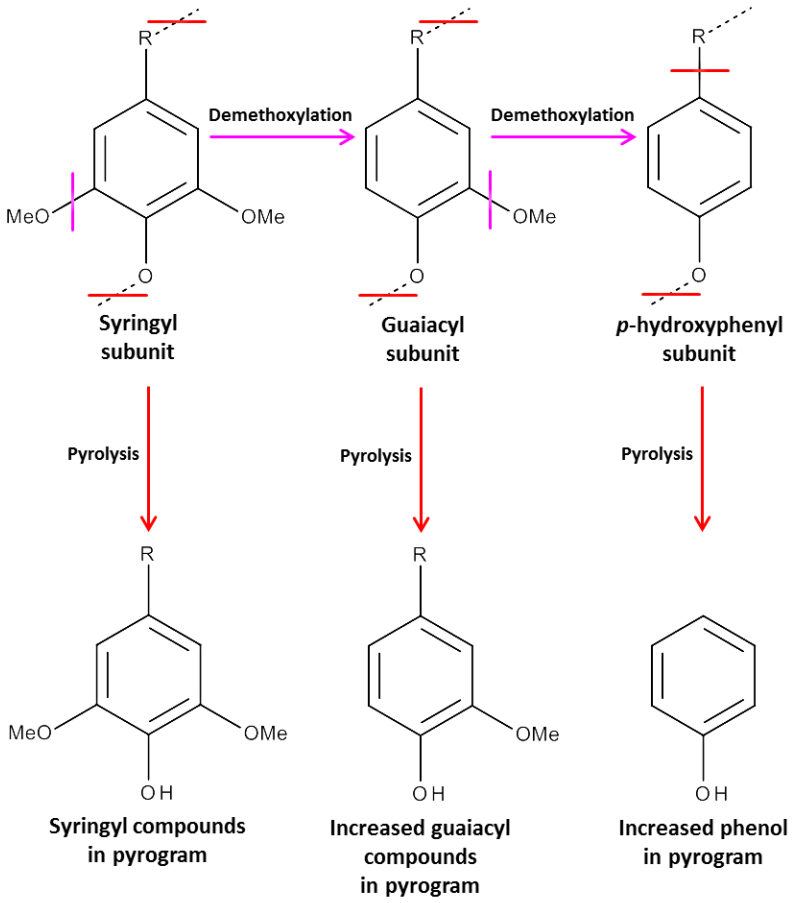

Figure 68. Postulated pathway for the demethoxylation of syringyl and guaiacyl lignin subunits, leading to the formation of phenol. Adapted from Schoemaker, 1990.

Demethylation of lignin phenols leads to the production of a range of benzenediol compounds. The demethylation of guaiacyl units yields catechol compounds (C; Figure 69a) whereas syringyl units can be mono-demethylated to produce methoxycatechol compounds (MC; Figure 69b). The pyrograms of both archaeological samples from Thaon reveal higher amounts of both C and MC species than for modern oak (Table 13). Demethylation of lignin phenol is commonly observed as a result of the action of the laccase enzymes of several fungi, including brown rot fungi (Martínez *et al*., 2005; Sánchez, 2009). Recent work characterising the emerging role of bacteria in lignin degradation has demonstrated that several species of soil bacteria (including species from the genera *Pseudomonas* and *Actinomycetes*) can also modify lignin by demethylation (Vicuña, 1988; Zimmermann, 1990; Bugg *et al*., 2011b).

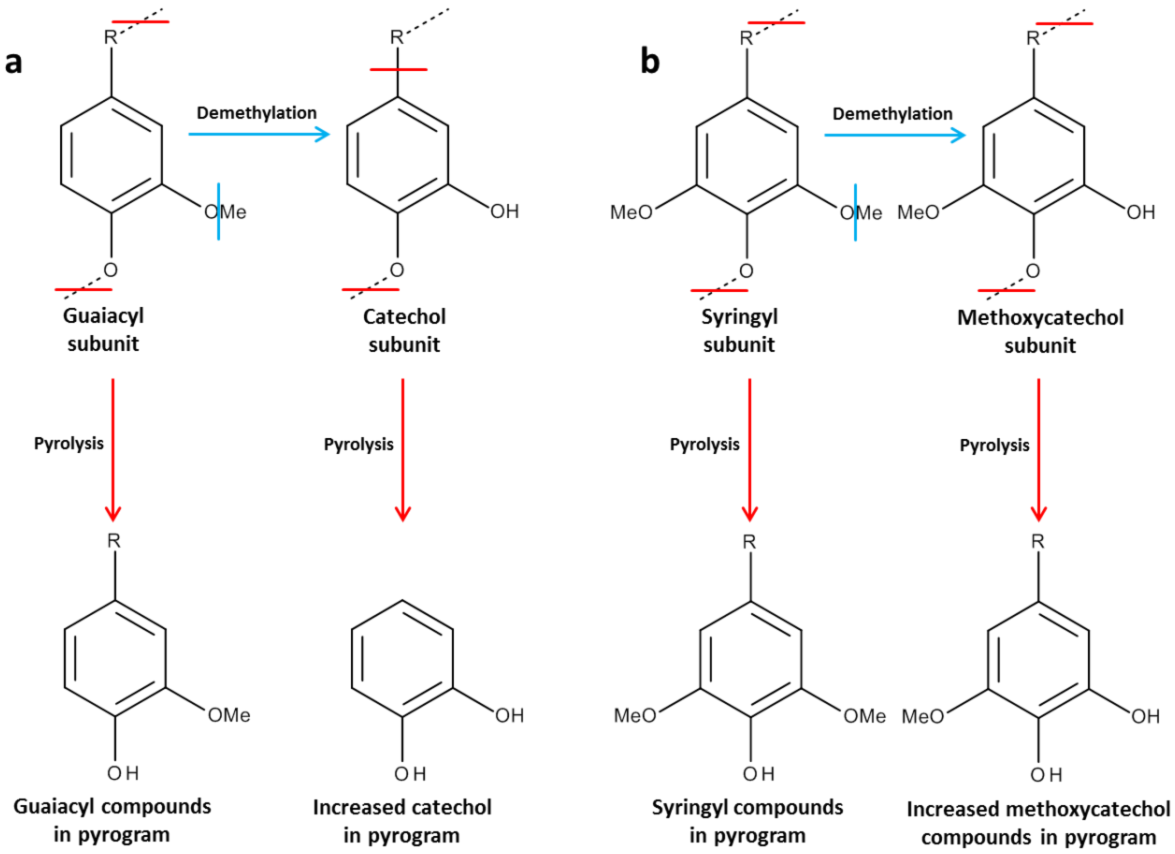

Figure 69. a) Postulated pathway for the demethylation of guaiacyl lignin subunits, leading to catechol formation, b) postulated demethylation of syringyl lignin subunits, leading to the formation of methoxycatechol derivatives.

5.7.2.2 SEM

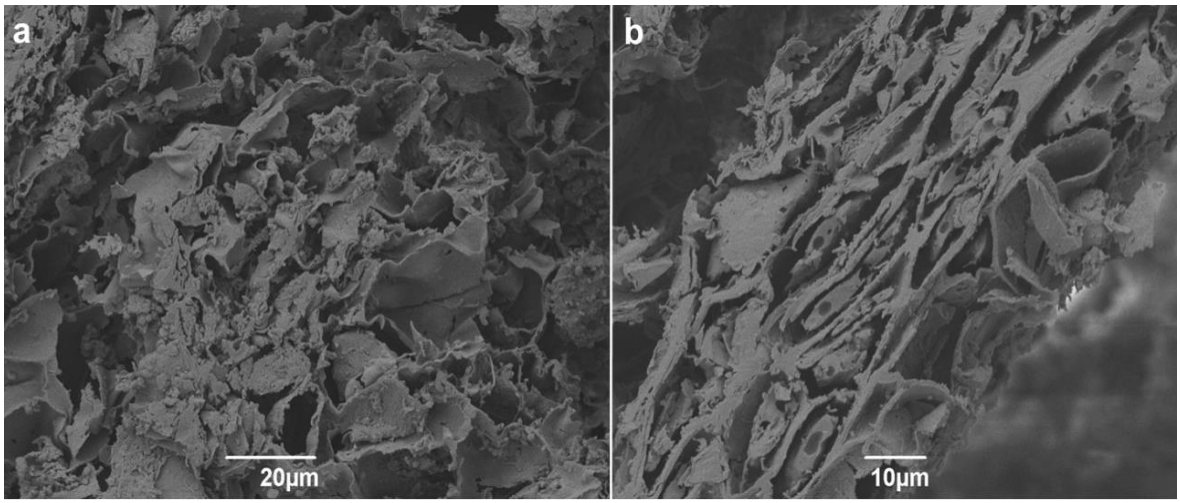

Figure 70. SEM images of coffin wood from SEP360 at the Thaon church excavation. The left image (a) shows that the cellular structure of the wood has been heavily distorted. The right image (b) shows that all holocellulose has been removed, leaving a weakened lignin skeleton.

Structurally, the wood from SEP360 at Thaon is heavily compromised. Figure 70a shows little of the cell structure that is typically observed in angiosperm woods at similar levels of magnification. The cell features that are present are very thin, suggesting a complete removal of cellulose to leave behind a lignin rich skeleton of middle lamellae (Rowell and Barbour, 1990). Other sections of the wood (seen in Figure 70b) show that the majority of the wood cells have collapsed and been compressed. Such damage is attributable to loss of secondary cell wall layers due to removal of holocellulose components (Blanchette, 2000). The fact that the cell walls are thinner than those of undegraded angiosperms wood also suggests that cellulose attrition has taken place. This finding fits with the lack of peaks in the carbohydrate region and an absence of levoglucosan (from cellulose) in the pyrograms of the coffin wood.

The physical damage to the wood structure is in excess of that expected given the levels of lignin still present in the material. Woods that are more heavily chemically modified still show a high degree of order; an example being the wood from the top of the coffin nail from grave 310 at Fewston (see Section 3.2.2). The disparity between the chemical and physical preservation of the wood may be due to the water levels at the site. During excavation, grave 360 was partially submerged in water. It is unknown if the water table fluctuates or whether the coffin was waterlogged continuously. Collapse and shrinkage similar to that observed in the SEM of the Thaon coffin wood has been reported in previous studies of waterlogged woods; the damage is attributed to the loss of the water when the wood is dried in an uncontrolled manner, leading to the collapse of the tracheid cells (Florian, 1990). A repeated change in the water level could have led to the wood from grave 360 experiencing periodic cycles of wetting and drying.

5.7.3 Summary and conclusions

The coffins from the graves at Thaon, SEP360 and SEP421, are both made from angiosperm wood, as indicated by the presence of both guaiacyl and syringyl lignin subunits. Burial in a hardwood coffin indicates that the individuals were of appreciable wealth. Neither wood yielded any carbohydrate derived pyrolysis products, indicating that the holocellulose has been completely degraded. In comparison with modern oak, both archaeological woods show degradation of the lignin component, exhibiting a smaller long:short chain lignin subunit ratio and evident demethoxylation (smaller S:G and G:P ratios) and demethylation (smaller S:MC ratio) of the lignin methoxyphenols. The wood from SEP360 also contained fewer oxidised lignin side chains. All of these metrics indicate that the archaeological materials are more degraded than the modern oak and that the wood from SEP360 is significantly more degraded than that from SEP421.

The SEM of wood from SEP360 reveals a complete loss of all secondary cell wall layers and a high degree of physical deformation, possibly due to fluctuations in the water table affecting the burial environment.

5.8 Hanson Logboat

5.8.1 Site and sampling information

The Hanson Logboat was discovered in the Hanson Gravel Pit in the village of Shardlow, Derbyshire, in 1998 (latitude: 52.860235, longitude: -1.368392). The boat was discovered when a quarrying machine uncovered and destroyed the stern (British Archaeology Magazine, 2003). Carved from the trunk of a single 300 year old oak tree (*Quercus robur*), the vessel still contained its cargo of Bromsgrove sandstone, suggesting that its sinking was not intentional (Crawshaw *et al.*, 2013). Radio carbon dating indicates that the tree from which the boat was constructed was felled between 1440 and 1310 BC, in the Middle Bronze Age (Crawshaw *et al.*, 2013). Its preservation for approximately 3400 years was undoubtedly facilitated by the waterlogged environment in which it resided. Waterlogged environments are often anoxic or anaerobic, conditions that retard microbial decay of wood and can result in wooden objects surviving for thousands of years (Blanchette, 1991). Such conditions do not, however, always prevent deterioration of wood; biological or chemical modification can still occur (Florian, 1990).

The surviving 11 metres of the logboat was cut into sections to enable its removal from the site and each section was conserved by York Archaeological Trust (Crawshaw *et al.,* 2013). The conservation process involved the replacement of water in the structure of the wood with two grades of the polymer polyethylene glycol (PEG); initially impregnating with PEG 200, followed by PEG 3400 (Crawshaw *et al.,* 2013). PEG is commonly used to impregnate wooden archaeological artefacts recovered from waterlogged environments during conservation (Graves, 2004). The polymer impregnates the wood, as water (which can constitute a large proportion of the mass of the artefact) is slowly removed. The PEG acts as a cell wall bulking agent and a consolidant, preventing the wood from cracking and deforming. Following impregnation with PEG the boat was freeze dried to remove any remaining water.

Whilst on display at Derby Museum and Art Gallery, the Hanson Logboat began to display signs of deterioration. Parts of the wood appeared to take on a darker colour and became brittle. Owing to concerns about the condition of the boat, samples were taken for analysis. In order to assess the preservation state of the boat, samples of the deteriorated wood (labelled HL 2011) were analysed alongside samples kept in refrigerated storage from after the conservation treatments were applied that did not exhibit the same changes in morphology (labelled HL 2003), and modern English Oak (*Quercus robur*). The polyethylene glycol conserving agents were removed by solvent extraction (Chapter 2.2.2.4) to enable degradation of the holocellulose and lignin components of the woods to be assessed. Materials were analysed by EA (CHNS and O), Py-GC-FID, Py-GC-MS and SEM.

Figure 71. A map of the region surrounding Shardlow, Derbyshire, with the location that the boat was found marked by a red star (top) and an image of the Hanson Logboat on display in Derby Museum and Art Gallery, showing the sandstone blocks found in the vessel and several other artefacts found in context with the boat (bottom).

5.8.2 Analysis of archaeological material

5.8.2.1 EA

The TOC content for modern oak was measured as 37.1% (Figure 72 and Table 14). The overall elemental composition from the CHO data accords to the formula $C_{22}H_{38}O_8$, with trace levels of N. The higher TOC content of HL 2003 (44.0%) is consistent with depletion of holocellulose and enrichment of the lignin component of the wood, lignin having a considerably higher proportion of carbon (57.7% ± 1.4) than holocellulose (41.4% ± 1.6) (Eglin *et al*., 2008). The elemental abundances of C, H, N and S are higher in the HL 2003 material than in fresh oak, and the oxygen content is similar (Figure 72 and Table 14). The calculated molecular formula for the sample is $C_{20}H_{44}O_8$, with traces of N and S. An enrichment in lignin, via attrition of cellulose, would be accompanied by a small decrease in hydrogen content, a larger decrease in oxygen content and an increase in the carbon content. The similarity in oxygen content together with higher levels of H, N and S indicates the presence of other organic matter contaminating the archaeological wood.

The TOC content of the 2011 sample (2.2%) is considerably less than both fresh oak and the 2003 sample. The low TOC content indicates that the sample is predominantly inorganic in composition, which signifies severe attrition of the organic components of the wood. The elemental abundances similarly reflect the low abundance of organic matter. The sulfur content (27.4%) is considerably higher than would be consistent with organic sulfur containing compounds; hence it is apparent that the wood contains high levels of inorganic sulfur species.

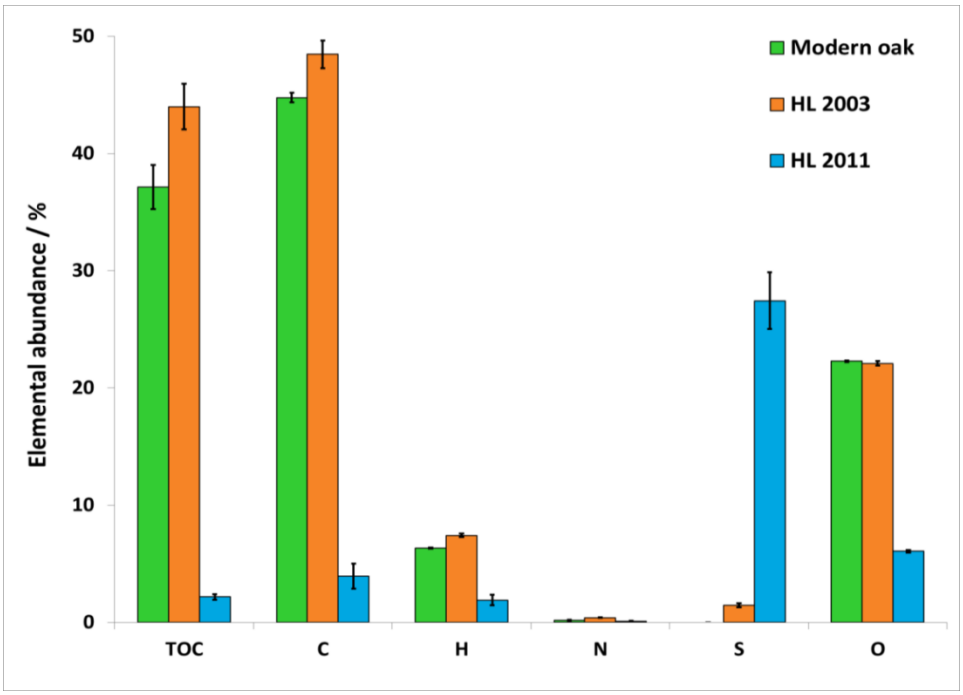

Figure 72. Mean element atomic abundances (n = 3) of fresh oak and wood from the two Hanson Logboat samples HL 2003 and HL 2011. Error bars show ± 1 standard deviation.

Table 14. Mean element atomic abundances (n = 3) of fresh oak and wood from the two Hanson Logboat samples HL 2003 and HL 2011 (%Δ represents the percentage difference in elemental composition compared with fresh oak).

Wood	TOC / % (%Δ)	SD	C / % (%Δ)	SD	H / % (%Δ)	SD	N / % (%Δ)	SD	S / % (%Δ)	SD	O / % (%Δ)	SD
Modern oak $C_{22}H_{38}O_9$	37.1	1.9	44.8	0.4	6.3	0.1	0.2	0.1	0.0	---	22.3	0.1
HL 2003 $C_{20}H_{44}O_8$	44.0 (18. 8)	1.9	48.5 (9.7)	1.2	7.4 (26.9)	0.1	0.41 (122)	0.4	1.5	0.2	22.1 (4.1)	0.2
HL 2011 $C_2H_{11}O_2$	2.2 (-94.1)	0.2	4.0 (-91.0)	1.1	1.9 (-67.5)	0.4	0.1 (-58.5)	0.1	27.4	2.4	6.1 (71.4)	0.1

5.8.2.2 Py-GC

Contrasting with the typical profile of monomer units from fresh oak (Figure 73a), the pyrogram of HL 2003 comprises a complex sequence of peaks eluting between 20 and 50 min (Figure 73b). The similarities in the elution times between peak clusters in the archaeological sample are typical of a large polymer with only a few unique monomeric units. Comparison with literature data suggested that the unknown polymer was polyethylene glycol (PEG), the pyrogram of PEG exhibiting very similar complex peak profiles (Voorhees *et al*., 1994). Combined with the knowledge that PEG was used in the conservation of the wood, the peaks in the conserved wood pyrogram can be attributed to PEG with confidence. The presence of PEG compromises the interpretation of the Py-GC chromatogram as it masks key signatures from the thermal breakdown of the wood polymers; for example, many of the lignin-derived peaks are obscured. Identification and assessment of the chemical integrity of the wood polymers cannot be performed on the wood without the PEG contaminant being removed.

The presence of PEG would be reflected in the elemental composition of the sample, partly explaining the atypical CHO values obtained. PEG impregnation would not, however, account for the observed increase in sulfur content (PEG does not contain any sulfur). A range of different molecular weights of PEG are used in conservation of wooden objects. PEG has the average formula $C_8H_{18}O_4$, which can be written as $C_{20}H_{40}O_{10}$ to aid comparison with wood formulae (Merck Index, 11th Ed). The presence of PEG in the 2003 sample would account for the elevated oxygen and hydrogen content, which would be expected to be depleted significantly in an archaeological wood sample due to the attrition of cellulose.

The pyrogram of 2011 (Figure 73c) reveals very extensive degradation of both the cellulose and lignin biopolymers. The pyrogram represents a signal strength one order of magnitude less than for the 2003 sample, obtained from an order of magnitude more material. The only identifiable peak in the pyrogram is that of phenol and no PEG was detected. These data combined with the EA data indicate that the material is very heavily decayed and – from a chemical perspective – is no longer recognisable as wood.

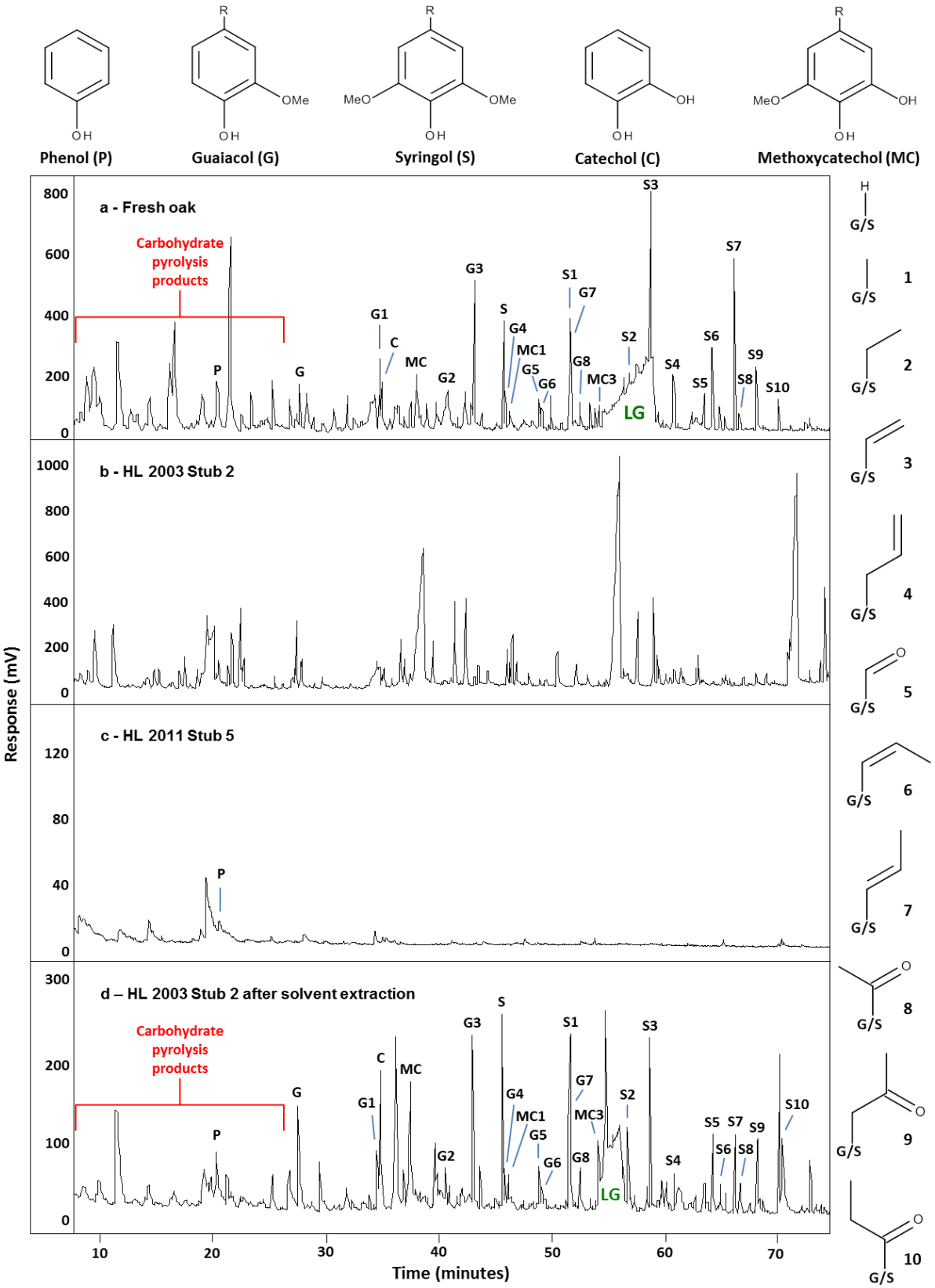

Figure 73. Partial Py-GC pyrograms of a) fresh oak, b) HL 2003, c) HL 2011 and d) HL 2003 after solvent extraction. P = phenol, G = guaiacol, C = catechol, MC = methoxycatechol, S = syringol and LG = levoglucosan (a cellulose pyrolysis product). The identities of the numbered peaks are shown in the key to the right of the pyrograms.

5.8.2.3 SEM

Under SEM the PEG can clearly be seen covering many of the interior surfaces of the HB 2003 wood (labelled as PEG in Figure 74a – d). The PEG is filling a large proportion of the tracheid cells and some of the lumen, which would suggest that the conservation treatment was successful in replacing water and incorporating the PEG consolidant into the wood. There is, however, substantial distortion of the wood structure, the majority of the cells appearing compressed. This is a feature typically observed when waterlogged wood is dried during conservation treatments (Florian, 1990). Despite the compression the substructure appears relatively intact, suggesting that the incorporation of the PEG is successfully preventing collapse of the dried wood. Although the tracheid cells appear to be thinner than those of modern oak (Fengel and Wegener, 1984; Florian, 1990), there is still evidence of secondary cell wall material (which is rich in holocellulose), indicating a reasonable level of preservation. No conclusive signs of microbial attack (such as pitting or fungal hyphae) are present.

The 2011 material bears little resemblance to the 2003 material or to modern oak, having a similar appearance to mineral or soil material (Figure 74e – h). There are several features which could be interpreted as being wood-like structures (labelled as PWT in Figure 74g). A crystalline material is visible on the surfaces of the sample, irregular polyhedra composed of 4, 5 and 6 sided polygons (labelled as CM in Figure 74e – h). The crystalline material is an inorganic mineral component. A crystal of the mineral (approximately 2 mm in diameter) was observed to have a golden colour during the preparation of samples for SEM, prior to the sputter coating. The geometry, colouration and high sulfur content of the wood are consistent with the material being pyrite (FeS_2).

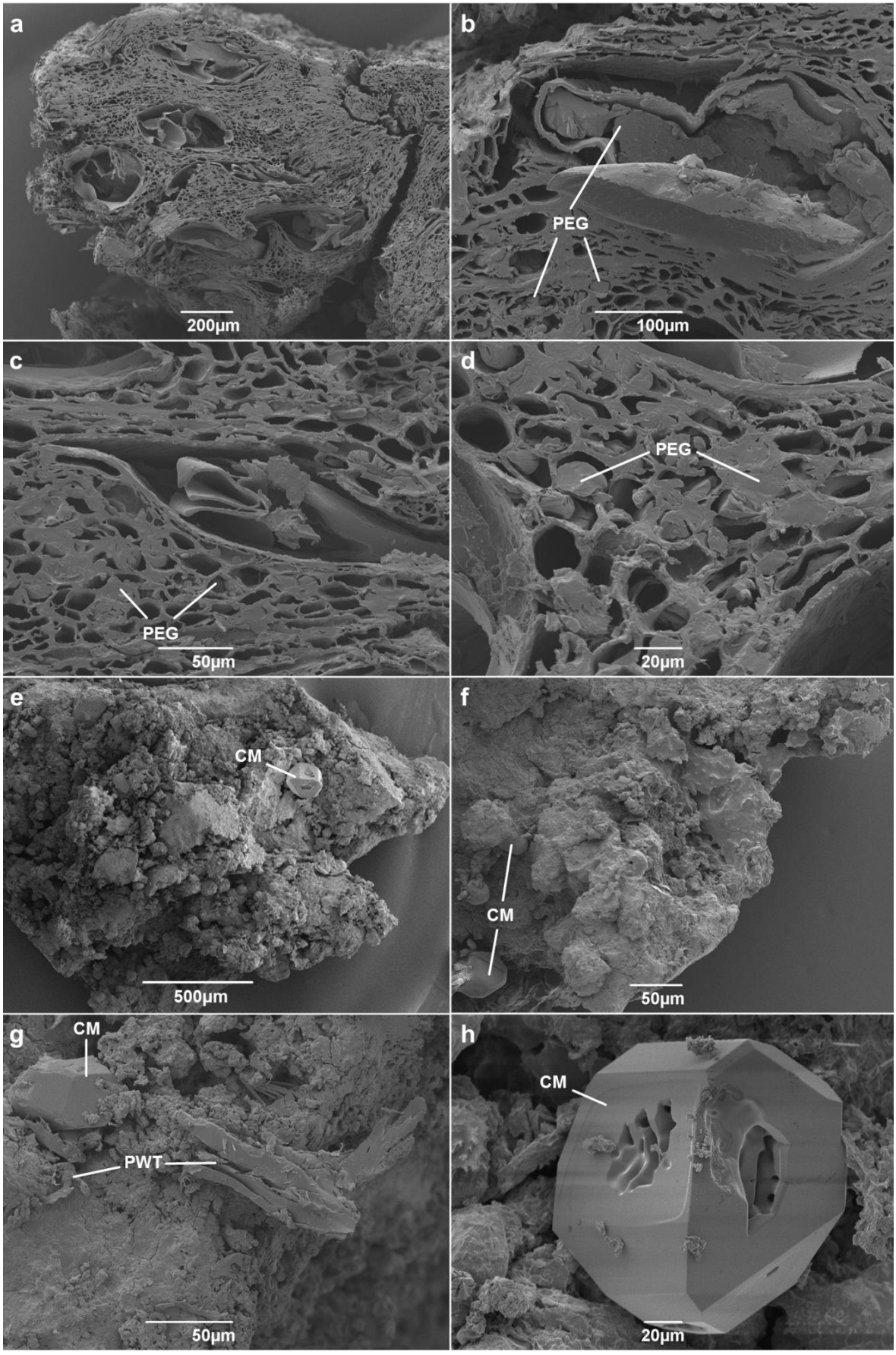

Figure 74. SEM images of HL 2003 (a to d), showing PEG imbedded in the voids of the woods substructure, and HL 2011 (e to h), showing crystalline material (CM) and possible woody tissues (PWT).

5.8.2.4 Accelerated solvent extraction

In an attempt to remove the PEG from HL 2003, the material was extracted sequentially with 9:1 DCM-methanol and acetone (see Chapter 2.2.2.4). Samples of modern oak and HL 2011 were also extracted to remove any non-polymeric materials that may have been contributing to the elemental composition.

The masses of each extract, percentage of the total extract mass and the percentage yields with respect to the mass of the HL 2003 wood extracted for each of the 9:1 DCM:methanol and acetone extractions are shown in Table 15. 59.7% of the mass of the 2003 material was removed by the applied solvents. Comparatively, samples of modern oak wood yield approximately 1% of their mass by extraction with similar solvents (Todaro *et al*., 2013; Kebbi-Benkeder *et al*., 2015). Assuming that a large proportion of the material extracted from the 2003 sample is PEG, the massive increase compared to modern wood demonstrates that – at the time sample was taken – PEG was a large constituent of the preserved wood. The removal of 91.7% of the total extractable material by the first DCM:methanol extraction suggests that a single extraction with this solvent mixture would remove sufficient PEG to allow for analysis by Py-GC.

Table 15. Mass and yield data for the solvent extraction of the 2003 Hanson Logboat material

Extract	Mass of extract / g	% of total extract mass	% yield of sample mass
DCM:MeOH 1	238.04	91.7%	54.8%
DCM:MeOH 2	12.03	4.6%	2.8%
DCM:MeOH 3	4.91	1.9%	1.1%
Acetone 1	2.34	0.9%	0.5%
Acetone 2	1.26	0.5%	0.3%
Acetone 3	0.88	0.3%	0.2%
Σ DCM:MeOH	254.98	98.3%	58.7%
Σ Acetone	4.48	1.7%	1.0%
Σ all extracts	259.46	100.0%	59.7%

5.8.2.5 EA after accelerated solvent extraction

The TOC content of the solvent extracted modern oak was the same as the unextracted sample (37.0%; Table 16 and Figure 75). The overall elemental composition accords to the formula $C_{22}H_{35}O_8$, with traces of N, very similar to that calculated before extraction ($C_{22}H_{38}O_8$). By contrast, the extracted HL 2003 sample gave a molecular formula of $C_{23}H_{32}O_7$, statistically distinguishable from the extracted oak and reflecting an appreciable difference in elemental composition. Thus, the extracted HL 2003 sample has a higher carbon content, and lower hydrogen and oxygen contents than the modern oak standard. Such changes are consistent with the attrition of the holocellulose fraction, which would be expected for an archaeological wood sample. Coupled with the observed differences between the TOC content before and after extraction, it is probable that a large quantity of the PEG has been removed by the extraction process, and that the elemental composition of HL 2003 after extraction reflects only the wood component.

Sulfur was absent from the solvent extracted wood from HL 2003 indicating that the sulfur in the unextracted sample represented elemental or organic sulfur species that are amenable to solvent extraction. The low TOC content of the solvent extracted wood from HL 2011 (2.1%) was the same as that of the unextracted wood (2.1%). The total carbon content (2.2%) is lower than in the unextracted material (4.0%) whereas the values for the sulfur contents of the native (27.4%) and solvent extracted woods (27.3%) are essentially identical. The resistance of the sulfurous material to extraction by organic solvents suggests it to comprise inorganic sulfur such as pyrite (FeS_2).

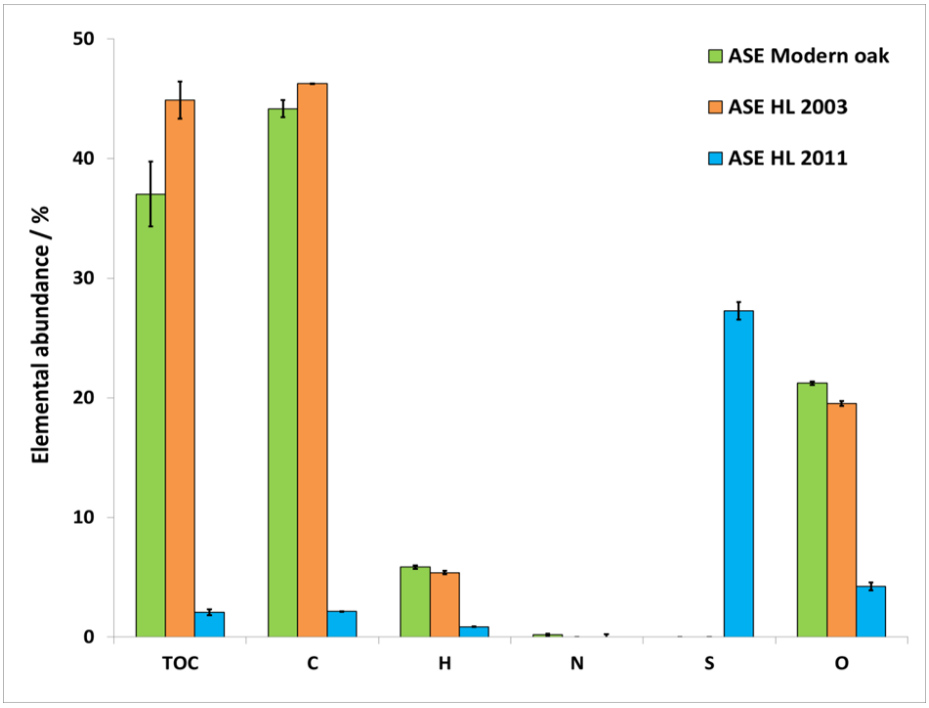

Figure 75. Mean element atomic abundances (n = 3) of fresh oak and wood from the two Hanson Logboat samples HL 2003 and HL 2011 after accelerated solvent extraction with 9:1 DCM-methanol and acetone. Error bars show ± 1 standard deviation.

Table 16. Mean element atomic abundances (n = 3) of fresh oak and wood from the two Hanson Logboat samples HL 2003 and HL 2011 after accelerated solvent extraction with 9:1 DCM-methanol and acetone (%Δ represents the percentage difference in elemental composition compared with fresh oak).

Wood	%TOC (%Δ)	SD	%C (%Δ)	SD	%H (%Δ)	SD	%N (%Δ)	SD	%S (%Δ)	SD	%O (%Δ)	SD
Modern Oak $C_{22}H_{38}O_9$	37.1	2.7	44.0	0.7	5.9	0.1	0.2	0.2	0.0	---	21.2	0.2
HL 2003 $C_{23}H_{32}O_7$	44.9 (21.2)	1.5	46.3 (4.7)	0.0	5.4 (-7.8)	0.2	0.0	---	0.0	---	19.6 (-7.9)	0.2
HL 2011 $C_1H_5O_2$	2.1 (94.4)	0.3	2.2 (-95.1)	0.0	0.9 (-85.2)	0.0	0.0	---	27.3	0.8	4.2 (-80.0)	0.3

5.8.2.6 Py-GC after solvent extraction

The absence of PEG signatures in the pyrogram of HL 2003 after solvent extraction (Figure 73d) indicates its complete removal from the wood. Pyrograms of the solvent extracts contained abundant signatures of PEG, consistent with it being removed by the DCM:methanol solvent (data not shown). The profile of the pyrolytic breakdown products from the extracted 2003 wood sample is very similar to that of modern oak (Figure 73a), but with several key differences. The lower relative abundance of carbohydrate pyrolysis products in the pyrogram of the archaeological wood is attributable to the degradation of cellulose and hemicellulose. The species eluting before 26 min are furan based aldehydes and ketones produced by thermally induced degradation reactions of 6-membered ring sugars from both cellulose and hemicellulose. As a result, the compounds cannot be assigned specifically to either polymer. A decrease in the peak area of levoglucosan, a product of the thermal degradation of cellulose, suggests that the cellulose component of the wood has certainly been degraded. The most commonly observed biological degraders of wood in waterlogged or aquatic environments are bacteria, fungi playing a subordinate role than is typically observed in other burial environments (Björdal *et al*., 1999; Blanchette, 1995). Typical bacterial wood degraders preferentially attack the carbohydrate components, with limited modification of the lignin component (Blanchette 1991; Blanchette, 1995; Blanchette and Hoffmann, 1994; Kim, 1990). The presence of only residual amounts of holocellulose in the 2003 sample indicates limited preservation of the more labile component of the original wood polymer composition.

Percentages of the individual lignin derived compounds produced upon pyrolysis of both materials were calculated with respect to the sum of all lignin phenol peak areas (shown in Table 17). The pyrograms of modern wood and HL 2003 material show clear differences in the lignin content.

Microbially mediated decay of lignin subunits typically results in a measurable decrease to the S:G ratio (Saiz-Jiminez *et al*., 1987; Martínez *et al*., 2001). Previous studies of archaeological wood recovered from waterlogged environments has suggested that the syringyl units are selectively degraded, either by being chemically modified in chain or involving their complete removal from the lignin polymer, leading to a lower S:G ratio than for undegraded wood of the same species ([van Bergen et al., 2000]). S:G ratios for corresponding guaiacyl and syringyl pyrolysis products are shown in Table 18. The total S:G ratio and those for the majority of corresponding guaiacyl and syringyl compounds are lower in the HL 2003 wood than in modern oak, suggesting a preferential loss of syringyl lignin components from the HL 2003 wood. This indicates that there has been some modification of the HL 2003 wood lignin component.

Table 17. Semiquantitative analysis of lignin derived phenols produced upon pyrolysis of solvent extracted modern oak and Hanson Logboat 2003 wood. Values are expressed as percentages of the sum of all lignin phenol peak areas.

Compound	Modern oak	Hanson Logboat 2003
(P) Phenol	5.45	3.39
(G) Guaiacol	3.44	7.61
(G1) 4-Methylguaiacol	6.15	2.28
(C) Catechol	3.09	7.36
(MC) Methoxycatechol	6.65	11.24
(G2) 4-Ethylguaiacol	6.22	1.44
(G3) 4-Vinylguaiacol	7.94	6.18
(S) Syringol	5.56	7.15
(G4) 4-Allylguaiacol	1.97	1.37
(MC1) 4-Methylmethoxycatechol	1.73	2.00
(G5) Vanillin	1.81	2.29
(G6) *cis*-Isoeugenol	1.08	0.85
(S1) 4-Methylsyringol	4.52	5.65
(G7) *trans*-Isoeugenol	4.59	4.02
(G8) Acetoguaiacone	2.19	1.67
(S2) 4-Ethylsyringol	1.33	0.31
(MC3) 4-Vinylmethoxycatechol	1.49	9.60
(S3) 4-Vinylsyringol	9.70	5.60
(S4) 4-Allylsyringol	2.75	1.01
(S5) Syringaldehyde	2.24	2.90
(S6) *cis*-4-Propenylsyringol	4.62	3.55
(S7) *trans*-4-Propenylsyringol	8.02	2.70
(S8) Acetosyringone	1.16	1.22
(S9) Syringylacetone	4.62	2.83
(S10) Propiosyringone	1.69	5.79

Table 18. Ratios for corresponding syringyl, guaiacyl, phenol and methoxycatechol subunits from solvent extracted modern oak and Hanson Logboat 2003 wood. ^ denotes an increase in the S:G ratio.

Ratio	Modern oak	Hanson Logboat 2003
SH:GH	1.62	0.94
S1:G1	0.74	^2.48
S2:G2	0.21	0.21
S3:G3	1.22	0.91
S4:G4	1.39	0.73
S5:G5	1.24	^1.27
S6:G6	4.28	4.19
S7:G7	1.75	0.67
S8:G8	0.53	^0.73
Σ S:G	1.13	1.09
Σ S:MC	4.68	1.69
Σ G:C	11.44	3.76

Several mechanisms for the direct attrition of syringyl moieties have been proposed, the two most often postulated being demethoxylation and demethylation. Demethoxylation would result in an increase in mono-methoxylated guaiacyl units, contributing to an observed decrease in the S:G ratio (Saiz-Jiminez *et al*., 1987). One of the most characteristic pyrolysis signatures of heavily degraded lignin in archaeological wood is the increase in *para*-hydroxyphenyl with respect to guaiacyl and syringyl subunits. The increase is typically a result of the complete demethoxylation of guaiacyl and syringyl subunits, leading to the liberation of large amounts of phenol on pyrolysis (Figure 68). An increase in the amount of phenol is not evident in the Hanson Logboat pyrolysis results, suggesting that complete demethoxylation of syringyl to *para*-hydroxyphenyl lignin subunits has not occurred.

Demethylation of lignin phenols leads to the production of a range of benzenediol-related compounds. The demethylation of guaiacyl units yields catechols (C; Figure 69a) whereas syringyl units can be mono-demethylated to produce methoxycatechols (MC; Figure 69b). The pyrogram of solvent extracted wood from the 2003 sample reveals a marked increase in both C and MC species, the G:C and S:MC ratios both being approximately three times smaller in the HL 2003 wood than in modern oak (Table 18). Demethylation of lignin phenols is commonly observed as a result of the action of the laccase enzymes of fungi including brown rot fungi (Martínez *et al.,* 2005; Sánchez, 2009). Recent work characterising the emerging role of bacteria in lignin degradation has demonstrated that several species of soil bacteria (including species from the genera *Pseudomonas* and *Actinomycetes*) can also modify lignin by demethylation (Vicuña, 1988; Zimmermann, 1990; Bugg *et al.,* 2011a). Low levels of methoxycatechols have also been identified in modern wood standards and suggested to result from demethylation of syringyl subunits in the earliest stages of wood diagenesis (van Bergen *et al.,* 2000). Alternatively, the methoxycatechols may be residual lignin precursors (such as 5-hydroxy-coniferaldehyde; Boerjan *et al.,* 2003).

In comparison with modern oak, the abundance of lignin phenols with shorter side chains is higher and the prevalence of longer side chains is lower in the HL 2003 wood. Higher levels of guaiacol, syringol, 4-methylsyringol (S1) and 4-ethylsyringol (S2) in the HL 2003 wood suggest that some modification to the three carbon linkages between the phenolic moieties has occurred, leading to depolymerisation of the lignin. Cleavage of the Cα–Cβ linkages of the lignin polymer (generating 4-methylsyringol) and demethoxylation (producing guaiacol) both occur following aromatic radical formation induced by microbial lignolytic peroxidases (Eriksson *et al*., 1990; Martínez *et al.,* 2005). Similar changes are reported by del Rio *et al.* (2002) when angiosperm wood is exposed to a range of delignifying *basidiomycetes.* Contrary to the overall reduction in molecular weight of HL 2003 pyrolysis products, is the substantially large amount of propiosyringone (10), containing a ketone functionality. Two other oxidised lignin compounds occurring in high relative abundance are vanillin (G5) and acetosyringone (S8). Such oxidative

alteration to lignin side chains has been previously reported when wood is treated with white rot fungi and is also attributed to the cascade of depolymerisation reactions that follow enzymatic radical generation (Faix *et al*., 1991; del Rio *et al*., 2002). Whether this reflects degradation of the wood prior to its burial or degradation during the time between excavation and the commencement of conservation treatments is not known. Such oxidative degradation processes may have been limited *in situ* as the conditions rapidly become anoxic in waterlogged environments (McGrail, 2014).

The pyrogram of solvent extracted 2011 wood showed no differences to the unextracted material (Figure 73c), suggesting that what little organic material remaining in the sample is not amenable to solvent extraction and is therefore probably polymeric. The lack of peaks in the carbohydrate region of the pyrogram, and the simplicity of the peak patterns compared with those from fresh oak, implies that none of the holocellulose remains and any remaining lignin is in an extremely degraded form. The heavily degraded lignin has lost much of its peripheral functionality, the defunctionalised remnants producing phenol upon pyrolysis (as in the final step in Figure 68). Recent experimental work produced very similar pyrograms by treating modern angiosperm wood with sulfuric acid (pH 1 for 16 weeks at 80 °C; High, 2014). Inorganic sulfurous species such as pyrite have been shown to aggregate in the microstructures of wood, originating either directly from the environment or being produced by the reaction of iron(III) oxide (Fe_2O_3) with dissolved sulfides (H_2S, HS^- or S^{2-}) (Macleod and Kenna , 1990; Sandström *et al*., 2005). Reduced sulfur-containing species are known to degrade by oxidation in the presence of atmospheric oxygen, producing various oxides of iron as well as sulfate anions, as shown in Equation 1 (Ghisalberti *et al.,* 2002; Jerz and Rimstidt, 2004; Sandström *et al*., 2005).

Sulfates react with moisture in the air (the attraction to conserved archaeological materials being facilitated by the hygroscopic properties of PEG) to produce sulfuric acid, which has been shown to damage archaeological woods (Macleod and Kenna, 1990; Sandström *et al*., 2002; Sandström *et al*., 2005). Acidification of the wood due to the generation of acidic species is likely the cause of the damage seen in the Hanson Logboat after its period of museum display.

$$FeS_2 + 3.5O_2 + (n+1)H_2O \longrightarrow FeSO_4 \cdot nH_2O + H_2SO_4$$

Equation 1. The reaction of pyrite with water and oxygen, producing hydrated iron sulfates and sulfuric acid (Jerz and Rimstidt, 2004).

Further work on this material, to identify the type of inorganic sulfur compounds present, could be carried out. Possible methods of analysis include X-ray diffraction (either by isolation of the sulfurous material or in conjunction with scanning electron microscopy) and sulfur and iron K-edge XANES (Fors *et al*., 2011).

5.8.3 Summary and conclusions

The two logboat samples are in very different states of preservation. HL 2003 displays some attrition of the holocellulose fraction. The lignin component has also been degraded, measurable by a decrease in the lignin S:G ratio, partial modification of the lignin by demethylation producing substituted aromatic phenols, and higher amounts of short chain and oxidised lignin compounds as a result of oxidative depolymerisation. Degradation of celluloses and demethylation of lignin both occur early during the decomposition of wood in archaeological burials, whereas depolymerisation and oxidation of the aryl three carbon linkages typically occur in oxic environments as a direct result of microbial decay. It is uncertain if the decay to the biopolymers occurred preburial, within the burial environment, or post excavation. SEM imaging suggests that the microstructure of the wood is relatively well preserved, owing to the successful impregnation by PEG. By contrast, HL 2011 is very heavily degraded, with no cellulose and only very little, heavily modified lignin remaining. The high level of inorganic sulfur-containing mineral in the material indicates a likely route to enhanced degradation of the wood, through oxidation to generate sulfuric acid and lower the pH of microenvironments within the wood. Finding a solution to the 'sulfur problem' is a major focus of current research in the conservation community (Fors *et al*., 2014; Chaumat, 2016; Pearson *et al*., 2016; Sandström and Schofield, 2016).

A particularly novel and interesting aspect of this study of archaeological wood samples is the ability to perform a comprehensive set of analyses following the removal of PEG conservation treatments that accurately and directly reflect the preservation state of the constituent biopolymers. Previous work on the analysis of woods conserved with PEG have either used expensive solid state NMR techniques combined with data manipulation to remove the responses from the PEG (Bardet *et al*., 2007; Fors *et al*., 2011) or have analysed the wood using Py-GC-MS without the removal of the PEG, giving limited data on the condition of the wood (Tamburini *et al*., 2016).The ability to remove chemical contaminants easily and completely from materials that have undergone similar conservation processes and their subsequent analysis by readily available, highly informative techniques potentially allows for the future analysis of precious artefacts in collections. This is an exciting prospect as it could facilitate the analysis and assessment of objects that hold vast cultural, social and historical significance.

5.9 Analysis of intersite trends

The number of lignin derived compounds analysed for each sample and the large number of samples analysed resulted in a large, multidimensional dataset. In order to assess any patterns and trends present across all of the experimental and archaeological burial environments, principal component analysis (PCA) using PAST v3.15 (Hammer *et al*., 2001) was used to interpret the relative lignin phenol compositions of both the gymnosperm (Chapter 5.7.1) and the angiosperm (Chapter 5.7.2) datasets. Missing values in individual data rows were filled using iterative imputation; blanks were initially replaced by the column mean, then the data was subjected to subsequent PCA runs until convergence (Ilin and Raiko, 2010).

5.9.1 PCA of gymnosperm wood lignin phenol data

The PCA scatter plot for lignin phenol composition data of all experimentally buried and archaeological gymnosperm wood samples is shown in Figure 76. A simplified biplot, showing the weighting of each lignin phenol variable on PC1 and PC2 is shown in Figure 77. The first two principal components (PC1 and PC2) account for 61.9% and 29.5% of the variation, a total of 91.4%. PC1 is positively correlated to G1 (0.23), G3 (0.37) and G12 (0.31), and negatively correlated to T (0.41), P (-0.68) and G (-0.18). PC2 is positively correlated to T (0.41). G3 (0.19) and G14 (0.36), and negatively correlated to G (0.72).

Using the PCA data points in combination with the data presented in the site specific sections of this chapter, three general trends are apparent. The green arrow in Figure 76 indicates wood samples where preferential lignin degradation has occurred, with extensive modification of the lignin components of the wood leading to a much larger predominance of short chain, defunctionalised lignin subunits (T and P; see Figure 77), and relatively little damage to the holocellulose. From the analytical pyrolysis data and SEM images in Chapter 5.3, it was reasoned that the wood samples from SK310 at Fewston were likely degraded by lignin-preferring white rot fungus, and that the wood from the bottom of the copper coffin nail is the least degraded, the wood from the top of the nail is the most degraded and that the coffin wood away from the nail has a preservation state that is in between the two. The wood from SK26 at Mechelen was also postulated to have been modified by a lignin-specific decay agent, although there was no clear evidence to determine if the cause was fungal, bacterial or chemical. This wood has a lignin pyrolysis profile that is very different from that of the modern pine, suggesting it to be very degraded. The trend highlighted in green in the PCA supports that these materials were all degraded in a similar manner, and that the wood from SK26 at Mechelen and the top of the coffin nail of SK310 at Fewston are the most degraded in this trend line. It is, therefore, reasonable to

conclude that the green arrow represents the decomposition trajectory for gymnosperm woods that are degraded by microfauna with similar lignin-specific degradation capabilities.

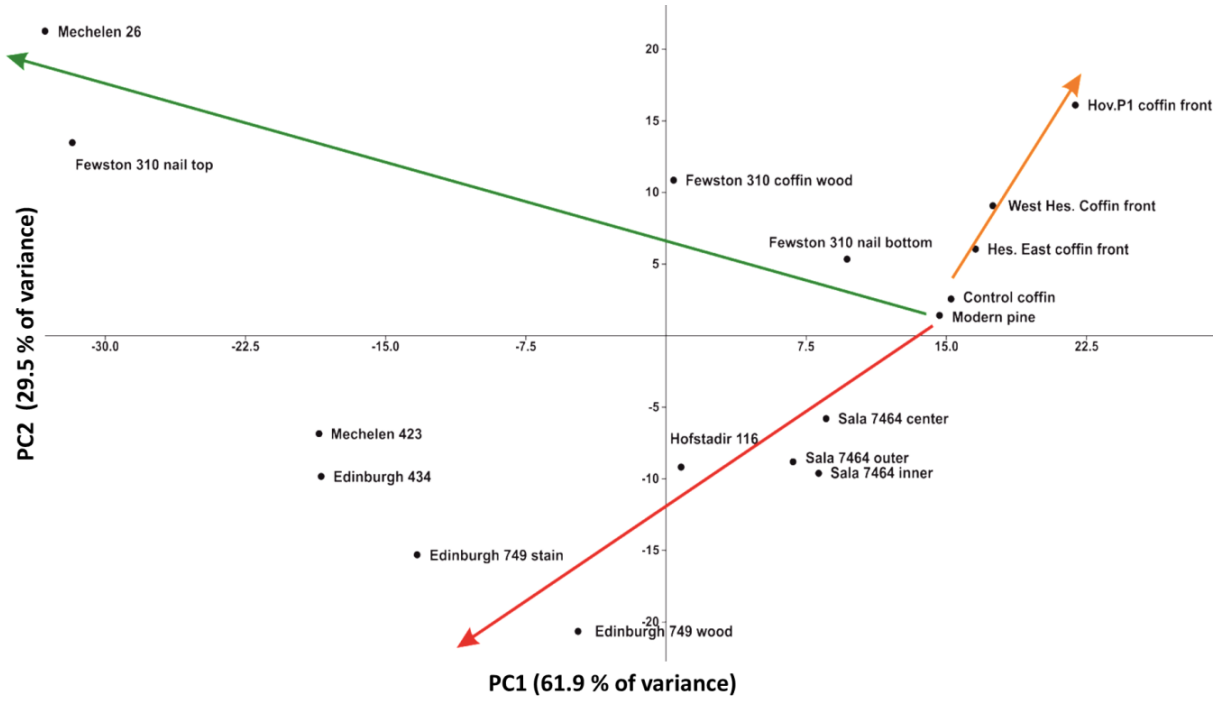

Figure 76. PCA scatter plot of PC1 and PC2 for gymnosperm wood lignin phenol composition data, accounting for 91.4% of total variance.

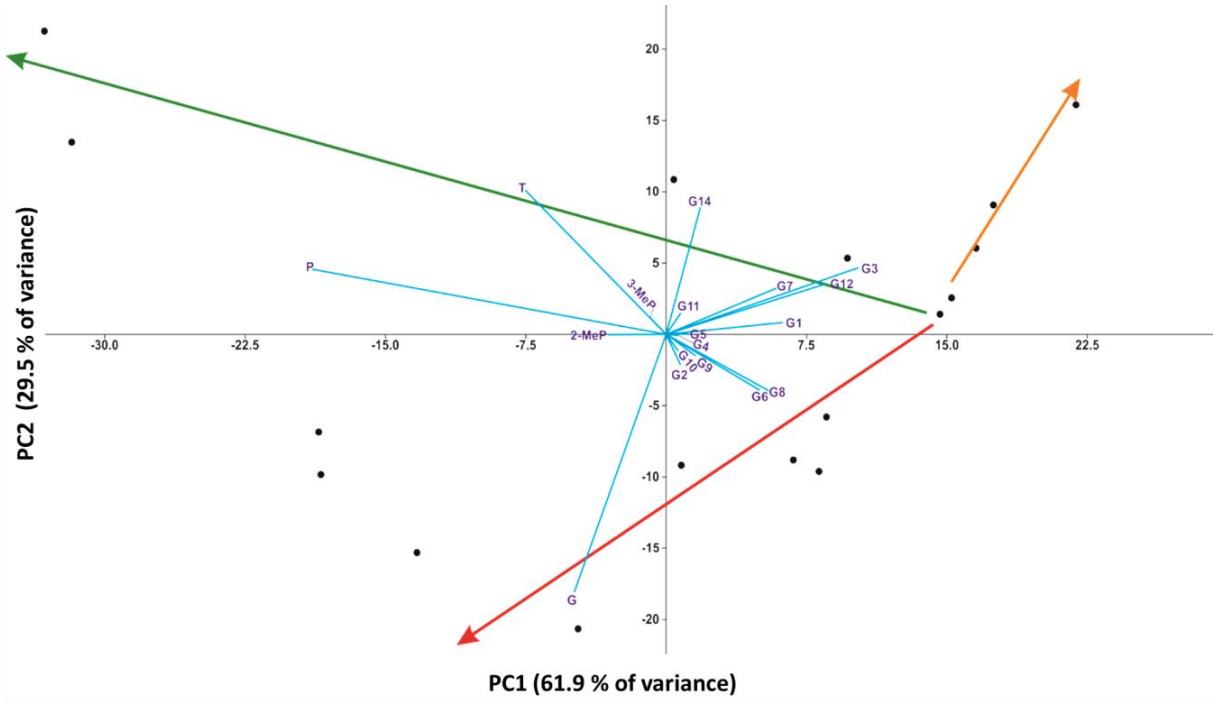

Figure 77. PCA loadings plot of gymnosperm wood lignin phenol composition data, showing the major contributions of each compound to PC1 and PC2.

The red arrow in Figure 76 correlates with increasing difference in the lignin pyrolysis profile from modern pine, with increasing percentage composition of G down the trend. These materials were all postulated to have been degraded by factors that affect both the holocellulose and lignin components of the wood, such as brown rot or non-lignin-specific white rot fungus, with the material from the soil stain at Edinburgh having a lignin compound profile most different to that of the modern pine. The trend seen in this case is less well defined than that seen for lignin-specific white rot (green arrow), with the points around the red arrow being more disperse. Whilst far less convincing and less certain than that seen for lignin-specific degradation, this trend may represent the decomposition trajectory of gymnosperm wood when subjected to microfauna that do not selectively degrade lignin, or degrade both lignin and holocellulose in the burial environment.

The third evident trend in Figure 76 is that for the coffins from the burial experiments, represented by the orange arrow. The lowest point of the trend is that of the unburied control wood, which is obviously the least degraded. The point that is most distant to the control point is wood from the Hovingham Piglet 1 coffin, which, on the basis of the pyrolysis data in Chapter 4.2, the Piglet 1 coffin was concluded to be the most degraded gymnosperm piglet coffin wood. The other two gymnosperm piglet coffin samples lie between the control and that fore Hovingham Piglet 1, which suggests that these are in an intermediate state of preservation. This trend shown in the PCA is in agreement with the conclusions reasoned in Chapter 4.2. This is, however, a very small dataset as the majority of the wood from the experimental burials was angiosperm. The fact that the trend is moving away from the two trends for the archaeological gymnosperm materials is likely due to the wood being treated with modern preservation techniques (see Chapter 4.2.2.1).

5.9.2 PCA of angiosperm wood lignin phenol data

The PCA scatter plot for lignin phenol composition data of all experimentally buried and archaeological angiosperm wood samples is shown in Figure 78. A simplified biplot, showing the weighting of each lignin phenol variable on PC1 and PC2 is shown in Figure 79. The first two principal components (PC1 and PC2) account for 42.4% and 29.9% of the variation, a total of 72.3%. PC1 is positively correlated to P (0.71) and G (0.30), and negatively correlated to G1 (-0.44) and G7 (-0.24). PC2 is positively correlated to G1 (0.39), S3 (0.37) and S10 (0.22), and negatively correlated to P (-0.40).

In comparison with the archaeological gymnosperm PCA presented in section 5.9.1, the archaeological angiosperm wood dataset is far smaller, with angiosperm wood only being recovered from two archaeological sites. Despite this, all three of the archaeological angiosperm data points and that for modern oak form a well correlated, linear trend, shown by the brown arrow in Figure 78. Following the arrow away from the modern oak, samples of archaeological angiosperm wood are increasingly degraded, the pyrograms showing higher proportions of P and G, and lower proportions of syringyl derived compounds and long chain guaiacyl compounds. Analytical pyrolysis and SEM data indicate that the wood from the Hanson Logboat directly after conservation is in a relatively good state of preservation (Chapter 5.8). The analyses of wood from Thaon (Chapter 5.7) indicate that the two wood samples are relatively heavily degraded, with the material from SEP360 being in a more advanced state of decomposition than that from SEP421. The trend seen in the PCA plot agrees with the independent findings from the respective subsections of this chapter, and allows for the materials to be accurately ranked in terms of their lignin degradation. The trend may represent a degradation trajectory for angiosperm woods within archaeological burial environments, although the data set is far too small to make such a conclusion with any degree of certainty.

The angiosperm woods from the experimental burials are all loosely clustered away from the archaeological wood samples, highlighted in green in Figure 78. Due to the pre-treatment of the piglet coffin wood using unknown methods (see Chapter 4.2.2), the lignin profile of these materials is very different to untreated modern wood or any of the archaeological wood samples. As a result, the piglet coffin wood data points are not directly comparable with the modern or archaeological wood. Two of the more degraded wood samples from the burial experiments – those from Piglet 2 at Hovingham and Piglet 9 at West Heslerton – are in the lower right quadrant of the plot, the region where the most degraded angiosperm coffin wood is located. Whilst the pre-treatment of the piglet coffin woods prevents any direct comparison with the archaeological data set, the wood from the Hovingham Piglet 2 coffin was is the most advanced state of decay of all the experimentally buried woods, having an increased proportion of shorter chain and

defunctionalised lignin subunits. As a result of this, the location of the data point in a region of the PCA plot that corresponds to increased abundance of P and G is unsurprising. As this piglet burial wood is compositionally different from untreated and archaeological wood, further investigation as to the degradation trajectories of these materials is not warranted.

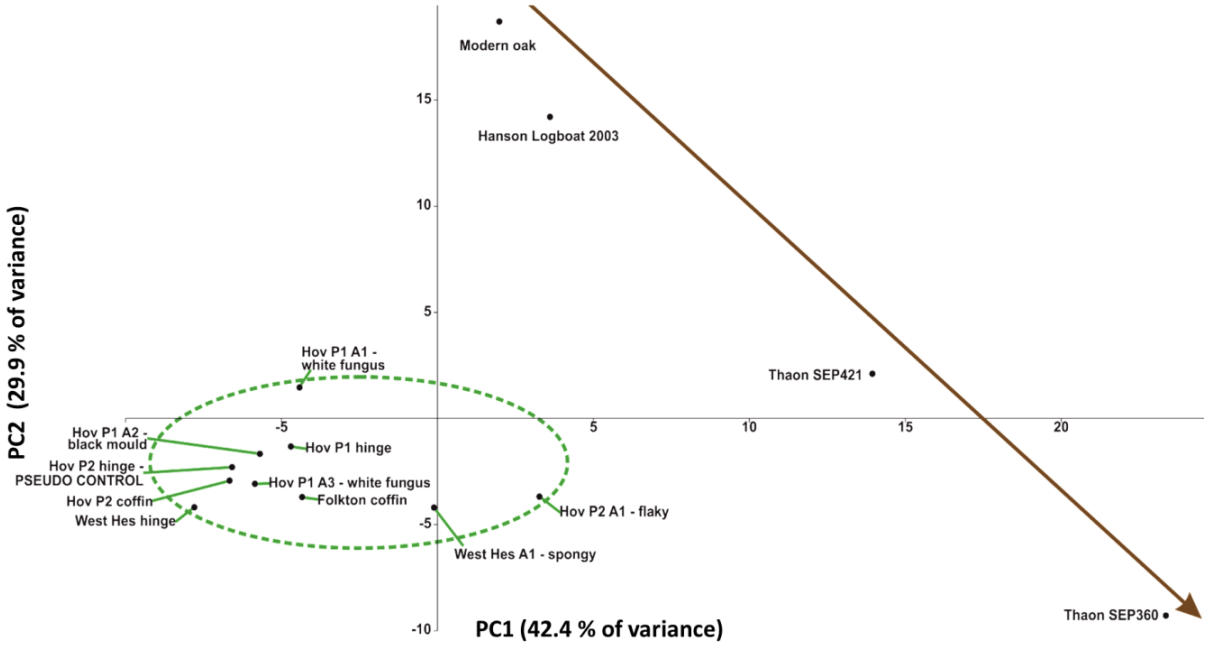

Figure 78. PCA scatter plot of PC1 and PC2 for angiosperm wood lignin phenol composition data, accounting for 72.3% of total variance.

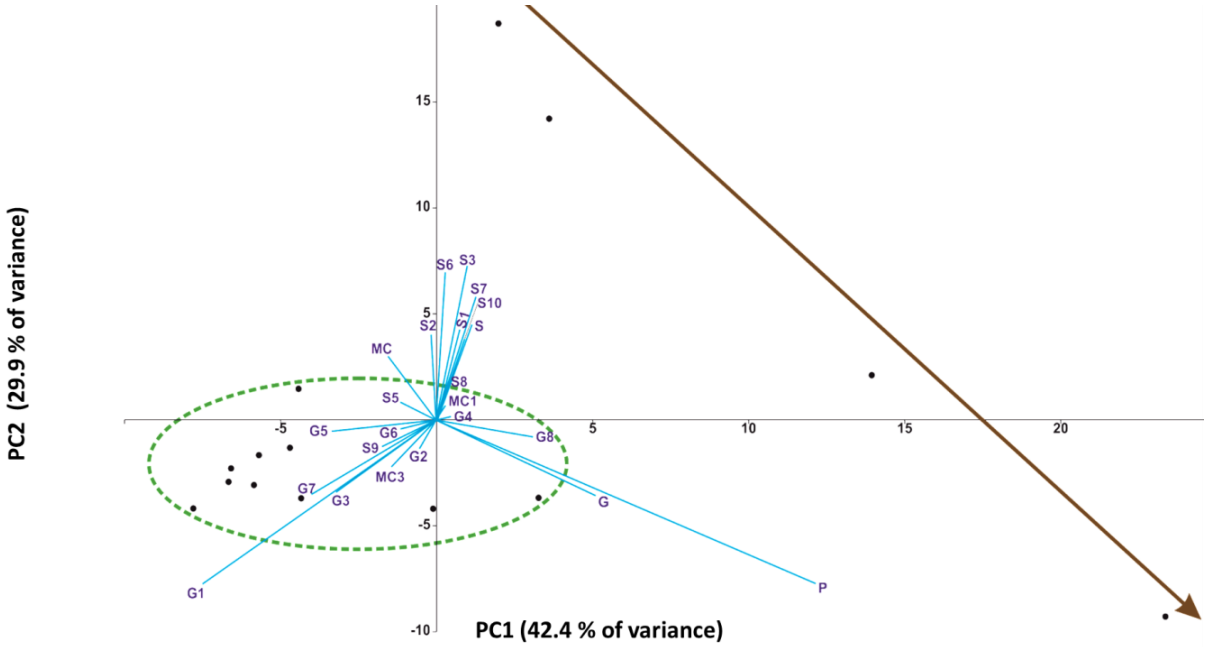

Figure 79. PCA loadings plot of angiosperm wood lignin phenol composition data, showing the major contributions of each compound to PC1 and PC2.

5.10 Conclusions

5.10.1 Decomposition of wood in archaeological burials

Table 19 presents the burial conditions and estimated dates of burial for the archaeological woods from the 7 excavation sites in Northwestern Europe and outlines some of the key findings from the analyses by Py-GC and SEM.

Table 19. Summary of findings from the analyses performed on the archaeological woods.

Site	Burial matrix	Burial date	Wood type	Preservation state	Suspected cause of decay
Edinburgh	Sand	1500 – 1700 AD	Gymnosperm	**G434**: no holocellulose and heavily modified lignin **G758**: only heavily modified lignin metabolites remain. **G749**: extreme degradation of holocellulose and decay of lignin.	**G434**: Non-selective white rot or lignolytic bacteria **G758**: Not known **G749**: Two different unknown causes
Fewston	Well drained coarse loamy soils	G271: not known G310: March 1886	Gymnosperm	**G271**: complete loss of organic polymers, mineralised. **G310**: varying with distance from copper nail, from extensive degradation of all polymers to excellent preservation. Evident fungal bodies.	**G271**: not known **G310**: lignin preferring white rot fungus
Hofstaðir	Histic andosol, pH 4 – 6	900 – 1300 AD	Gymnosperm	Loss of holocellulose and oxidative depolymerisation of lignin. Evident fungal bodies.	Non-selective white rot fungus
Mechelen	Sandy, likely acidic pH	Not known	Gymnosperm	**G26**: selective delignification, leading to extensive depolymerisation. Holocellulose intact. **G423**: loss of holocellulose, some lignin modification. Evident fungal bodies.	**G26**: lignin preferring white rot fungus **G423**: brown rot fungus
Sala	Sandy podzol, likely acidic pH	1400 – 1600 AD	Gymnosperm	Loss of holocellulose and secondary cell wall layers, demethoxylation and limited depolymerisation of lignin. Evident fungal bodies.	Brown rot fungus
Thaon	Waterlogged	1300 – 1840 AD	Angiosperm	Loss of all holocellulose and secondary cell wall layers, varying lignin degradation. Cell structure distorted.	Not known
Hanson Logboat	Waterlogged gravel pit	1440 – 1310 BC	Angiosperm, European oak	**2003**: preservation of cellulose and hemicellulose and some lignin modification. Cell distortion due to conservation. **2011**: complete destruction of all organic polymers.	**2003**: possible bacterial in burial environment. **2011**: inorganic iron sulfur compounds form sulfuric acid in humid air, producing sulfuric acid.

The majority of the materials analysed were identified as softwoods from gymnosperm trees. Wood from gymnosperms is often cheaper than that of angiosperms, the faster growth rates making the wood more readily available and less valuable than hardwood. The lower density and mechanical strength of softwoods makes them easier to fell, transport and work, reducing the labour required and, as a result, the cost. The lower cost and labour demand of softwoods make them a more common material for coffin construction. The hardwood coffins from Thaon therefore indicate that their occupants were of sufficient status to afford the luxury of sought after wood for their caskets; possibly indicating nobility or a high ranking member of the clergy. The exception to the lower value of softwoods is that of the coffin from Hofstaðir. Around the time of burial, the majority of trees in Iceland were angiosperms (downy birch, rowan and aspen; Eysteinsson, 2004) indicating that the wood used was a rarity. The use of a sought after commodity in the construction of a coffin is a strong indication that this individual was of high status.

Only two of the woods sampled showed exceptional levels of preservation; the coffin wood in close proximity to a copper nail from G310 at Fewston, and the Hanson Logboat. The wood in close proximity to the copper coffin nail illustrates the presence of a toxic substance that retarded microbial activity. Wood from the same grave that is in much poorer condition illustrates the unique microenvironments that can exist within burial matrices. The Hanson Logboat was preserved due to a waterlogged burial environment that led to anoxic, anaerobic conditions that were not supportive of microbial growth. This wood was interred for nearly 3500 years, making it the oldest wood analysed and yet it is the least degraded. This indicates that the conditions within the burial environment can play a greater role than time in the decay of woods. These two cases highlight the key role that microorganisms play in degrading buried wood. The remarkable preservation of the Hanson Logboat due to anoxia highlights the propensity for anoxic environments to preserve buried wood. Hence, less well preserved woods may imply less persistent anoxia or a generally more variable environment.

The degradation of wood by microfauna that specifically target lignin (such as white rot fungi) is identifiable by both Py-GC and SEM, the specificity of their enzyme action in metabolising lignin make their degradation signatures readily detectable by both techniques. Brown rot is more difficult to detect by Py-GC alone as it can lead to some modification of lignin, meaning that differentiating between brown rot induced degradation and limited decay by white rots can be difficult. A combination of Py-GC analysis with SEM imaging provides a clearer picture on which to interpret the results. Elimination of soft rots and a range of lignocellulose degrading bacteria as possible culprits of decay is more easily achieved from SEM evidence as the characteristic pits and cavities they form in the cell walls of wood are distinctive and easily visible under SEM (Eriksson *et al*., 1990; Blanchette *et al*., 2004). Although these types of microbe were not implicated as agents

of wood decay in this study, their presence was easily ruled out by the absence of their decay signatures.

The detection of lignin and holocellulose derived compounds in the Py-GC analysis of the soil stain from Edinburgh has a potential significance for the archaeological community. Features uncovered during excavations are often attributed to the decay of wood; 'post holes' are a good example of this (Reynolds, 1994; Andrews *et al.*, 2000). If the technique can be applied to these materials and detect lignocellulosic residues, the interpretation of the soil features can be more guided and the conclusions more certain.

Aside from the PEG applied to the Hanson Logboat during its conservation, no evidence of preservative treatments was found in any of the coffin woods. The removal of the PEG from the preserved Hanson Logboat and the subsequent analysis by a range of chemical techniques is the first reported instance of conserved wood being analysed by EA and Py-GC. The option to employ these techniques to wooden objects and gain more meaningful data than before gives rise to the prospect of analysing materials in private and museum collections – the majority of which are conserved with PEG treatments – in ways previously thought not to be possible (Hocker *et al*., 2012). The wealth of potential information that may be available cannot be overstated. The successful employment of the solvent extraction and chemical analysis is also of use to conservators, who currently face similar issues with sulfur accumulation and the concomitant degradation of archaeological woods recovered from waterlogged environments.

The use of PCA (Chapter 5.9) to compare all lignin pyrolysis product data of the same type (gymnosperm or angiosperm) allowed for wood samples to be ranked in terms of their degradation and also highlighted trends in the change of the lignin compound profile resulting from different types of degradation. The trends noticed in the PCA of the gymnosperm wood data add confidence to the hypothesised type and cause of degradation of the wood in the burial environment, and suggest that the lignin modifications resulting from lignin-specific and non-lignin-specific degradation are different. One trend suggests that the wood from the top of the coffin nail of Fewston SK310 and the coffin wood from SK26 at Mechelen are the most heavily modified by lignin-specific decay agents. The other gymnosperm degradation trend is less certain (due to lower correlation of data points) but it does agree with the findings from the respective subsection of this chapter, that the coffin wood from SK434 and the soil stain from SK749 at Edinburgh, and the wood from Mechelen SK423 are the most heavily degraded materials that have seen modification to both their lignin and holocellulose components. The lignin pyrolysis dataset for archaeological angiosperm wood is much smaller, but a degradation trend is apparent in the analysed data that enables the materials to be ranked in terms of their lignin modification and, hence, their preservation state.

5.10.2 Appraisal of techniques employed

5.10.2.1 EA

Compared with the amount of structural information provided by Py-GC, EA is less informative on the chemical preservation state of archaeological wood. It can, however, be useful in analysing waterlogged archaeological woods. An accumulation of sulfur containing species from the burial environment can often lead to the generation of sulfuric acid, which leads to extensive damage to the component biopolymers (Sandström *et al*., 2002; Sandström *et al*., 2005). Detecting high levels of sulfurous compounds before the damage is apparent may well be vital to preventing the loss of objects of cultural and historical significance.

5.10.2.2 Py-GC

Compared with other techniques commonly employed to study the polymers of wood, Py-GC provides more compositional and structural information than FTIR, with far less data analysis than is required for NMR methods. The use of TD to remove bound volatiles makes sample cleaning rapid. It also has the benefit of removing degraded holocellulose and lignin subunits that may be loosely bound within the remaining polymer, which would otherwise be counted in the analysis, biasing the result and giving a false impression of the preservation state.

The need for MS data is vital to establish the identities of the compounds detected by FID. The number of compounds generated by pyrolysis of woods produces results in pyrograms that are highly complex. Comparison with literature data that were acquired using methods which vary only slightly can make the assignment of all relevant peaks difficult and inaccurate. The differing responses of FID and MS for each compound also make the assignment of peaks difficult, even when the data are collected using the same experimental conditions. The use of daily retention time standards was crucial is enabling accurate identification of peaks in the FID pyrograms. The more accurate quantitation of FID over MS outweighs the effort required for reliable peak assignment.

Crucially, the hypotheses made based on the analytical pyrolysis data were largely confirmed by the SEM imaging. This shows that although the use of a standard error, (see Chapter 3.1.5) instead of replicate Py-GC analyses for each wood sample, is far from perfect, it is accurate enough to allow for valid observations to be made in the analysis of the archaeological materials.

5.10.2.3 ASE

This study highlights the use of solvent extraction techniques in the removal of compounds not native to wood. As well as the removal of volatile compounds, solvent extraction was able to remove the PEG impregnated into the Hanson Logboat wood, allowing for a comprehensive suite of chemical analyses to be performed. The automation of solvent extraction by ASE enables

materials to be extracted rapidly, allowing large batches of samples to be extracted in the time it would take to extract a single sample by Soxhlet extraction techniques (Mortensen *et al*., 2007). ASE also uses far less solvent than Soxhlet extractions (10 ml of solvent per ASE extraction compared to 50 ml per Soxhlet extraction; Mortensen *et al*., 2007), which has financial, safety and environmental benefits.

5.10.2.4 SEM

Unlike published Py-GC data of modern and degraded woods, SEM images are not affected by variation in the method and conditions used, making the images 'universal' and identification of decay patterns easier. Due to the features of interest only being visible in cross section, one disadvantage of SEM is that the data is only for a single point and axis in the wood, whereas Py-GC data gives an average of the whole homogenised sample. Nevertheless, given that the archaeological woods studied had all been buried for at least a hundred years, it would appear that in most cases (with the exception of the coffin nail preserving wood in grave 310 at Fewston) the degradation had progressed uniformly throughout the wood. The correlation between the SEM and Py-GC results is evidence of this.

The other key drawback of SEM is the drying process required for archaeological woods. The solvent replacement and critical point drying are time intensive and can lead to fragile samples being destroyed in the process. However, the majority of the wood samples analysed by SEM in this study were prepared without issue.

Despite these caveats, the use of SEM in conjunction with data from chemical analyses has been invaluable in assessing the preservation state of the wood samples, by allowing for the interpretations of the chemical data to be tested by visualising the changes to the microstructures of the wood.

CHAPTER 6

ANALYSIS OF ARCHAEOLOGICAL TEXTILE AND LEATHER

6.1 Introduction

Textiles and animal hide materials recovered from burials of the deceased are an excellent repository of data about the technological capabilities and social practices of the period. In cases where no similar objects have been inherited or their knowledge lost, burial artefacts allow modern society to rediscover part of the past. The funerary customs of many cultures involve burial of the dead in their finest clothing or in ceremonial garments, the composition and constructions of which can be hugely informative (Lieberman, 1991; Scarre and Fagan, 2008). The burial environment can enable clothing materials to survive for thousands of years, albeit in a modified form.

The focus of this chapter is the analysis of textile and hide material fragments recovered from archaeological burials across Western Europe. The locations of the five sites from which these materials were collected are shown in Figure 80. As with the woods analysed in the previous chapter, one of the aims of analysing these materials was to identify the material from which they were made, which could potentially provide information that could aid in the interpretation of the archaeology. These analyses also set out to examine the preservation state of the materials, in order to assess modes of degradation and conditions that existed within the burial environments, allowing a clearer picture of how textiles and leathers degraded when placed into human burials in a limited number of conditions.

The samples were prepared and analysed using a range of appropriate techniques (detailed in Chapter 3). Elemental analysis (C, H, N, S and O) was used to distinguish between plant derived and animal derived materials, allowing for more informative, polymer specific analyses to be performed. Materials with elemental compositions similar to those of modern plant based textiles were analysed by analytical pyrolysis (Py-GC with FID and MS detection), to examine the remaining holocellulose and lignin. Samples that had elevated nitrogen contents, or elemental compositions similar to modern animal based materials, were analysed by RP-HPLC, to determine the amino acid contents, compositions, and racemisation values. Following the chemical analyses of these materials, SEM was performed to visualise the microscopic features of the materials, to look for macromolecular signs of degradation, and to test the hypotheses made on the basis if the chemical data.

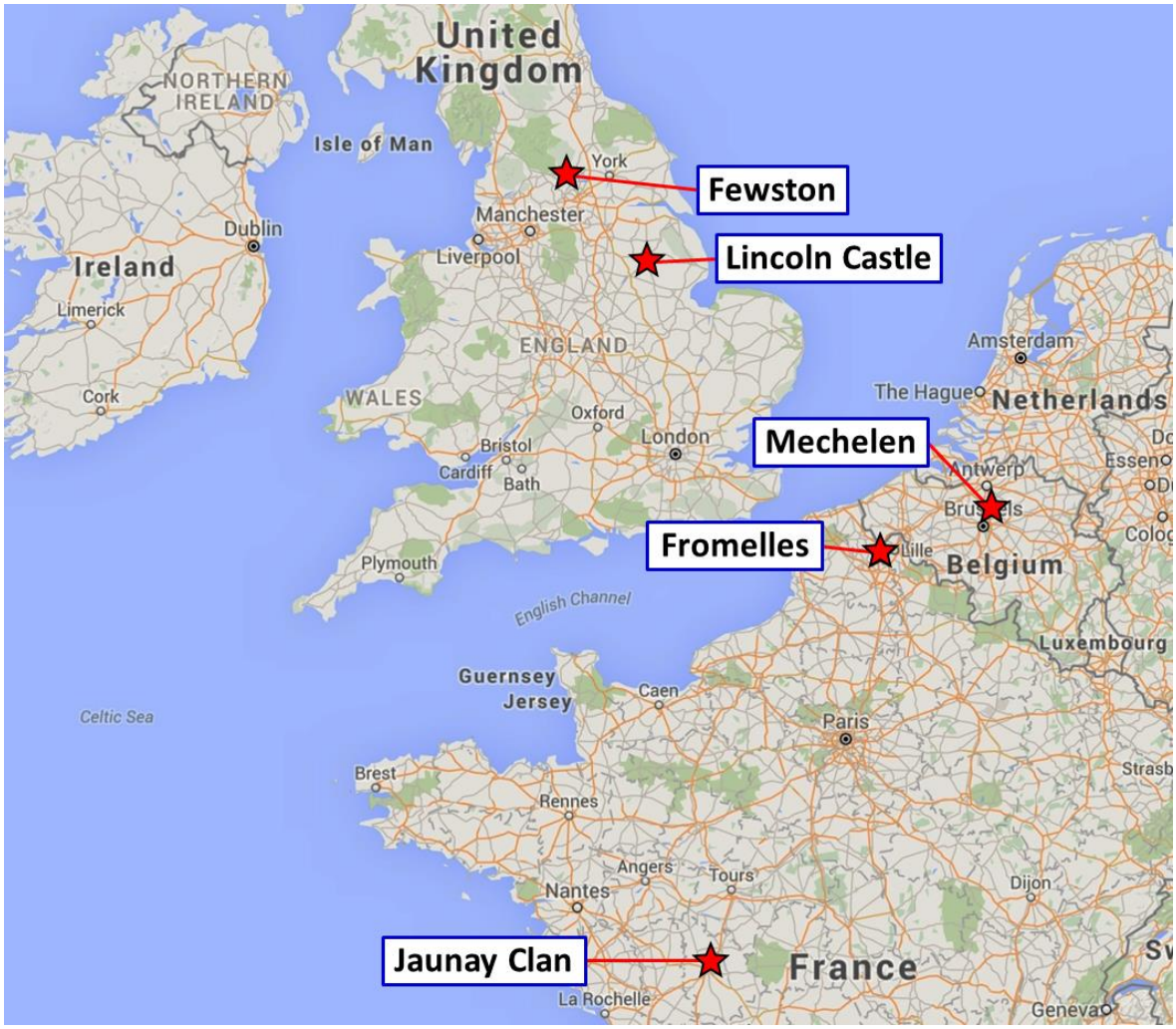

Figure 80. A map of Northwest Europe showing the archaeological sites from which the InterArChive Project team collected samples of textile and leather materials.

6.2 Fromelles

6.2.1 Site and sampling information

Eight First World War mass graves located on the southern border of Pheasant Wood, Fromelles, Northern France (15 km east of Lille at latitude: 50.609850, longitude: 2.854541) were identified in 2007. The location and positioning of the graves is shown in Figure 81.

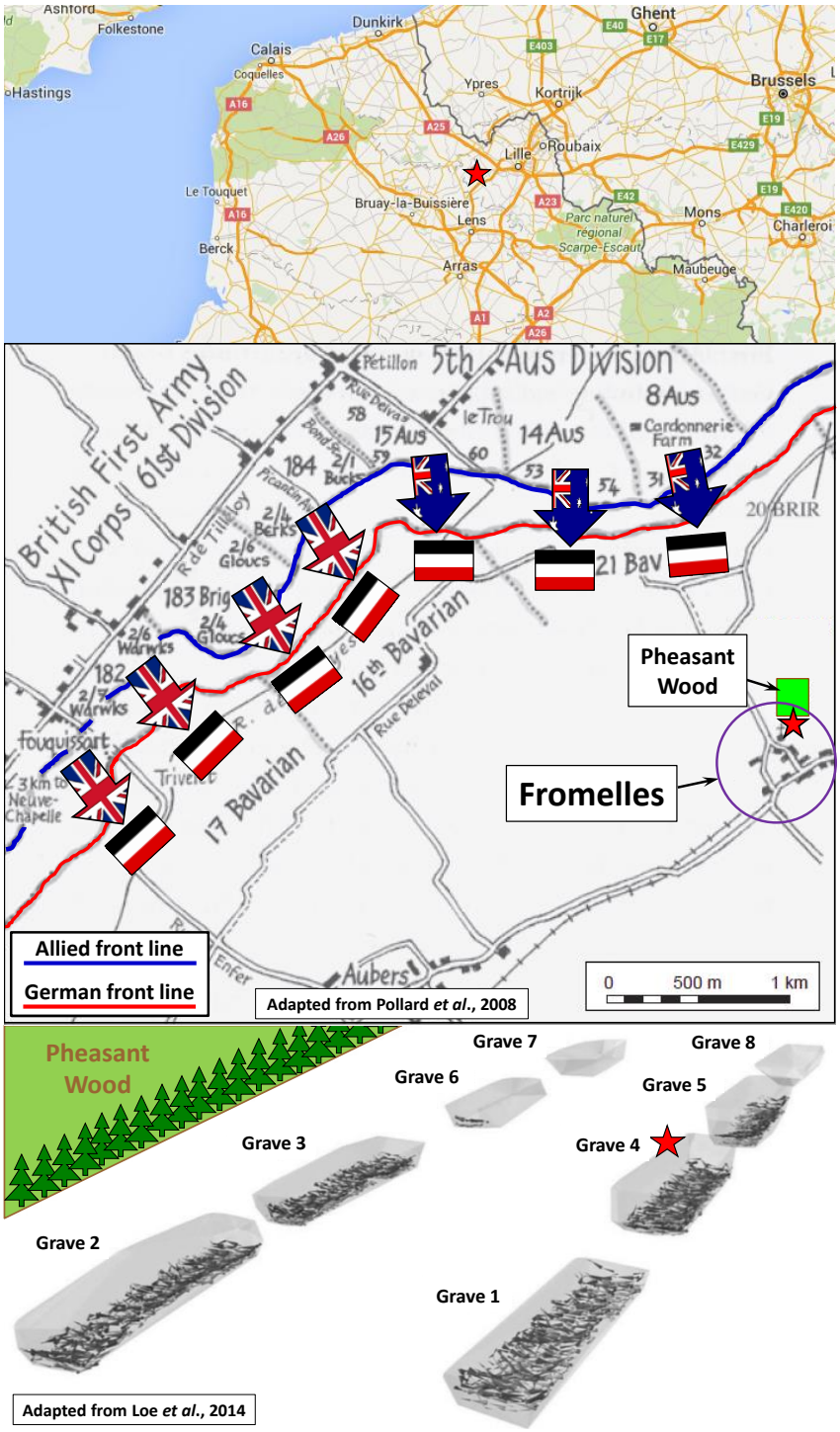

Figure 81. The location of Grave 4, on the south border of Pheasant Wood, Fromelles, Northern France in relation to Northwest Europe (top), the Allied and German front lines in July 1916 (middle; adapted from Pollard et al., 2008) and the excavation of all 8 mass graves in 2009 (bottom; adapted from Loe et al., 2014a).

The burial pits were dug by men from the 21st Bavarian Infantry Reserve Regiment in late July 1916 for the interment of the dead from the Australian 5th Division and British 61st Division who had been killed in and around the overrun German positions during The Battle of Fromelles, fought on 19th and 20th July (see Figure 82; Barton, 2007). Each grave was investigated in 2007 by the excavation of a small trench, after which the remains were covered with geotextile and the trenches backfilled with sand, vermiculite and clay (Pollard *et al.,* 2008). The site was completely excavated in 2009 by Oxford Archaeology, during which each individual and their associated finds were extensively catalogued. The remains were subjected to osteological analysis and DNA testing in order to identify the individuals. All of the 250 bodies were subsequently reburied in the newly built Fromelles Military Cemetery, and many of the finds are on display in the adjoining Museum of the Battle of Fromelles.

Figure 82. Men of the 53rd Battalion, 5th Australian Division at the Battle of Fromelles. Several minutes after this photograph was taken the order was given for the men to break from the cover of their trench and advance on the German positions across 'no man's land'. It is not known what happened to the individuals in this photograph. Photograph taken by Charles Henry Lorking (Australian War Memorial ID: H16396).

Soil analyses carried out by McKenzie (in Pollard *et al*., 2008) concluded that the burial matrix was primarily silt and fine grained Ypresian (Flanders) clay, which is known for its low water permeability and tendency to create bodies of standing surface water (Doyle *et al*., 2002; Doyle, 2014). The site was noted to be waterlogged during the excavation, and iron hydromorphism in the sediment (reddish, oxidised iron deposits at the surface giving way to grey, reduced iron deposits; Duchaufour, 2012) demonstrated that the lower levels of the matrix were waterlogged and anaerobic. Grave 4 was noted to be the most waterlogged of the eight. The average pH of soil at the site was neutral to mildly alkaline (pH 7 to pH 8). By contrast, the pH at the level of the burials in Grave 4 was measured to be 4.7 (Pollard *et al*., 2008).

The InterArChive team collected organic material finds from 4 sets of remains from Grave 4 (Figure 81a). The grave measured 9.60 m by 2.20 m, and was approximately 1.51 m deep (Pollard *et al*., 2008). The individuals were all arranged in an approximate north-south orientation in two layers, one directly on top of the other (Loe *et al*., 2014a). The materials sampled were related to SK1523, SK1525, SK1527 and SK1750, individuals lying on the bottom layer of the burial in contact with the base of the grave (see Table 20 for a list of samples). The majority of the materials have an obvious weave and are readily identifiable as fragments of textile from the uniforms worn by the deceased. One textile find, from the feet of SK1750, was red in colour and interpreted by the archaeological excavation team to be a red sock. The exceptions to the above are material from the feet of SK1525 and the pelvis of SK1527, which have no observable features typical of woven materials. One of the aims for the analysis of these samples was to assess their chemical composition and deduce the identity of the material, as well as assessing the preservation state of all samples.

6.2.2 Analysis of archaeological materials

Samples of material finds unearthed alongside the buried skeletal remains were collected by the InterArChive team. These samples were named to denote the identity of the skeleton and approximate anatomical location of the find. Analyses of the 12 samples were carried out according to methods detailed in Chapter 2.2.1.

6.2.2.1 Py-GC analysis

The organic material samples from Grave 4 were all analysed by Py-GC. An example of the Py-GC data is shown in Figure 83 and the results for all of the samples outlined in Table 20. All of the material finds analysed were determined to be protein based, their pyrograms being similar to those of modern wool and silk.

Table 20. The samples collected from Grave 4 at Fromelles and the summarised results of Py-GC analysis. Samples are marked with an asterisk (*) to indicate materials that have no observable weave or physical features to indicate they are textiles or fibres from clothing.

Skeleton no.	Sample name	Py-GC results
SK1523	Pelvis textile	Protein based
	Head textile A	Protein based
	Head textile B	Protein based
SK1525	Pelvis fibres	Protein based
	Pelvis textile	Protein based
	Foot textile	Protein based
	Foot material *	Protein based
SK1527	Head textile	Protein based
	Pelvis textile	Protein based
	Pelvis material *	Protein based
	Foot textile	Protein based
SK1750	Foot textile	Protein based

Pyrolysis of proteins leads to thermally induced modification reactions to the constituent amino acids (Takekoshi *et al.*, 1997; Hendricker and Voorhees, 1998). Several amino acids can produce the same thermal degradation product; Table 21 outlines typical protein pyrolysis products detected and the amino acids they are derived from (Takekoshi *et al.*, 1997). The thermal degradation of amino acids induced by this technique results in potentially valuable information being lost. In order to gather more comprehensive data on the composition and levels of preservation of the protein based textiles, the amino acid compositions of the samples were analysed by RP-HPLC, following hydrolysis at 110°C for 18 hours (see Chapter 2.5).

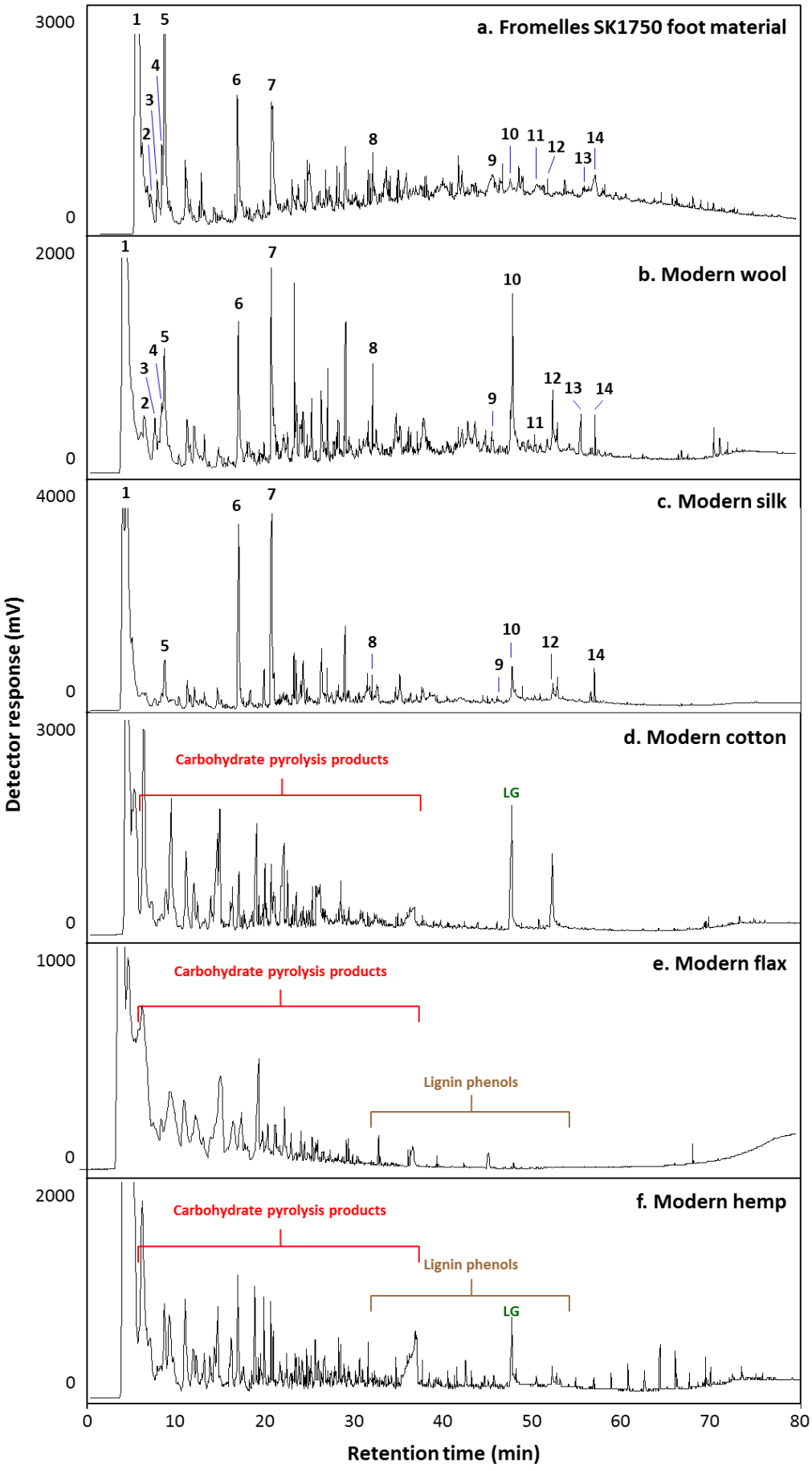

Figure 83. Partial pyrolysis – GC traces of textile from the feet of SK1750 at Fromelles (a), compared with modern wool (b), silk (c), cotton (d), flax (e) and hemp (f). LG = levoglucosan, a cellulose pyrolysis product. 1 to 14 are thermal decomposition products of amino acids and peptides (Table 21).

Table 21. The identities of peaks 1 to 14 in Figure 83, detailing the pyrolysis products detected and the amino acids or peptides from which they are produced by thermal decomposition. DKP = 2,5-diketopiperazine. (Takekoshi et al., 1997; Kurata and Ichikawa, 2008).

Peak	Protein pyrolysis product	Origin
1	Acetonitrile	Alanine, proline
2	3-Methylbutanal	Leucine
3	Isovaleronitrile	Leucine
4	Pyrrole	Proline
5	Toluene	Phenylalanine
6	Phenol	Tryptophan
7	*p*-Creosol	Tyrosine
8	Indole	Tryptophan
9	Gly-Ala DKP	Glycine-Alanine
10 & 11	Pro-Ala DKP	Proline-Alanine
12	Pro-Gly DKP	Proline-Glycine
13 & 14	Pro-Val DKP	Proline-Valine

6.2.2.2 Chiral AA content analysis by RP-HPLC

The majority of samples from Fromelles have total amino acid contents that are within the range of variability seen in modern wools (see Figure 84). The textiles from the head of SK1525, the pelvis of SK1527 and the feet of SK1750 display measurably lower amino acid contents than the modern analogues (Student's t tests; all *p* values = <0.041). This may well be indicative of degradation; inorganic materials from the burial matrix replacing the degraded proteins would account for the observed lower amino acid content per unit of sample mass.

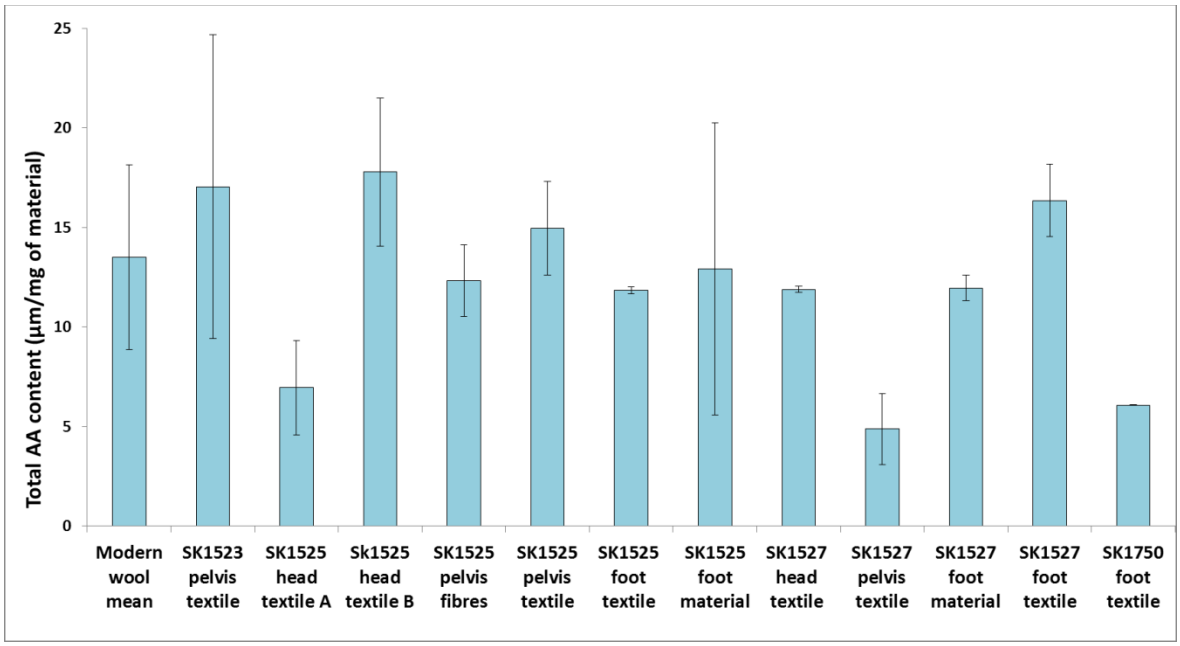

Figure 84. Total amino acid concentrations of the Fromelles wool materials compared with the mean value calculated for the 6 types of modern wool analysed. Error bars represent +/- 1 standard deviation; n=10 for modern wool and n=2 for archaeological materials.

The amino acid compositions of selected materials from SK1523, SK1525, for SK1527 and SK1750 are shown in Figure 85. The data displayed are a representative sample of all the material analysed. All of the textile samples collected from Grave 4 at Fromelles have very similar amino acid compositions to that of modern wools, and as such can be identified as being woollen textiles with confidence. There are, however, some differences between the profiles of modern wool and the archaeological materials, these being higher amounts of Ser and Gly and lower amounts of Asx, Arg, Ile and Leu in the archaeological materials (Student's t tests; all *p* values = <0.05). The differences are outside of the range of amino acid composition values for all of the modern wools studied and are apparent across all of the samples studied. This suggests that the cause is not due to a difference in the wool that the textiles were made from, as it is highly unlikely that all of the wool was obtained from a single breed of sheep that has a vastly different wool amino acid composition.

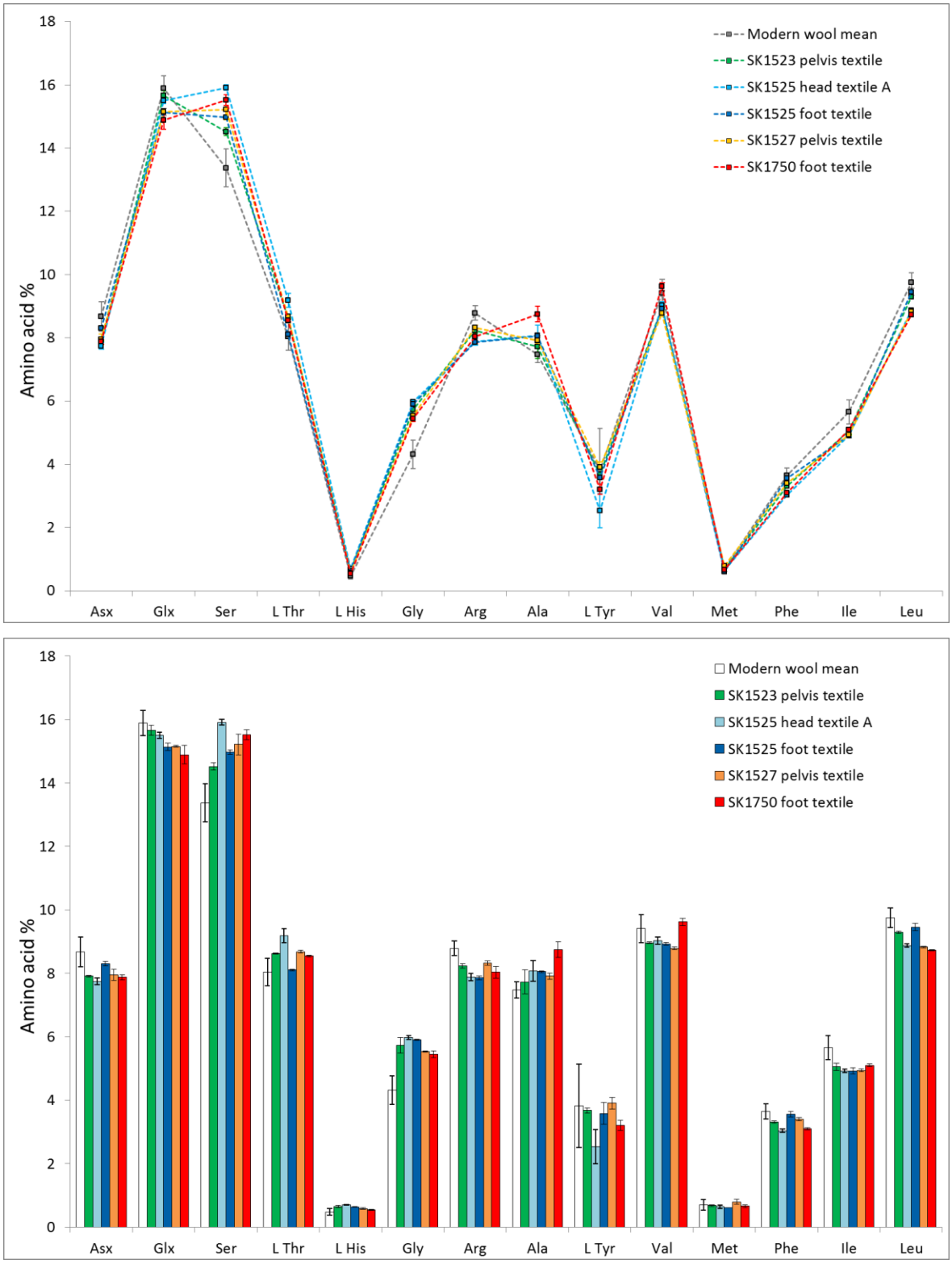

Figure 85. Amino acid compositions for selected materials recovered from grave 4 at the Fromelles mass burial. The data are expressed as percentages of the sum of all amino acid peak areas. Error bars represent +/- 1 standard deviation; n=10 for modern wool and n=2 for archaeological materials.

The variation is likely to be due to a specific form of biological attack that leads to preferential degradation of particular substructures of the wool fibres over others. Notably, the proteins that comprise the cuticular scales have a different amino acid composition to the proteins that constitute the inner cortex (see Table 22). The preferential degradation of one type of protein would alter the overall amino acid composition of the remaining material. Table 22 shows the

amino acid compositions of whole wool fibres, wool cuticle proteins, and wool cortex proteins. With the exception of Thr – which is marginally higher in proportion than in modern wool – the samples from Fromelles appear to have an amino acid profile consistent with an increased proportion of cuticle material. This suggests that the cortex components of the wool have been degraded, while the outer cuticle remains in a better state of preservation. Certain microbes are known to cause loss of cortex spindle cells whilst leaving the outer cuticle untouched, producing hollow tubes of degraded wool fibres (Gabriel, 1932; Kidd, 1977; Janaway, 2001; Mahall, 2003). As a result of the amino acid compositions suggesting preferential degradation of the wool cortex material, SEM was carried out to assess the physical damage to the fibres and to see if the predicted hollowing had indeed occurred. SEM analysis is presented in Section 2.2.3.

Table 22. Amino acid compositions of whole wool fibres, proteins of the wool cuticle and proteins that compose the wool cortex (Church et al., 1997).

Amino acid	**Whole wool fibre** Bradbury *et al*., 1967; Leeder & Marshall, 1982	**Wool cuticle** Bradbury & Ley, 1972	**Wool cortex** Bradbury, 1973
Alanine	5.4	5.8	5.5
Arginine	6.9	4.3	6.7
Aspartate	6.5	3.5	6.5
Glutamate	11.9	8.7	12.4
Glycine	8.4	8.2	8.1
Histidine	0.9	0.8	0.7
Isoleucine	3.1	2.7	3.3
Leucine	7.7	6.1	7.9
Lysine	2.9	2.7	2.6
Methionine	0.5	0.3	0.4
Phenylalanine	2.9	1.7	2.5
Serine	10.4	14.3	10.3
Threonine	6.4	4.4	6.5
Tyrosine	3.8	2.8	2.9
Valine	5.6	7.5	5.7

The ratios of measured D and L form amino acids for selected materials sampled from SK1523, SK1525, SK1527 and SK1750 at the Fromelles excavation are shown in Figure 86. The data displayed are a representative sample of all the material analysed. With the exceptions of Asx and Ser, amino acids only racemise when terminally bound. All samples from grave 4 at Fromelles exhibit greater extents of racemisation of Asx and Ser than modern materials (Mann-Whitney u tests; all p values = <0.027). Other amino acids (which require terminal sequence locations for racemisation to occur) show increased racemisation, which most likely indicates that hydrolysis of

the wool proteins produced a greater number of terminal residues. This finding is in agreement with the amino acid composition data that suggests degradation of the wool structure.

Textile sample A from the head of SK1525 exhibits larger D/L values for many amino acids than all other material recovered from grave 4 (with a notably large Leu D/L value). The difference in the D/L values and the amino acid composition of this material combined with the significantly depleted overall amino acid content suggest that textile A from the head of SK1525 is the most degraded material recovered from the site.

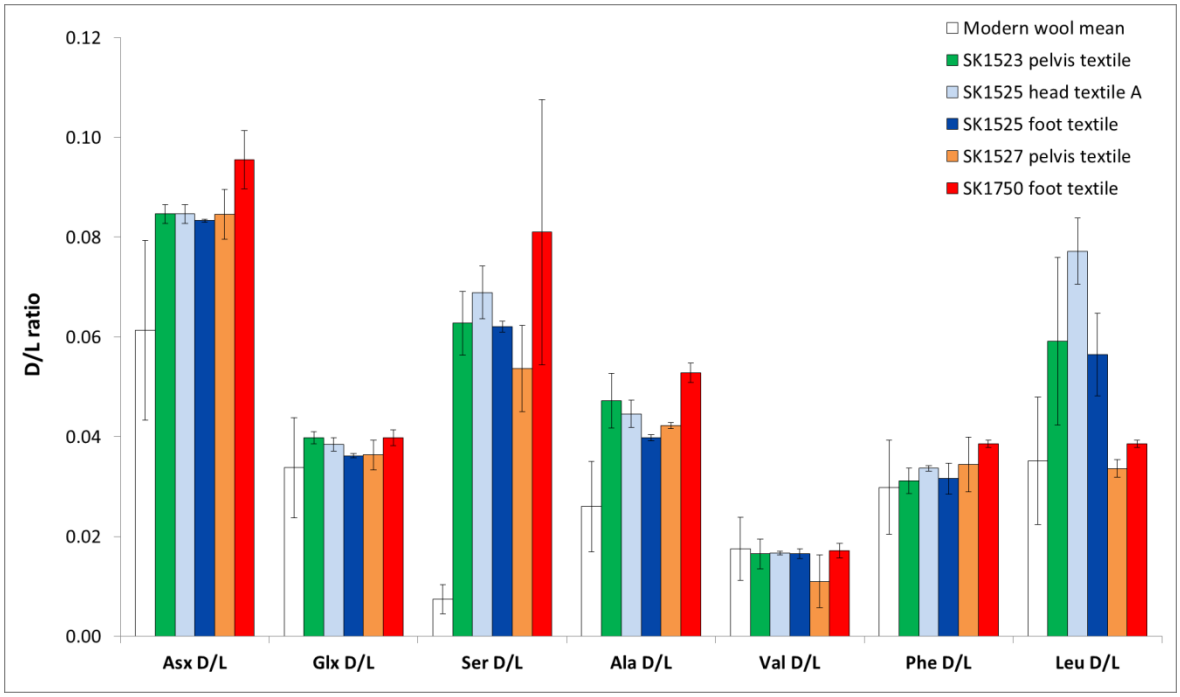

Figure 86. Selected amino acid D/L values for several materials recovered from the four skeletons sampled in grave 4 at the Fromelles mass burial. Error bars represent +/- 1 standard deviation; n=10 for modern wool and n=2 for archaeological materials.

6.2.2.3 SEM

To assess the physical state of the microstructures of the wool and test the hypothesis of fibre hollowing reasoned on the basis of the amino acid data, SEM analysis was performed on two separate subsamples of material taken from the SK1750 'red sock' (Figure 14 c to h). In comparison with modern wool (Figure 87a and b), the archaeological material shows signs of extensive damage, with most wool fibres appearing to have been affected. Many fibres exhibit damage to only one half, the other side remaining less affected, a pattern of deterioration that is characteristic of bacterial attack (Mahall, 2003). The individual wool strands are hollow and straw-like; many have been pressed flat due to the loss of the interior material. The cuticular layers remain intact and much of the inner cortex and medulla material is not present. The cuticular scales exhibit no lifting but do show some smoothing of their edges. Visible penetration and pitting of the outer structure of the fibres is limited. The damage to the cuticles could have been caused by mechanical processes within the burial environment, during excavation or cleaning, which have resulted in the snapping of the hollow structures, parting the cuticular scales in the process.

The evidence from the SEM images confirms the interpretation from the amino acid composition data that the cortex had been preferentially degraded. Thus, the high relative abundance of Ser reflects the greater proportion of this amino acid in the proteins that constitute the cuticle than in the cortex. A higher proportion of cuticular protein relative to cortex protein than in undegraded wool fibres can account for the elevated Ser content of the archaeological material.

Pink rot (*Bacillus subtilis*), a bacterium found in soil and the human digestive tract, has been shown to degrade keratinaceous material including wool (Hong *et al.,* 2009; Zaghloul *et al.,* 2011; Pekhtasheva *et al.,* 2012). The deterioration of wool fibres to produce hollowed tubes of cortical cells has been observed in previous studies (Gabriel, 1932; Molyneux, 1959). In a case reported by Gabriel (1932), a sample of Romney wool inoculated with *B. subtilis* was shown to release the individual cortical cells into solution, leaving "an empty tube of [cuticular] scale cells". *B. subtilis* disrupts the adhesion of cortical cells, releasing them from the fibre to leave a hollow structure composed of cuticular material. It is a facultative anaerobe, capable of respiring aerobically in oxygen rich environments and also producing ATP by anaerobic respiration (fermentation) in anoxic conditions, such as those found in Grave 4 (Nakano and Zuber, 1998).

On excavation of the find the red colour of the material was assumed to be attributable to an intentional dyeing of the wool during its manufacture. The location by the foot of the remains combined with the course weave, indicative of a knitted garment and not the woven cloth that made up the uniform trousers or puttees (Tynan, 2013), strongly imply that the material is part of a sock. Military regulations at the time prohibited the wearing of clothing that was not khaki or

'drab' coloured (Chappell, 2000). Despite extensive literature searching no reference can be found to any of the Allied divisions at Fromelles wearing red socks.

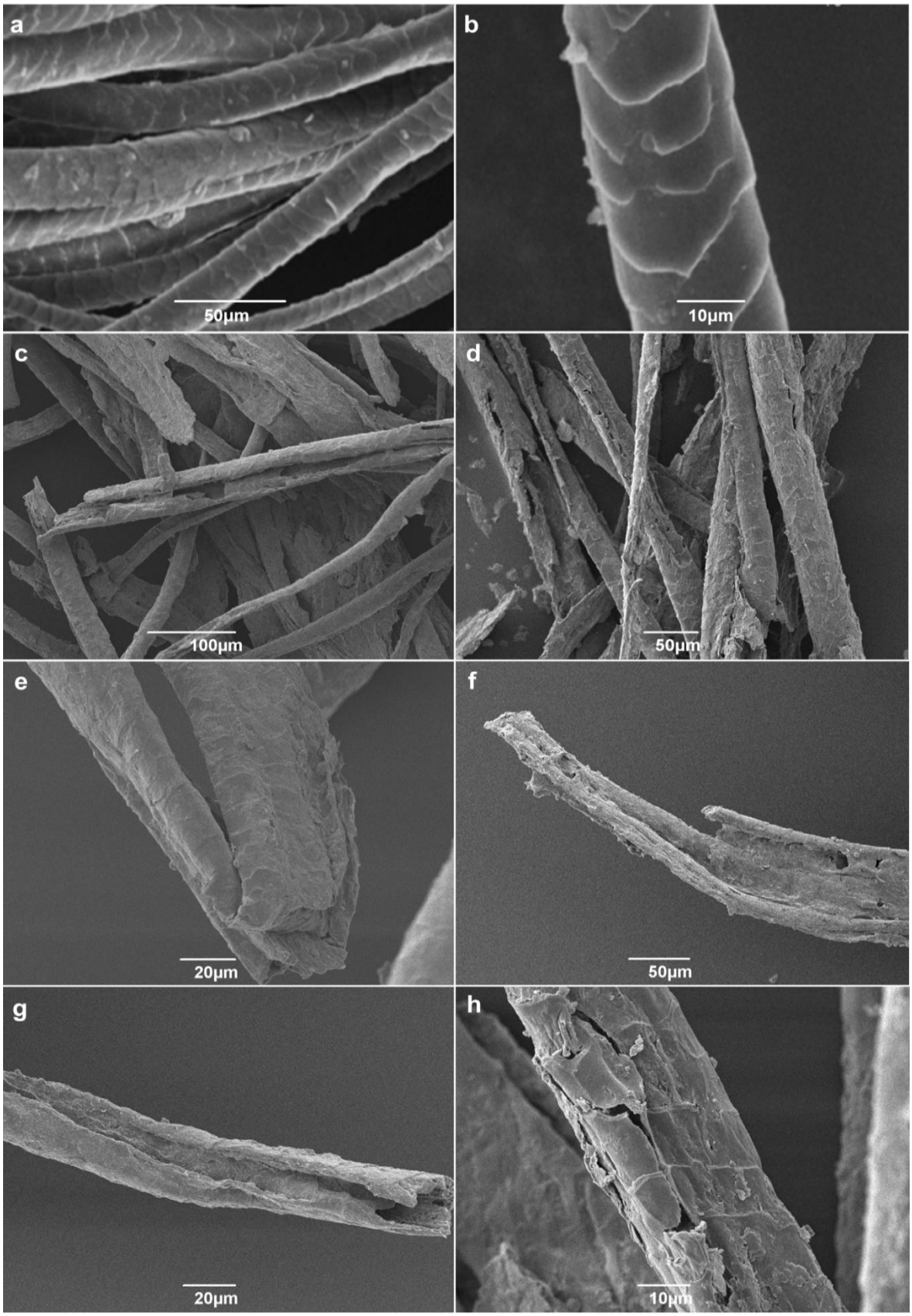

Figure 87. SEM images of modern wool (a and b; adapted from Chakraborty and Madān, 2014) and two wool samples taken from the SK1750 'red sock' (c to h). The archaeological wool fibres are hollowed; a result of the destruction of cortex material whilst the outer cuticular scales remain in good condition.

A subsample of the material was solvent extracted by another member of the InterArChive research team using 9:1 DCM:methanol solvent (see Chapter 2.2.2.4) and the extract was analysed by UV spectroscopy. No absorption due to an organic dye material was observed. Subsequent GC-MS analysis of the extract did not reveal the presence of any compounds commonly used in the colouration of textiles (Hicks, 2017). *B. subtilis* is known to sometimes impart a pink colouration to wools and fleece that is extremely difficult to remove by washing, hence the common name for the bacteria being pink rot (Nay and Watts, 1977; D'Arcy, 1990). Therefore, the colour of the archaeological wool may be due to the exposure to *B. subtilis* or similar microorganisms in the burial environment. Some soil microorganisms can produce chromophore containing compounds (such as carotenoids) through metabolic processes (Khaneja *et al.,* 2010). Many wool pretreatment methods in the textile industry rely on exposing fibres to enzymatic and chemical agents in order to increase the colour fastness of the dyes applied, the current consensus being that the enzyme mediated hydrolysis of the wool proteins produces more binding sites for the applied dye molecules (Kim *et al*., 2005; Kang *et al*., 2006; Araujo *et al*., 2008a; Araujo *et al*., 2008b). Thus, the activity of keratinolytic enzymes may have facilitated covalent crosslinking of microbially produced 'natural' dyes to the modified wool fibres, leading to the fastness of the colouration of the material. Alternatively, the loss of the cortex material may have changed the way that the material interacts with light, resulting in the perceived change in colour.

Thr is reportedly found in lower abundance in the cuticular proteins of undegraded wools when compared to the average values of whole wool fibres (Table 22; Church *et al.,* 1997). The Thr content is slightly higher in the hollowed wools from Fromelles, indicating a discrepancy between the experimental and literature data. It is likely that the differences are due to this study employing different analytical techniques than those used in the literature work. The techniques used in this investigation differentiate between D and L forms of the amino acids detected, with good reproducibility and accuracy. This enables a more precise amino acid composition to be determined, implying that the composition detected is an accurate representation of the materials analysed.

6.2.3 Summary and conclusions

Based on the amino acid composition data all archaeological materials sampled during the excavation at Fromelles were determined to be made from woven or felted wool. All of the archaeological samples exhibit very similar amino acid distributions to modern wools and they also exhibit a characteristic difference in amino acid compositions. The increase in the relative abundances of particular amino acids, including Ser which is found in higher abundance in the cuticular scales, suggests that the cores of a significant proportion of the wool have been preferentially degraded, most likely by microbial attack. This suggestion was confirmed by SEM imaging, which shows that the majority of the wool fibres are hollow, having been stripped of the cortex materials.

A range of preservation states are evident among the samples, though there does not appear to be an obvious pattern relating to conditions in the burial matrix that would account for the variation in preservation. It is likely that the acidic, waterlogged conditions found at the bottom of grave 4 contributed to preservation of the material for nearly 100 years without more extensive degradation.

The wool from the pelvis of SK1527 has a low total amino acid content, but, the amino acid composition and the D/L values for this material are no more dissimilar to modern wool than the other archaeological samples that have higher amino acid contents. It is possible that the anomalous value is due to a non-proteinaceous component of the textile sample that persisted through the cleaning procedures. If so, the lower amino acid content would not be indicative of the preservation state of the material.

Textile sample A from the head of SK1525 also exhibits a lower amino acid content but does show significant variation in the other amino acid values. The sample has a higher percentage composition of Ser and larger D/L values for many amino acids than all other material recovered from grave 4, suggesting that this material is the most degraded of all samples recovered from the site.

6.3 Fewston

6.3.1 Site and sampling information

During March and April of 2010 excavation was carried out to recover buried remains from graves in the construction footprint of a new Heritage Centre attached to the church of St Michael and St Lawrence at Fewston, North Yorkshire (latitude: 53.982745, longitude: -1.704312; Figure 88). A total of 163 sets of human remains were found and removed from graves in the churchyard. The temporal range of the burials was from the church's founding in the 14th century and extended after the last recorded burial in 1896 to a burial in 1921 (Buglass, 2010). The burial soils are well drained coarse loamy soils that lie atop Namurian millstone grit of the Upper Carboniferous period (Buglass, 2010).

Members of the InterArChive team collected textile fragments from two sets of remains at the Fewston site. SK408 was identified as Richard Gill who died in May 1883 at the age of 78. Mr Gill was buried in a wooden coffin that had leather adornments and a copper alloy breastplate (Buglass, 2010). Samples of textile from around the feet of the remains were sampled. The material had a course weave and was thought by the excavating archaeologists to be the part of socks or long johns. SK289 was an unidentified individual, the sex was tentatively identified as female although less than 60% of the skeleton remained and what was left was in poor condition (Caffell and Holst, 2010). The individual was estimated to be between 35 and 45 years of age and the date of burial was undetermined. The hair of the individual remained, detached from the skull (as the scalp had completely decomposed) and still bound by a hair tie made from a woven material. The locations of both SK289 and SK408 within the church grounds are given in Figure 88 (bottom).

Both samples of textile were initially analysed by Py-GC-FID (Chapter 2.4.2) with the intention of conducting further analysis of the amino acid content of any materials found to be protein based (Chapter 2.5).

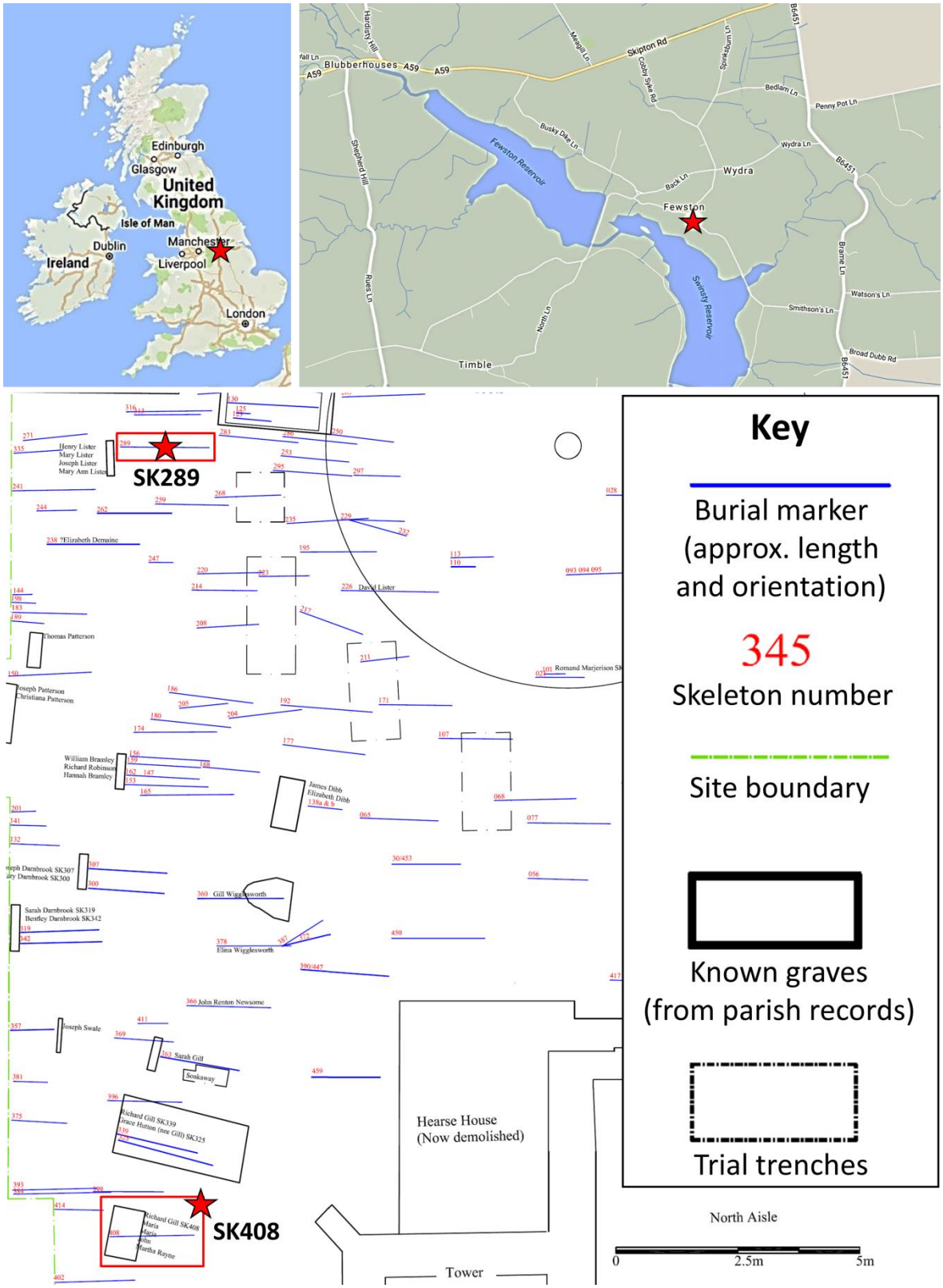

Figure 88. A map of the area surrounding the church of St Michael and St Lawrence at Fewston (top) and a site plan from the 2009 archaeological excavations, highlighting the positions of SK289 and SK408 (bottom).

6.3.2 Analysis of archaeological material

6.3.2.1 Py-GC analysis

Both samples of textile from the Fewston excavations had similar pyrograms to modern protein based materials, the pyrograms containing peaks attributable to amino acid thermal degradation products (see Figure 89). Amino acid analysis was therefore performed to examine amino acid concentrations, D/L values, and the overall protein content of the materials (Section 3.2.2).

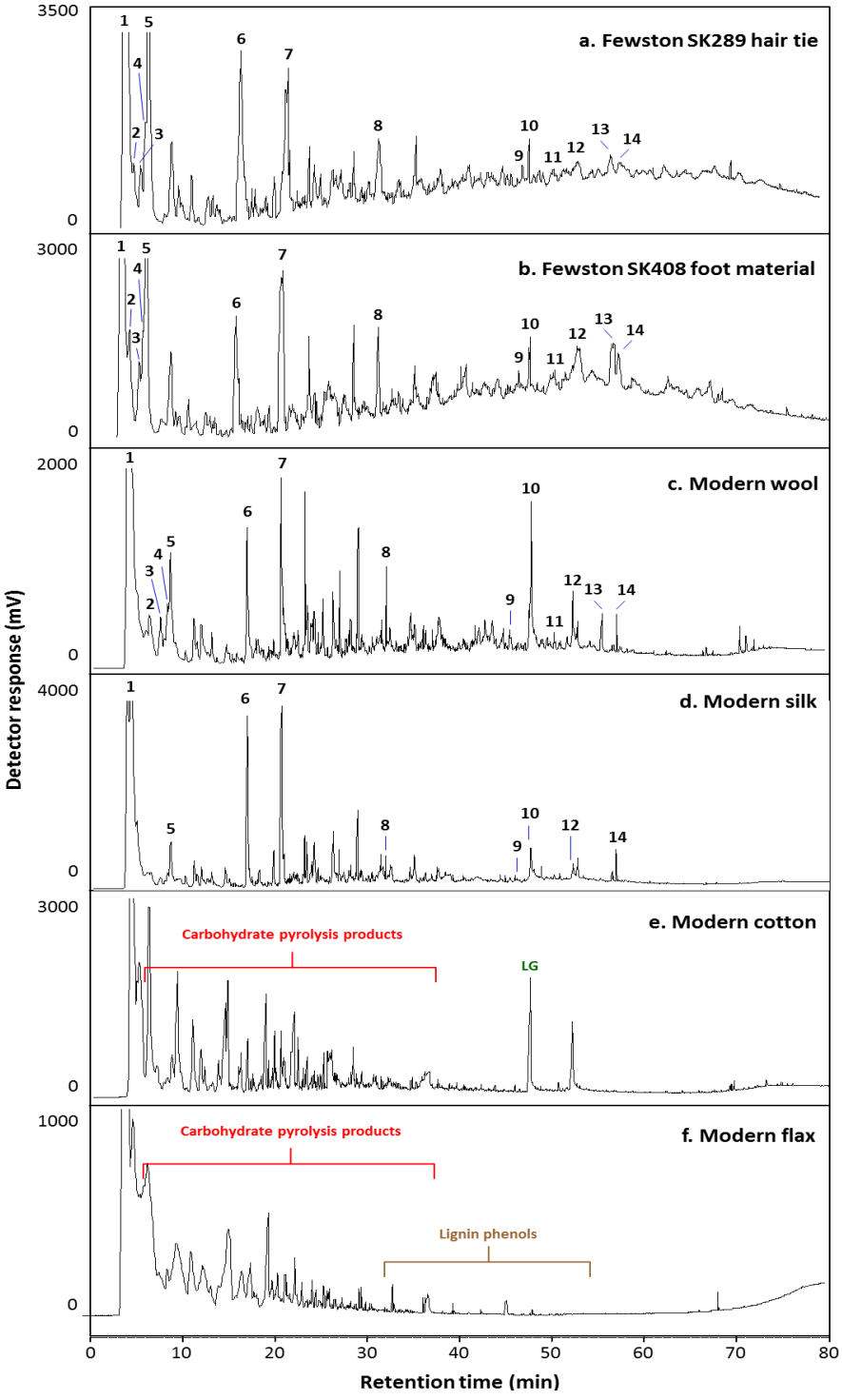

Figure 89. Partial pyrolysis – GC traces of the SK289 hair tie (a) and the SK408 foot textile (b) from Fewston compared with a range of modern materials (c – f). LG = levoglucosan, a cellulose pyrolysis product. 1 to 14 are thermal decomposition products of amino acids and peptides (Table 21).

6.3.2.2 Chiral AA content analysis by RP-HPLC

The total amino acid contents of the textiles from SK289 and SK408 are within the range of variability of the modern wools analysed (see Figure 90), suggesting that both materials are in an excellent state of preservation.

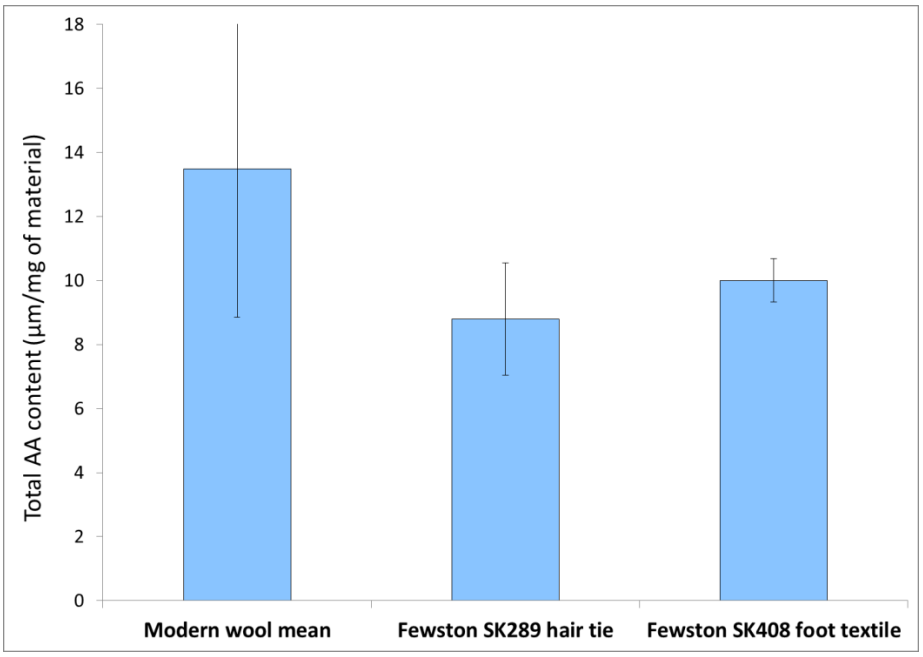

Figure 90. Total amino acid concentrations of the Fewston wool materials compared with the mean value calculated for the 6 types of modern wool analysed. Error bars represent +/- 1 standard deviation; n=10 for modern wool and n=2 for archaeological materials.

The amino acid compositions of the textiles recovered from SK289 and SK408 are shown in Figure 91. The material from the head of SK289 and that from the feet of SK408 both have amino acid compositions that are very similar to modern wool. Given the physical appearance of the textiles and the amino acid profiles, it is safe to conclude that both samples of textile are made from woven wool. The percentage abundance of the majority of the amino acids from both samples fall within the range demonstrated by modern wool, those that lie outside this range only differ marginally (Student's t tests; all *p* values = <0.024). Thus, it is unlikely that these materials have undergone any significant microbially mediated decomposition.

The D/L values of selected amino acids (Figure 92) reveal statistically significant increases in the racemisation of Asx and Ser for both materials (Mann-Whitney u tests; all *p* values = <0.027). None of the other amino acids analysed exhibited significant racemisation. The magnitude of the increase in the Asx and Ser D/L values is small by comparison with materials from other sites where definite signs of degradation are evident (such as Fromelles, see section 6.2.2.2). These observations suggest that the racemisation of Asx and Ser has most likely occurred in chain. Consequently, new terminal residues generated by hydrolysis of the peptides of the wool would be limited, giving further evidence of good preservation for both textiles.

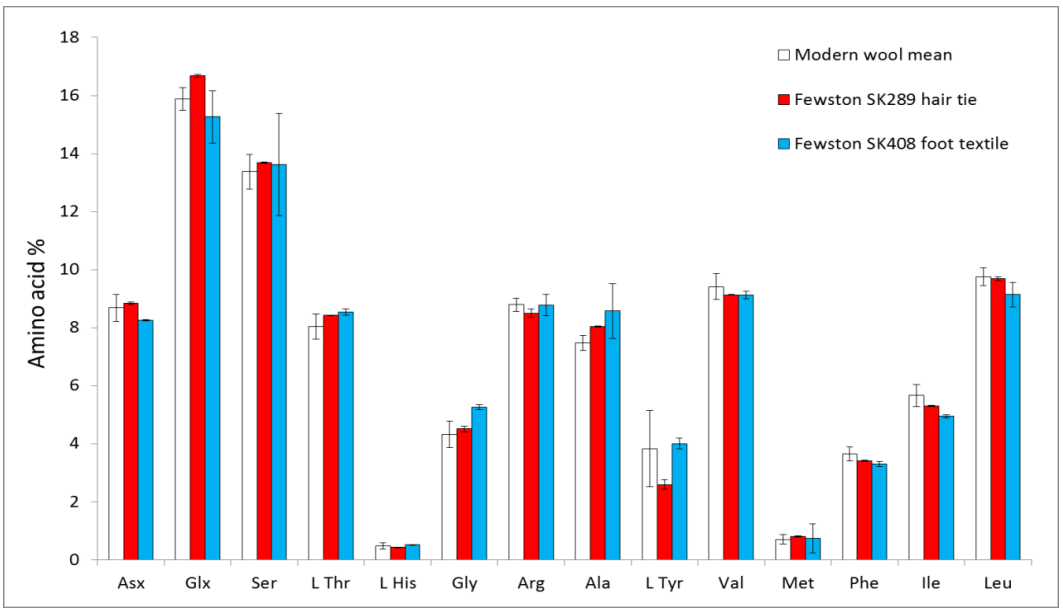

Figure 91. Amino acid compositions for the material recovered from SK289 and SK408 during the Fewston excavation. The data are expressed as percentages of the sum of all amino acid peak areas. Error bars represent +/- 1 standard deviation, n=10 for modern wool and n=2 for archaeological materials.

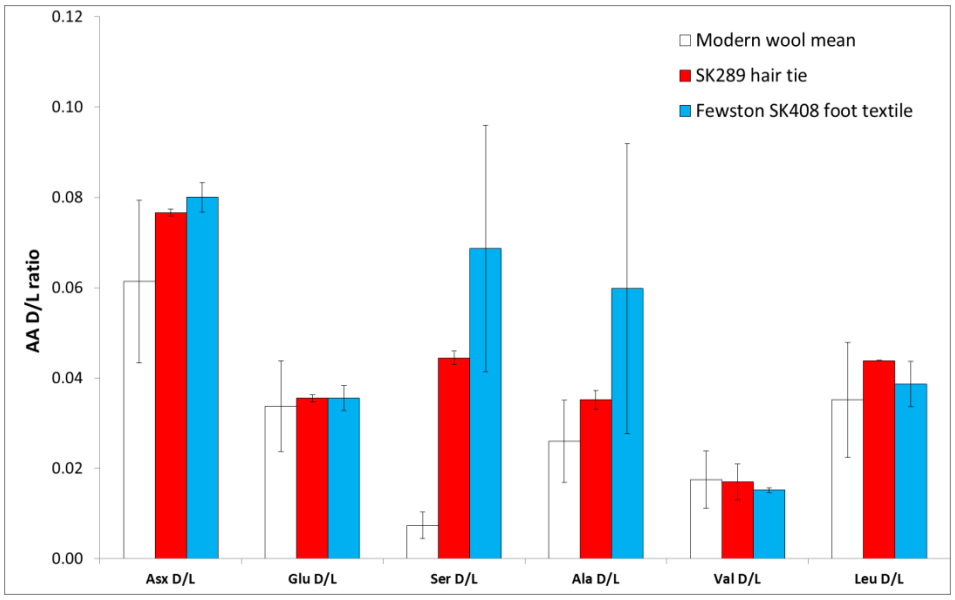

Figure 92. Amino acid D/L values for the material recovered from SK289 and SK408 during the Fewston excavation. Error bars represent +/- 1 standard deviation; n=10 for modern wool and n=2 for archaeological materials.

6.3.3 Summary and conclusions

The amino acid compositions of both of the materials recovered from Fewston enabled their identification of their compositions as wool. The material from the hair of SK289 is a hair tie used to keep the hair from falling in the face. The appearance of the material from the feet of SK408 would suggest that it is part of a knitted sock or garment covering the legs. The amino acid compositions, the amino acid D/L values and the total amino acid contents of the wools from both materials suggest they are in a reasonably good state of preservation, with neither having experienced any measurable deterioration during their periods of internment.

6.4 Mechelen

6.4.1 Site and sampling information

In 2009 members of the InterArChive team sampled from a former churchyard next to the Cathedral of Saint Rumbold in Mechelen, Belgium, approximately 23 miles north east of Brussels in the Flanders Region (latitude: 51.028858, longitude: 4.479221; Figure 93). The site was used from the early 12th century until 1785 as the sole burial site for the deceased of the parish of Mechelen. Records show the site to contain the remains of at least 4200 individuals. From a total of 3675 burials the excavation located and removed 4166 articulated skeletons and 100 collections of disarticulated bones resulting from secondary burials (reburial of the remnant bones following an initial phase of decomposition elsewhere; Depuydt *et al*., 2013). The site comprised four distinct layer of sediment. The uppermost two layers (dated to the 17th and 18th century AD) were a "dark brown, greyish sandy soil" (Depuydt *et al*., 2013). The third layer (dated to the 15 and 16th century AD) was "a brownish soil of light loamy sand" and the fourth layer being "yellow – brown sand" (Depuydt *et al*., 2013).

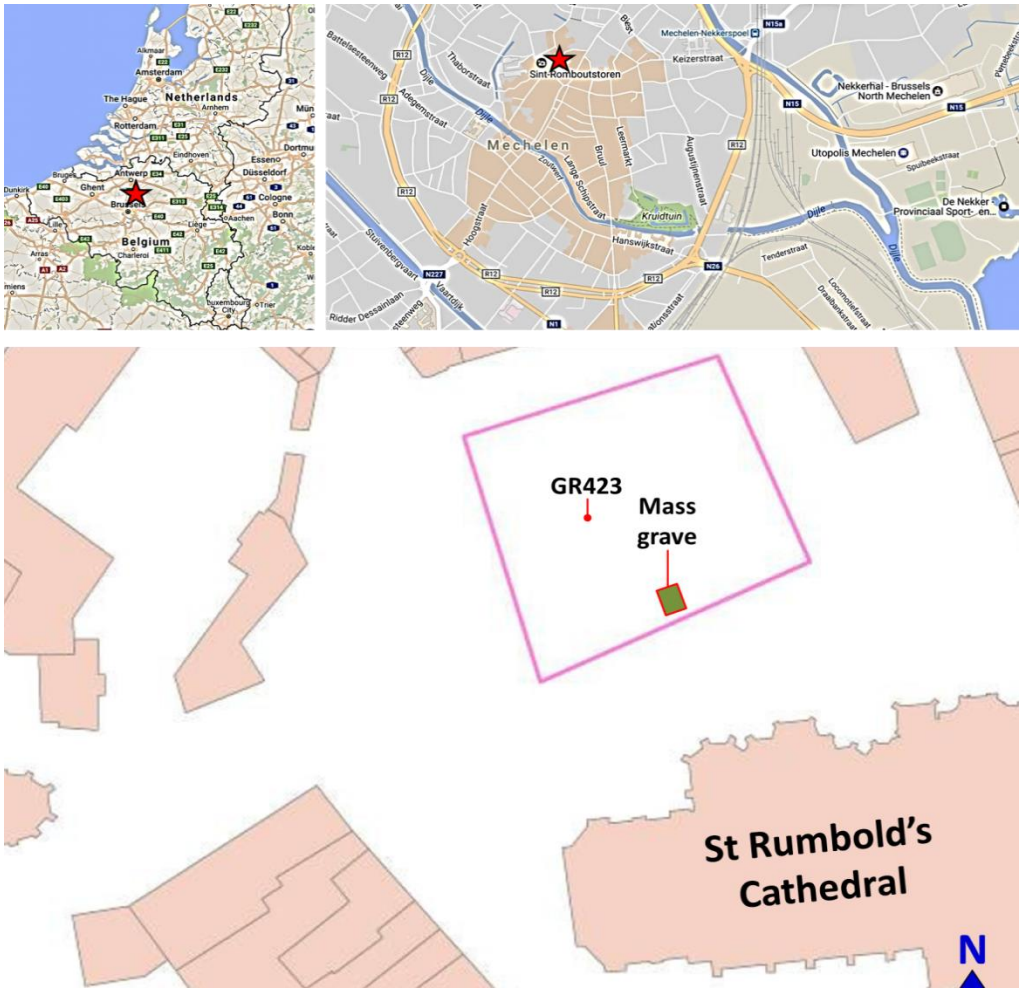

Figure 93. A map of the region surrounding Mechelen (top) and a plan of the 2009 archaeological excavation of the former churchyard next to Saint Rumbold's Cathedral in Mechelen, Belgium showing the locations of GR423 and the mass grave – GR1651 (bottom).

Along with the more typical burials found at the site, GR1651 contained over 41 individuals occupying a single rectangular pit, measuring 2.28 m by 3.16 m (Figure 94). The remains are of those executed on 23rd October 1798 by French soldiers (Van de Vijver and Kinnaer, 2014) at the time of the French occupation of parts of Flanders and Brabant. Local people who were opposed to the French rule took up arms against the French in what became known as The Peasants' War. The deceased in GR1651 had been found guilty and sentenced to death (Figure 95). Most were prone or supine, and those that were sexed by an osteologist were identified as males. Several sets of silver cuff or collar links were found, three in context with one skeleton. Markings on one of the links were used to date the production of the object to 1780.

Many textile fragments were recovered from the burial and conserved by Artesis University College of Antwerp. Visual assessment of the textiles by the conservation team concluded that most of the textile was wool based, with some incidences of surviving leather. Prior to their conservation the InterArChive team collected samples of material from SK2, SK3 and SK40; the materials having been visually identified as leather, wool and felt, in turn. The sample from SK3 was taken adjacent to a green stain surrounding a copper button. A large sample of dark blue/black, finely woven textile and the surrounding dark, stained soil was also recovered from the remains of SK14. The textile was very fragile and brittle; handling fragments of the sample with tweezers resulted in unravelling of the weave and shedding of threads. Woollen textiles recovered from the site were much thicker and more pliable by comparison.

The strategy for analysis of the set of samples was to establish if the materials were derived from animal materials (being protein based) or from plant materials by the implementation of EA. Detection of a significant nitrogen content would distinguish a material as being predominantly protein based, leading to subsequent analysis of the amino acid content by RP-HPLC. Samples found to be lacking a substantial nitrogen component would suggest that the material is plant based, prompting their analysis by Py-GC-MS.

Figure 94. GR1651 mass grave uncovered during the excavation of the churchyard adjacent to Saint Rombold's Cathedral in Mechelen.

Figure 95. "De gefusilleerden van Mechelen tijdens de Boerenkrijg" painted by Léon Rotthier (1897), depicting the execution of brigands who rebelled against the French rule of Flanders in October 1798. The painting is of those shot by French troops on 23rd October 1798 in the cemetery of St Rombold, who were buried in the mass grave (GR1651). © Stedelijke Musea Mechelen.

6.4.2 Analysis of archaeological material

6.4.2.1 EA

EA was carried out using the methods outlined in Chapter 2.3. As elemental analysis was only being employed to distinguish between animal and plant material based primarily on the nitrogen content, no TOC or O analyses were performed. The results from the CHNS analyses are shown in Table 23.

Table 23. CHNS contents of the samples obtained from Mechelen compared with a range of modern materials. Either AA or Py-GC were then carried out based on the nitrogen content.

Sample	C	H	N	S	AA% analysis	Py-GC-MS analysis
Modern cotton	42.11	6.13	0.67	0.00		✓
Modern flax	41.94	6.17	0.00	0.00		✓
Modern hemp	42.41	6.41	0.00	0.00		✓
Modern human hair	46.16	6.83	14.56	4.93	✓	
Modern sheep wool	45.34	6.86	15.49	3.91	✓	
Modern silk	45.09	6.19	17.79	0.00	✓	
Modern cow leather	43.41	5.94	11.05	1.23	✓	
Modern suede	41.56	6.61	14.34	0.46	✓	
GR1651 SK14 black textile	49.86	3.05	0.10	0.18		✓
GR1651 SK2 leather	33.10	4.39	6.73	0.17	✓	
GR1651 SK3 brown textile	41.18	5.93	13.20	3.11	✓	
GR1651 SK40 felt	28.79	4.05	6.96	1.35	✓	

The black textile from SK14 exhibited a low nitrogen content (0.10), within the range of the three modern plant derived textiles analysed (0.00 to 0.67). This indicates that the material has a very low amino acid content and is likely to be a plant based textile. Further analyses of this material using Py-GC and SEM are presented in Section 6.4.2.2 and Section 6.4.2.4 respectively. The three samples of material from SK2, SK3 and SK40 all have nitrogen contents that suggest their structural composition to contain a high percentage of protein. The EA data fits with the tentative identification by the on-site conservation team. Further analyses of these materials by RP-HPLC and SEM are presented in Chapter 6.4.2.3 and Chapter 6.4.2.4 respectively.

6.4.2.2 Py-GC-MS analysis

The pyrogram of the plant based textile from GR1651 SK14 is dissimilar to any of the modern analogues that were analysed alongside the sample. No pyrolysis products that are typically attributable to carbohydrate or lignin were detected by MS. All of the modern plant materials studied contain high proportions of polysaccharides in the form of cellulose and hemicellulose, with small amounts of lignin (Table 24). As has been shown in previous work (Perez-Ceollo *et al.,* 1997) the celluloses in materials in buried materials are readily degraded.

Table 24. The cellulose, hemicellulose and lignin percentage compositions of the modern plant textiles analysed by Py-GC-MS as standards with which to compare the archaeological material from SK14, GR1651, Mechelen.

Material	Cellulose %	Hemicellulose %	Lignin %
Cotton *de* Morais Teixeira *et al*., 2010)	95.5 – 99.9	0.1 – 0.9	0.3 – 0.5
Flax (Li *et al*., 2007)	71	18.6 – 20.6	2.2
Hemp (Li *et al*., 2007)	57 - 77	14.0 – 22.4	3.7–13.0

From a chemical perspective, the material from SK14 cannot be definitively classified as being from a plant or an animal source, despite indications from the EA data that it is unlikely to be animal derived. The complete lack of any peaks derived from organic polymers found in textiles must be rationalised with the physical presence of the textile.

Preservation of the physical structure of textiles by partial or complete mineralisation has been studied previously (Sibley and Jakes, 1982; Gillard *et al*., 1994; Chen *et al*., 1998; Janaway, 2001; Solazzo *et al*., 2014). The organic matrix of polymers is degraded and replaced with inorganic minerals present in the burial environment, the latter often being derived from metal objects buried in close proximity. The mineralisation can be limited to an exterior shell of inorganic materials with surviving biopolymers within, or can involve complete replacement of the organic components, producing a wholly inorganic replica known as a pseudomorph (Sibley and Jakes, 1982). The complete mineralisation of the textile is a likely explanation for the lack of detectable biopolymer signatures in the Py-GC data of the sample from SK14. To test this hypothesis, SEM imaging of the textile was carried out to examine the microstructure of the material (see Chapter 6.2.6).

6.4.2.3 Chiral AA content analysis by RP-HPLC

The three samples of material from the mass burial that had significant nitrogen contents were prepared and analysed by RP-HPLC as described in Chapter 2.5. The total amino acid contents of all three materials are shown in Figure 96.

The total amino acid content of the leather recovered from GR1651 SK2 is within the range of the modern hide materials analysed, indicating that it has undergone little observable degradation. The brown wool from SK3 also has an amino acid content that is well within the range of the modern wools analysed. The felt from SK40 has a total amino acid content slightly below that observed for modern wools (Mann-Whitney u test; *p* value = 0.041). Although this may be due to degradation, it could also be due to the manufacturing processes used in producing felt (Schroeder *et al*., 2004). The felting processes employed may have had some impact on the wool fibres before the material entered the burial environment. The issue of cleaning the felted material must also be discussed. Due to the density and close knitting of the fibres in the material, microscopic particles of sediment trapped within may not have been removed by the cleaning process. This would conceivably increase the mass of the material and decrease the amount of detected amino acids per mg of sample.

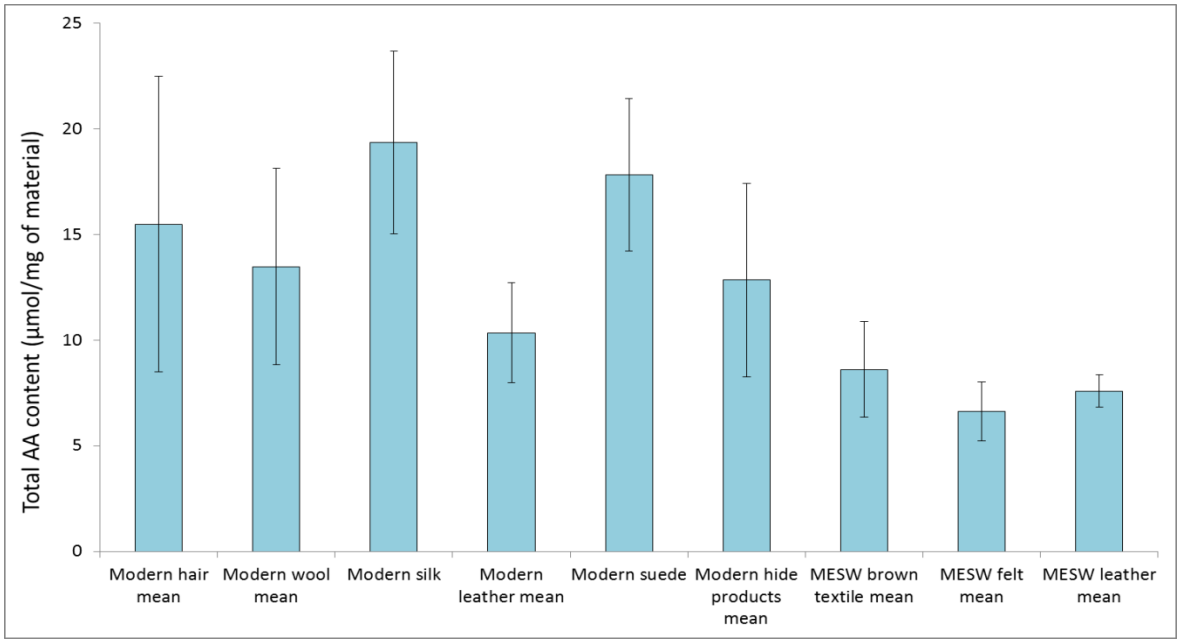

Figure 96. Total amino acid concentrations of the three animal derived materials samples from the mass burial at Mechelen compared with a range of modern materials. Error bars represent +/- 1 standard deviation; n=10 for modern hair and wool, n=3 for modern silk and suede, n=6 for modern leather and n=2 for archaeological materials.

The amino acid compositions of the nitrogen rich textiles are shown in Figure 97. The SK3 brown textile and the material from SK40 have amino acid compositions similar to that of modern wools. This data, combined with the assessment by the conservators from the Artesis University College of Antwerp establish the brown textile from SK3 as a woven or knitted wool garment and the matted material from SK40 is a felted material, produced from wool fibres. The amino acid composition of the material from SK2 matches that of modern leather. As with the previous two samples this finding is in agreement with the observations made by the conservation team.

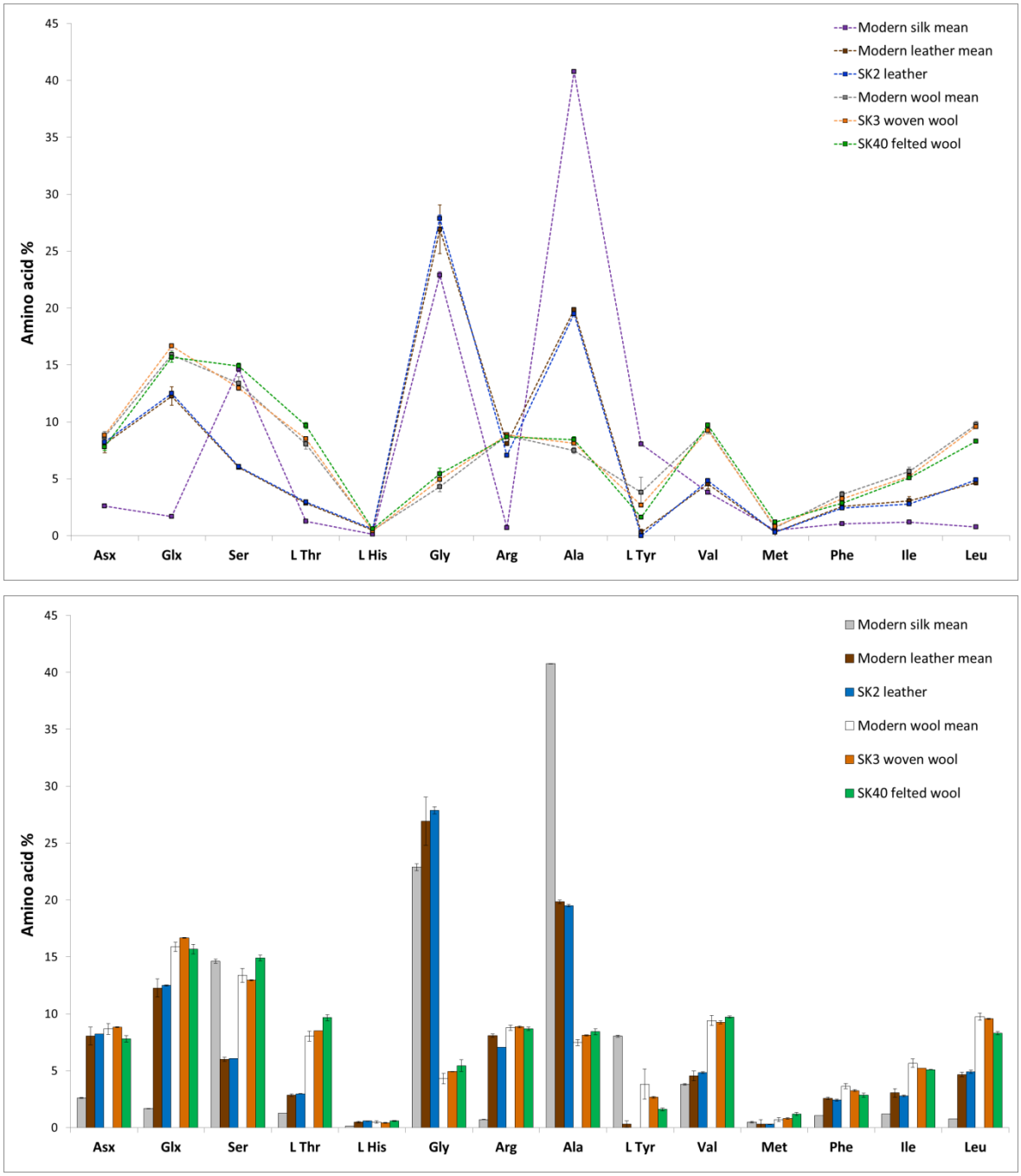

Figure 97. Amino acid compositions of the materials recovered from SK2, SK3 and SK40 in grave 1651 at Mechelen. The data are expressed as percentages of the sum of all amino acid peak areas. Error bars represent +/- 1 standard deviation; n=10 for modern wool, n=6 from modern leather and n=2 for archaeological materials.

The amino acid compositions of the SK2 leather and the SK3 brown textile closely match those of their modern counterparts, with no differences in amino acid compositions (no statistical differences when subjected to Student's t tests; all *p* values >0.05). Any degradation that has taken place has therefore occurred uniformly, in all tissues of the materials and probably reflects chemical and not microbially mediated mechanisms. Attack by proteolytic enzymes produced by microfauna in the burial environment would most likely cleave at specific amino acid sequences and preferentially attack different substructures within the materials; such degradation would produce an evident change in the amino acid compositions (Wilson *et al.,* 2007a, Wilson *et al*., 2010). Degradation of woollen materials that affects fibres uniformly and non-preferentially is typically characterised by amino acid ratios being unchanged from those of the unaltered wool (Wilson *et al.,* 2007a, Wilson *et al*., 2010). No evidence of microbially induced degradation was found during subsequent SEM analysis (see Section 4.2.4).

Slight differences in the amino acid composition of the felt from SK40 are evident by comparison with modern wools. The archaeological felt exhibits higher levels of Ser, L Thr and Ala, and lower levels of Asx, Phe and Leu than the ranges exhibited by the modern wools (Student's t tests; all *p* values = <0.038). As with the textiles analysed from Fromelles (Section 2.2.2) higher Ser content than modern wool can reflect preferential loss of wool fibre cortex proteins, leaving an increased abundance of the Ser rich cuticular layers. Degradation of this kind is almost certainly microbially mediated, signatures of which were found during subsequent SEM analysis (see Section 4.2.4).

The D/L values of selected amino acids from the wool recovered from SK3 show little difference to those of modern wools. The only amino acid that does show any substantial increase in racemisation is Ser (Mann-Whitney u test; *p* value <0.001), but as racemisation has been shown to occur in chain as well as when terminally bound it is not necessarily indicative of any significant breakdown of the wool keratin. For the felt from SK40, on the other hand, increased levels of D Asx and D Ala provide (Mann-Whitney u tests; *p* values <0.027), which may be evidence of modification to the component wool during the felt making process or degradation within the burial environment.

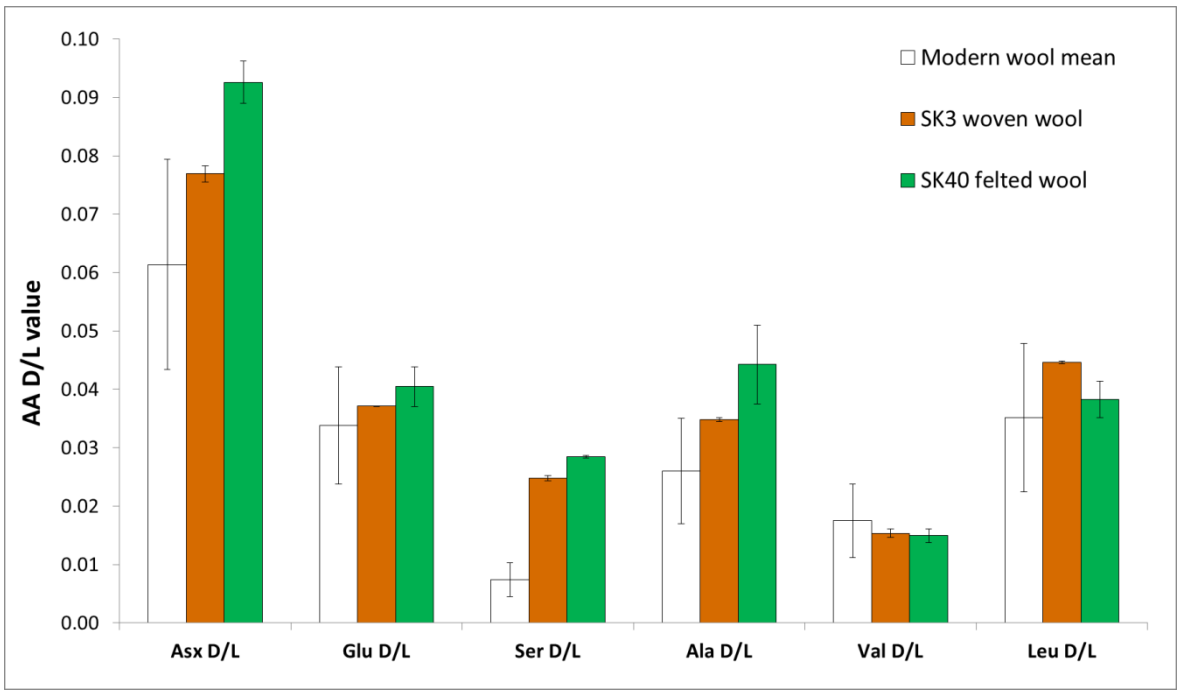

Figure 98. Selected amino acid D/L values for the material recovered from SK3 and SK40 in grave 1651 at Mechelen. Error bars represent +/- 1 standard deviation; n=10 for modern wool and n=2 for archaeological materials.

A small increase in Asx racemisation in the leather from SK2 (Mann-Whitney u test; p <0.001) indicates that there has been little degradation. Given that the material had been buried for around 200 years, any substantial damage by hydrolysis would lead to a greater difference in the D/L values. Thus, the amino acid ratio provides further evidence that the leather from SK2 is well preserved.

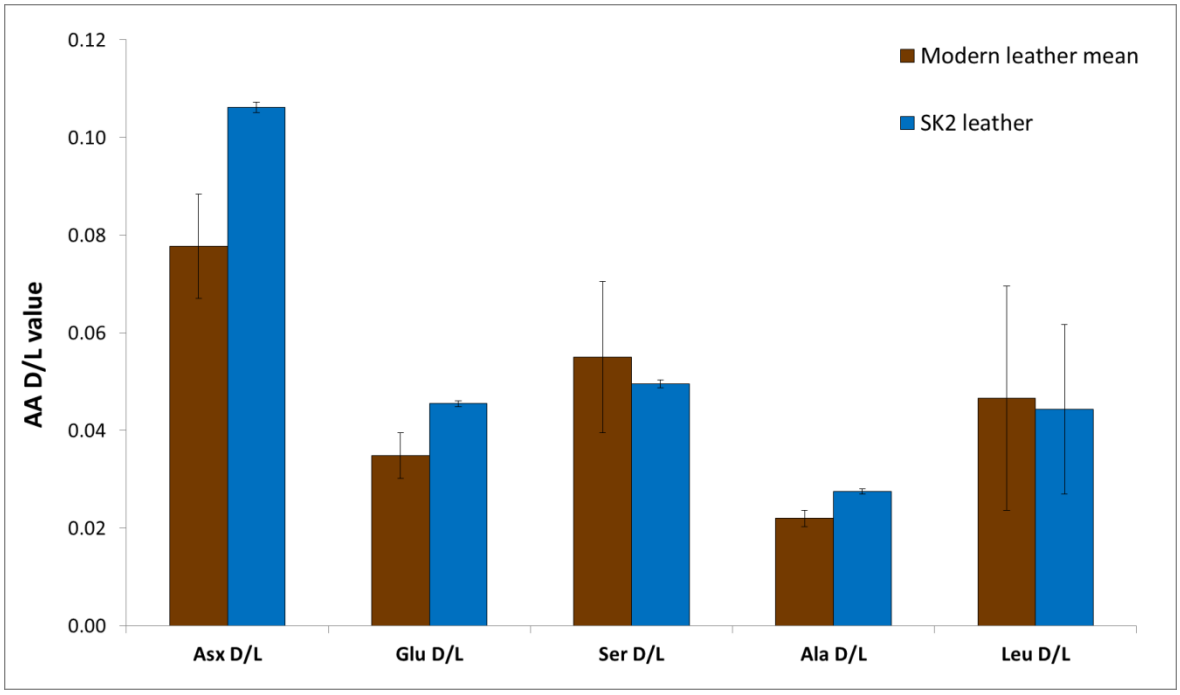

Figure 99. Selected amino acid D/L values for the material recovered from SK2 in grave 1651 at Mechelen. Error bars represent +/- 1 standard deviation; n=6 for modern leather and n=2 for archaeological materials.

6.4.2.4 SEM

The diameters of the fibres that make up the black textile from GR423 (Figure 100) were measured between 5 and 10 µm using SEM, smaller than is typical of individual wool strands (20 - 50 µm). The hollow structure and angular shape is the same as that of bast fibres, harvested from the phloem tissue of dicot plants (Dusenbury, 1992; Ferrero *et al*., 1998; El-Gaoudy *et al*., 2011). This confirms that the material was originally a plant based textile. An in depth examination of the geometry and dimensions of the fibres by Serchisu (2014) indicate them to be flax, the raw material used to produce linen. In the 18th century the Flanders region was a major producer and consumer of linen, making it likely that the material found in context with the occupant of grave 423 was once linen (Van der Wee and Aerts, 1978; Spufford, 2006; Gray, 2003; Ronsijn, 2015). Given the absence of biopolymers in the pyrolysis analyses, it is evident that the material has survived as a totally mineralised pseudomorph.

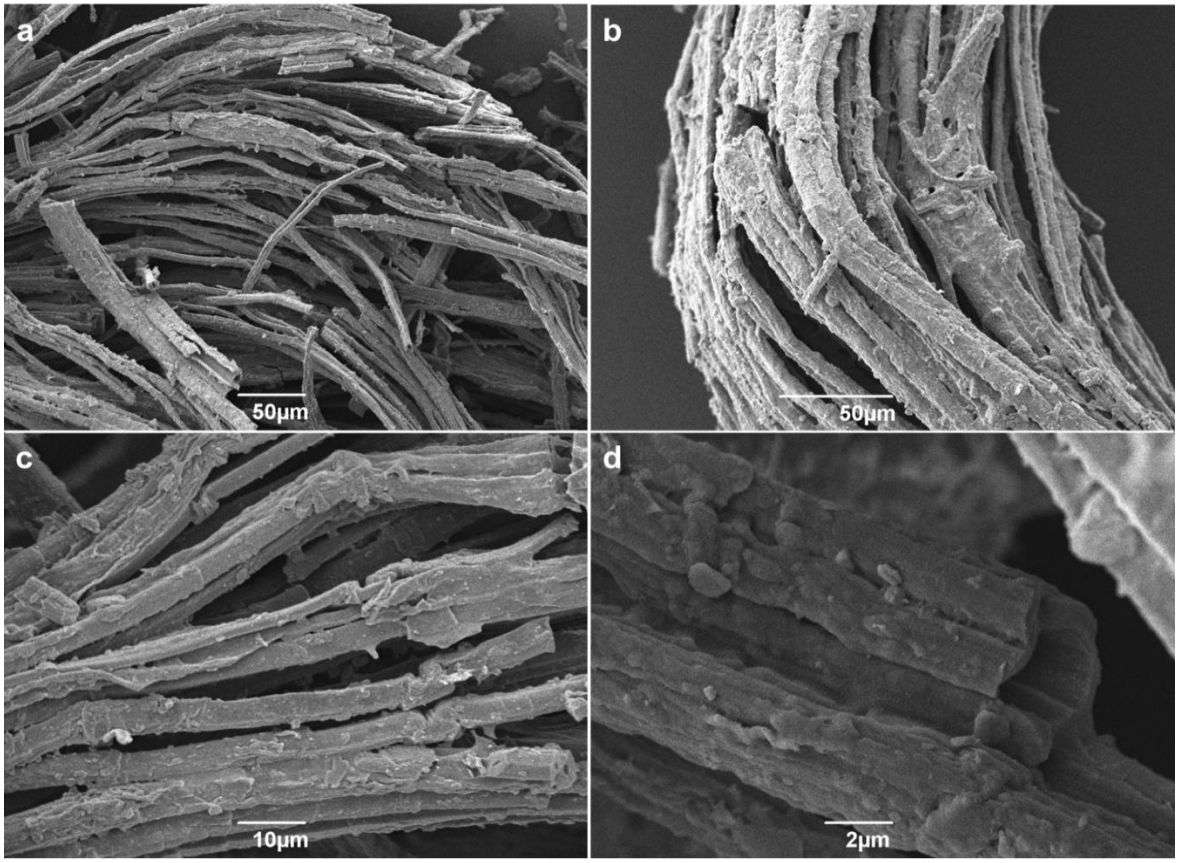

Figure 100. Selected SEM images of the black textile recovered from GR423 at Mechelen.

The black textile from GR423 represents the only example of plant based textile collected from the five sites in this study. In comparison with wool based textiles, plant based materials have a much lower incidence of recovery from archaeological sites (Wild, 1988). There are, however, examples of such textiles surviving for thousands of years (Burnham, 1965; Schick, 1986). Typically, the survival of plant textiles is limited to dry and arid conditions; the two previously mentioned examples are both desert environments, where microbial growth is not supported.

The burial environment at Mechelen was extremely sandy, giving excellent drainage and minimising the water content of the soils. These conditions may have slowed microbial degradation of the textile sufficiently as to allow mineralisation to occur at a comparable rate, and the pseudomorphic textile to be formed. The coarse grain structure of the matrix may also have played a part in the recovery of the textile by archaeologists. Unlike more loamy or clay rich soils the sand would not have adhered to the material, resulting in its detection upon excavation. Given the fragility of the material, a burial matrix that would have adhered to the textile may have resulted in it being missed or destroyed during excavation.

Another possible factor enabling the survival of this textile surviving is the low pH often attributed to sandy soils. The excellent drainage leads to the rapid removal of pH increasing calcium ions from the matrix, leading to a lowered pH (Day and Ludeke, 1993). The acidic conditions may have slowed the progress of decay, resulting in the material surviving, albeit in a heavily modified form. Lower pH soils are known to inhibit microbial growth significantly and to severely limit the biodiversity of the microfauna (Rousk *et al*., 2010).

The woven wool textile from SK3 (Figure 101) in the mass burial exhibits a rough surface coating that covers a large proportion of the wool fibres. The cuticular scales that are visible though the detrital coating appear intact, with little erosion or smoothing. The structural integrity of the fibres suggests that they were undamaged before they were covered.

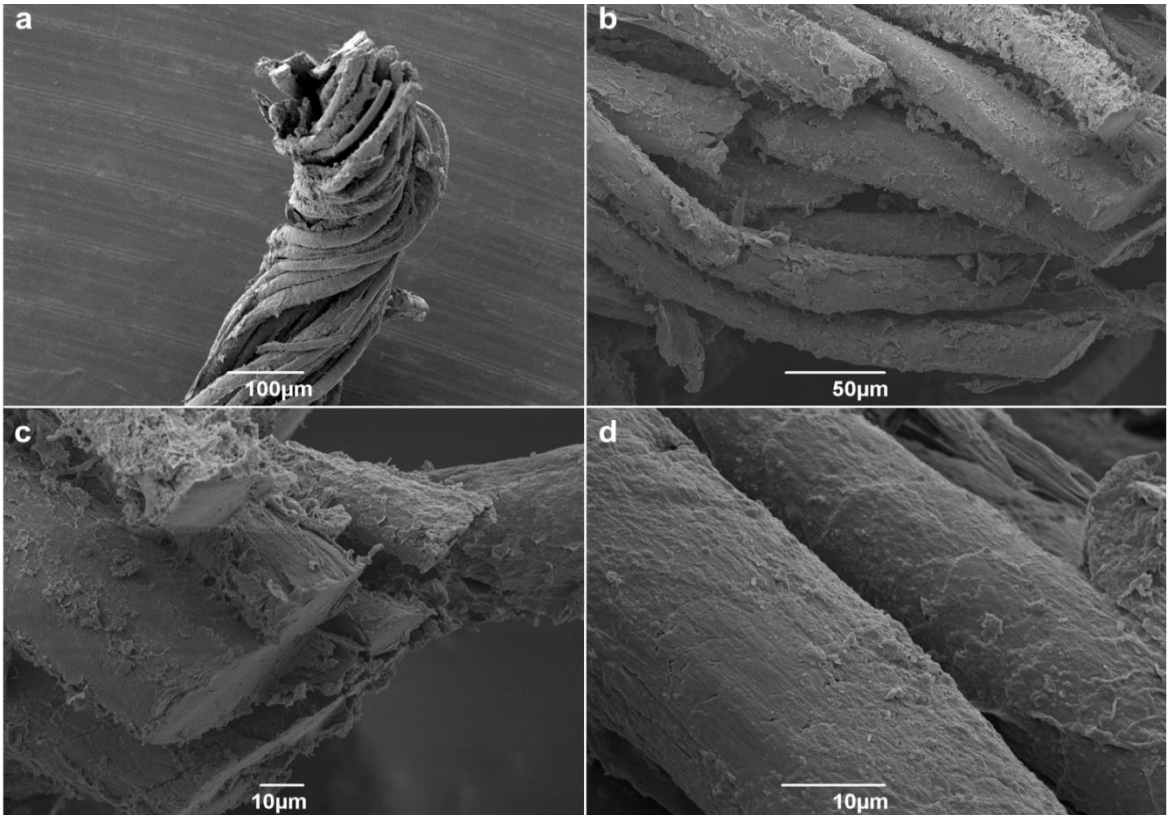

Figure 101. Selected SEM images of the woven wool textile recovered from SK3 in the mass burial at Mechelen.

The cross sections of the wool fibres reveal the cortex and medulla to be intact with no observable deterioration. In some strands of the spun wool thread the fibres are tightly wound and appear cracked. This may be a result of mechanical stress applied in the burial environment or during preparation for SEM. The textile exhibits none of the characteristic signs of microbial or insect degradation. The observations made by SEM analysis concur with the finding of the amino acid analysis in Section 6.4.2.3.

The proximity of this woollen material to the copper staining most likely accounts for its remarkable preservation. Copper is known to have antimicrobial properties that aid in the preservation of grave goods; fragments of textile are often found close to copper artefacts despite the remainder of the article having been destroyed by decomposition (Chen *et al.,* 1998).

The leather from SK2 (Figure 102) exhibits signs of unravelling of the dermal fibres, a trait that often occurs due to mechanical stresses and prolonged immersion in water (Dempsey, 1974; Spangenberg *et al.,* 2010). The overall structure, however, seems intact with no evidence of microbial or insect attack. This supports the evidence for good preservation of the material provided by the amino acid analysis.

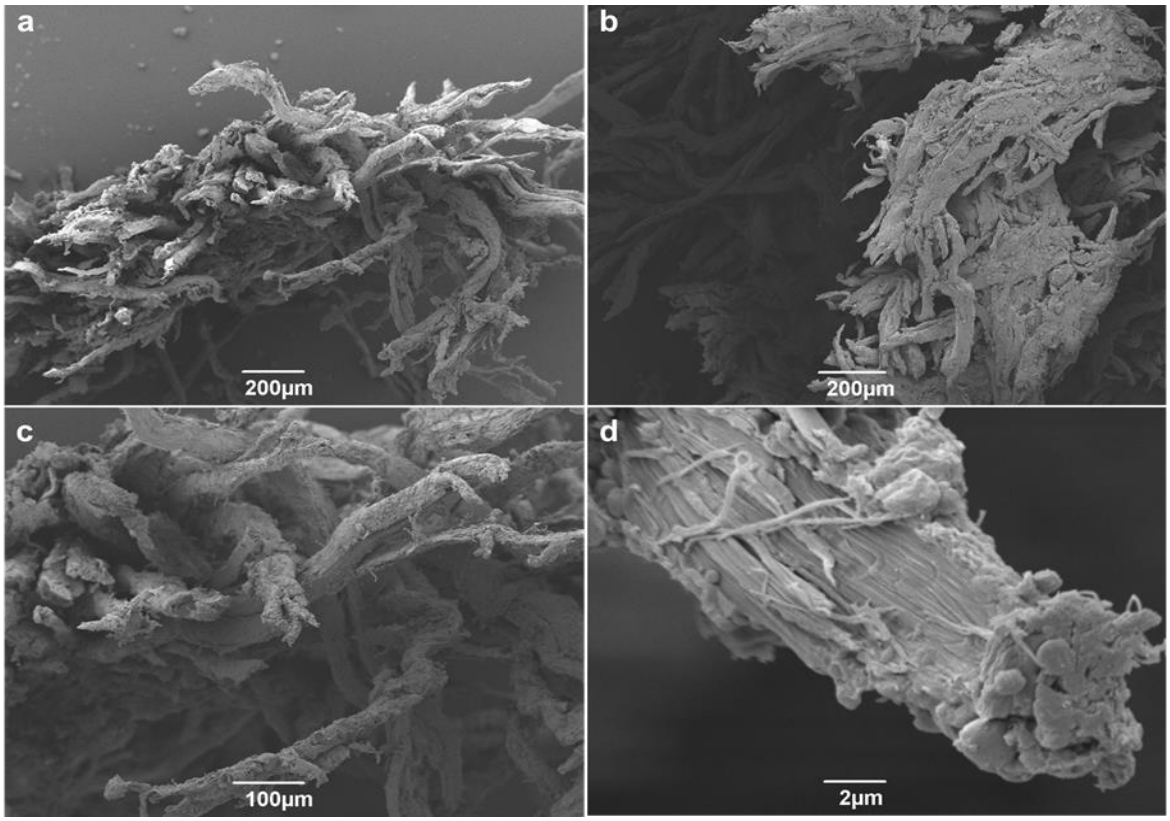

Figure 102. Selected SEM images of the animal hide material recovered from SK2 in the mass burial at Mechelen.

Figure 103 shows some key features observed during the SEM analysis of the felted wool material from SK40 in GR1561. The individual wool strands are interlocked and meshed together in a manner consistent with that of felt. Many of the individual fibres show signs of deterioration

which appear to be concentrated on degradation of the cortex material. Some areas of the cuticle are damaged, with erosion of the cuticular scales. In other areas the scales appear well defined and undamaged. Many strands have holes in the outer cuticles, which expose areas of cortex removal and attrition. Many fibres also appear to be longitudinally split; the visible inner surfaces are heavily pitted and damaged.

Several of the features in Figure 103b may be remains of fungal bodies that contributed to the decay of the felted wool. Figure 103c shows clear evidence of fungal spores adhering to the wool strands. The fact that a fungal organism has sporulated suggest that it had been in a supportive environment with sufficient material to metabolise. The proximity of the spores to the degraded wool fibres in Figure 103c make the parent fungal organism a likely suspect in the decay of this material.

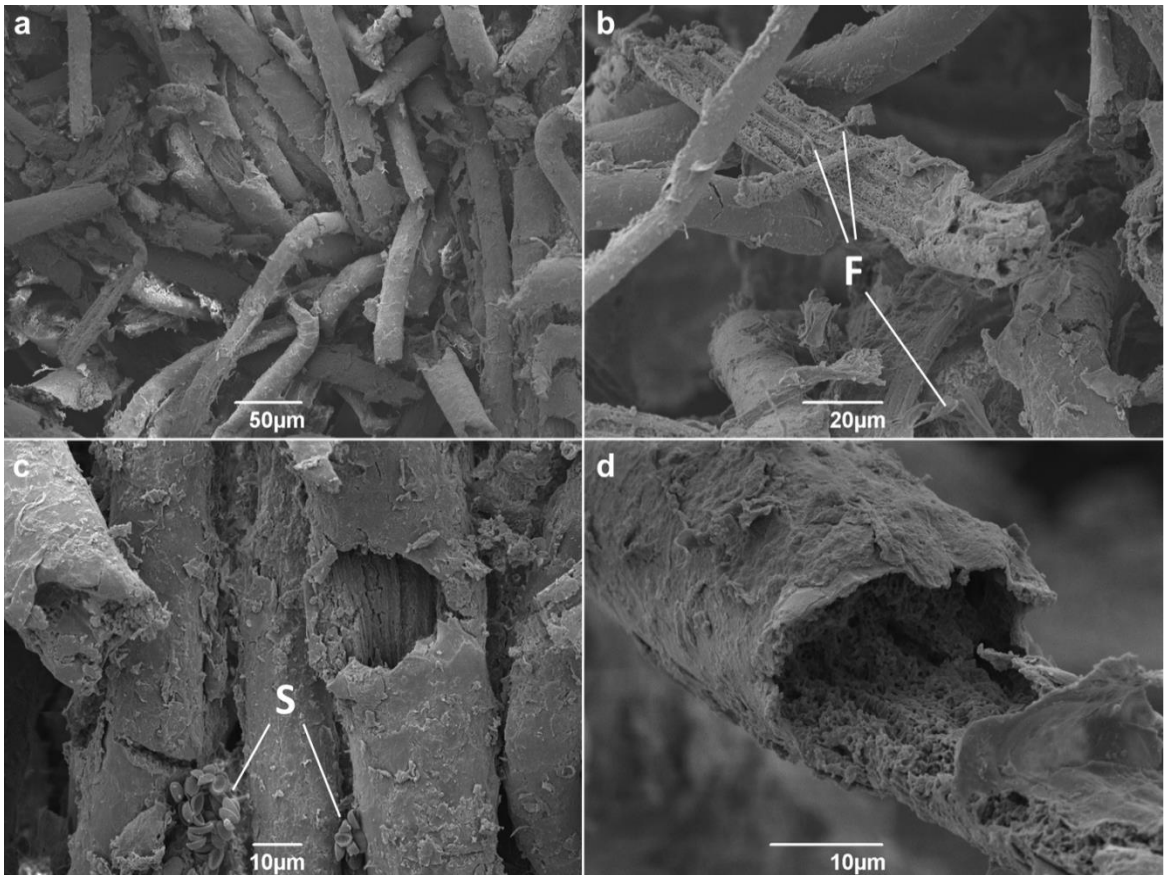

Figure 103. Selected SEM images of the felted wool material recovered from SK40 in the mass burial at Mechelen. F indicates possible fungal bodies. S indicates fungal spores.

It is evident that the felted material from SK40 is more degraded than the woven wool from SK3, suggesting differences in the decay processes affecting these two materials. This would indicate that at least two distinct microenvironments existed within the mass burial pit at some point during the period of interment. Given the presence of copper in proximity to the woven wool from SK3, there is therefore a strong likelihood that the copper did indeed have an antimicrobial effect, protecting the wool from the damage evident in the SK40 felt.

6.4.3 Summary and conclusions

EA indicates that three of the four samples from the mass grave at Mechelen are protein based materials. Amino acid analysis identifies two as woollen textiles, the morphology suggesting that one is a woven textile and the other a felted material. The third material was identified as a remnant of an animal hide similar to modern leather. The amino acid data suggest that the woven wool and the leather are in excellent states of preservation, which is confirmed by SEM imaging. The felted wool has significant differences in its amino acid composition, suggesting that some microbially induced decay has occurred. Damage to the wool, possible fungal structures and fungal spores can all be observed in the SEM images.

The fourth material, a woven textile that has no appreciable nitrogen content, contained no detectable compounds in the Py-GC profiles that relate to known textile biopolymers. SEM revealed that the material was made from bast fibres from flax, hence the textile was a linen fabric. The absence of any biopolymers implies that the textile is a pseudomorph, a material in which all of the organic components have been replaced by inorganic materials. The now mineralised textile is a fragile remnant that bears no chemical similarity to the original material.

The preservation of the protein based materials may well be due to the well drained, and most likely acidic, burial matrix features known to inhibit the growth of the majority of potential microbial degraders.

6.5 Lincoln Castle

6.5.1 Site and sampling information

In 2013 renovation work at Lincoln Castle in Lincolnshire (latitude: 53.234604, longitude: -0.540714) unearthed nine sets of remains buried 3 metres below ground level within the footprint of an ancient church (Figure 104, top). One of the skeletons was enclosed in a limestone sarcophagus (Norton, 2014). One set of remains found in close proximity to the sarcophagus were radiocarbon dated to between 1035 and 1070 AD (Isles, 2015). The mortar seal between the body and the lid of the sarcophagus was not intact at the time of excavation and had presumably been degraded for some time, given the amount of sediment that had accumulated around the remains. It is unknown when the seal was broken or if the seal created a closed system.

Members of the InterArChive team collected 4 samples of what were believed to be clothing materials from the remains in the sarcophagus; three from the chest and one from a mass of dark material by the feet (Figure 104, bottom). All of the samples were flat, amorphous masses, with no discernible weave or stranded structures. The sample from the area surrounding the feet had a small hole in the material, which was suspected as being an eyelet as would typically be found in leather clothing or footwear. The samples available for analysis were very small. Given that one of the four samples was suspected of being protein based (leather), amino acid content assessment by hydrolysis and RP-HPLC was the sole method of analysis performed on this sample set.

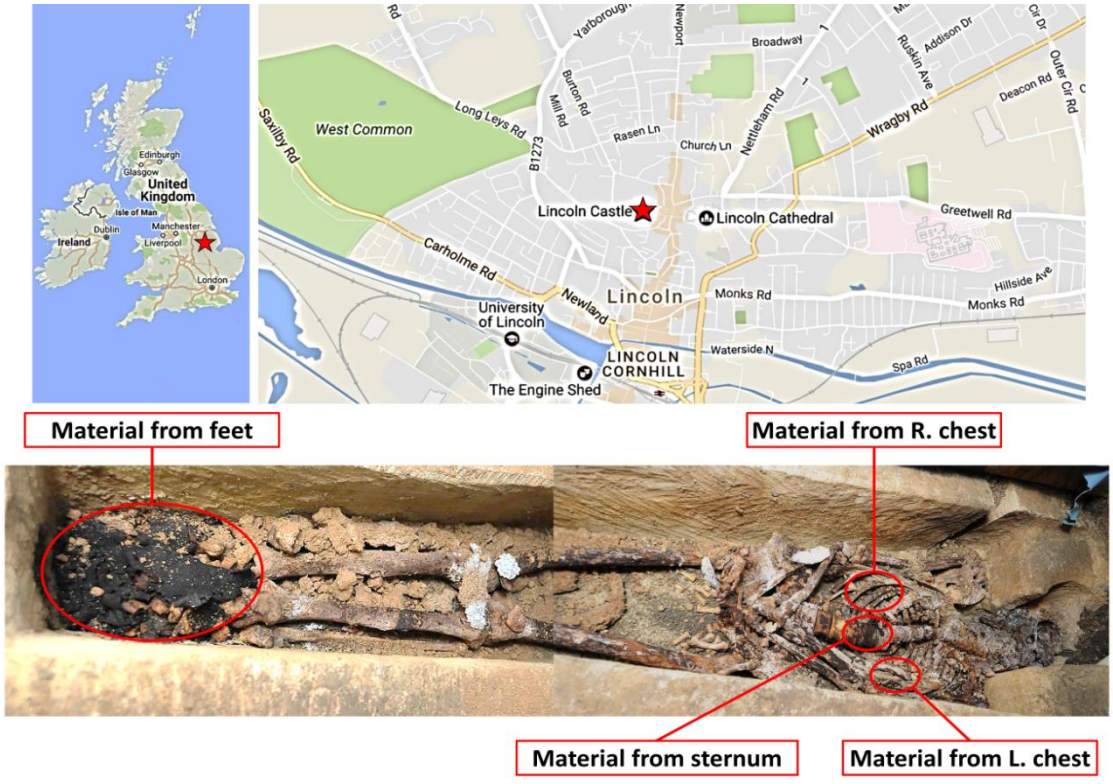

Figure 104. The location of Lincoln Castle in Lincolnshire (top), and a composite image of the remains within the sarcophagus, showing the locations from which the samples were taken (bottom).

6.5.2 Analysis of archaeological material

6.5.2.1 Chiral AA content analysis by RP-HPLC

The total amino acid contents of all four archaeological samples (Figure 105) are significantly lower than for modern materials, suggesting that they are all heavily degraded. All three samples from the chest area of the remains have similar amino acid contents, suggesting that the samples are all from the same type of material, possibly from the same item of clothing. The 'leather' from the feet of the remains has a much lower amino acid content than the samples from the chest, indicating that this material is much more degraded.

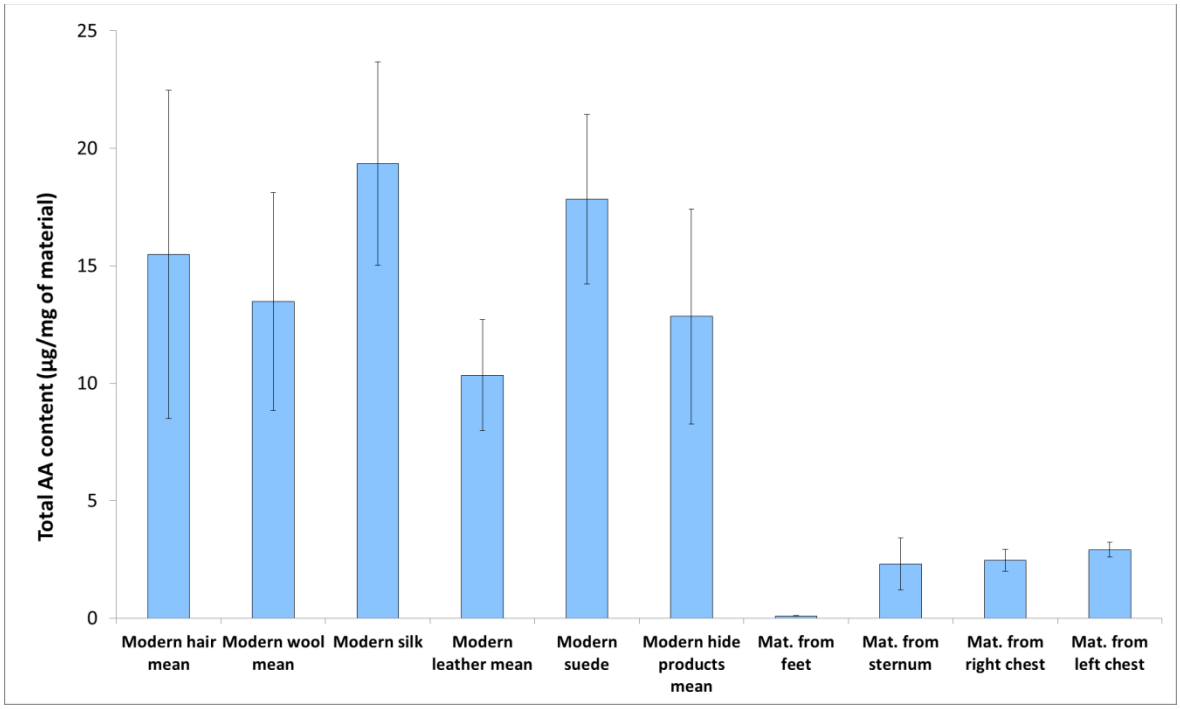

Figure 105. Total amino acid concentrations of the materials sampled from the Lincoln Castle sarcophagus compared with a range of modern materials. Error bars represent +/- 1 standard deviation; n=10 for modern hair and wool, n=3 for modern silk and suede, n=6 for modern leather and n=9 for modern hide products (the mean averages of leather from 2 sources and modern suede) and n=2 for archaeological materials.

The amino acid compositions of the four samples from the sarcophagus are shown in Figure 106. The material from the foot end of the coffin is most similar to modern materials made from animal skins (suede and leather), with large proportions of Gly and Ala that are typical of skin tissues. This similarity combined with the location in which the sample was found and the observation of a hole, consistent with an eyelet, led to the conclusion that the material is most likely part of footwear that the individual was wearing at the time of burial. Despite the similarity in amino acid composition there are significant differences. The majority of the amino acid percentages show significant variation from those of modern hides, suggesting that the material has been significantly degraded.

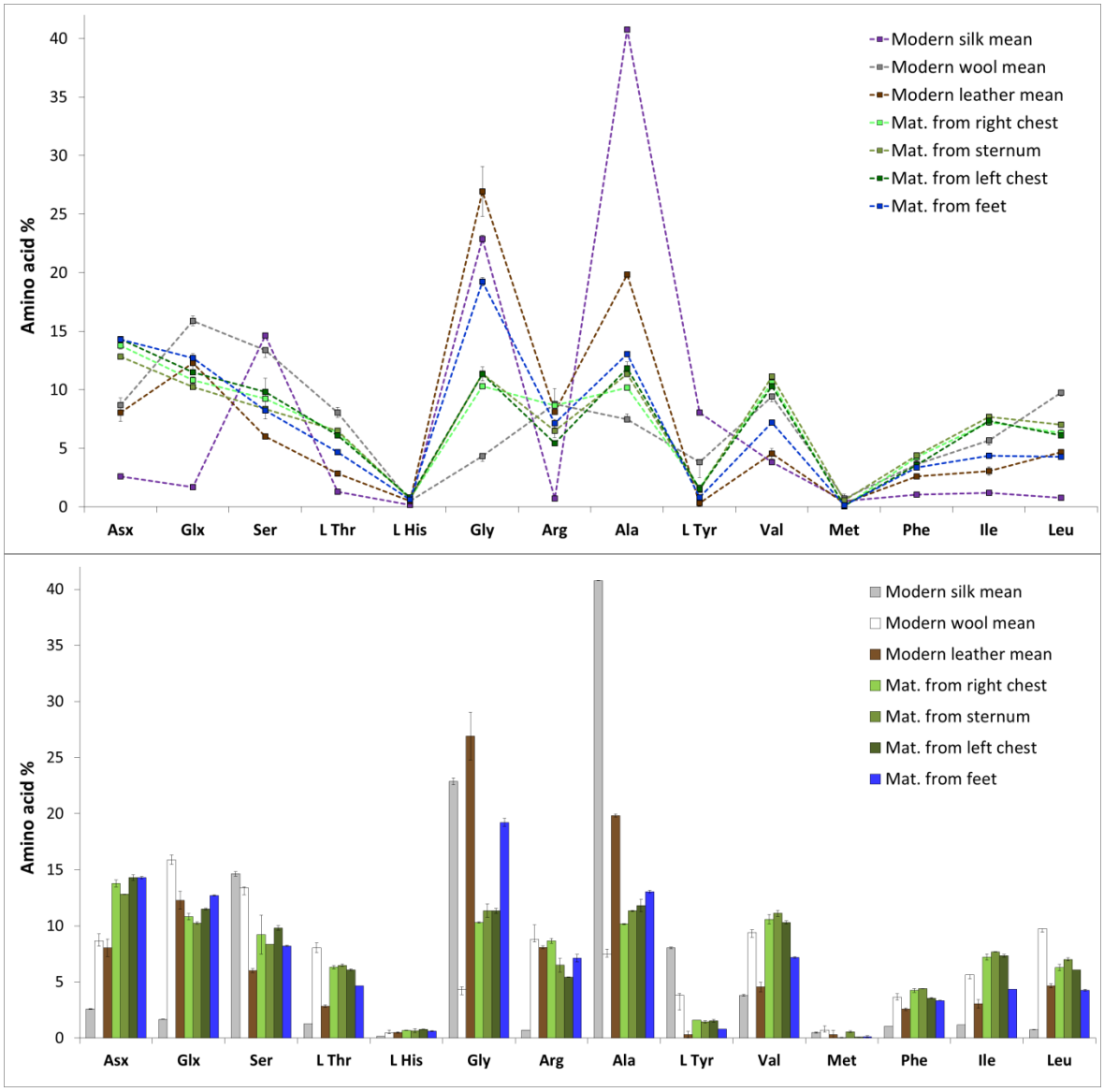

Figure 106. Amino acid compositions of the materials recovered from the remains in the sarcophagus at Lincoln Castle. The data are expressed as percentages of the sum of all amino acid peak areas. Error bars represent +/- 1 standard deviation; n=10 for modern wool, n=6 from modern leather and n=2 for archaeological materials. NB. Mat. is an abbreviation of material.

The decomposition of the body tissues strongly suggests that microbes capable of digesting collagen had colonised the remains, most likely within the sarcophagus. Thus, it is plausible that the types of microbe that degraded the collagen of the corpse also played a role in the observed decomposition of the leather artefact. Non biological degradation of the leather, such as chemically induced hydrolysis and oxidative degradation are also a possibility (Larsen, 1994). Elevated Asx content has been reported in previous studies of degraded leathers to be due to oxidation, although it is commonly accompanied by an increase in Glx which is not seen in this case (Florian, 2007).

The three samples from the chest area all have very similar AA compositions. This suggests that they are made from the same type of material, possibly even from the same piece of clothing. The AA profiles of the archaeological materials are markedly different to any of the modern materials

but are most similar to those composed of hard α-keratin (sheep wool and animal hairs). The Glx:Ser ratio suggests that the material is wool and not human hair, although degradation may well have altered this ratio. The most likely materials used in clothing during the period of burial are woollen textiles, animal skins or tanned hides. Given that the amino acid compositions do not closely match any of the modern analogues of these materials it is highly likely that these three samples of textile from the sarcophagus are heavily degraded.

All of the D/L values for the amino acids studied are higher in the archaeological samples than the mean values obtained from modern leathers (Figure 107). This suggests that the proteins that the materials are made from are in a more fragmented state, producing more terminal residues that have undergone racemisation. The most distinctive feature of the data set is the higher value of the Ile D/L value for modern leather and the material from the foot of the sarcophagus than for modern wool and the other three archaeological samples. The data for modern leather is a mean average based on triplicate analysis of material from two different leather sources. Samples of modern suede also show a very similar Ile D/L value (0.1401, SD: 0.0007, *n*=3). Since D-amino acids are rarely found in living tissues (Barker and Hopkinson, 1977) this increase in Ile D/L value of the modern hide products is almost certainly due to the conditions applied during the tanning process, which is known to lead to racemisation of amino acids (Maxwell *et al*., 2006; Covington and Covington, 2009). Despite this acknowledgement in the literature of increased racemisation upon tanning, there is no previous report of the specific predominance of Ile racemisation over other amino acids. Possible explanations for this level of selectivity may be the specific location of Ile in collagen peptides or the fact that Ile has two stereocenters, whereas most other amino acids only have one. The observation that both the modern animal hide materials and the sample from the foot end of the sarcophagus both display this elevated Ile D/L value is further evidence that the material is indeed a tanned animal hide.

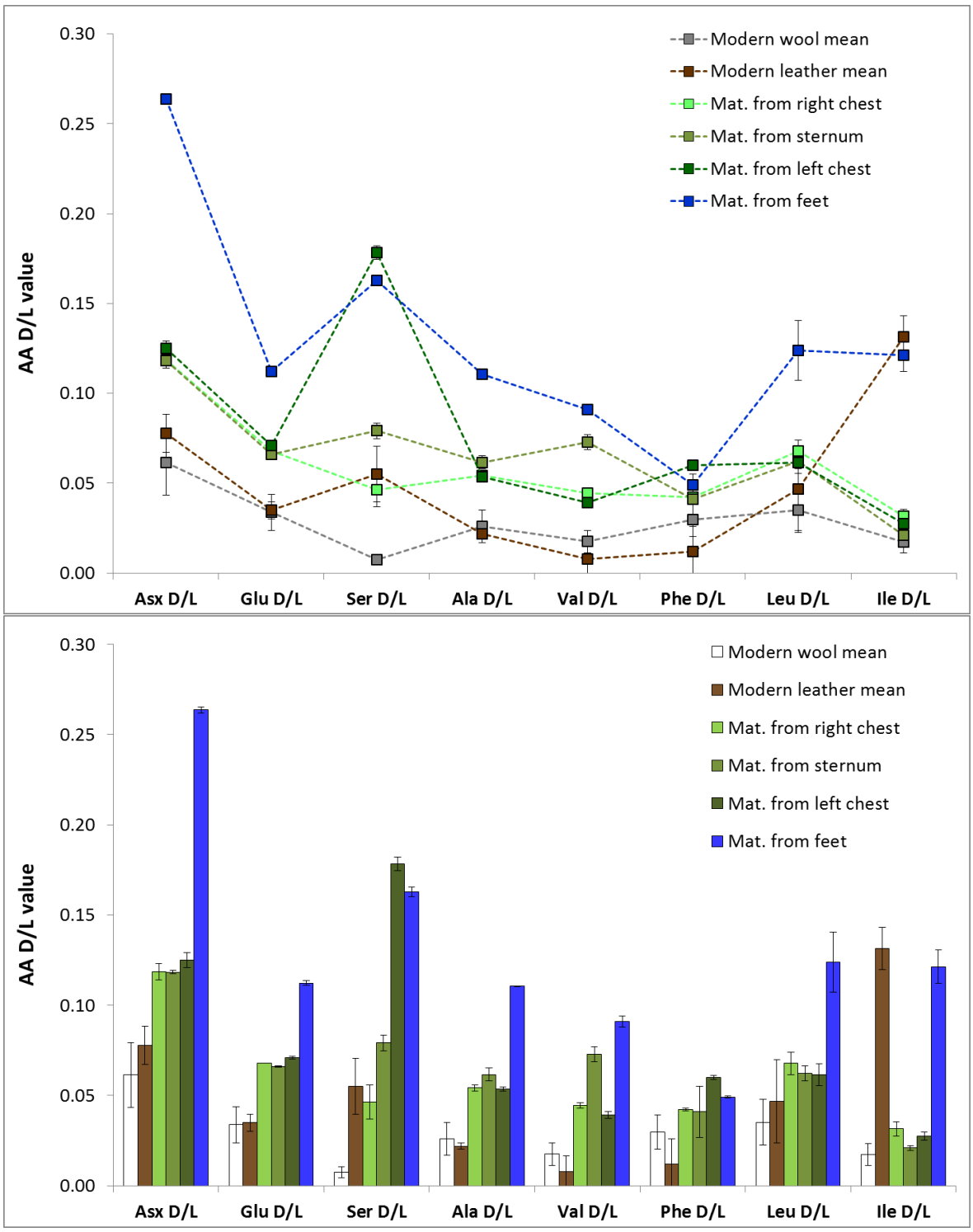

Figure 107. Selected amino acid D/L values for the material recovered from the sarcophagus at Lincoln Castle. Error bars represent +/- 1 standard deviation; n=10 for modern wool, n=6 for modern leather and n=2 for archaeological materials. NB. Mat. is an abbreviation of material.

6.5.3 Summary and conclusions

The material recovered from the feet of the remains in the sarcophagus has an amino acid composition that more closely resembles that of modern animal hide materials than any of the other modern comparators. Given the substantial difference from modern leathers, the amino acid composition is of limited use in identifying the material. The higher levels of racemisation of Ile found in both the modern tanned animal hides and the suspected archaeological leather provides more certainty in the identity of the material as leather.

The three samples from the chest all have similar amino acid compositions, suggesting that they probably originate from the same garment. They are most similar to modern wool, but as with the material from the feet, there are substantial differences that preclude identification of the material based on the amino acid composition with any degree of certainty.

All three of the amino acid parameters measured provide strong evidence that all four samples of material are heavily degraded. This is not surprising given that the materials are approximately 1000 years old. The mechanisms of decay cannot be determined based on the data collected.

6.6 Jaunay-Clan

6.6.1 Site and sampling information

During 2012 a rescue excavation to discover, record and remove all burials and materials of archaeological interest was carried out at the site of a disused cemetery in the town of Jaunay-Clan (latitude: 46.684867, longitude: 0.376976). The town lies in the west of France approximately 170 km south east of Nantes and 12 km north of Poitiers (Figure 108, top). The cemetery occupied an area of 6690 m² and was used for the burial of the dead since Neolithic times (Segard, 2013). During the archaeological excavations two limestone sarcophagi were discovered in the subsurface remains of a mausoleum building (Figure 108, bottom). When the sarcophagi were opened it was found that the occupants were sealed within lead coffins. A team of experts in the fields of palaeopathology, palynology, parasitology, textiles, chemistry and DNA residues was assembled to analyse the contents of the sealed coffins. The InterArChive team were part of the interdisciplinary panel invited to study the burials.

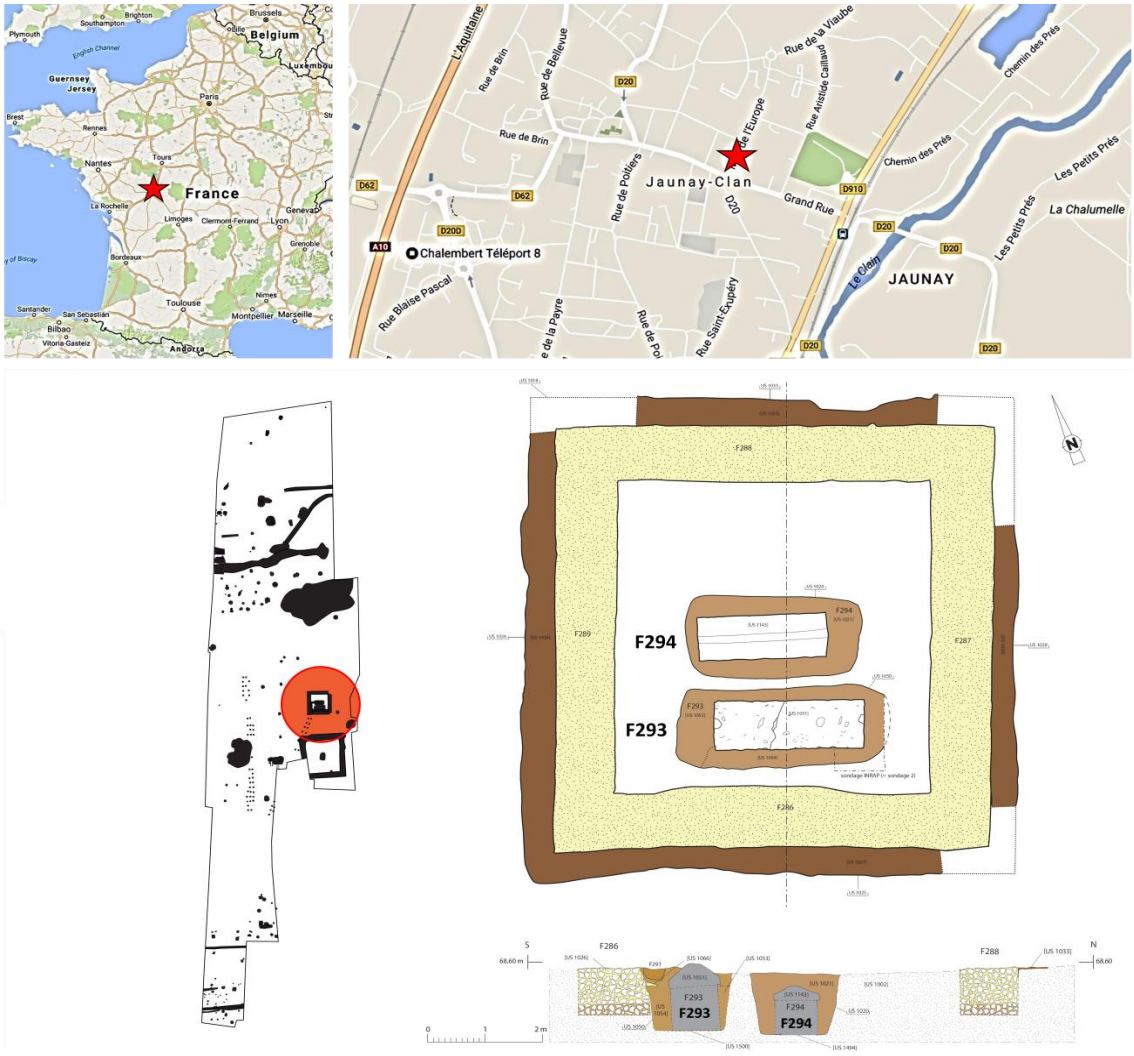

Figure 108. The location of the Jaunay-Clan excavation, in the mid-west of France (top), a plan of the site showing the location of the mausoleum remains containing the sarcophagi (bottom left) and a diagram showing the locations and burial depths of the two sarcophagi within the mausoleum (bottom right).

The sarcophagus labelled F293 contained the remains of an older male, judged to be more than 60 years of age. Radiocarbon dating of bone samples estimated the year of death to be 70 - 230 AD. The base of the lead coffin was damaged near the head and the feet, resulting in holes that exposed the outer limestone sarcophagus. The bone in close proximity to these areas was very heavily degraded. A total of 13 samples of material were taken for analysis within the InterArChive project (Figure 109 and Table 25).

The sarcophagus labelled F294 contained the remains of a 9 to 14 year old child. The sex was not determined due to the undeveloped skeletal features typically used to infer gender. Radiocarbon dating of the bones places the year of death between 240 and 390 AD. A total of eight samples of material were taken for analysis within the InterArChive project (Figure 109 and Table 25).

All of the samples resembling textile materials were very fragile and readily disintegrated when manipulated. It was clear that if any of the samples were indeed the remnants of textile materials they were in an advanced state of decomposition. EA was performed on these samples in order to assess if any had similar elemental compositions to modern textile materials (see Chapter 2.3).

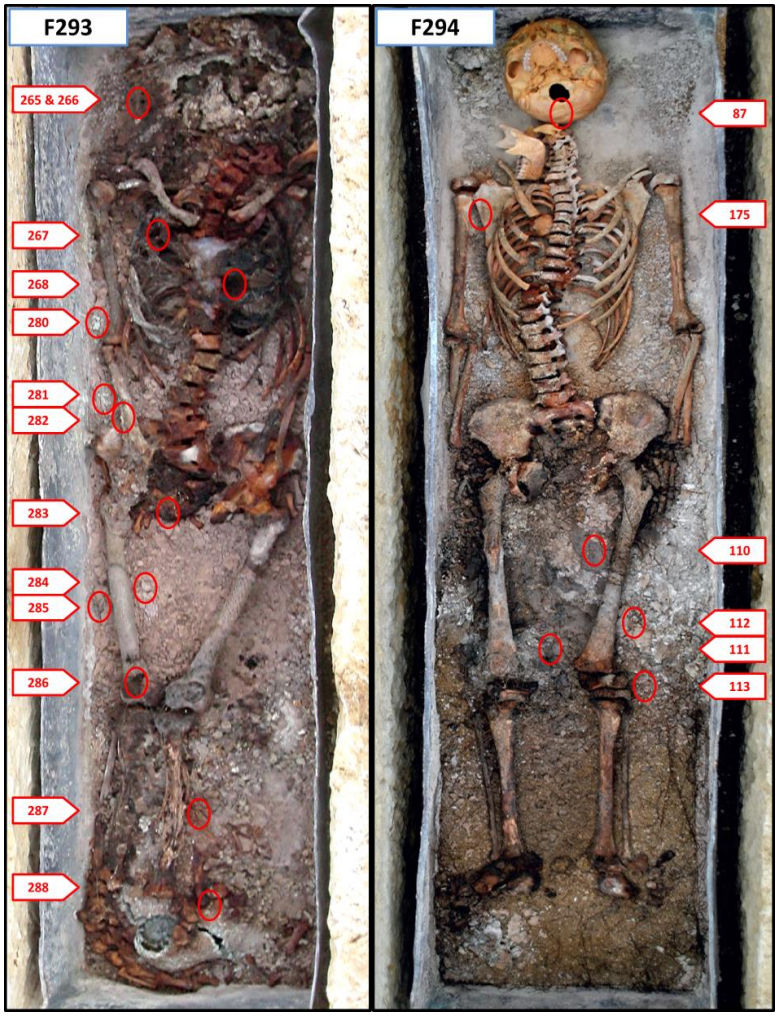

Figure 109. Images of the remains inside the two lead coffins found within the limestone sarcophagi at Jaunay-Clan, France. The red ovals show the approximate positions from which samples were collected for analysis (see Table 25).

6.6.2 Analysis of archaeological material

6.6.2.1 EA

CHNS and TOC analyses of suspected organic material finds were carried out. Several samples exhibited elemental compositions that differed from those of the controls (samples of modern textiles) and of the majority of soils collected from the burial matrix. The most notable and characteristic features was an elevated nitrogen component, often seen in protein based materials (see Table 25). The samples displaying high nitrogen contents were subsequently cleaned, hydrolysed and analysed by RP-HPLC to assess their amino acid compositions compared with modern materials (Chapter 2.5).

Table 25. CHNS and TOC contents of the samples from Jaunay-Clan compared with a range of modern materials.Samples displaying an elevated nitrogen content were then analysed by RP-HPLC

Burial	Sample	C	H	N	S	TOC	AA% analysis
Modern	Cotton	42.11	6.13	0.67	0.00	-	
Modern	Flax	41.94	6.17	0.00	0.00	-	
Modern	Hemp	42.41	6.41	0.00	0.00	-	
Modern	Human hair	46.16	6.83	14.56	4.93	-	✓
Modern	Sheep wool	45.34	6.86	15.49	3.91	-	✓
Modern	Silk	45.09	6.19	17.79	0.00	-	✓
Modern	Cow leather	43.41	5.94	11.05	1.23	-	✓
Modern	Suede	41.56	6.61	14.34	0.46	-	✓
F293	265 – R. of skull, fragmented material	13.41	1.33	0.25	0.41	2.50	✓
	266 – R. of skull, more intact material	33.10	4.36	1.96	0.34	5.73	✓
	267 – R. ribcage	46.14	6.00	5.26	0.59	7.01	✓
	268 – L. ribcage	50.37	5.43	4.73	0.52	6.21	✓
	280 – R. humerus	5.58	0.16	0.07	0.00	0.53	
	281 – R. Ulna	5.21	0.11	0.00	0.00	0.96	
	282 – R. radius	14.30	2.76	0.00	0.00	2.89	
	283 – Pelvis symphysis	39.55	4.72	4.68	0.55	7.00	✓
	284 – Inside R. femur	7.66	0.79	0.00	0.00	3.11	
	285 – Outside R. femur	6.17	0.34	0.00	0.00	1.21	
	286 – Dark material from R. patella	39.08	5.27	6.03	0.61	7.18	✓
	287 – L. of L. tib/fib	4.95	0.06	0.00	0.00	0.41	
	288 – L. foot	4.13	0.07	0.00	0.00	0.66	
F294	87 – under skull	4.30	0.39	0.00	0.00	2.29	
	88 – Fibrous material from the left of C1	5.05	0.35	0.00	0.00	1.07	
	110 – Below pelvis, inside L. femur	5.51	0.73	0.00	0.00	2.12	
	111 – Below pelvis, between femurs	14.69	1.73	1.90	0.56	5.10	✓
	112 – Below pelvis, L. of L. femur	5.61	0.61	0.00	3.07	1.90	
	113 – Below pelvis, L. of L. knee	7.56	0.74	0.00	0.00	1.95	
	184 – above skull	3.90	0.37	0.00	0.00	1.41	
	175 – under R. scapula	5.23	0.21	0.00	0.00	1.26	

All of the material sampled around the head, ribcage and pelvis of F293 have elemental nitrogen contents that suggest they could be protein based. The distribution of these samples would be consistent with a woollen/leather tunic, covering the torso of the deceased. At the time of burial the grave site was in Aquitania, a region of the Roman Empire. Short tunics worn to cover the torso and extending to the thighs were the accepted style of dress for the period (Bunson, 2014). The shoulders, vertebrae, ribs and pelvis all exhibit a red-brown staining that is absent from the bones of the arms and upper legs. The staining of the bones would also be consistent with the presence of a tunic worn by the deceased at the time of entombment. Clothing could conceivably have altered the decay environment of the adjacent tissues in these areas or the dyes may have leached out of the fabric, staining the bone and resulting in the discolouration.

The samples that exhibited no detectable nitrogen also contained very little carbon, hydrogen and sulfur. This indicates that the samples collected are either inorganic residues resulting from the decomposition of the body or heavily degraded textiles with little or no remaining biopolymer. As with the nitrogen rich samples discussed above, the locations of the nitrogen deficient samples could also indicate the presence of fabric or clothing in relation to the body. The proximity of these materials to the arms and legs could be due to the individual being buried in a cloak or toga. The advanced attrition of these materials by comparison with those around the torso could be indicative of the two garments having different textile compositions.

Only one of the samples from F294 exhibited a nitrogen content consistent with proteinaceous organic matter. As with the samples containing no nitrogen in F293, the majority of those in F294 contained little carbon, hydrogen or sulfur. The lack of nitrogen rich material in F294 could be due to many factors, including differing burial dress, methods of preparing the deceased, as well as unique populations of microbes that colonised each set of the buried remains. The issue of the F293 lead coffin being breached may also be a key factor. The holes in the coffin of F293 may well have allowed the fluids rendered from the decaying remains to leak out into the surrounding sarcophagus, removing with it vast quantities of microfauna that would be capable of digesting a range of biopolymers that make up many textiles and clothing materials. The loss of these microorganisms would have likely altered the rate and possibly trajectories of the degradation within the burial.

Sample 112 exhibits a higher sulfur content than all of the other samples from the F294 sarcophagus. Given that the non-sulfur elemental values are similar to the majority of samples analysed from the burial, the high levels of sulfur point to an inorganic source. Sulfur had many uses within the cultures of the Roman Empire. Being synonymous with purification and regarded as cleansing, sulfur was used as a disinfectant to treat wounds and was also burned to ward off illness and plague and to purify the home after the death of a loved one (Block, 2001). It is

possible that sulfur was placed in the sarcophagus with the deceased as a symbolic gesture. Another possible source of inorganic sulfur is the clothing worn by individual. Textiles were cleaned (or fulled) using elemental sulfur (Bradley, 2002); remnants of this process may have persisted in the textile at the time of burial, resulting in the elevated sulfur content of the material thought to be textile remnants.

6.6.2.2 Chiral AA content analysis by RP-HPLC

The total amino acid contents of the materials recovered from the sarcophagi at Jaunay-Clan are lower than in all of the modern comparators (Figure 110). This is evidence of advanced degradation of the materials during their many hundreds of years of burial.

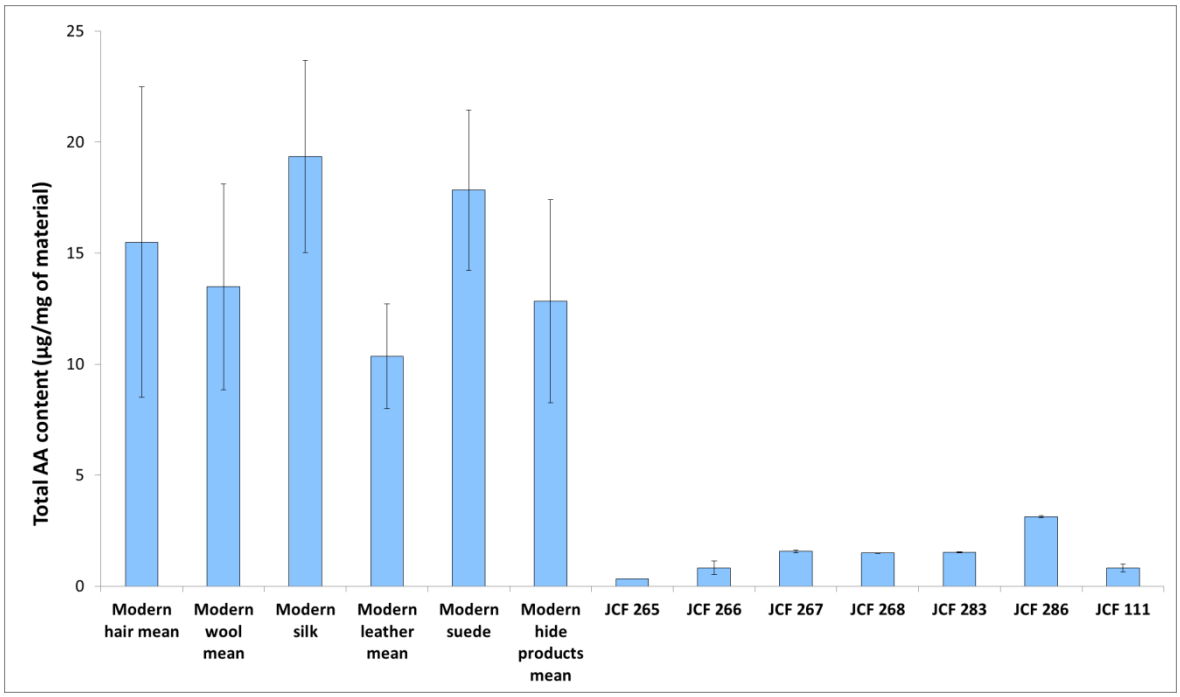

Figure 110. Total amino acid concentrations of the materials sampled from the sarcophagi discovered at Jaunay-Clan compared with a range of modern materials. Error bars represent +/- 1 standard deviation; n=10 for modern hair and wool, n=3 for modern silk and suede, n=6 for modern leather and n=9 for modern hide products (the mean averages of leather from 2 sources and modern suede) and n=2 for archaeological materials.

The amino acid compositions of the materials recovered from the sarcophagi at Jaunay-Clan are shown in Figure 111 and Figure 112. Many of the materials recovered from F293 and F294 show very little similarity to the range of modern materials examined, including literature data for human dermal tissue (data not shown). Several of the samples do show similarities to modern materials, JCF265 and JCF111 having similar AA compositions to those of modern wool and human hair.

The amino acid compositions of samples 266, 267, 268, 283 and 286 are all similar to each other, with 265 having a distinctly different amino acid composition. This could indicate that the samples are from two different sets of material within sarcophagus F293. Given that sample 265 was taken from beneath the head the material could be the degraded remains of hair from the scalp, the remaining samples being from another source. Analysis of the skeleton suggested that the skull has rolled back, away from the neck vertebrae during the period of burial (Segard, 2013). An explanation put forward for this is that the head of the deceased was resting on a pillow which decomposed allowing the skull to roll. A pillow of a different material to that covering the torso of

the remains (such as fur or feathers) could also explain the distinct amino acid composition of sample 265 from F293.

The similarity in the amino acid compositions of the samples covering the torso, together with the similarities in the elemental abundances are consistent with a single piece of material, such as a tunic, covering these areas. If the garment was indeed woollen, the vastly different amino acid composition to modern wool would be indicative of significant degradation of the fibres. The absence of any visible hair along with the remains may indicate the presence of conditions or microorganisms capable of metabolising keratin based matter. The degradation of woollen materials by proteolytic enzymes is often found to be accompanied by an alteration in amino acid composition. The specific sites at which the enzymes cleave proteins render some tissues more liable to modification than others and also results in a range of different peptide products being produced. Some of the peptides are metabolised and lost in the burial environment whereas others are retained and contribute the overall amino acid composition of the sample (Wilson *et al.,* 2007a, Wilson *et al.,* 2010).

All archaeological materials show increased extents of racemisation of the amino acids (Figure 113). This is indicative of a breakdown of the proteins that compose the materials, suggesting degradation.

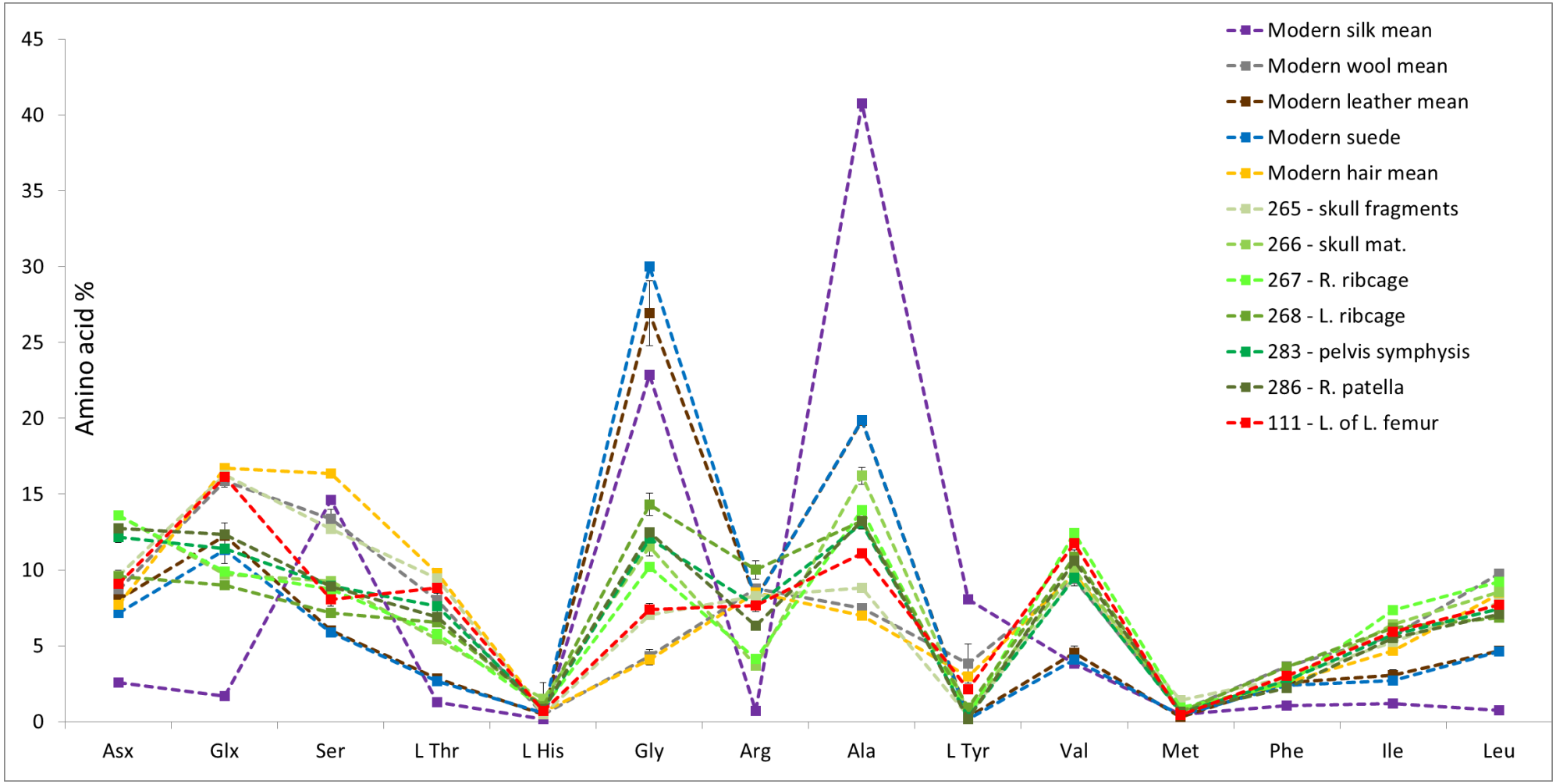

Figure 111. Amino acid compositions for the materials recovered from sarcophagi F293 and F294 at Jaunay Clan. The data are expressed as percentages of the sum of all amino acid peak areas. Error bars represent +/- 1 standard deviation; n=10 for modern hair and wool, n=3 for modern silk and suede, n=6 for modern leather and n=2 for archaeological materials.

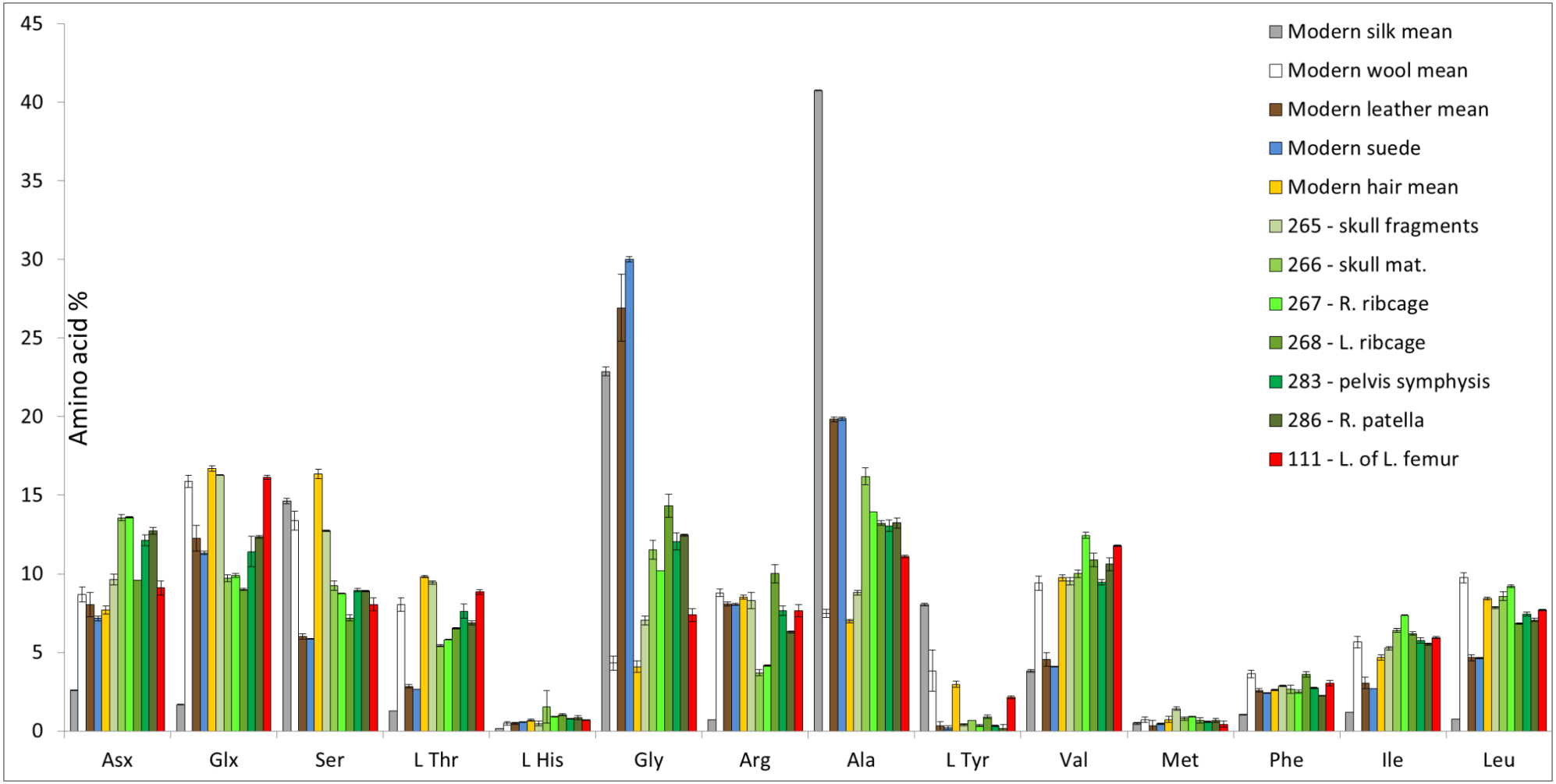

Figure 112. Amino acid compositions for the materials recovered from sarcophagi F293 and F294 at Jaunay Clan. The data are expressed as percentages of the sum of all amino acid peak areas. Error bars represent +/- 1 standard deviation; n=10 for modern hair and wool, n=3 for modern silk and suede, n=6 for modern leather and n=2 for archaeological materials.

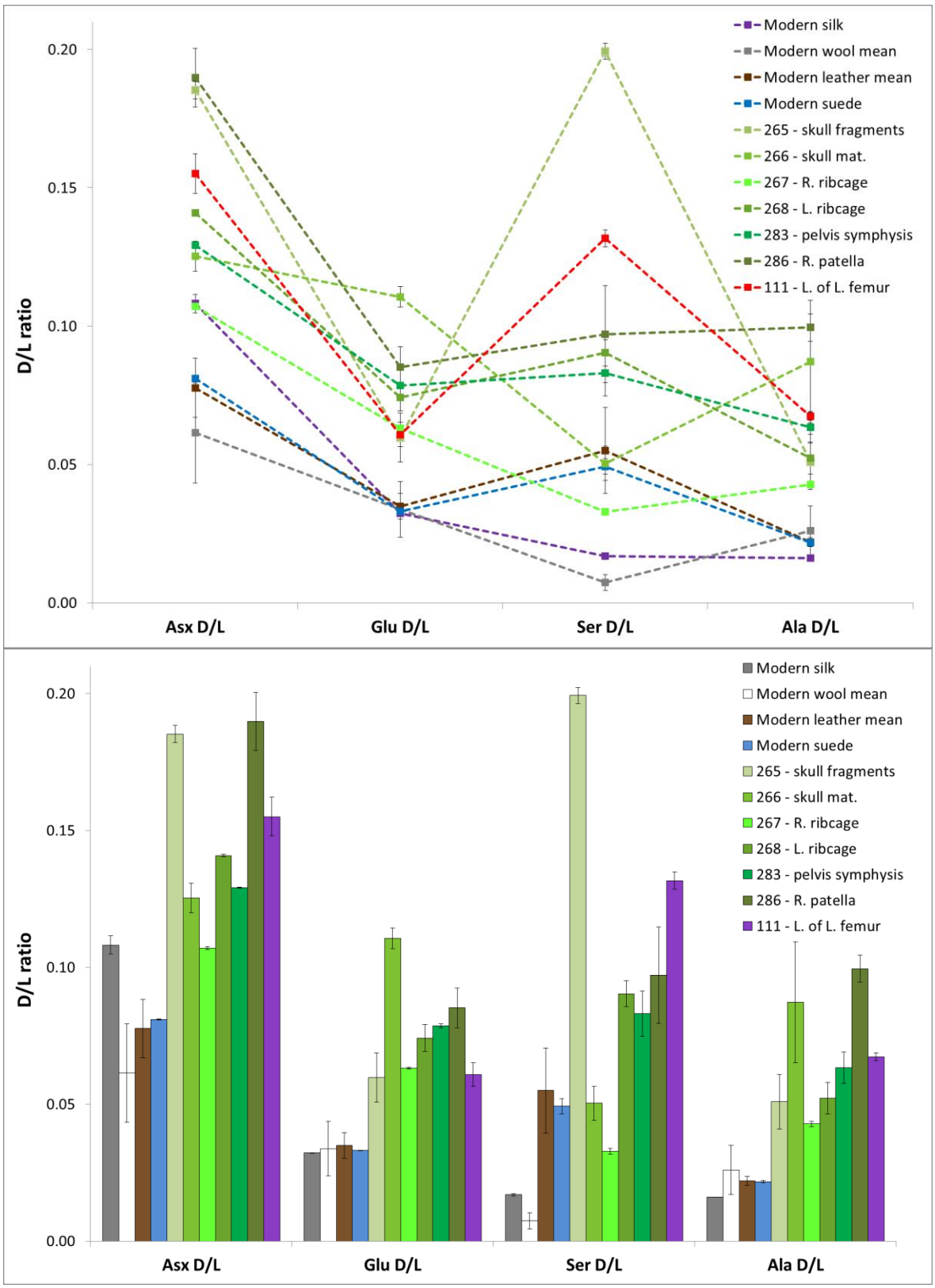

Figure 113. Selected amino acid D/L values for the material recovered from the sarcophagi at Jaunay-Clan. Error bars represent +/- 1 standard deviation; n=3 for modern silk and suede, n=10 for modern wool, n=6 for modern leather and n=2 for archaeological materials.

6.6.3 Summary and conclusions

Based on the EA data, the materials that showed no appreciable nitrogen content (and therefore no amino acid and protein content) are either inorganic residues remaining from the decomposition of the human remains or heavily degraded plant materials that have no elemental compositional similarity with modern materials. The sample with an elevated sulfur content is most likely an inorganic sulfur containing material. The C, H and N content is similar to that of the other materials found within the grave, meaning that the sulfur content is due to a compound containing none of these elements and therefore cannot be organic. It may well be due to an item placed in the grave with the deceased.

All of the protein based material samples from the two sarcophagi at Jaunay-Clan are also heavily degraded, as shown by the amino acid compositions being different to any of the modern materials, by the high degree of racemisation of the amino acids, and by the low overall amino acid contents.

There are differences in the amino acid compositions of the materials from around the torso of F293 from that sampled from under the skull of 265. The most likely explanation for this is that 265 is hair or material from a pillow under the head, and the remaining samples are of clothing that covered the torso. The staining of the torso, pelvis and upper arms may also be indicative of fabric covering these areas; the discolouration being a result of either textile dyes or due to differing decompositional processes caused by the textile.

6.7 Analysis of intersite trends

The number of amino acids analysed for each sample and the large number of samples analysed resulted in a large, multidimensional dataset. In order to assess any patterns and trends present across all of the experimental and archaeological burial environments, principal component analysis (PCA) using PAST v3.15 (Hammer *et al.*, 2001) was used to interpret both the amino acid composition (Chapter 6.7.1) and the D/L value (Chapter 6.7.2) datasets. Missing values in individual data rows were filled using iterative imputation; blanks were initially replaced by the column mean, then the data was subjected to subsequent PCA runs until convergence (Ilin and Raiko, 2010).

6.7.1 PCA of amino acid composition data

The PCA scatter plot for the amino acid composition data of all experimentally buried and archaeological textile and leather samples is shown in Figure 114. A simplified biplot, showing the weighting of each amino acid variable on PC1 and PC2 is shown in Figure 115. The first two principal components (PC1 and PC2) account for 87.3% and 7.6% of the variation, a total of 94.9%. PC1 is positively correlated to Gly% (0.75) and Ala% (0.44), and negatively correlated to Ser% (-0.33). PC2 is positively correlated to Ser% (0.41) and Glx% (0.38), and negatively correlated to Asx% (-0.60), Val% (-0.35) and Ile% (-0.30).

Several distinct clusters of data points are apparent in Figure 114. The cluster highlighted in red contains data points for all of the wool samples analysed. Modern, undegraded wool is at the bottom of the cluster, with the more degraded samples appearing higher up in the cluster. The literature data for the composition of wool cuticle material (Bradbury and Ley, 1972) lies above the cluster. The linearity of the cluster enables the wool materials recovered to be ranked by the difference in amino acid composition from that of modern wool, and thus establish a scale of degradation. The woven wool from Mechelen SK3 is the least chemically degraded archaeological wool, followed by the hair tie from SK289 at Fewston and then the textile from the feet of SK408 at Fewston. As was reasoned on the basis of chemical and SEM data (Chapter 6.4.2), the PCA indicates that the felt from SK40 at Mechelen is more degraded than the woven wool from SK3 at the same site, the felt having a similar amino acid composition to woollen textile from the feet of SK1525 at Fromelles. The remaining samples from Fromelles are all tightly grouped, indicating that these wool materials all have similar amino acid compositions and are, therefore, are in a similar state of preservation. Their position at the top of the cluster indicates that this group of samples are the most chemically different to modern wool and are the most degraded samples of wool that can be confidently identified as such. The data point for sample 265 from beneath the skull of SK293 at Jaunay-Clan lies close to the red wool cluster, which may indicate that this

material is keratin based, and is either degraded wool or hair. The data point for sample 265 is also very far away from that of sample 266. Both of these observations add further support to the hypothesis derived in Chapter 6.6, which indicates that samples 265 and 266 may be two different types of material.

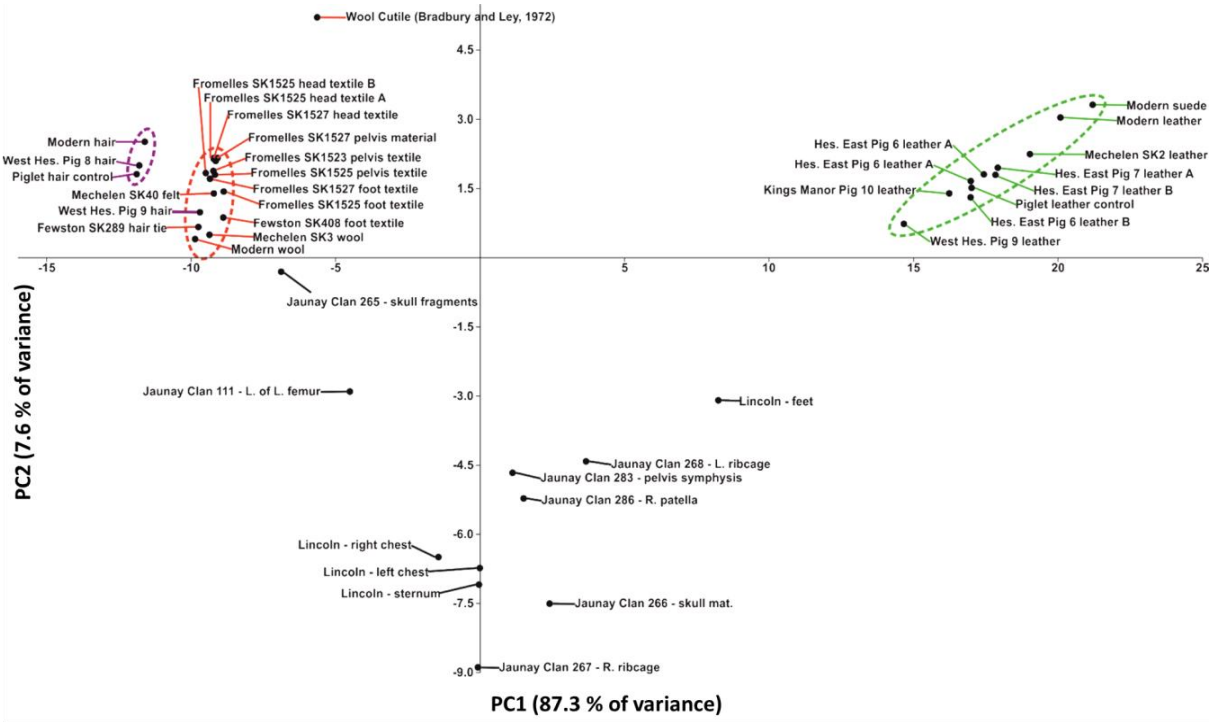

Figure 114. PCA scatter plot of PC1 and PC2 for textile and leather amino acid composition data, accounting for 94.9% of total variance. The data points and cluster highlighted in red are the wool, those in green are leathers and those in purple are human hair.

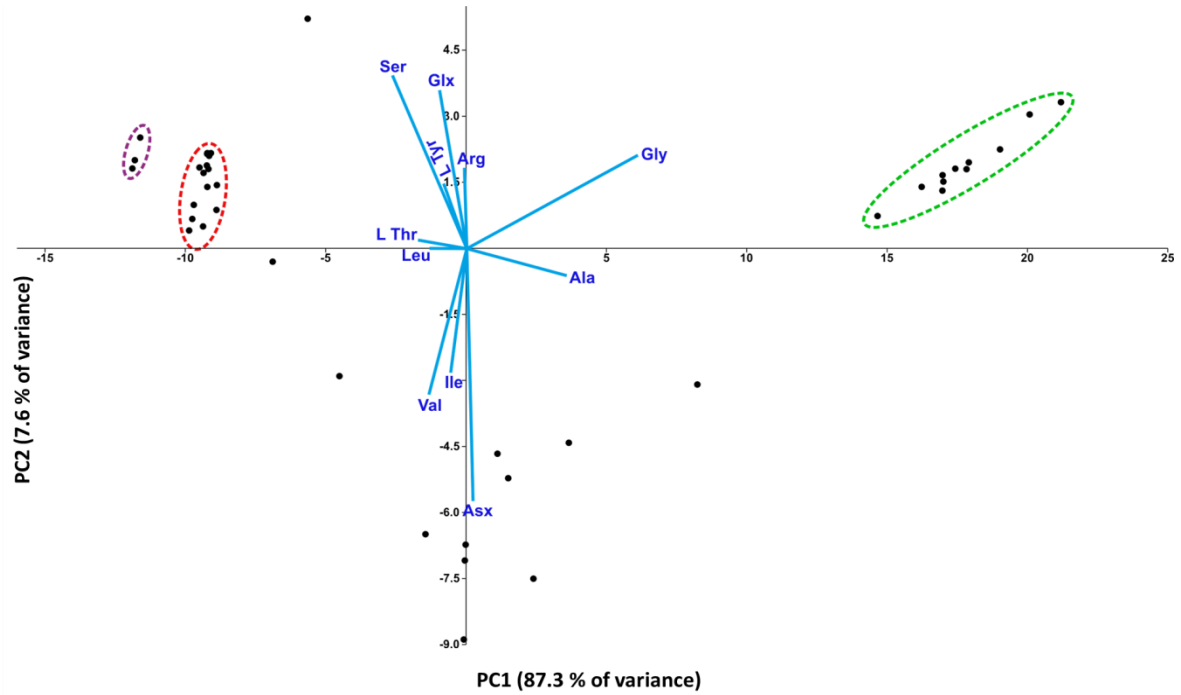

Figure 115. PCA loadings plot of amino acid composition data, showing the major contributions of each amino acid to PC1 and PC2. The data points and cluster highlighted in red are the wool, those in green are leathers and those in purple are human hair.

Three of the four data points for human hair are tightly grouped and highlighted in purple. The proximity to the hair data point cluster to the wool cluster is likely due to their similar amino composition (Robbins, 2012). The fact that both of these clusters are well resolved from each other demonstrates that there is a measurable difference between the two, and illustrates the suitability of the chemical and statistical methods employed during this investigation. The hair buried with Piglet 8 at West Heslerton lies between those of the unburied hair control and the mean value for modern hair, suggesting that these materials all have very similar amino acid compositions. This implies that the hair from Piglet 8 has undergone little compositional change in the burial environment. The remaining human hair sample is that recovered from the West Heslerton Piglet 9 burial experiment, which does not lie with the other three hair samples, it is instead in the red wool cluster. This indicates that the piglet 9 hair is significantly compositionally different from the modern, unburied human hairs, which supports the findings in Chapter 4.3.

The data points for all animal hide samples analysed also group into a distinct, linear cluster, highlighted in green in Figure 114. Modern hide materials (leather and suede) occupy the top of the cluster, the only positively identified archaeological leather – that from SK2 at Mechelen – being below the modern materials, and the piglet leathers forming the lower portions of the cluster. The piglet leather control is in the lower half of the cluster, along with the experimentally buried leathers. This suggests that the leather used in the experimental burials is compositionally different from the other modern leathers analysed as part of the InterArChive project. As a result of the leather data subset being smaller than that of wool, no firm conclusions can be drawn about decomposition trajectories based on this data. However, the material sampled from the feet of the remains in the sarcophagus uncovered at Lincoln Castle (Chapter 6.6) could not be definitively identified as leather based upon the amino acid composition, but it was tentatively assigned as such. In the amino acid composition PCA plot, the data point for this sample is outside the leather cluster, but if a best fit line were drawn using the points in the leather cluster and extrapolated towards the y axis, the line would come very close to the Lincoln feet material. This may be further evidence of this material being highly degraded leather.

The remaining, more heavily degraded samples from Lincoln Castle and Jaunay-Clan are scattered in the lower half of the plot, where higher percentage compositions of the more hydrophobic residues Ile and Val are more prevalent. The three samples from the chest area of the Lincoln Castle remains all lie close to one another. This grouping reinforces the hypothesis made in Chapter 6.5, which suggest that these samples may all be from the same piece of textile or item of clothing. Samples 268, 283 and 286 from Jaunay-Clan form their own small cluster, which also supports the idea that these samples are from the same materials source (Chapter 6.6). The remaining data points do not show any trend or correlation.

6.7.2 PCA of amino acid D/L value data

The PCA scatter plot for the D/L values of all experimentally buried and archaeological textile and leather samples is shown in Figure 116. A simplified biplot, showing the weighting of each amino acid variable on PC1 and PC2 is shown in Figure 117. The first two principal components (PC1 and PC2) account for 79.7% and 11.9% of the variation, a total of 91.6%. PC1 is positively correlated to Asx D/L value (0.96), Ser D/L value (0.57) and Leu (0.31). PC2 is positively correlated to Val D/L value (0.39) and Glx D/L value (0.34), and negatively correlated to Ser D/L value (-0.77).

As with the amino acid composition PCA plot, several distinct groupings of data points are apparent. All four of the hair samples form a cluster (highlighted in purple), with modern hair, the unburied piglet control hair and the hair buried with West Heslerton Piglet 8 all being very close together. This indicates that the Piglet 8 hair has undergone little racemisation. The hair from Piglet 9 has a lower y value than the other three hairs, indicating that this material may have undergone the most racemisation of the hair samples.

The data point for modern wool is close to the hair cluster, likely due to the similarity of their chemical composition and low amount of D amino acids observed in undegraded mammalian proteins (Michal and Schomburg, 1999). All of the Fromelles wool data points are grouped together, shown in the red oval in Figure 116. The woollen textile from the feet of Fewston SK408 also lies close to this grouping. The data points for these wool samples are furthest from that of modern wool, indicating that these materials are most different in terms of their D and L amino acid compositions. Looking at the PCA loading plot in Figure 117, data points that have more negative PC2 values are more likely to have a higher Ser D/L value, indicating that these have undergone more Ser racemisation. Between this cluster and the modern wool are the remaining archaeological wood samples; their increasing distance from the modern wool data point indicating an increase in Ser racemisation, shown by the red arrow. Using this trend it can be inferred that the wools from Mechelen have undergone the least amount of Ser racemisation, and that the wool sample from Fewston SK289 has undergone comparatively more L-Ser to D-Ser conversion, with the Fromelles and Fewston SK408 wool experiencing the most Ser racemisation. If the red arrow were extended, it would intersect with the data points for samples from the left chest area of the Lincoln Castle remains (Chapter 6.5) and sample 265 from under the skull of F293 from Jaunay-Clan (Chapter 6.6). Both these samples have been hypothesised to be heavily degraded keratinaceous materials. The extension of this line, with its origin near the data points for modern wool and hair, would add further weight to these ideas.

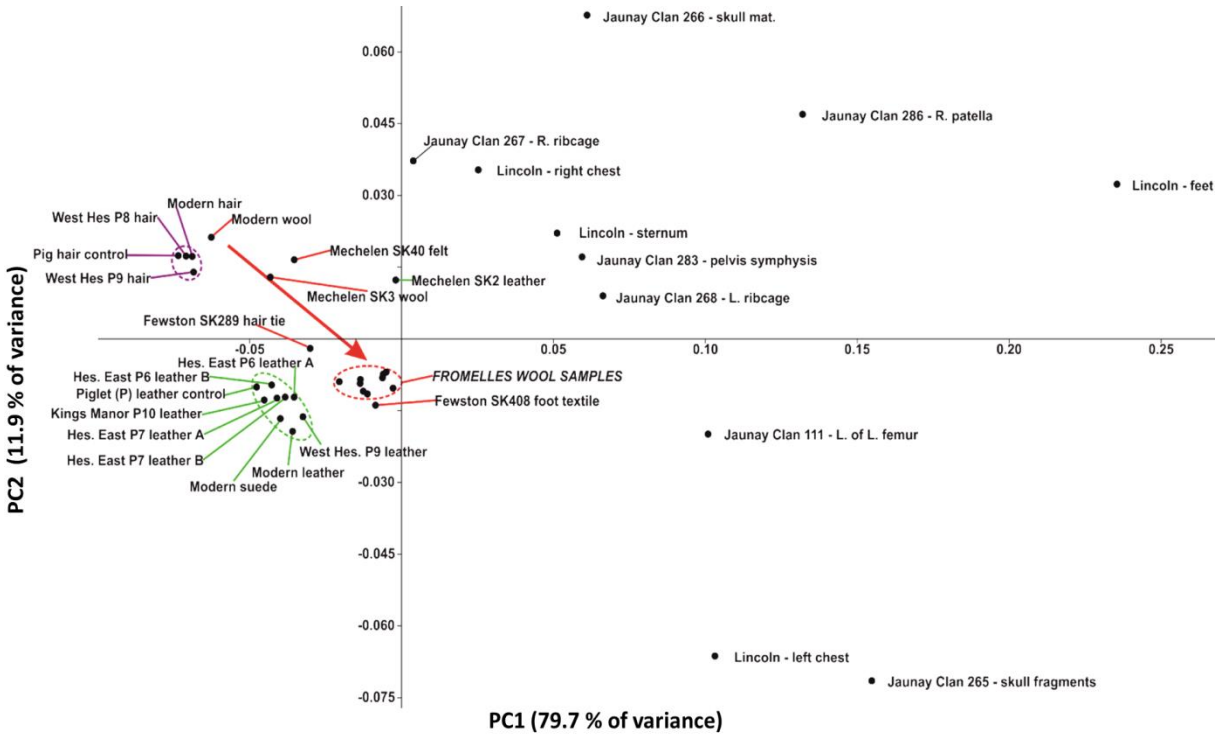

Figure 116. PCA scatter plot of PC1 and PC2 for textile and leather D/L values, accounting for 91.6% of total variance. The data points and cluster highlighted in red are the wool, those in green are leathers and those in purple are human hair.

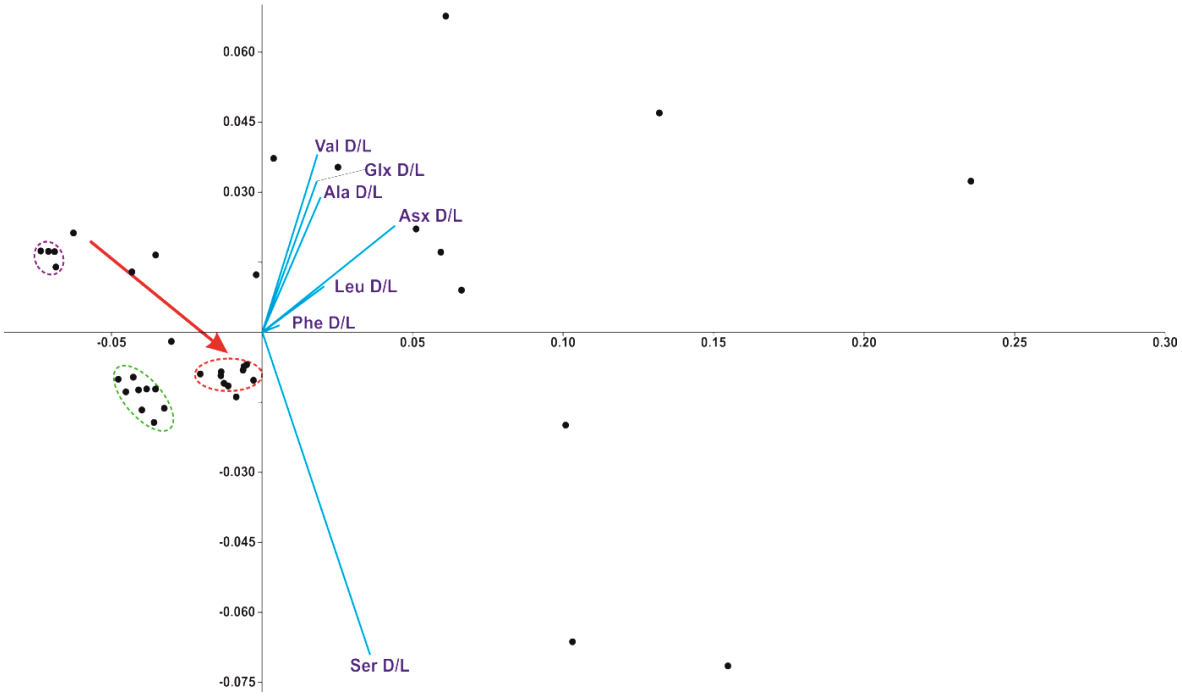

Figure 117. PCA loadings plot of amino acid D/L values, showing the major contributions of each amino acid to PC1 and PC2. The data points and cluster highlighted in red are the wool, those in green are leathers and those in purple are human hair.

All of the modern and experimentally buried leather data points group together, highlighted in green. The close grouping of the unburied and experimentally buried materials is likely due to their relatively brief burial duration leading to limited racemisation. The only archaeological sample that can be confidently identified as leather, from SK3 at Mechelen, is away from this grouping (near the positive y axis). Due to this being the only leather point away from the main cluster, no conclusions can be drawn about decomposition trajectories based on this data.

The remaining data points are scattered at positive x values, both above and below the x axis. As all of the undegraded materials have negative x values, all materials with positive x values are more racemised (see the loading plot in Figure 117). Other than this, no further conclusions can be drawn about these data points.

6.8 Conclusions

6.8.1 Decomposition of textile and leather in archaeological burials

Table 26 provides a summary of the findings from the analyses of the archaeological clothing materials. With the exception of the material from Fromelles, there is a trend of increasing degradation with longer burial time. This is to be expected, as the more time a material is exposed to the conditions within the burial environment the more likely they are to be subject to chemical and microbial modifying agents.

Table 26. A summary of the findings from the analyses performed on the entire set or archaeological textiles collected.

Site	Coffin	Burial matrix	Burial date	Material type	Preservation state
Fromelles	No	Clay, waterlogged, anoxic, pH 4.7	July 1916	12 samples of woven or felted wool	Extensive degradation of wool fibre cortex, leaving hollow tubes of cuticular scales
Fewston	Yes	Well drained course loamy soil	Late 1800	2 samples of woven wool	Good preservation, with some measurable degradation
Mechelen	No	Sandy	October 1798	1 woven and 1 felted wool, 1 leather and 1 linen	Excellent preservation of woven wool and leather, some fungal attack on felt and complete mineralisation of linen
Lincoln	Yes	Not known	Early 1000 AD	1 leather, 3 possibly wool	Extreme degradation
Jaunay-Clan	Yes	Not known	70 – 390 AD	Too degraded for identification, 265 possibly keratin based	Extreme degradation

The use of principal component analysis in Chapter 6.7 allowed for the comparison of all experimentally buried and archaeological textile and leather data. Using the amino acid composition and D/L value data sets it was possible to rank the degradation of samples based on their distance from the data points for the unburied, modern materials. It was noted that, unsurprisingly, the archaeological materials are more degraded than those from the relatively short term burial experiments. Both the wool amino acid composition and D/L PCA indicated that the wool from Mechelen was the least degraded, the wool from Fewston was more degraded and the wool from Fromelles was the most degraded.

The woollen textiles recovered from Fromelles are the youngest materials that have spent least time in the burial matrix, yet they are extensively degraded. Conversely, older materials – such as those from Fewston – are in a much better state of preservation. The clay rich makeup of the burial matrix of the Fromelles mass graves likely led to a retention of liquid, both from the burial

environment and from the decaying remains. The moisture levels combined with nutrients released from the mass of decomposing bodies may have allowed many strains of bacteria and fungi to proliferate, leading to an initial period of decay of the clothing materials before sufficient water entered the grave to cause waterlogged, anoxic conditions that prevented further degeneration.

The fast draining soil at Fewston combined with the fact that both sets of remains were in wooden coffins are likely the cause of the excellent preservation of the organic materials recovered from the burials. The bases of the wooden coffins were probably not watertight, allowing the fluids evolved from the decomposition of the remains to escape by gravity. The lids of the coffins would have diverted any surface water percolating down through the sediment, preventing the vast majority of the downflowing water from entering the coffin. The result of these processes would have created a relatively dry environment within the coffins, which would have retarded the growth of any microfauna capable of degrading the textiles.

The preservation of the leather at Mechelen is likely due to the sandy soil that was well drained and acidic (Day and Ludeke, 1993; Depuydt *et al*., 2013). Such conditions are known to restrict the growth of microorganisms, leading to excellent preservation. There is a disparity between the preservation states of the woven and felted wools recovered from the site. The excellent condition of the woven materials is likely due to its proximity to a copper button, a metal that is known to be toxic to potential microbial degraders (Chen *et al.,* 1998). There is evident degradation of the felt by fungi, but the extent is limited. The felt has numerous deposits of fungal spores. Many types of fungus only engage in sporulation when the environment is hostile and the survival of the organism is unlikely, which suggests that the conditions within the burial matrix limited the fungal activity (Sheaffer and Moncada, 2012). The felting process of wools leads to abrasion of the cuticular scales, which undoubtedly produced exposed areas of protein that were more vulnerable to fungal attack.

Lincoln and Jaunay-Clan are the two oldest burials and represent an extreme period of interment. The amino acid compositions of the materials recovered from these sites are vastly different from those of the modern controls, implying that they are heavily degraded. The deterioration of the materials suggests that none of the conditions required for the preservation of organic materials (anoxia, waterlogging or low humidity) could have been present in these burials, lest the materials would likely have survived in better condition. Such condition would only have been possible if the sarcophagi were airtight. It is, however, possible that the sealed bases of the sarcophagi concentrated the decompositional fluids of the bodies, aiding in the degradation of the clothing materials. Although all of the materials from these two sites were extremely degraded, the application of suitable analytical techniques has allowed information to be obtained from the

samples. The ability to differentiate between different types of materials and, hence, different articles of clothing and the detection of an inorganic sulfur residue allow for additional interpretation of the archaeology. The use of PCA has provided evidence that the sample recovered from the feet of the Lincoln Castle sarcophagus may be an extremely degraded animal hide material, and that sample 265 from under the skull of SK293 at Jaunay-Clan is different from sample 266, the former possibly being a heavily degraded keratin-based material.

6.8.2 Appraisal of methods of analysis

6.8.2.1 EA

EA is a useful tool that can be used to screen compounds to detect elemental compositions that may indicate an organic content. When archaeological materials are analysed alongside modern reference materials the technique can give some indication of the material being from a plant or an animal source. Given that the samples need only be weighed into the appropriate crucible and folded, sample preparation is rapid. The automated sampling and data acquisition systems that come with most elemental analysers lead to quick and easy data collection.

The method employed requires 2-3 mg of material for a reliable data set, which is more than for Py-GC (0.1-1 mg) and RP-HPLC analysis (approximately 0.5 mg). With smaller samples this can limit the number of analyses or render it not possible (as was the case for the material recovered from the sarcophagus at Lincoln Castle). Given the limited value of the elemental composition data compared against the more informative polymer subunit quantitation that can be elucidated using Py-GC and RP-HPLC, EA is less informative and should only be used as a preliminary to further analysis.

6.8.2.2 Py-GC(MS)

Py-GC is an excellent tool for analysing plant based textiles to assess holocellulose and lignin content and composition. Using a sample as small as 0.1 mg a material can be identified and its preservation state assessed by comparison of the peak profiles and the relative peak areas with those of modern materials. When used to analysed protein based materials, thermal degradation reactions occur, with some amino acids producing the same degradation product, resulting in a loss of information that would be retained by the use of other techniques. The analysis and data interpretation times for Py-GC are another drawback. Each sample takes 2 hours to run and pyrolysers typically do not have an automated sample carousel. Depending on the material being analysed the resulting pyrogram can be complex, with each peak having to be identified in turn. The use of MS to identify the compounds eluting from the GC vastly improves the accuracy and reliability of the peak assignments. Whether as the primary means of detection, or as a complementary technique whereby selected samples are used to aid the interpretation of those analysed without MS, attempting to interpret data without definite identification of peaks is extremely difficult.

6.8.2.3 RP-HPLC

RP-HPLC analysis of hydrolysed protein based materials is far superior to any of the other methods used in this investigation. Accurate quantitation of D and L forms of a wide range of amino acids allows for reliable identification and preservation state assessment with all but the

most heavily degraded materials. Correct interpretation of the data has been shown to reveal structural damage to woollen materials (samples from Fromelles and felt from Mechelen) that was confirmed by SEM analysis. The sample preparation steps are longer than for EA and Py-GC, but less than for whole peptide analysis techniques, and the quality and usefulness of the data outweigh the time costs.

6.8.2.4 SEM

SEM imaging provides a useful overview of the preservation state of materials. Features such as fungal bodies and spores, areas of damage and foreign bodies can be key to supporting interpretations and theories reasoned using data from chemical analyses. The preparation techniques can be destructive to fragile materials, making the technique unsuitable for samples that are mechanically weak or heavily degraded.

6.8.2.5 PCA

The application of PCA to the combined experimental burial and archaeological dataset has provided further evidence in support of many of the hypotheses and conclusions reasoned on the basis of the amino acid and SEM evidence. By resolving the complex, multivariate data into key variables that account for the majority of the variability between samples, PCA has allowed for the comparison of samples between sites, and allow for degradation tends to be examined.

CHAPTER 7

CONCLUSIONS AND FUTURE WORK

7.1 Overall conclusions

The aim of this thesis was to investigate the state of preservation of a range of organic materials excavated from archaeological graves during the InterArChive project, in order to gain a better insight into what information this currently under exploited archive may hold.

7.1.1 Appraisal of analytical techniques

The application of a range of analytical techniques has been shown to allow information on the identity, preservation state and likely causes of decay to be gained from fragments of wood, textiles and leather buried with human remains. Py-GC techniques provide detailed information on the biopolymer composition of wood and plant based textiles; the attrition of cellulose and hemicellulose, and modification of the lignin are all evident, with significant changes in composition compared with modern undegraded materials. The use of thermal desorption (TD) prior to pyrolysis eliminates lengthy sample pretreatment and reduces the levels of volatile compounds, which would otherwise obscure the peaks arising from the pyrolysis of the component biopolymers. Accelerated solvent extraction (ASE) techniques have also shown to be useful in removing a range of organic compounds from wood. Although incorporation of the extraction step is more time consuming and requires the requisite equipment, the approach allows for the removal of treatments that have penetrated deep into wood, including PEG in conserved wood from the Hanson Logboat (Chapter 5). Small differences in the amino acid composition and racemisation of protein based materials from archaeological burials are detectable by use of RP-HPLC. This has been shown to be useful in identifying degradation of specific substructures, enabling suggestions as to the causal agents to be made. SEM imaging has been valuable in testing and supporting the conclusions based on the chemical data, providing direct visual evidence of known microbial degraders and characteristic degradation patterns. The use of principal component analysis to compare the preservation state of materials between sites aided with the elucidation of trends and the postulation of degradation trajectories.

7.1.2 Degradation of organic materials in archaeological graves

The recovery of wood, textile and leather from archaeological burials indicates that these materials can survive over extended periods of time, if the conditions within those burial environments or in microenvironments in the soils are conducive to slowing their degradation by microorganisms. However, the modifications to these materials during even the relatively short burial experiments indicates that materials placed in human burials begin to decay (at different rates depending on their composition) within the first few years of interment.

The observed modification of lignocellulose (in wood and plant derived textiles) and proteins (in animal derived textiles and animal skin products) is indicative that chemical or biological

degradation processes were at one time active within the archaeological burials. These modifications, in even the most visibly well preserved materials, may be evidence that the conditions needed for inhibition of microbial decay are not immediately present; instead the burial environment changes due to the decomposition of the cadaver or as a result of geological or hydrological processes, eventually supporting the long term survival of the materials.

Proximity to metal objects was observed to alter the decomposition of coffin wood. Analysis of the wood polymers revealed areas of more and less severe damage inflicted by white rot fungus in comparison to wood from the same coffin that was not in proximity to the metal. This observation lends support to reports in the literature and shows that unique microenvironments can result in enhanced preservation of materials.

Throughout the InterArChive project, it was noted that wood and textiles were more commonly recovered from the archaeological sites with soils that had good drainage. Thus, these environments are likely to have had conditions which are not favourable to microbial degraders, the key antimicrobial factors likely being low moisture levels and acidic pHs. Permanently waterlogged conditions also resulted in excellent preservation of wood, for example that sampled from the Hanson Logboat, whereas temporary or periodic waterlogging resulted in degradation, evident in coffin wood from Thaon and the piglet burial in the Folkton bog. The degradation of the piglet coffin wood buried in a bog with seasonal fluctuations in the water level after only three years of burial provides clear evidence that this type of hydrological regime is more conducive to organic degradation than a stagnant or dry environment.

Analysis of wood both from the short term experimental graves and from archaeological burials provides evidence of multiple microorganisms degrading wood in the same burial. This highlights the diverse array of microfauna that are active in burial environments. In comparison with protein based materials, it is far easier to establish potential causes of wood decay, as there are far fewer, specialised microfauna that are able to degraded lignocellulose materials. Brown and white rot fungi were found to be the chief degraders of wood. These fungi require oxygen to thrive and degrade wood, which suggests that the burial environments in which they proliferated were not anoxic for the entirety of the burial period. The damage observed to fragments of wool (in the archaeological burials) and human hair (in the experimental burials) was likely caused by both bacterial and fungal degraders. The ubiquitous nature of protein in all living organisms make them far less recalcitrant than lignocellulose materials. As proteins are degraded by a much wider array of microorganisms than lignin, and mean that they can be more readily degraded by a much wider range of soil biota. The use of PCA to resolve large, multivariate data sets into the components responsible for the majority of the variation observed within the wood and amino acid textile data sets allowed for samples to be ranked in terms of most degraded to least degraded. PCA also

allowed degradation trends to be visualised, and in some cases allowed for degradation trajectories of some materials to be hypothesised.

7.1.3 Identification of materials using chemical techniques

The application of an array of analytical techniques has demonstrated the ability to identify different polymeric materials using chemical techniques. Py-GC has allowed the differentiation between gymnosperm and angiosperm woods, wood from gymnosperm trees being the most common wood identified from the archaeological burials. This is highly suggestive that softwoods were the most commonly used wood for the construction of coffins in Northwest Europe, probably due to the relative abundance of gymnosperm trees in the geographic regions studied (at the time of the burials), and the ease with which softwoods can be worked. This ability to distinguish between types of wood has the potential to significantly aid archaeological interpretation. An example is provided by the grave analysed from Hofstaðir, where the presence of a pine coffin may indicate a high profile burial.

The ability to distinguish between types of animal protein using RP-HPLC has also been demonstrated. Even in the most degraded burial, that from Jaunay-Clan, chemical analysis was able to identify that two different types of materials were present, lending further evidence to the interpretation of the archaeologists that a pillow may have been laid under the deceased's head. Use of PCA provided further evidence that this sample may be from a severely degraded keratin based material. PCA also suggested that the sample from the feet of the Lincoln Castle sarcophagus may be an extremely degraded leather or similar animal hide material.

7.1.4 Contribution to the archaeological record

The identification of lignin in soil stains believed to be due to the presence of heavily decayed wood (Chapter 5) has not been previously reported in the literature. The result confirms the presence of a coffin and demonstrates that even heavily degraded wood can provide recognisable signatures. From an archaeological perspective, the ability to detect the previous presence of wood is significant. Often, when wood has fully degraded the location of features such as post holes relies solely on the interpretation of the excavator. Confirming the former presence of wood has the potential to greatly enrich the interpretation in both archaeological and forensic settings.

The removal of PEG from the Hanson Logboat wood and the subsequent chemical assessment has far reaching consequences, as wooden objects have been preserved using PEG worldwide for decades. The treatment is now widely acknowledged to be problematic in terms of carrying out certain chemical analysis (e.g. analytical pyrolysis and radiocarbon dating), as well as contributing to the acidification of wood via the formation of sulfuric acid. The application of the PEG removal

technique to other artefacts in museums and private collections has the potential to reveal a wealth of information that was previously considered to be inaccessible.

Finally, the analysis of the 'red sock' from Fromelles illustrates how the application of analytical techniques and an understanding of degradative processes may prevent the incorrect interpretation of the archaeological record. Whilst the chemical analysis suggesting that the colour of the sock is the result of bacterial decay, and not due to it being a non regulation clothing item sent by the soldier's family is less glamorous, the analysis has likely provided a more accurate reflection of reality.

7.1.5 Summary

It has been shown during this investigation that the fragments of wood, textile and leather that do survive in human burials contain valuable information that has yet to be accessed. The use of a combination of analytical techniques has demonstrated that these small fragments can yield information regarding the provenance of the materials, degradation trajectories, and the nature of the burial environment. This information has the potential to contribute significantly to the archaeological interpretation of a site, as well as have broader applications, such as aiding with forensic and conservation questions.

By demonstrating this ability, it is hoped that this study will lead to the wider chemical analysis of such materials in future, leading to an increased knowledge base and the further development of methodologies to study a set of materials that are rarely exploited to their full potential.

7.2 Future work

Given the information that was obtained from the burial experiments in spite of the problems encountered, more burial experiments, with the specific aim of studying the decomposition of materials buried with human remains, should be carried out. Coffins with panels of different untreated angiosperm and gymnosperm woods would enable the degradation of wood from different species of tree to be studied in the same burial experiment. The burial of leather from different animals which has been tanned using methods common during antiquity, as well as woven and felted wool, silk, cotton, hemp, and linen would allow for the study of a wider range of materials. The textile and leather materials should be buried both in coffins and without coffins to examine the differences in degradation between these two distinctly different burial styles. A wider range of soil types, hydrologies and burial durations would also increase the understanding of the diagenesis of these materials during the years immediately following their burial. Lack of SEM analysis of material from the burial experiments was unfortunate, and a result of time and financial constraints. Based on the usefulness of the data obtained by SEM of archaeological materials (Chapter 5 and 6), SEM of material from future experimental burials would be immensely worthwhile and should be factored into the planning.

The analysis of archaeological wood, textile and leathers from a wider range of archaeological burial environments would enable a wider understanding of degradation of these materials, and to enable the trends and hypothesises degradation trajectories to be fully explored. The geographical area from which the samples are taken could also be extended beyond Northwestern Europe, allowing a wider range of climates and burial environments to be studied. In addition, this may provide the opportunity to examine materials that are less common within Europe, or more typically used in funerary practises further afield. Reaching out to the archaeological, conservation and forensic communities could provide a vast set of materials to be analysed.

The study of wood from the Hanson Logboat represents a novel approach to the analysis of materials that have undergone conservation treatments. The application of the developed solvent extraction technique and subsequent Py-GC analysis should be expanded to other artefacts that have been treated in a similar manner, and possibly developed so that it is applicable to larger objects. A manuscript describing this work has been submitted to allow for its communication to the relevant communities. The identification of the inorganic minerals present in the degraded Hanson Logboat samples would aid in the elucidation of the decay mechanisms, contributing to a solution to the common problem of acidic degradation observed in wooden artefacts that have been treated with PEG.

The analysis of Py-GC data could be simplified by using a GC system fitted with both MS and FID detection. The column eluent could be split between both detectors, providing the desired quantitative FID data with simultaneous collection of MS data for compound identification. The data from both detectors would have the same retention times and eliminate the inherent variability of using two different Py-GC systems.

The use of proteomic techniques to examine the peptide cleavage sites of degraded hair, leather and wool could provide more clues as to the enzymes and even the specific microbe that is responsible for degrading a material. Identification of the microbes found in areas of decay using microscopic methods or genome sequencing could also be carried out, although these analyses would have to be carefully planned and executed, in order to account for microorganisms present near areas of degradation that were responsible for causing the damage.

REFERENCES

Abbott, A. (2001). Earliest malaria DNA found in Roman baby graveyard. *Nature*, 412(6850), 847.

Adelson, D. L., Cam, G. R., DeSilva, U., & Franklin, I. R. (2004). Gene expression in sheep skin and wool (hair). *Genomics*, 83(1), 95-105.

Ajuong, E. M., & Redington, M. (2004). Fourier transform infrared analyses of bog and modern oak wood (Quercus petraea) extractives. *Wood Science and Technology*, 38(3), 181-190.

Allington-Jones, L. (2015). The Clacton spear: The last one hundred years. *Archaeological Journal*, 172(2), 273-296.

Almkvist G. (2008). *The Chemistry of the Vasa – Irons, acids and degradation*. PhD Thesis, Swedish University of Agricultural Sciences, Uppsala

Alves, A., Schwanninger, M., Pereira, H., & Rodrigues, J. (2006). Analytical pyrolysis as a direct method to determine the lignin content in wood: Part 1: Comparison of pyrolysis lignin with Klason lignin. *Journal of Analytical and Applied Pyrolysis*, 76(1), 209-213.

Ander, P., & Eriksson, K. E. (1977). Selective degradation of wood components by white-rot fungi. *Physiologia Plantarum*, 41(4), 239-248.

Andrews, G., Barrett, J. C., & Lewis, J. S. (2000). Interpretation not record: the practice of archaeology. *Antiquity*, 74(285), 525-530.

Araujo, R., Casal, M., & Cavaco-Paulo, A. (2008a). Application of enzymes for textile fibres processing. Biocatalysis and Biotransformation, 26(5), 332-349.

Araújo, R., Cavaco-Paulo, A., & Casal, M. (2008b). Strategies towards the functionalization of Subtilisin E from *Bacillus subtilis* for wool finishing applications. *Engineering in Life Sciences*, 8(3), 238-249.

Arias, M. E., Polvillo, O., Rodríguez, J., Hernández, M., González-Pérez, J. A., & González-Vila, F. J. (2006). Thermal transformations of pine wood components under pyrolysis/gas chromatography/mass spectrometry conditions. *Journal of Analytical and Applied Pyrolysis*, 77(1), 63-67.

Arnalds, O. (2004). Volcanic soils of Iceland. *Catena*, 56(1), 3-20.

Arneborg, J., Heinemeier, J., Lynnerup, N., Nielsen, H. L., Rud, N., & Sveinbjörnsdóttir, Á. E. (1999). Change of diet of the Greenland Vikings determined from stable carbon isotope and 14C dating of their bones. *Radiocarbon*, 41(2), 157-168.

Asunmaa, S., & Lange, P. W. (1954). *The distribution of "cellulose" and "hemicellulose" in the cell wall of spruce, birch and cotton.* Svenska träforskningsinstitutet, träkemi och pappersteknik.

Australian Wool Exchange. (2010). *Preparation of Australian Wool Clips, Code of Practice 2010–2012.*

Backa, S., Brolin, A., & Nilsson, T. (2001). Characterisation of fungal degraded birch wood by FTIR and Py-GC. *Holzforschung*, *55*(3), 225-232.

Bäckström, Y., & Sundström, A.I. (2014) Sala gruvkyrkogård: Innanför och utanför vid Sala silvergruva. Etapp 3. (Sala mining cemetery: Inside and outside the Sala silver mine. 3rd Stage). *Societas Archaeologica Upsaliensi.*

Bada, J. L., Schroeder, R. A., Protsch, R., & Berger, R. (1974). Concordance of collagen-based radiocarbon and aspartic-acid racemization ages. *Proceedings of the National Academy of Sciences*, *71*(3), 914-917.

Bada, J. L. (1985a). Amino acid racemization dating of fossil bones. *Annual Review of Earth and Planetary Sciences*, 13, 241.

Bada, J. L. (1985b). *Racemization of amino acids. In Chemistry and biochemistry of the amino acids* (pp. 399-414). Springer Netherlands.

Barber, E. J. W. (1991). *Prehistoric textiles: the development of cloth in the Neolithic and Bronze Ages with special reference to the Aegean*. Princeton University Press, New Jersey, USA

Bardet, M., Gerbaud, G., Trân, Q. K., & Hediger, S. (2007). Study of interactions between polyethylene glycol and archaeological wood components by 13 C high-resolution solid-state CP-MAS NMR. *Journal of Archaeological Scie*nce, 34(10), 1670-1676.

Barham, L. (2013). *From hand to handle: the first industrial revolution*. Oxford University Press, Oxford, UK.

Barker, R. F., & Hopkinson, D. A. (1977). The genetic and biochemical properties of the D-amino acid oxidases in human tissues. *Annals of human genetics*, 41(1), 27-42.

Barton, P. (2007). *Fromelles: A Report Based Upon Research in the Hauptstaatsarchiv Kriegsarchiv, Munich*. Carried out on behalf of the Australian Army History Unit, unpublished typescript.

Bauer, W. D., Talmadge, K. W., Keegstra, K., & Albersheim, P. (1973) The Structure of Plant Cell Walls. *Plant Physiology*, 61, 174-187.

Bell, E. L. (1990). The historical archaeology of mortuary behavior: coffin hardware from Uxbridge, Massachusetts. *Historical Archaeology*, 54-78.

Bergfjord, C., & Holst, B. (2010). A procedure for identifying textile bast fibres using microscopy: Flax, nettle/ramie, hemp and jute. *Ultramicroscopy*, 110(9), 1192-1197.

Beukens, R. P., Pavlish, L. A., Hancock, R. V., Farquhar, R. M., & Wilson, G. C. (1992). Radiocarbon dating of copper-preserved organics. *Radiocarbon,* 34(3), 890-897.

Bienkiewicz, K. J. (1983). Physical chemistry of leather making. Krieger Publishing Co. Inc..

Björdal, C. G., Nilsson, T., & Daniel, G. (1999). Microbial decay of waterlogged archaeological wood found in Sweden applicable to archaeology and conservation. *International Biodeterioration & Biodegradation*, 43(1), 63-73.

Blanchette, R. A., Nilsson, T., Daniel, G., and Abad, A. (1990). Biological degradation of wood. In *Archaeological Wood Properties, Chemistry, and Preservation. Developed from a symposium sponsored by the Cellulose Paper and Textile Division at the 196th National Meeting of the American Chemical Society, Los Angeles, California, September 25-September 30, 1988* (pp. 141-174). American Chemical Society.

Blanchette, R. A. (1991). Delignification by wood-decay fungi. *Annual Review of Phytopathology*. 29:381–98.

Blanchette, R. A., & Simpson, E. (1992). Soft rot and wood pseudomorphs in an ancient coffin (700 BC) from Tumulus MM at Gordion, Turkey. *IAWA Journal*, 13(2), 201-213.

Blanchette, R. A., & Hoffmann, P. (1994). Degradation processes in waterlogged archaeological wood. In *Proceedings of the fifth ICOM Group on Wet Organic Archaeological Materials conference, Portland, Maine, 16-20 August 1993*, 111-142. ICOM Committee for Conservation Working Group on Wet Organic Archaeological Materials; Ditzen Druck und Verlags-GmbH.

Blanchette, R. A., Obst, J. R., & Timell, T. E. (1994). Biodegradation of compression wood and tension wood by white and brown rot fungi. *Holzforschung – International Journal of the Biology, Chemistry, Physics and Technology of Wood*, 48(s1), 34-42.

Blanchette, R. A. (1995). Degradation of the lignocellulose complex in wood. *Canadian Journal of Botany*, 73(S1), 999-1010.

Blanchette, R. A. (2000). A review of microbial deterioration found in archaeological wood from different environments. *International Biodeterioration & Biodegradation*, 46(3), 189-204.

Blanchette, R. A., Held, B. W., Jurgens, J. A., McNew, D. L., Harrington, T. C., Duncan, S. M., & Farrell, R. L. (2004). Wood-destroying soft rot fungi in the historic expedition huts of Antarctica. *Applied and Environmental Microbiology*, 70(3), 1328-1335.

Blanchette, R. A., Haight, J. E., Koestler, R. J., Hatchfield, P. B., & Arnold, D. (2013). Assessment of deterioration in archaeological wood from ancient Egypt. *Journal of the American Institute for Conservation.* 33:1, 55-70.

Block, R. J. (1939). The composition of keratins the amino acid composition of hair, wool, horn, and other eukeratins. *Journal of Biological Chemistry*, 128(1), 181-186.

Block, S. S. (Ed.). (2001). *Disinfection, sterilization, and preservation*. Lippincott Williams & Wilkins.

Boer, W., Folman, L. B., Summerbell, R. C., & Boddy, L. (2005). Living in a fungal world: impact of fungi on soil bacterial niche development. *FEMS Microbiology Reviews*, 29(4), 795-811

Boerjan, W., Ralph, J., & Baucher, M. (2003). Lignin biosynthesis. *Annual Review of Plant Biology*, 54(1), 519-546.

Bonaduce, I., Ribechini, E., Modugno, F., & Colombini, M. P. (2016). Analytical Approaches Based on Gas Chromatography Mass Spectrometry (GC/MS) to Study Organic Materials in Artworks and Archaeological Objects. *Topics in Current Chemistry*, 374(1), 1-37.

Bonani, G., Ivy, S. D., Hajdas, I., Niklaus, T. R., & Suter, M. (1994). AMS 14C age determinations of tissue, bone and grass samples from the Otztal ice man. *Radiocarbon*, 36(2), 247-250.

Borysiak, S., & Doczekalska, B. (2005). X-ray diffraction study of pine wood treated with NaOH. *Fibres and Textiles in Eastern Europe*, 13(5), 87-89.

Bouslimi, B., Koubaa, A., & Bergeron, Y. (2014). Effects of biodegradation by brown-rot decay on selected wood properties in eastern white cedar (*Thuja occidentalis L.*). *International Biodeterioration & Biodegradation*, 87, 87-98.

Bowes, J. H., & Kenten, R. H. (1948). The amino-acid composition and titration curve of collagen. *Biochemical Journal*, 43(3), 358.

Bradbury, J. H., Chapman, G. V. & King, N. L. R. (1967) in *Symposium on Fibrous Proteins*, W. G. Crewther, Ed., Butterworths, Australia, p.368.

Bradbury, J. H. & Ley, K. F. (1972). The chemical composition of wool. XI. Separation and analysis of exocuticle and endocuticle. *Australian Journal of Biological Sciences,* 25 (6), 1235-1247

Bradbury, J. H. (1973). The structure and chemistry of keratin fibers. *Advances in Protein Chemistry*, 27, 111-211.

Bradley, M. (2002). 'It all comes out in the wash': Looking harder at the Roman fullonica. *Journal of Roman Archaeology*, *15*, 20-44.

Brandt, L. Ø., Schmidt, A. L., Mannering, U., Sarret, M., Kelstrup, C. D., Olsen, J. V., & Cappellini, E. (2014). Species identification of archaeological skin objects from Danish bogs: Comparison between mass spectrometry-based peptide sequencing and microscopy-based methods. *PLOS One*, 9(9), e106875.

Braovac, S., Tamburini, D., Łucejko, J. J., McQueen, C., Kutzke, H., & Colombini, M. P. (2016). Chemical analyses of extremely degraded wood using analytical pyrolysis and inductively coupled plasma atomic emission spectroscopy. *Microchemical Journal*, 124, 368-379.

British Archaeology online (March 2003). Tale of the Bronze Age barge sunk in Trent. *British Archaeology*, issue 39, News. (http://www.archaeologyuk.org/ba/ba69/news.shtml) – retrieved 08/04/2014

Brosse, N., El Hage, R., Chaouch, M., Pétrissans, M., Dumarçay, S., & Gérardin, P. (2010). Investigation of the chemical modifications of beech wood lignin during heat treatment. *Polymer Degradation and Stability*, 95(9), 1721-1726.

Brothwell, D. R. (1958). Evidence of leprosy in British archaeological material. *Medical history*, 2(04), 287-291.

Brothwell, D. R. (1981). *Digging up bones: the excavation, treatment, and study of human skeletal remains*. Cornell University Press.

Brothwell, D. R. (2016). *A faith in archaeological science: reflections on a life*. Archaeopress Publishing, Oxford, UK.

Brown, M. E., & Chang, M. C. (2014). Exploring bacterial lignin degradation. *Current Opinion in Chemical Biology*, 19, 1-7.

Brown, M. E., Walker, M. C., Nakashige, T. G., Iavarone, A. T., & Chang, M. C. (2011). Discovery and characterization of heme enzymes from unsequenced bacteria: application to microbial lignin degradation. *Journal of the American Chemical Society*, 133(45), 18006-18009.

Buckley, S. A., Stott, A. W., & Evershed, R. P. (1999). Studies of organic residues from ancient Egyptian mummies using high temperature-gas chromatography-mass spectrometry and sequential thermal desorption-gas chromatography-mass spectrometry and pyrolysis-gas chromatography-mass spectrometry. *Analyst,* 124(4), 443-452.

Bugg, T. D., Ahmad, M., Hardiman, E. M., & Singh, R. (2011a). The emerging role for bacteria in lignin degradation and bio-product formation. *Current Opinion in Biotechnology*, 22(3), 394-400.

Bugg, T. D., Ahmad, M., Hardiman, E. M., & Rahmanpour, R. (2011b). Pathways for degradation of lignin in bacteria and fungi. *Natural Product Reports*, 28(12), 1883-1896.

Buglass, J. (2010) The Church of St Michael And St Lawrence, Fewston, North Yorkshire. Final assessment report on the archaeological investigation. Unpublished report by John Buglass Archaeological Services, Northallerton.

Bull, I. D., Simpson, I. A., Van Bergen, P.F. and Evershed R.P. (1999) Muck-'n'-molecules: Organic geochemical methods for detecting ancient manuring. *Antiquity*, 73(279), pp.86–96.

Bunson, M. (2014). *Encyclopedia of the Roman Empire*. Infobase Publishing.

Burnham, H. B. (1965). Çatal Hüyük—The Textiles and Twined Fabrics. *Anatolian Studies*, 15, 169-174.

Burns, A. (2015). *Post-depositional alterations across varying sediment types from archaeological inhumation burials - a geoarchaeological approach*. PhD thesis, University of York.

Caffel, A., & Holst, M. (2010) Osteological analysis: The Church of St Michael and St Lawrence, Fewston, North Yorkshire. Unpublished report by York Osteoarchaeology Ltd, York.

Calvo-Flores, F. G., & Dobado, J. A. (2010). Lignin as renewable raw material. *ChemSusChem,* 3(11), 1227-1235.

Campbell, A. G., Kim, W. J., & Koch, P. (2007). Chemical variation in lodgepole pine with sapwood/heartwood, stem height, and variety. *Wood and Fiber Science*, 22(1), 22-30.

Cardamone, J. M., K. M. Keister, & A. H. Osareh. (1991). Degradation and conservation of cellulosics and esters. In: *Polymers in Conservation,* eds. Allen, N. S., Edge, M., and Horie, C. V., pp. 108–124. Royal Society of Chemistry, London.

Cartwright, C. R. (2015). The principles, procedures and pitfalls in identifying archaeological and historical wood samples. *Annals of Botany*, mcv056.

Cevasco, R., & Moreno, D. (2015). Historical Ecology in Modern Conservation in Italy. In: *Europe's Changing Woods and Forests: From Wildwood to Managed Landscapes*, eds. Kirby, K. & Watkins, C., pp. 227. CABI.

Chakraborty, J. N., & Madān, P. P. S. (2014). Imparting anti-shrink functionality to wool by individual and simultaneous application of keratinase and papain. *Indian Journal of Fibre & Textile Research* (IJFTR), 39(4), 411-417.

Chapman, G. V., & Bradbury, J. H. (1968). The chemical composition of wool 7. Separation and analysis of orthocortex and paracortex. *Archives of Biochemistry and Biophysics*, 127, 157-163.

Chappell, M. (2000). British Infantry Equipments (2) 1908-2000 (Vol. 108). Osprey Publishing.

Chaumat, G. (2016) Use of sebacate salts to cure or prevent acidification of waterlogged wood artefacts contaminated by iron-sulphur compounds. Conference paper presented *at WOAM 2016: 13th ICOM-CC Wet Organic Archaeological Materials Conference, 16-20 May 2016, Florence, Italy.*

Chen, H. L., Jakes, K. A., & Foreman, D. W. (1998). Preservation of archaeological textiles through fibre mineralization. *Journal of Archaeological Science*, 25(10), 1015-1021.

Chesworth, W. (2008). Biomes and their soils. In *Encyclopedia of soil science* (pp. 61-68). Springer Netherlands.

Church, J. S., Corino, G. L., & Woodhead, A. L. (1997). The analysis of merino wool cuticle and cortical cells by Fourier transform Raman spectroscopy. *Biopolymers*, 42(1), 7-17.

Collins, M. J., Nielsen–Marsh, C. M., Hiller, J., Smith, C. I., Roberts, J. P., Prigodich, R. V., ... & Turner–Walker, G. (2002). The survival of organic matter in bone: a review. *Archaeometry*, 44(3), 383-394.

Colombini, M. P., Giachi, G., Modugno, F., Pallecchi, P., & Ribechini, E. (2003). The characterization of paints and waterproofing materials from the shipwrecks found at the archaeological site of the Etruscan and Roman harbour of Pisa (Italy). *Archaeometry*, 45(4), 659-674.

Cook, B. (1988). Fibre damage in archaeological textiles. In *Archaeological Textiles,* eds, O'Connor, S.A. & Brooks, M.M., *pp. 5–15. UKIC Occasional Papers No. 10*, United Kingdom Institute for Conservation, London.

Corfield, M. C., & Robson, A. (1955). The amino acid composition of wool. *Biochemical Journal*, 59(1), 62.

Courty, M. A. (1992). Soil micromorphology in archaeology. *Proceeding of the British Academy* (Vol. 77, pp. 39-59).

Covington, A. D. (1997). Modern tanning chemistry. *Chemical Society Reviews*, 26(2), 111-126.

Covington, A. D., & Covington, T. (2009). *Tanning chemistry: the science of leather*. RSC Publishing, Cambridge, UK.

Crawshaw, A., Panter, I., & Richardson, C. (2013). The Shardlow Boat – a conservation case study. In: *Proceedings of the 12th ICOM-CC Group on Wet Organic Archaeological Materials Conference, Istanbul, 13th – 17th May 2013,* 252-257. ICOM Committee for Conservation Working Group on Wet Organic Archaeological Materials; Eds. Grant, T., & Cook, C.

Crestini, C., El Hadidi, N. M., & Palleschi, G. (2009). Characterisation of archaeological wood: A case study on the deterioration of a coffin. *Microchemical Journal*, 92(2), 150-154.

Crighton, J.S. (1977). Characterisation of textile materials by thermal degradation: a critique of pyrolysis GC and thermogravimetry. In: *Analytical pyrolysis: proceedings of the Third International Symposium on Analytical Pyrolysis held in Amsterdam, September 7-9, 1976* (p. 337). Elsevier Science & Technology.

Crockford, D. J., Holmes, E., Lindon, J. C., Plumb, R. S., Zirah, S., Bruce, S. J., ... & Nicholson, J. K. (2006). Statistical heterospectroscopy, an approach to the integrated analysis of NMR and UPLC-MS data sets: application in metabonomic toxicology studies. *Analytical Chemistry*, 78(2), 363-371.

Cutter, W. (1992). *The Jewish Mourner's Handbook*. Behrman House, Inc.

D'arcy, J. B. (1990). Sheep management and wool technology. *UNSW Press*.

Darragh, A. J., & Moughan, P. J. (2005). The effect of hydrolysis time on amino acid analysis. *Journal of AOAC International*, *88*(3), 888-893.

Day, A. D., & Ludeke, K. L. (1993). Soil acidity. *Plant Nutrients in Desert Environments*. Springer Berlin Heidelberg, 31 – 33.

de Goyet, C. D. V. (2004). Epidemics caused by dead bodies: a disaster myth that does not want to die. *Pan American Journal of Public Health*, 15, 297-299.

de Morais Teixeira, E., Corrêa, A. C., Manzoli, A., de Lima Leite, F., de Oliveira, C. R., & Mattoso, L. H. C. (2010). Cellulose nanofibers from white and naturally colored cotton fibers. *Cellulose*, 17(3), 595-606.

DeGaetano, D. H., Kempton, J. B., & Rowe, W. F. (1992). Fungal tunnelling of hair from a buried body. *Journal of Forensic Science*, 37(4), 1048-1054.

del Rıo, J. C., Gutiérrez, A., Martınez, M. J., & Martınez, A. T. (2001). Py–GC/MS study of Eucalyptus globulus wood treated with different fungi. *Journal of Analytical and Applied Pyrolysis*, 58, 441-452.

Del Rıo, J. C., Speranza, M., Gutiérrez, A., Martínez, M. J., & Martínez, A. T. (2002). Lignin attack during eucalypt wood decay by selected basidiomycetes: a Py-GC/MS study. *Journal of Analytical and Applied Pyrolysis*, 64(2), 421-431.

Demarchi, B., Williams, M. G., Milner, N., Russell, N., Bailey, G., & Penkman, K. (2011). Amino acid racemization dating of marine shells: a mound of possibilities. *Quaternary International*, 239(1), 114-124.

Demarchi, B., Collins, M., Bergström, E., Dowle, A., Penkman, K., Thomas-Oates, J., & Wilson, J. (2013). New experimental evidence for in-chain amino acid racemization of serine in a model peptide. *Analytical chemistry*, 85(12), 5835-5842.

Dempsey, M. (1974). Scanning electron microscope studies of the grain surface of leather. *Journal of Materials Science*, 9(4), 651-657.

Depuydt, S., Kinnaer, F., & Van de Vijver, K. (2013). In the Shadow of the Tower: Results of the archaeological investigation of Saint Rumbold's Churchyard in Mechelen, Belgium. *City of Mechelen Archaeology Service, Legal Deposit D/2013/0797/036.*

Dickson, J. H., Oeggl, K., & Handley, L. L. (2003). The iceman reconsidered. *Scientific American,* 288(5), 70-79.

DiCosimo, R., & Szabo, H. C. (1988). Oxidation of lignin model compounds using single-electron-transfer catalysts. *The Journal of Organic Chemistry*, 53(8), 1673-1679.

Dittmer, J. K., Patel, N. J., Dhawale, S. W., & Dhawale, S. S. (1997). Production of multiple laccase isoforms by Phanerochaete chrysosporium grown under nutrient sufficiency. *FEMS microbiology letters*, 149(1), 65-70.

Doyle, P. (2014). Geology and the War on the Western Front, 1914–1918. *Geology Today*, 30(5), 183-191.

Doyle, P., Barton, P., Rosenbaum, M., Vandewalle, J., & Jacobs, K. (2002). Geo-environmental implications of military mining in Flanders, Belgium, 1914–1918. *Environmental Geology*, 43(1-2), 57-71.

Drewett, P. (2011). *Field archaeology: an introduction*. Routledge, Oxon, UK.

Duchaufour, R. (2012). *Pedology: pedogenesis and classification*. Springer Science & Business Media.

Dusenbury, M. (1992). A wisteria grain bag and other tree bast fiber textiles of Japan. In: *Textiles in Daily Life: Proceedings of the Third Biennial Symposium of the Textile Society of America, September 24–26, 1992.* Textile Society of America.

Eastoe, J. E. (1955). The amino acid composition of mammalian collagen and gelatin. *Biochemical Journal*, 61(4), 589.

Eglin, T., Maunoury-Danger, F., Fresneau, C., Lelarge, C., Pollet, B., Lapierre, C., Francois, C., & Damesin, C. (2008). Biochemical composition is not the main factor influencing variability in carbon isotope composition of tree rings. *Tree Physiology*, 28(11), 1619-1628.

El Hadidi, N. M. (2016). Decay of softwood in archaeological wooden artifacts. *Studies in Conservation,* 1-13.

El-Gaoudy, H., Kourkoumelis, N., Varella, E., & Kovala-Demertzi, D. (2011). The effect of thermal aging and color pigments on the Egyptian linen properties evaluated by physicochemical methods. *Applied Physics A*, 105(2), 497-507.

Eriksson, K. E. L., Blanchette, R. A., & Ander, P. (1990). *Microbial and enzymatic degradation of wood and wood components*, 225-333. Springer Berlin Heidelberg.

Evershed, R. P. (2008). Organic residue analysis in archaeology: the archaeological biomarker revolution. *Archaeometry*, 50(6), 895-924.

Eysteinsson, T. (2004). Forestry in a treeless land. *Lustgården*.

Fagan, B. M. (2016). *Archaeology: a brief introduction*. Routledge, Oxon, UK.

Faix, O., Bremer, J., Schmidt, O., & Tatjana, S. J. (1991). Monitoring of chemical changes in white-rot degraded beech wood by pyrolysis—gas chromatography and Fourier-transform infrared spectroscopy. *Journal of Analytical and Applied Pyrolysis*, 21(1), 147-162.

Falkovich, A. H., & Rudich, Y. (2001). Analysis of semivolatile organic compounds in atmospheric aerosols by direct sample introduction thermal desorption GC/MS. *Environmental Science & Technology*, 35(11), 2326-2333.

Felix, W. D., McDowall, M. A., & Eyring, H. (1963). The differential thermal analysis of natural and modified wool and mohair. *Textile Research Journal*, 33(6), 465-471.

Fengel, D. & D. Grosser (1975). Chemische zusammensetzung von Nadel- und Laubholzern. Holz roh-werkst 33**:** 32-34.

Fengel, D., & Wegener, G. (Eds.). (1984). *Wood: chemistry, ultrastructure, reactions*. Walter de Gruyter, Berlin

Ferrero, F., Testore, F., Malucelli, G., & Tonin, C. (1998). Thermal degradation of linen textiles: the effects of ageing and cleaning. *Journal of the Textile Institute*, 89(3), 562-569.

Fiebach, K., & Grimm, D. (2000). Resins, Natural. *Ullmann's Encyclopedia of Industrial Chemistry*.

Filley, T. R., Blanchette, R. A., Simpson, E., & Fogel, M. L. (2001). Nitrogen cycling by wood decomposing soft-rot fungi in the "King Midas tomb," Gordion, Turkey. *Proceedings of the National Academy of Sciences*, 98(23), 13346-13350.

Florian, M. L. E (1990). Scope and history of archaeological wood. In: *Archaeological Wood Properties, Chemistry, and Preservation. Developed from a symposium sponsored by the Cellulose Paper and Textile Division at the 196th National Meeting of the American Chemical Society, Los Angeles, California, September 25-September 30, 1988* (pp. 141-174). American Chemical Society.

Florian, M. L. E. (2007). Protein facts: fibrous proteins in cultural and natural history artefacts. Archetype Publications, London, UK

Forbes, S. L., Keegan, J., Stuart, B. H., & Dent, B. B. (2003). A gas chromatography-mass spectrometry method for the detection of adipocere in grave soils. *European Journal of Lipid Science and Technology*, 105(12), 761-768.

Fors, Y., Grudd, H., Rindby, A., Jalilehvand, F., Sandström, M., Cato, I., & Bornmalm, L. (2014). Sulfur and iron accumulation in three marine-archaeological shipwrecks in the Baltic Sea: The Ghost, the Crown and the Sword. *Nature Scientific reports*, 4:4222.

Fors, Y., Jalilehvand, F., & Sandström, M. (2011). Analytical aspects of waterlogged wood in historical shipwrecks. *Analytical Sciences*, 27(8), 785.

Foston, M., Hubbell, C. A., Samuel, R., Jung, S., Fan, H., Ding, S. Y., ... & Gjersing, E. (2011). Chemical, ultrastructural and supramolecular analysis of tension wood in *Populus tremula x alba* as a model substrate for reduced recalcitrance. *Energy & Environmental Science*, 4(12), 4962-4971.

Fountoulakis, M., & Lahm, H. W. (1998). Hydrolysis and amino acid composition analysis of proteins. *Journal of Chromatography A*, 826(2), 109-134.

Frisk, M. (2015). *Concerning Mass Graves: The use, development and identities within mass graves during the Scandinavian Iron age and Middle ages*. PhD thesis, Uppsala University.

Fu, Q., Argyropoulos, D. S., Tilotta, D. C., & Lucia, L. A. (2008). Understanding the pyrolysis of CCA-treated wood: Part I. Effect of metal ions. *Journal of Analytical and Applied Pyrolysis*, 81(1), 60-64.

Gabriel, M. T. (1932). The cortical cells of Merino, Romney and Lincoln wools. *Journal of the Textile Institute Transactions*, 23(8), T171-T176.

Geib, S. M., Filley, T. R., Hatcher, P. G., Hoover, K., Carlson, J. E., del Mar Jimenez-Gasco, M., ... & Tien, M. (2008). Lignin degradation in wood-feeding insects. *Proceedings of the National Academy of Sciences*, 105(35), 12932-12937.

Gelbrich, J., Mai, C. & Militz, H. (2008). Chemical Changes in wood degraded by Bacteria. *International Biodeterioration & Biodegradation,* 61, 24-32.

Gelbrich, J., Kretschmar, E. I., Lamersdorf, N., & Militz, H. (2012). Laboratory experiments as support for development of in situ conservation methods. *Conservation and Management of Archaeological Sites*, 14(1-4), 7-15.

Ghisalberti, E. L., Godfrey, I. M., Kilminster, K., Richards, V. L., & Williams, E. (2002). The analysis of acid-affected Batavia timbers. In: *Proceedings of the 8th ICOM Group on wet organic archaeological materials conference, Stockholm, 11-15 June 2001, 281-307.* Deutsches Schiffahrtsmuseum.

Gillard, R. D., Hardman, S. M., Thomas, R. G., & Watkinson, D. E. (1994). The mineralization of fibres in burial environments. *Studies in Conservation*, 39(2), 132-140.

Gilligan, I. (2010). The prehistoric development of clothing: archaeological implications of a thermal model. *Journal of Archaeological Method and Theory*, 17(1), 15-80.

Good, I. (2001). Archaeological textiles: a review of current research. *Annual Review of Anthropology*, 209-226.

Goring, D. A. I., & Timell, T. E. (1962). Molecular weight of native celluloses. *Tappi*, 45(6), 454-460.

Graham, R. D. (1973). History of wood preservation. In: *Wood deterioration and its prevention by preservative treatments,* (pp. 1 – 25), Ed, Nicholas, D. D. Syracuse University Press, Syracuse, NY.

Grant, J., Gorin, S., & Fleming, N. (2015). *The archaeology coursebook: an introduction to themes, sites, methods and skills*. Routledge, Oxon, UK.

Grave, P., & Kealhofer, L. (1999). Assessing bioturbation in archaeological sediments using soil morphology and phytolith analysis. *Journal of Archaeological Science*, 26(10), 1239-1248.

Graves, D. (2004). A comparative study of consolidants for waterlogged wood: polyethylene glycol, sucrose, and silicone oil. *SSCR Journal (Scottish Society for Conservation and Restoration),* 15 (3), 13–17.

Gray, J. (2003). The Irish, Scottish and Flemish linen industries during the long eighteenth century. In: *The European Linen Industry in Historical Perspective.* Oxford University Press, 159-186.

Green, K. A. (2013). *The fate of lipids in archaeological burials*. PhD thesis, University of York.

Gupta, B. S. (2008). *Friction in textile materials*. Woodhead Publishing, Cambridge, UK.

Hagelberg, E., Hofreiter, M., & Keyser, C. (2015). Ancient DNA: the first three decades. *Philosophical Transactions of the Royal Society B: Biological Sciences*, 370(1660).

Haines, B. M. (2006). The fibre structure of leather. In: *Conservation of leather and related materials*, eds. Kite, M., & Thomson, R., pp 11. Routledge, Oxon, UK.

Hammer, Ø., Harper, D.A.T., Ryan, P.D. 2001. PAST: Paleontological statistics software package for education and data analysis. *Palaeontologia Electronica* 4(1): 9.

Hardin, I. R. (1996). Investigation of textiles by analytical pyrolysis. In: *Modern Textile Characterization Methods*, ed. Raheel, M., (p 173). CRC Press, Boca Raton, USA.

Hardin, I. R., & Wang, X. Q. (1989). The use of pyrolysis-gas chromatography in textiles as an identification method. *Textile Chemist & Colorist*, 21(1).

Harris, D., C. (1999). Gas Chromatography. In: *Quantitative chemical analysis (Chapter 24) (Fifth ed.).* W. H. Freeman and Company.

Hays, M. D., Smith, N. D., Kinsey, J., Dong, Y., & Kariher, P. (2003). Polycyclic aromatic hydrocarbon size distributions in aerosols from appliances of residential wood combustion as determined by direct thermal desorption—GC/MS. *Journal of Aerosol Science*, 34(8), 1061-1084.

Hearle, J. W. S. (2000). A critical review of the structural mechanics of wool and hair fibres. *International Journal of Biological Macromolecules*, 27(2), 123-138.

Hedges, R.E.M., 1990. The chemistry of archaeological wood In: *Archaeological Wood Properties, Chemistry, and Preservation. Developed from a symposium sponsored by the Cellulose Paper and Textile Division at the 196th National Meeting of the American Chemical Society, Los Angeles, California, September 25-September 30, 1988* (pp. 111-141). American Chemical Society, Washington DC, USA.

Hedges, R. E., Thompson, J., & Hull, B. D. (2005). Stable isotope variation in wool as a means to establish Turkish carpet provenance. *Rapid Communications in Mass Spectrometry*, 19(22), 3187-3191.

Henderson, J. (1987). Factors determining the state of preservation of human remains. In: *Death, decay and reconstruction: approaches to archaeology and forensic science*, 43-54. Eds, Boddington, A., Garland A. N., and Janaway, R. C. Manchester University Press, Manchester, UK.

Hendricker, A. D., & Voorhees, K. J. (1998). Amino acid and oligopeptide analysis using Curie-point pyrolysis mass spectrometry with in-situ thermal hydrolysis and methylation: mechanistic considerations. *Journal of Analytical and Applied Pyrolysis*, 48(1), 17-33.

Hicks, S. A. (2017). *Fate and preservation of lipids in the soils of archaeological and experimental burials*. PhD thesis, University of York.

Hiendleder, S., Kaupe, B., Wassmuth, R., & Janke, A. (2002). Molecular analysis of wild and domestic sheep questions current nomenclature and provides evidence for domestication from two different subspecies. *Proceedings of the Royal Society of London B: Biological Sciences*, 269(1494), 893-904.

High, K. E. (2014). *Fading Star: Understanding accelerated decay of organic remains at Star Carr.* PhD thesis, University of York.

High, K., Milner, N., Panter, I., Demarchi, B., & Penkman, K. E. (2016). Lessons from Star Carr on the vulnerability of organic archaeological remains to environmental change. *Proceedings of the National Academy of Sciences*, 201609222.

Higson, S. P. J. (2004) *Analytical chemistry*. Oxford University Press, Oxford, UK.

Higuchi, T. (1990). Lignin biochemistry: biosynthesis and biodegradation. *Wood Science and Technology*, 24(1), 23-63.

Hirs, C. H. W., Stein, W. H., & Moore, S. (1954). The amino acid composition of ribonuclease. *Journal of Biological Chemistry*, 211(2), 941-950.

Hoch, G. (2007). Cell wall hemicelluloses as mobile carbon stores in non-reproductive plant tissues. *Functional Ecology*, 21, 823–834.

Hocker, E., Almkvist, G., & Sahlstedt, M. (2012). The Vasa experience with polyethylene glycol: A conservator's perspective. *Journal of Cultural Heritage*, 13(3), S175-S182.

Hoffman, P. (1981). Chemical wood analysis as a means of characterising archaeological wood. In: *Proceedings of the ICOM Waterlogged Wood Working Group Conference*, Ed Grattan, D.W., Ottawa, 73-83.

Hoffmann, P., & Jones, M. A. (1990). Structure and degradation process for waterlogged archaeological wood. In: *Archaeological Wood Properties, Chemistry, and Preservation. Developed from a symposium sponsored by the Cellulose Paper and Textile Division at the 196th National Meeting of the American Chemical Society, Los Angeles, California, September 25-September 30, 1988* (pp. 35-65). American Chemical Society.

Hong, H. A., Khaneja, R., Tam, N. M., Cazzato, A., Tan, S., Urdaci, M., Brisson, A., Gasbarrini A., Barnes A., & Cutting, S. M. (2009). *Bacillus subtilis* isolated from the human gastrointestinal tract. *Research in microbiology*, 160(2), 134-143.

Hori, C., Ishida, T., Igarashi, K., Samejima, M., Suzuki, H., Master, E., ... & Larrondo, L. F. (2014). Analysis of the *Phlebiopsis gigantea* genome, transcriptome and secretome provides insight into its pioneer colonization strategies of wood. *Public Library of Science Genetics*, 10(12), e1004759.

Huisman, D. J. (Ed.). (2009). *Degradation of archaeological remains*. Sdu Uitgevers, The Hague, Netherlands.

Hunt, S. (1985) "Degradation of amino acids accompanying in vitro protein hydrolysis." *Chemistry and Biochemistry of the Amino Acids*. Springer Netherlands, 376-398.

Hunter, J., Roberts, C. A., & Martin, A. (1996). Studies in crime: an introduction to forensic archaeology. *Psychology Press*, Oxon, UK.

Iiyama, K., N. Kasuya, L.T.B. Tuyet, J. Nakano & H. Sakaguchi. (1988). Chemical characterisation of ancient buried wood. *Holzforschung* 42: 5–10.

Ilin, A. & T. Raiko. 2010. Practical approaches to Principal Component Analysis in the presence of missing values. *Journal of Machine Learning Research* 11:1957-2000.

Isles, R. (2015) Dundee experts recreate face of Saxon man at Lincoln Castle. University of Dundee Online. “http://www.dundee.ac.uk/news/2015/dundee-experts-recreate-face-of-saxon-man-at-lincoln-castle”. Retrieved on 15/04/2016.

Jackson, M. G. (1977). Review article: the alkali treatment of straws. *Animal Feed Science and Technology*, 2(2), 105-130.

Jacobsen, T. W., & Cullen, T. (1990). The work of JL Angel in the Eastern Mediterranean. *A Life in Science: Papers in Honor of JL Angel, Kampsville, IL: Center for American Archeology, Scientific Paper*, 6, 38-51.

Jakubke, H. D., & Sewald, N. (2008). *Peptides from A to Z: a concise encyclopedia*. John Wiley & Sons.

Janaway, R. (1983). Textile fibre characteristics preserved by metal corrosion: the potential of SEM studies. *The Conservator*, 7(1), 48-52.

Janaway, R. C. (2001). Degradation of clothing and other dress materials associated with buried bodies of archaeological and forensic interest. In: *Advances in Forensic Taphonomy: Method, theory, and archaeological perspective* (pp. 379-402). Eds, Haglund, W. D., & Sorg, M. H. CRC Press, Boca Raton, USA.

Janaway, R. C., Wilson, A. S., Díaz, G. C., & Guillen, S. (2009). Taphonomic changes to the buried body in arid environments: an experimental case study in Peru. In: *Criminal and Environmental Soil Forensics* (pp. 341-356). Eds, Ritz, K., Dawson, L., & Miller, D. Springer, Netherlands.

Jerz, J. K., & Rimstidt, J. D. (2004). Pyrite oxidation in moist air. *Geochimica et Cosmochimica Acta*, 68(4), 701-714.

Jones, M., & Eaton, R. (2006). Conservation of Ancient Timbers from the sea. In: *Conservation Science: Heritage Materials.* Eds, May, E. & Jones, M. RSC Publishing, Cambridge.

Jupp, P. (1992). Cremation or burial? Contemporary choice in city and village. *The Sociological Review*, 40(S1), 169-197.

Kaiser, K., & Benner, R. (2005). Hydrolysis-induced racemization of amino acids. *Limnology and Oceanography: Methods, 3, 318*-325.

Kang, S. M., Cha, M. K., Kim, S. J., & Kwon, Y. J. (2006). The effect of quality improvement for wool and silk treated with protease produced by *B. subtilis* K-54. *Fashion & Textile Research Journal*, 8(2), 239-244.

Kebbi-Benkeder, Z., Colin, F., Dumarçay, S., & Gérardin, P. (2015). Quantification and characterization of knotwood extractives of 12 European softwood and hardwood species. *Annals of Forest Science*, 72(2), 277-284.

Kelley, J. O., & Angel, J. L. (1987). Life stresses of slavery. *American Journal of Physical Anthropology*, 74(2), 199-211.

Khaneja, R., Perez-Fons, L., Fakhry, S., Baccigalupi, L., Steiger, S., To, E., Sandmann, G., Dong, T.C., Ricca, E., Fraser, P.D., & Cutting, S. M. (2010). Carotenoids found in Bacillus. *Journal of Applied Microbiology*, 108(6), 1889-1902.

Kidd, F. (1977). Other animal fibres. In: *Chemistry of Natural Protein Fibers* (pp 370 – 409). Ed, Asquith, R. S. Springer Science & Business Media.

Kim, S. J., Cha, M. K., Oh, E. T., Kang, S. M., So, J. S., & Kwon, Y. J. (2005). Use of protease produced by Bacillus sp. SJ-121 for improvement of dyeing quality in wool and silk. *Biotechnology and Bioprocess Engineering*, 10(3), 186-191.

Kim, Y. S., & Singh, A. P. (2000). Micromorphological characteristics of wood biodegradation in wet environments: a review. *IAWA Journal*, 21(2), 135-155.

Kim, Y. S., & Singh, A. P. (2016). Wood as Cultural Heritage Material and its Deterioration by Biotic and Abiotic Agents. In: *Secondary Xylem Biology: Origins, Functions, and Applications* (pp. 233). Eds. Kim, Y.S., Funada, R. & Adya, P. Academic Press, Cambridge, USA.

Kim, Y.S. (1990). Chemical characteristics of water-logged archaeological wood. Holzforschung, 44, 169-172.

King, H. H., & Solomon, P. R. (1983). Modelling tar composition in lignin pyrolysis. *Symposium on Mathematical Modelling of Biomass Pyrolysis Phenomena Washington, D.C.*

King, T. E., Fortes, G. G., Balaresque, P., Thomas, M. G., Balding, D., Delser, P. M., ... & Tonasso, L. (2014). Identification of the remains of King Richard III. *Nature Communications*, 5.

Kurata, S., & Ichikawa, K. (2008). Identification of small bits of natural leather by pyrolysis gas chromatography/mass spectrometry. *Bunseki Kagaku*, 57(7), 563-569.

Kvavadze, E., Bar-Yosef, O., Belfer-Cohen, A., Boaretto, E., Jakeli, N., Matskevich, Z., & Meshveliani, T. (2009). 30,000-year-old wild flax fibers. *Science*, 325(5946), 1359-1359.

Larsen, R. (1994). STEP leather project: evaluation of the correlation between natural and artificial ageing of vegetable tanned leather and determination of parameters for standardization of an artificial ageing method. *Royal Danish Academy of Fine Arts & European Commission*.

Larsen, R. (2008). The chemical degradation of leather. *CHIMIA International Journal for Chemistry*, 62(11), 899-902.

Latourette, K. S. (1978). *A History of the Expansion of Christianity*. Zondervan Publishing House, Grand Rapids, USA.

Leeder, J. D., & Marshall, R. C. (1982). Readily-extracted proteins from Merino wool. *Textile Research Journal*, 52(4), 245-249.

Leonowicz, A., Matuszewska, A., Luterek, J., Ziegenhagen, D., Wojtaś-Wasilewska, M., Cho, N. S., ... & Rogalski, J. (1999). Biodegradation of lignin by white rot fungi. *Fungal Genetics and Biology*, 27(2), 175-185.

Levin, L., Forchiassin, F., & Ramos, A. M. (2002). Copper induction of lignin-modifying enzymes in the white-rot fungus Trametes trogii. *Mycologia*, 94(3), 377-383.

Lewis, N. G., & Yamamoto, E. (1990). Lignin: occurrence, biogenesis and biodegradation. *Annual Review of Plant Biology*, 41(1), 455-496.

Li, X., Tabil, L. G., & Panigrahi, S. (2007). Chemical treatments of natural fiber for use in natural fiber-reinforced composites: a review. *Journal of Polymers and the Environment*, 15(1), 25-33.

Lieberman, P. (1991). *Uniquely human: The evolution of speech, thought, and selfless behavior*. Harvard University Press, Cambridge, USA.

Liesowska, A. (2015). Shigir Idol is oldest wooden sculpture monument in the world, say scientists. *The Siberian Times*, 26th August 2015. Retrieved on 5th July 2016.

Lillie, M., & Smith, R. (2007). The in situ preservation of archaeological remains: using lysimeters to assess the impacts of saturation and seasonality. *Journal of Archaeological Science*, 34(9), 1494-1504.

Loe L., Barker C., & Wright RV. (2014a) An osteological profile of trench warfare: peri-mortem trauma sustained by soldiers who fought & died in the Battle of Fromelles. *The Routledge Handbook of the Bioarchaeology of Human Conflict* (pp. 575-601). Routledge, Oxon, UK.

Loe, L., Boyle, A., Webb, H., & David, S. (2014b). *'Given to the Ground': A Viking Age Mass Grave on Ridgeway Hill, Weymouth.* Oxford Archaeology.

Łucejko, J. J., Modugno, F., Ribechini, E., & José, C. (2009). Characterisation of archaeological waterlogged wood by pyrolytic and mass spectrometric techniques. *Analytica Chimica Acta*, 654(1), 26-34.

Łucejko, J. J., Modugno, F., Ribechini, E., Tamburini, D., & Colombini, M. P. (2015). Analytical instrumental techniques to study archaeological wood degradation. *Applied Spectroscopy Reviews,* 50(7), 584-625.

MacKinnon, M. (2007). Osteological research in classical archaeology. *American Journal of Archaeology*, 473-504.

MacLeod, I. D., & Kenna, C. (1990). Degradation of archaeological timbers by pyrite: oxidation of iron and sulphur species. In: *Archaeological Wood Properties, Chemistry, and Preservation. Developed from a symposium sponsored by the Cellulose Paper and Textile Division at the 196th National Meeting of the American Chemical Society, Los Angeles, California, September 25-September 30, 1988* (pp. 133-142). American Chemical Society, Washington DC, USA.

Mahall, K. (2003). *Quality assessment of textiles: damage detection by microscopy*. Springer Science & Business Media.

Malim, T., Morgan, D., & Panter, I. (2015). Suspended preservation: Particular preservation conditions within the Must Farm–Flag Fen Bronze Age landscape. *Quaternary International*, 368, 19-30.

Marte, B. (2003). Proteomics. *Nature*, 422(6928), 191-191.

Martínez, A. T., Camarero, S., Gutiérrez, A., Bocchini, P., & Galletti, G. C. (2001). Studies on wheat lignin degradation by Pleurotus species using analytical pyrolysis. *Journal of Analytical and Applied Pyrolysis*, 58, 401-411.

Martínez, A. T., Speranza, M., Ruiz-Dueñas, F. J., Ferreira, P., Camarero, S., Guillén, F., Martínez, M. J., Gutiérrez, A. & del Río, J. C. (2005). Biodegradation of lignocellulosics: microbial, chemical, and enzymatic

aspects of the fungal attack of lignin. *International microbiology: the official journal of the Spanish Society for Microbiology*, 8(3), 195.

Maxwell, C. A., Wess, T. J., & Kennedy, C. J. (2006). X-ray diffraction study into the effects of liming on the structure of collagen. *Biomacromolecules*, *7*(8), 2321-2326.

McGrail, S. (2014). Ancient Boats in North-West Europe: The archaeology of water transport to AD 1500. Routledge, Oxon, UK .

Menkart, J., Wolfram, L. J., & Mao, I. (1966). Caucasian hair, Negro hair and wool: similarities and differences. *Journal of the Society of Cosmetic Chemists*, 17(13), 769-788.

Merck Index, Twelfth Edition. Merck and Company. 1305.

Meylan, B. A., & Butterfield, B. G. (1972). Three-dimensional structure of wood: a scanning electron microscope study (Vol. 2). Syracuse University Press, Syracuse, USA.

Michal, G., & Schomburg, D. (Eds.). (1999*). Biochemical pathways: an atlas of biochemistry and molecular biology* (No. QP171. B685 1999). New York: Wiley.

Mitterer, R. M., & Kriausakul, N. (1984). Comparison of rates and degrees of isoleucine epimerization in dipeptides and tripeptides. *Organic Geochemistry*, 7(1), 91-98.

Mohan, D., Pittman, C. U., & Steele, P. H. (2006). Pyrolysis of wood/biomass for bio-oil: a critical review. *Energy & Fuels*, 20(3), 848-889.

Mohanty, A. K., Misra, M., & Drzal, L. T. (Eds.). (2005). *Natural fibers, biopolymers, and biocomposites.* CRC Press, Boca Raton, USA.

Moldoveanu, S. C. (1998). *Analytical pyrolysis of natural organic polymers* (Vol. 20). Elsevier.

Molyneux, G. S. (1959). The digestion of wool by a keratinolytic Bacillus. *Australian Journal of Biological Sciences*, 12(3), 274-281.

Morrison, W. H., & Archibald, D. D. (1998). Analysis of graded flax fiber and yarn by pyrolysis mass spectrometry and pyrolysis gas chromatography mass spectrometry. *Journal of Agricultural and Food Chemistry*, 46(5), 1870-1876.

Mortensen, M. N., Egsgaard, H., Hvilsted, S., Shashoua, Y., & Glastrup, J. (2007). Characterisation of the polyethylene glycol impregnation of the Swedish warship Vasa and one of the Danish Skuldelev Viking ships. *Journal of Archaeological Science*, 34(8), 1211-1218.

Nakano, M. M., & Zuber, P. (1998). Anaerobic growth of a "strict aerobe"(*Bacillus subtilis*). *Annual Reviews in Microbiology*, 52(1), 165-190.

Nay, T., & Watts, J. E. (1977). Observations on the wool follicle abnormalities in Merino sheep exposed to prolonged wetting conducive to the development of fleece-rot. *Crop and Pasture Science*, 28(6), 1095-1105.

NIST 08 (2008). Mass spectral library (NIST/EPA/NIH). National Institute of Standards and Technology, Gaithersburg, USA. NIST Mass Spectrometry Data Center Collection

NIST Mass Spec Data Center, S.E. Stein, director, "Mass Spectra" in NIST Chemistry WebBook, NIST Standard Reference Database Number 69, Eds. P.J. Linstrom and W.G. Mallard, National Institute of Standards and Technology, Gaithersburg MD, 20899, http://webbook.nist.gov

Norton, E. (2014) Story of Lincoln Castle Saxon skeletons revealed. *The Lincolnite*. http://thelincolnite.co.uk/2014/06/story-lincoln-castle-saxon-skeletons-revealed/. Retrieved on 15/04/2016

O'Sullivan, N. J., Teasdale, M. D., Mattiangeli, V., Maixner, F., Pinhasi, R., Bradley, D. G., & Zink, A. (2016). A whole mitochondria analysis of the Tyrolean Iceman's leather provides insights into the animal sources of Copper Age clothing. *Scientific Reports*, 6.

Obreza, T. A., Alva, A. K., & Calvert, D. V. (1993). *Citrus fertilizer management on calcareous soils. Cooperative Extension Service*, Institute of Food and Agricultural Sciences. University of Florida.

Obst, J. R. (1982). Guaiacyl and syringyl lignin composition in hardwood cell components. *Holzforschung*, 36:143–152.

Oonk, S., Slomp, C. P., Huisman, D. J., & Vriend, S. P. (2009). Geochemical and mineralogical investigation of domestic archaeological soil features at the Tiel-Passewaaij site, The Netherlands. *Journal of geochemical exploration*, 101(2), 155-165.

Otjen, L., Blanchette, R., Effland, M., & Leatham, G. (1987). Assessment of 30 white rot basidiomycetes for selective lignin degradation. *Holzforschung,* 41(6), 343-349.

Pacchiarotta, T., Nevedomskaya, E., Carrasco-Pancorbo, A., Deelder, A. M., & Mayboroda, O. A. (2010). Evaluation of GC-APCI/MS and GC-FID as a complementary platform. *Journal of Biomolecular Techniques*: JBT, 21(4), 205.

Palmieri, G., Giardina, P., Bianco, C., Fontanella, B., & Sannia, G. (2000). Copper induction of laccase isoenzymes in the ligninolytic fungus Pleurotus ostreatus. *Applied and Environmental Microbiology*, 66(3), 920-924.

Pandey, K.K. (1998). A study of chemical structure of soft and hardwood and wood polymers by FTIR Spectroscopy. *Journal of Applied Polymer Science,* 71, 1969-1975.

Pandey, K. K., & Pitman, A. J. (2003). FTIR studies of the changes in wood chemistry following decay by brown-rot and white-rot fungi. *International Biodeterioration & Biodegradation,* 52(3), 151-160.

Parnell, J. J., Terry, R. E., & Nelson, Z. (2002). Soil chemical analysis applied as an interpretive tool for ancient human activities in Piedras Negras, Guatemala. *Journal of Archaeological Science*, 29(4), 379-404.

Patt, R., Kordsachia, O., & Süttinger, R. (2002). *Pulp* In: Ullmann's Encyclopaedia of Industrial Chemistry. Wiley-VCH, Weinheim

Payen, A. (1838). Sur un moyen d'isoler le tissu élémentaire des bois. *Comptes Rendus Hebdomadaires des Séances de l'Académie des Sciences*, 7, 1125.

Pe´rez-Coello, M. S., Sanz, J., & Cabezudo, M. D. (1997). Analysis of volatile components of oak wood by solvent extraction and direct thermal desorption-gas chromatography-mass spectrometry. *Journal of Chromatography A*, 778(1), 427-434.

Peachy, P. (2015). Body farms: British researchers looking for site to set up laboratory for dead human remains. *The Independent Online.* http://www.independent.co.uk/news/uk/home-news/body-farms-british-researchers-looking-for-site-to-set-up-laboratory-for-dead-human-remains-a6751991.html. Retrieved on 20/07/16.

Pearce, J. (2016). Status and burial. In: *The Oxford Handbook of Roman Britain*. Eds.Millett, M.,Revell, L& Moore, A. OUP Oxford.

Pearson, M. P. (1999). *The archaeology of death and burial* (p. 44). Phoenix Mill, UK: Sutton.

Pearson, D., Schofield, E., & Butler, H. (2016). Discussion on the practicalities and effectiveness of re-treating a wooden gun carriage with DTPA. Conference paper presented *at WOAM 2016: 13th ICOM-CC Wet Organic Archaeological Materials Conference, 16-20 May 2016, Florence, Italy.*

Pekhtasheva, E. L., Neverov, A. N., Kubica, S., & Zaikov, G. E. (2012). Biodegradation and biodeterioration of some natural polymers. *Polymers Research Journal*, *5*(1), 77.

Penkman, K. E. H., Kaufman, D. S., Maddy, D., & Collins, M. J. (2008). Closed-system behaviour of the intra-crystalline fraction of amino acids in mollusc shells. *Quaternary Geochronology*, 3(1), 2-25.

Perez-Coello, M. S., Sanz, J., & Cabezudo, M. D. (1997). Analysis of volatile components of oak wood by solvent extraction and direct thermal desorption-gas chromatography-mass spectrometry. *Journal of Chromatography A*, 778(1), 427-434.

Perlin, J. (2005). A forest journey: The story of wood and civilization. The Countryman Press, Woodstock, USA

Pipes, M. L., Kruk, J., & Milisauskas, S. (2014). Assessing the archaeological data for wool-bearing sheep during the Middle to Late Neolithic at Bronocice, Poland. In: *Animal Secondary Products: Domestic Animal Exploitation in Prehistoric Europe, the Near East and the Far East* (pp 80-102). Ed, Greenfield, H. Oxbow Books, Oxford, UK.

Pokines, J. T., & Baker, J. E. (2013). Effects of burial environment on osseous remains. In: *Manual of Forensic Taphonomy,* pp. 73-114) CRC Press, Boca Raton, USA.

Pollard, P., Lelong, O., MacKinnon, G., Banks, I., Barton, P., Cropper, C., & McKenzie, J. (2008) Pheasant Wood Fromelles, Data Structure Report. *Glasgow University Archaeology Research Division (GUARD) Project 12008.* Glasgow University, UK.

Popescu, C., & Wortmann, F. J. (2010). Wool–structure, mechanical properties and technical products based on animal fibres. In: *Industrial Applications of Natural Fibres: Structure, Properties and Technical Applications*. Eds. Mussig, J. & Stevens, C. pp 255-266.

Public Health (Control of Disease) Act, (1984). Chapter 22, Part III. Disposal of Dead Bodies (in England and Wales).

Rackham, H. (1945). *Pliny: Natural History,* Vol. 4. Harvard University Press, Cambridge, USA..

Radbout University Department of Biology online reference collection: http://www.vcbio.science.ru.nl/image-gallery/show/print/PL0223/ - retrieved on 01/09/2016

Ralph, J., & Hatfield, R. D. (1991). Pyrolysis-GC-MS characterization of forage materials. *Journal of Agricultural and Food Chemistry*, 39(8), 1426-1437.

Ramsay, L. M., Sayer, J. A., & Gadd, G. M. (1999). Stress responses of fungal colonies towards toxic metals. *The Fungal Colony*, 178-200.

Rencoret, J., Gutiérrez, A., Nieto, L., Jiménez-Barbero, J., Faulds, C. B., Kim, H., ... & José, C. (2010). Lignin composition and structure in young versus adult Eucalyptus globulus plants. *Plant Physiology*, 155(2), 667–682.

Reynolds, P. J. (1994). The life and death of a post-hole. *Interpreting Stratigraphy*, 5, 21-25.

Rice, A. V., Tsuneda, A., & Currah, R. S. (2006). In vitro decomposition of Sphagnum by some microfungi resembles white rot of wood. *FEMS Microbiology Ecology*, 56(3), 372-382.

Rich, A., & Crick, F. H. C. (1961). The molecular structure of collagen. *Journal of Molecular Biology*, 3(5), 483IN1-506IN4.

Richards, G. N., & Zheng, G. (1991). Influence of metal ions and of salts on products from pyrolysis of wood: applications to thermochemical processing of newsprint and biomass. *Journal of Analytical and Applied Pyrolysis*, 21(1), 133-146.

Riello, G., & Parthasarathi, P. (2011). *The spinning world: a global history of cotton textiles, 1200-1850*. Oxford University Press, Oxford, UK.

Robbins, C. R. (2012*). Chemical composition of different hair types. In Chemical and physical behavior of human hair*. (pp. 105-176). Springer Berlin Heidelberg.

Robinson, N., Evershed, R. P., Higgs, W. J., Jerman, K., & Eglinton, G. (1987). Proof of a pine wood origin for pitch from Tudor (Mary Rose) and Etruscan shipwrecks: application of analytical organic chemistry in archaeology. *Analyst*, 112(5), 637-644.

Rodrigues, J., Meier, D., Faix, O., & Pereira, H. (1999). Determination of tree to tree variation in syringyl/guaiacyl ratio of *Eucalyptus globulus* wood lignin by analytical pyrolysis. *Journal of Analytical and Applied Pyrolysis,* 48(2), 121-128.

Ronsijn, W. (2015). The household, the labour market or the commodity market? Enabling the division of labour within proto-industries: the case of the Flemish linen industry during a period of decline (first half of nineteenth century). In *Datini-Ester Advanced Seminar* (No. 2015/2).

Rosato, D. V., Rosato, D. V., & Rosato, M. (2004). *Plastic product material and process selection handbook.* Elsevier.

Rousk, J., Bååth, E., Brookes, P. C., Lauber, C. L., Lozupone, C., Caporaso, J. G., ... & Fierer, N. (2010). Soil bacterial and fungal communities across a pH gradient in an arable soil. *The ISME Journal*, 4(10), 1340-1351.

Rowell, R. M., & Barbour, R. J. (1990). Archaeological Wood Properties, Chemistry, and Preservation. pp. 35-65. American Chemical Society.

Rudenberg, H. G., & Rudenberg, P. G. (2010). Origin and Background of the Invention of the Electron Microscope: Commentary and Expanded Notes on Memoir of Reinhold Rüdenberg. *Advances in Imaging and Electron Physics*, 160, 207-286.

Sáiz-Jiménez, C., Boon, J. J., Hedges, J. I., Hessels, J. K. C., & De Leeuw, J. W. (1987). Chemical characterization of recent and buried woods by analytical pyrolysis: Comparison of pyrolysis data with 13C NMR and wet chemical data. *Journal of Analytical and Applied Pyrolysis*, 11, 437-450.

Saiz-Jimenez, C. (1994). Analytical Pyrolysis of Humic Substances: Pitfalls, Limitations, and Possible Solutions. *Environmental Science Technology*, *28*, 1773-1780.

Salisbury, F. B., & Ross, C. W. (1992). Plant physiology. 4th. Edn. Wadsworth Publishers, Belmont, USA.

Sánchez, C. (2009). Lignocellulosic residues: biodegradation and bioconversion by fungi. *Biotechnology Advances*, 27(2), 185-194.

Sandström, M., Jalilehvand, F., Persson, I., Gelius, U., Frank, P., & Hall-Roth, I. (2002). Deterioration of the seventeenth-century warship Vasa by internal formation of sulphuric acid. *Nature*, 415(6874), 893-897.

Sandström, M., Jalilehvand, F., Damian, E., Fors, Y., Gelius, U., Jones, M., & Salomé, M. (2005). Sulfur accumulation in the timbers of King Henry VIII's warship Mary Rose: A pathway in the sulfur cycle of conservation concern. *Proceedings of the National Academy of Sciences of the United States of America*, 102(40), 14165-14170.

Sandström, J., & Schofield, E. (2016). Investigating the use of cellulose for the application of carbonate particles to neutralise acids in waterlogged wood. Conference paper presented *at WOAM 2016: 13th ICOM-CC Wet Organic Archaeological Materials Conference, 16-20 May 2016, Florence, Italy.*

Sayle, K. L., Hamilton, W. D., Cook, G. T., Ascough, P. L., Gestsdóttir, H., & McGovern, T. H. (2016). Deciphering diet and monitoring movement: multiple stable isotope analysis of the Viking Age settlement at Hofstaðir, Lake Mývatn, Iceland. *American Journal of Physical Anthropology*, 160: 126-136.

Scarre, C., & Fagan, B. M. (2008). *Ancient civilizations*. Prentice Hall, Upper Saddle River, USA.

Scheller, H. V., & Ulvskov, P. (2010). Hemicelluloses. *Plant Biology*, 61(1), 263.

Schick, T. (1986). Perishable remains from the Nahal Hemar Cave. *Mitekufat Haeven: Journal of the Israel Prehistoric Society/האבן מתקופת*, 95-97.

Schlegel, H. G. (1986) General Microscopy, Cambridge University Press, Cambridge, U.K.

Schoch, W. H. (2011). Wood and charcoal anatomy: Problems and solutions. *SAGVNTVM Extra*, 11, 43-44.

Schoemaker, H. E. (1990). On the chemistry of lignin biodegradation. *Recueil des Travaux Chimiques des Pays-Bas*, 109(4), 255-272.

Schroeder, M., Schweitzer, M., Lenting, H. B. M., & Guebitz, G. M. (2004). Chemical modification of proteases for wool cuticle scale removal. *Biocatalysis and Biotransformation,* 22(5-6), 299-305.

Schultz, T. P., Nicholas, D. D., & Preston, A. F. (2007). A brief review of the past, present and future of wood preservation. *Pest Management Science*, 63(8), 784-788.

Schwarze, F. W., Engels, J., & Mattheck, C. (2000). Fundamental aspects. In: *Fungal Strategies of Wood Decay in Trees* (pp. 5-31). Springer Berlin Heidelberg.

Scott, N. A., Cole, C. V., Elliott, E. T., & Huffman, S. A. (1996). Soil textural control on decomposition and soil organic matter dynamics. *Soil Science Society of America Journal*, 60(4), 1102-1109.

Sealy, J. C., van der Merwe, N. J., Sillen, A., Kruger, F. J., & Krueger, H. W. (2015). 87Sr86Sr as a dietary indicator in modern and archaeological bone. *Journal of Archaeological Science*, 18(3), 399-416.

Segard, M. (2013) Jaunay-Clan, Sous Clan 2: Rapport final d'opération d'archéologie preventive. Unpublished archaeological report.

Serchisu, Fabio (2014*) Textile fibre preservation and statistical variation in burials: Clothing evidence in Anglo-Saxon and Roman inhumations*. PhD thesis, University of York

Serpico, M., & White, R. (2000), Adhesives and binders, in *Ancient Egyptian materials and technology* (eds. P.Nicholson and I.Shaw), 475–94, Cambridge University Press, Cambridge.

Shakespeare, W. (1599). *The most excellent and lamentable tragedy of Romeo and Juliet* (Act 3, Scene 4). Cuthbert Burby, London, UK.

Sheaffer, C. C., & Moncada, K. M. (2012). Introduction to Agronomy: Food, Crops, and Environment. *Delmar Cengage Learning*.

Shedrinsky, A. M., Wampler, T. P., Indictor, N., & Baer, N. S. (1989). Application of analytical pyrolysis to problems in art and archaeology: a review. *Journal of Analytical and Applied Pyrolysis*, 15, 393-412.

Sibley, L. R., & Jakes, K. A. (1982). Textile fabric pseudomorphs, a fossilized form of textile evidence. *Clothing and Textiles Research Journal*, 1(1), 24-30.

Sibley, L. R., & Jakes, K. A. (1984). Survival of protein fibers in archaeological contexts. *Science and Archaeology,* 26:17-27.

Sigfusson, B., Gislason, S. R., & Paton, G. I. (2008). Pedogenesis and weathering rates of a Histic Andosol in Iceland: Field and experimental soil solution study. *Geoderma*, 144(3), 572-592.

Silvester, F. D. (2013). *Timber: Its mechanical properties and factors affecting its structural use*. Elsevier.

Smith, C. W., & Cothren, J. T. (1999). *Cotton: origin, history, technology, and production* (Vol. 4). John Wiley & Sons.

Sobeih, K. L., Baron, M., & Gonzalez-Rodriguez, J. (2008). Recent trends and developments in pyrolysis–gas chromatography. *Journal of Chromatography A*, 1186(1), 51-66.

Solazzo, C., Dyer, J. M., Clerens, S., Plowman, J., Peacock, E. E., & Collins, M. J. (2013). Proteomic evaluation of the biodegradation of wool fabrics in experimental burials. *International Biodeterioration & Biodegradation,* 80, 48-59.

Solazzo, C., Rogers, P. W., Weber, L., Beaubien, H. F., Wilson, J., & Collins, M. (2014). Species identification by peptide mass fingerprinting (PMF) in fibre products preserved by association with copper-alloy artefacts. *Journal of Archaeological Science*, 49, 524-535.

Spangenberg, J. E., Ferrer, M., Tschudin, P., Volken, M., & Hafner, A. (2010). Microstructural, chemical and isotopic evidence for the origin of late neolithic leather recovered from an ice field in the Swiss Alps. *Journal of Archaeological Scien*ce, 37(8), 1851-1865.

Spanou, S. (2012) Edinburgh Trams Project: South Leith parish church graveyard, Constitution Street, Leith. Archaeological excavations for Transport Initiatives Edinburgh Ltd. Headland Archaeology excavation report for job number ETCS08.

Spufford, P. (2006). From Antwerp and Amsterdam to London: the decline of financial centres in Europe. *De Economist*, 154(2), 143-175.

Sreeram, K. J., & Ramasami, T. (2003). Sustaining tanning process through conservation, recovery and better utilization of chromium. *Resources, Conservation and Recycling*, 38(3), 185-212.

Stephenson, R. C., & Clarke, S. (1989). Succinimide formation from aspartyl and asparaginyl peptides as a model for the spontaneous degradation of proteins. *Journal of Biological Chemistry*, 264(11), 6164-6170.

Strzelczyk, A. B., Kuroczkin, J., & Krumbein, W. E. (1987). Studies on the microbial degradation of ancient leather bookbindings: Part I. *International Biodeterioration*, 23(1), 3-27.

Swift, J. A., & Bews, B. (1976). The chemistry of human hair cuticle. III: the isolation and amino acid analysis of various sub-fractions of the cuticle obtained by pronase and trypsin digestion. *Journal of the Society of Cosmetic Chemists of Great Britain*, 27, 289-300.

Takekoshi, Y., Sato, K., Kanno, S., Kawase, S., Kiho, T., & Ukai, S. (1997). Analysis of wool fiber by alkali-catalyzed pyrolysis gas chromatography. *Forensic Science International*, 87(2), 85-97.

Tamburini, D., Łucejko, J. J., Modugno, F., Ribechini, E., & Colombini, M. P. (2016). Chemical parameters to evaluate the preservation state of wet archaeological wood: the critical interpretation of the Holocellulose/Lignin ratio. Conference paper presented *at WOAM 2016: 13th ICOM-CC Wet Organic Archaeological Materials Conference, 16-20 May 2016, Florence, Italy.*

Tame, N. W., Dlugogorski, B. Z., & Kennedy, E. M. (2007). Formation of dioxins and furans during combustion of treated wood. *Progress in Energy and Combustion Science*, 33(4), 384-408.

Taylor, R. P. (2000). Death and the afterlife: A cultural encyclopedia. ABC-CLIO, California.

Taylor, A. M., Gartner, B. L., & Morrell, J. J. (2002). Heartwood formation and natural durability- a review. *Wood and Fiber Science*, 34(4), 2002: 587-611.

Thieme, H. (1997). Lower Palaeolithic hunting spears from Germany. *Nature*, 385(6619), 807-810.

Tien, M. (1987). Properties of ligninase from Phanerochaete chrysosporium and their possible applications. *CRC Critical Reviews in Microbiology*, 15(2), 141-168.

Tien, M., & Kirk, T. K. (1984). Lignin-degrading enzyme from Phanerochaete chrysosporium: purification, characterization, and catalytic properties of a unique H2O2-requiring oxygenase. *Proceedings of the National Academy of Sciences*, 81(8), 2280-2284.

Tjeerdsma, B. F., & Militz, H. (2005). Chemical changes in hydrothermal treated wood: FTIR analysis of combined hydrothermal and dry heat-treated wood. *Holz als roh-und Werkstoff*, 63(2), 102-111.

Tjeerdsma, B. F., Boonstra, M., Pizzi, A., Tekely, P., & Militz, H. (1998). Characterisation of thermally modified wood: molecular reasons for wood performance improvement. *Holz als Roh-und Werkstoff,* 56(3), 149-153.

Todaro, L., Dichicco, P., Moretti, N., & D'Auria, M. (2013). Effect of combined steam and heat treatments on extractives and lignin in sapwood and heartwood of Turkey oak (*Quercus cerris L.*) wood. *BioResources*, *8*(2), 1718-1730.

Tongue, J. & Keely, B. J. (2008) Categorising organic remains from soil samples from burial grounds to determine correlation between them using chromatographic techniques. *MChem dissertation*, *University of York.*

Toups, M. A., Kitchen, A., Light, J. E., & Reed, D. L. (2011). Origin of clothing lice indicates early clothing use by anatomically modern humans in Africa. *Molecular biology and evolution*, *28*(1), 29-32.

Tridico, S.R. (2009) Natural animal textile fibres: structure, characteristics and identification. In: *Identification of Textile Fibers.* EdHouck, M.M. Elsevier.

Tsuge, S., Ohtani, H., & Watanabe, C. (2011*). Pyrolysis-GC/MS data book of synthetic polymers: pyrograms, thermograms and MS of pyrolyzates*. Elsevier.

Turner, B., & Wiltshire, P. (1999). Experimental validation of forensic evidence: a study of the decomposition of buried pigs in a heavy clay soil. *Forensic Science International*, 101(2), 113-122.

Tynan, J. (2013). British Army Uniform and the First World War: Men in Khaki. Palgrave Macmillan, London, UK.

Umezawa, T., Nakatsubo, F., & Higuchi, T. (1982). Lignin degradation by Phanerochaete chrysosporium: Metabolism of a phenolic phenylcoumaran substructure model compound. *Archives of Microbiology*, 131(2), 124-128.

Unger, A., Schniewind, A., & Unger, W. (2001). *Conservation of wood artifacts: a handbook*. Springer Science & Business Media, Berlin, Germany.

Updegraff, D. M. (1969). Semimicro determination of cellulose in biological materials. *Analytical Biochemistry*, 32(3), 420-424.

Usai, M. R., Pickering, M. D., Wilson, C.A., Keely, B. J., & Brothwell, D. R. (2014). 'Interred with their bones': soil micromorphology and chemistry in the study of human remains. *Antiquity*, March 2014.

van Bergen, P. F., Poole, I., Ogilvie, T., Caple, C., & Evershed, R. P. (2000). Evidence for demethylation of syringyl moieties in archaeological wood using pyrolysis-gas chromatography/mass spectrometry. *Rapid Communications in Mass Spectrometry*, 14(2), 71-79.

Van de Vijver, K., & Kinnaer, F. (2014). Reconstructing the execution and burial of 41 brigands in Mechelen during the Flemish Peasant's War in 1798. In: *The Routledge handbook of the bioarchaeology of human conflict* (pp. 490-510). Routledge, Oxon, UK.

Van der Wee, H., & Aerts, E. (1978). The History of the Textile Industry in the Low Countries. *Textile History*, *9*(1), 176-183.

Vane, C. H., Drage, T. C., & Snape, C. E. (2003). Biodegradation of oak (*Quercus alba*) wood during growth of the shiitake mushroom (*Lentinula edodes*): a molecular approach. *Journal of Agricultural and Food Chemistry*, 51(4), 947-956.

Vanholme, R., Demedts, B., Morreel, K., Ralph, J., & Boerjan, W. (2010). Lignin biosynthesis and structure. *Plant Physiology*, 153(3), 895-905.

Vicuña, R. (1988). Bacterial degradation of lignin. *Enzyme and Microbial Technology*, 10(11), 646-655.

Virchow, R. (1882). Zwergenkind. *Zeitschrift für Ethnologie*, 14, 215.

Vogt, F. G. (2010). Evolution of solid-state NMR in pharmaceutical analysis. *Future medicinal chemistry*, *2*(6), 915-921.

von Holstein, I. C. C., Penkman, K. E. H., Peacock, E. E., & Collins, M. J. (2014). Wet degradation of keratin proteins: linking amino acid, elemental and isotopic composition. *Rapid Communications in Mass Spectrometry*, 28(19), 2121-2133.

Voorhees, K. J., Baugh, S. F., & Stevenson, D. N. (1994). An investigation of the thermal degradation of poly (ethylene glycol). *Journal of Analytical and Applied Pyrolysis*, 30(1), 47-57.

Wampler, T. P. (Ed.). (2006). *Applied pyrolysis handbook*. CRC Press, Boca Raton, USA.

Ward, W. H., Binkley, C. H., & Snell, N. S. (1955). Amino acid composition of normal wools, wool fractions, mohair, feather, and feather fractions. *Textile Research Journal*, 25(4), 314-325.

Waterman, D., Horsfield, B., Leistner, F., Hall, K., & Smith, S. (2000). Quantification of polycyclic aromatic hydrocarbons in the NIST standard reference material (SRM1649A) urban dust using thermal desorption GC/MS. *Analytical chemistry*, 72(15), 3563-3567.

Weiland, J. J., & Guyonnet, R. (2003). Study of chemical modifications and fungi degradation of thermally modified wood using DRIFT spectroscopy. *Holz als Roh-und Werkstoff*, 61(3), 216-220.

Weiss, H. F. (1916). *The preservation of structural timber*. McGraw-Hill, New York City, USA.

Wild, J. P. (1988). *Textiles in archaeology* (Vol. 56). Osprey Publishing, Oxford, UK.

Wilson, K., & White, D. J. B. (1986). The anatomy of wood: its diversity and variability. *Stobart & Son Ltd.*

Wilson, M.A., Godfrey, I.M., Hanna, J.V., Quezada, R.A. & Finnie, K.S. (1993). The degradation of wood in old Indian Ocean shipwrecks. *Organic Geochemistry,* 20, 599-610

Wilson, A. S., Dodson, H. I., Janaway, R. C., Pollard, A. M., & Tobin, D. J. (2007a). Selective biodegradation in hair shafts derived from archaeological, forensic and experimental contexts. *British Journal of Dermatology*, 157(3), 450-457.

Wilson, A. S., Janaway, R. C., Holland, A. D., Dodson, H. I., Baran, E., Pollard, A. M., & Tobin, D. J. (2007b). Modelling the buried human body environment in upland climes using three contrasting field sites. *Forensic Science International*, 169(1), 6-18.

Wilson, C. A., Davidson, D. A., & Cresser, M. S. (2008). Multi-element soil analysis: an assessment of its potential as an aid to archaeological interpretation. *Journal of Archaeological Science*, 35(2), 412-424.

Wilson, A. S., Dodson, H. I., Janaway, R. C., Pollard, A. M., & Tobin, D. J. (2010). Evaluating histological methods for assessing hair fibre degradation. *Archaeometry*, 52(3), 467-481.

Wolfram, L. J., & Lindemann, M. K. (1971). Some observations on the hair cuticle. *Journal of the Society of Cosmetic Chemists of Great Britain*, 22, 839-850.

Wortmann, F. J., & Arns, W. (1986). Quantitative Fiber Mixture Analysis by Scanning Electron Microscopy Part I: Blends of Mohair and Cashmere with Sheep's Wool. *Textile Research Journal*, 56(7), 442-446.

Wu, G., Heitz, M., & Chornet, E. (1994). Improved alkaline oxidation process for the production of aldehydes (vanillin and syringaldehyde) from steam-explosion hardwood lignin. *Industrial & Engineering Chemistry Research*, 33(3), 718-723.

Yeh, T. F., Braun, J. L., Goldfarb, B., Chang, H. M., & Kadla, J. F. (2006). Morphological and chemical variations between juvenile wood, mature wood, and compression wood of loblolly pine (Pinus taeda L.). *Holzforschung*, 60(1), 1-8.

Yildiz, S., Gezer, E. D., & Yildiz, U. C. (2006). Mechanical and chemical behavior of spruce wood modified by heat. *Building and Environment*, 41(12), 1762-1766.

Yokoi, H., Nakase, T., Goto, K., Ishida, Y., Ohtani, H., Tsuge, S., ... & Ona, T. (2003). Rapid characterization of wood extractives in wood by thermal desorption-gas chromatography in the presence of tetramethylammonium acetate. *Journal of Analytical and Applied Pyrolysis*, 67(1), 191-200.

Zaghloul, T. I., Embaby, A. M., & Elmahdy, A. R. (2011). Key determinants affecting sheep wool biodegradation directed by a keratinase-producing Bacillus subtilis recombinant strain. *Biodegradation*, 22(1), 111-128.

Zhu, P., Sui, S., Wang, B., Sun, K., & Sun, G. (2004). A study of pyrolysis and pyrolysis products of flame-retardant cotton fabrics by DSC, TGA, and PY–GC–MS. *Journal of Analytical and Applied Pyrolysis,* 71(2), 645-655.

Zimmermann, W. (1990). Degradation of lignin by bacteria. *Journal of Biotechnology*, 13(2), 119-130.